Investigation into the role of PacC in *Epichloë festucae* development and symbiosis with perennial ryegrass

---

A thesis presented in partial fulfilment of the requirements for the degree of

Master of Science

in

Genetics

at Massey University, Palmerston North

New Zealand

Yonathan Lukito

2014

Abstract

In order to survive and adapt to the environment, it is imperative for fungi to be able to sense and respond to changes in extracellular pH conditions. In ascomycetes, sensing of extracellular pH is mediated by the Pal pathway which is activated by alkaline pH. The signal is subsequently relayed to changes in gene expression by activation of the transcription factor PacC, which is known to regulate various fungal metabolic pathways; including ion tolerance, cell-wall integrity and secondary metabolism. The role of PacC in regulating fungal virulence and pathogenicity has also been studied in several pathogenic fungi, but to date not in a symbiotic fungus. *Epichloë festucae* is a biotrophic fungal endophyte that forms a stable symbiosis with the perennial ryegrass *Lolium perenne*. In this mutualistic interaction, secondary metabolites are produced by the fungus that confer bioprotection for the host, and the host in turn provides nutrients and a means of dissemination for the fungus.

In this study, deletion (Δ*pacC*; acid-mimicking) and constitutively active (*pacC*^{CA}; alkaline-mimicking) mutants were generated to study the cellular roles of PacC in *E. festucae*. Deletion of *pacC* resulted in increased sensitivity to salt-stress and reduction in aerial hyphae formation, but did not affect the ability of the mutant to grow under alkaline pH conditions. The *pacC*^{CA} mutant on the other hand showed greater sensitivity to cell-wall and temperature stresses, and was able to grow under both acidic and alkaline conditions. Aberrant intrahyphal hyphae formation and abnormal conidiation were additionally observed in the *pacC*^{CA} mutant in culture, but hyphal fusion was unaffected. The expression of secondary metabolite genes both in culture and *in planta* was largely unaffected in both Δ*pacC* and *pacC*^{CA} mutants, and expression analysis of genes known to be pH- and PacC-dependent in other fungi showed that these genes were generally pH- and PacC-independent in *E. festucae*. The deletion and constitutive active *pacC* mutants were still able to sense and modify extracellular pH. Deletion of *pacC* did not affect the endophyte-host interaction, but ryegrass plants infected with the *pacC*^{CA} mutant were mildly hypertillered. Further examination of the growth of the *pacC*^{CA} mutant in the plant revealed formation of aberrant convoluted hyphal structures and an increase in hyphal breakage; possible reasons for the observed host plant phenotype.

This study provides novel insights into the role of PacC in the agriculturally important endophyte, *E. festucae*. In this fungus, PacC regulates salt tolerance and cell-wall integrity, but not secondary metabolism and growth at non-neutral pH conditions. The results also show that PacC is involved in the symbiotic interaction between *E. festucae* and perennial ryegrass but is not crucial in the establishment and maintenance of the symbiosis.

Acknowledgements

First of all, I would like to express my gratitude to my supervisor Prof. Barry Scott for his guidance, patience and dedication to bringing out my full potential. I am grateful for his immense knowledge and wisdom in identifying the right avenues for me to pursue and allowing me the freedom to be creative at the same time. Thank you to my co-supervisor Dr Tetsuya Chujo, for his guidance in my research, patience and for sharing with me his brilliant technical and analytical skills. It has been a privilege to work under the both of them and I am thankful for where they have brought me to today.

Thank you to the people of Scottbase, past and present. To Yvonne, Conni and Carla who were always happy to impart their skills and knowledge. To Arvina for the excessive chocolates; and Gemma for the cupcakes and other sugary stuffs… To Kim, Pip, Alex, Dan and Will thanks also for the fun, help and discussions.

My special thanks to Matthias for spending the many patient hours in training me with the confocal microscope, and to Matthew, Jordan, Doug and Nicky for assistance and also training with the various microscopes.

To William, Yang and Alvaro, thanks for the friendship and fun, for making and saving the dinner when I had to stay on at the lab.

Finally, to Mom and Dad, Joshua, Sandy and Samuel, thank you for the family and financial support.

To Monica, thank you, for everything.

YL was a recipient of a studentship funded from a grant from the Royal Society of New Zealand Marsden Fund, contract MAU1002.

Table of Contents

Table of Contents

List of Figures

List of Tables

List of Abbreviations

aM	attomolar
Amp	ampicillin
Amp^R	ampicillin-resistant
BCIP	5-bromo-4-chloro-3-indolyl-phosphate
BLAST	basic local alignment search tool
bp	base pair
cDNA	complementary DNA
cm	centimetre
Cp	crossing point
d	day(s)
DIC	differential interference contrast
DIG	digoxigenin
DMSO	dimethyl sulfoxide
DNA	deoxyribonucleic acid
dNTP	deoxynucleotide triphosphate
dUTP	deoxyuridine triphosphate
EDTA	ethylenediaminetetraacetic acid
EGFP	enhanced green fluorescent protein
ESCRT	endosomal sorting complex required for transport
Fab	fragment antigen-binding
g	gram
Gen	geneticin
Gen^R	geneticin-resistant
GFP	green fluorescent protein
h	hour
Hyg	hygromycin
Hyg^R	hygromycin-resistant
Kan	kanamycin
Kan^R	kanamycin-resistant
kb	kilobase
kV	kilovolts
L	litre
LB	Luria-Bertani
LiAc	lithium acetate
M	Molar
MAP	mitogen-activated protein
MAPK	mitogen-activated protein kinase
mg	milligram
min	minute
mL	millilitre
mm	millimetre
mM	millimolar
mRNA	messenger RNA
N.D.	not detectable
NADPH	nicotinamide adenine dinucleotide phosphate
NaOAc	sodium acetate
NB-LRR	nucleotide-binding leucine-rich repeat
NBT	nitro-blue tetrazolium
NES	nuclear export signal

ng	nanogram
NLS	nuclear localisation signal
nm	nanometre
nM	nanomolar
Nox	NADPH oxidase
PCR	polymerase chain reaction
PD	potato dextrose
PDA	potato dextrose agar
PEG	polyethylene glycol
PIPES	piperazine-N,N′-bis(2-ethanesulfonic acid)
pM	picomolar
PR	pathogenicity response
qRT-PCR	quantitative reverse transcription PCR
rcf	relative centrifugal force
RG	regeneration
RNA	ribonucleic acid
RNA	ribonucleic acid
ROS	reactive oxygen species
rpm	revolutions per minute
RT-PCR	reverse transcription PCR
s	second
SAM	shoot apical meristem
SDS	sodium dodecyl sulphate
SD-Ura	synthetic defined uracil dropout
SM	secondary metabolite
SOB	super optimal broth
spp.	species
SSC	saline-sodium citrate
TB	transformation buffer
TBE	Tris/Borate/EDTA
tBLASTn	search of translated nucleotide databases with a protein query
TMD	trans-membrane domain
ura	uracil
UTR	untranslated region
UV	ultraviolet
V	volt
v/v	volume to volume
vol	volume
w/v	weight to volume
WGA	wheat germ agglutinin
wpi	weeks post-inoculation
WT	wild-type
YPD	yeast-extract peptone dextrose
YRC	yeast recombinational cloning
µF	microfarad
µg	microgram
µL	microlitre
µm	micrometre
µM	micromolar

1. Introduction

1. Introduction

In the natural ecosystem, almost all plants form associations with fungi which can range from a symbiotic to an antagonistic interaction (Clay & Schardl, 2002). The most common and well-studied association is the symbiosis formed between 80% of all land plants and the arbuscular mycorrhizal fungi (Glomeromycota). In this interaction, the fungus helps to improve water and nutrient uptake for the plant; and in exchange, the plant provides carbohydrates such as glucose and sucrose for the fungus (Parniske, 2008). Equally important, but less intensively studied is the symbiotic association formed by the Epichloë endophytes (Ascomycota, Clavicipitaceae) and cool season grasses of the subfamily Pooideae. This family includes the perennial ryegrass *Lolium perenne*, a globally important pasture grass and the most commonly sown grass on New Zealand farms (Charlton, 2012). The term 'endophyte' is given to any microorganism that grows within a plant, in a non-antagonistic manner; as opposed to epiphytes, which grow on the plant surface (Clay & Schardl, 2002). In a grass-endophyte symbiosis, the endophyte produces several classes of secondary metabolites which confer upon the host benefits such as increased disease resistance, drought tolerance, and protection from animal and insect herbivory. The grass in return, provides nutrients, protection, and a means of dissemination for the fungus (Tanaka *et al.*, 2012).

1.1. *E. festucae* and *L. perenne* as a model experimental system

The Epichloë group of endophytes includes two distinct genera: *Epichloë*, which consists of species capable of sexual reproduction; and *Neotyphodium*, consisting strictly of asexual species that have lost this reproductive ability. Phylogenetic studies have suggested that the *Neothyphodium* spp. originally evolved from the *Epichloë* spp., and that most of the species within the former genus arose from interspecific hybridisation (Tsai *et al.*, 1994; Moon *et al.*, 2000). Both *Epichloë festucae* and *Neothyphodium lolii* species form stable mutualistic interactions with *L. perenne*, with *N. lolii* being the most commonly found symbiont in nature. *N. lolii* however, has a very slow rate of growth in axenic culture and often exhibits an unstable colony morphology; making it a less ideal organism to study in the lab (Latch & Christensen, 1985). In contrast, *E. festucae* is relatively fast growing (1-3 mm per day; Tanaka *et al.*, 2012) and retains stable colony morphology in culture. Protoplasts of *E. festucae* can be generated within a day and

transformed with linear or circular DNA; homologous recombination can subsequently be achieved with good frequencies of 1 to 25%, or more in the case of non-homologous recombination (Scott *et al.*, 2007). To date, several targeted gene replacements and reporter-tagged strains using GUS or GFP have been generated through such recombinational methods (Takemoto *et al.*, 2006; Christensen *et al.*, 2008; Eaton *et al.*, 2008; May *et al.*, 2008; Tanaka *et al.*, 2008). Cre-Lox recombination, as well as *Agrobacterium tumefaciens* T-DNA mutagenesis have also been used to generate and isolate mutants of *E. festucae* (Tanaka *et al.*, 2006; Florea *et al.*, 2009). In addition, complete genomic sequences of two *E. festucae* strains and other *Epichloë* species have been made available, facilitating genetic analysis and manipulation of the *Epichloë* spp (Genome Projects at University of Kentucky, URL: http://www.endophyte.uky.edu/).

L. perenne is a relatively easy grass to grow in the lab and inoculations with *E. festucae* typically achieve 90% infection rates in the case of wild-type *E. festucae* strain Fl1 (Schardl *et al.*, 2009). More importantly, in this artificially-generated association, the growth patterns of both plant and endophyte resemble that which is formed in nature; in which hyphal growth is strictly regulated, aligned parallel to the leaf axes, and seldom branching (Christensen *et al.*, 2006). Fescues manually infected with *Epichloë* endophytes also produce endophyte-infected seeds, as is the case in a natural infection (Latch & Christensen, 1985).

1.2. Growth of *E. festucae* in axenic culture

E. festucae grows on potato dextrose agar (PDA) as a white and fluffy mycelial colony (Figure. 1A). At the edge of the colony, hyphae grow as a single layer attached to the agar, unbranched, and organised in parallel bundles (Figure. 1B) (Scott *et al.*, 2012). Towards the middle of the colony, hyphal branching can be observed which usually occurs near the apical tip of a growing hypha (Figure. 1C). In this region, in addition to the first layer of hyphae growing attached to the agar for continued access to nutrients, a second layer is formed consisting of more hyphal bundles and aerial hyphae (Figure. 1D). Characteristically coiled aerial hyphal structures are formed within this region which often develop into conidiophores; although, most strains of *E. festucae* sporulate sporadically (Figure. 1E). Hyphal fusions or anastomosis are frequently observed at the centre and older areas of the colony (Figure. 1F). Vegetative hyphal fusion in this respect may serve to maintain homeostasis of the colony as a whole, by allowing

intrahyphal communication and exchange of nutrients (Glass *et al.*, 2004). The exact mechanism of such fusions in *E. festucae* is yet to be fully elucidated, but seems to involve reactive oxygen species, the NADPH oxidase enzyme, and several polarity proteins (Kayano *et al.*, 2013; Tanaka *et al.*, 2013).

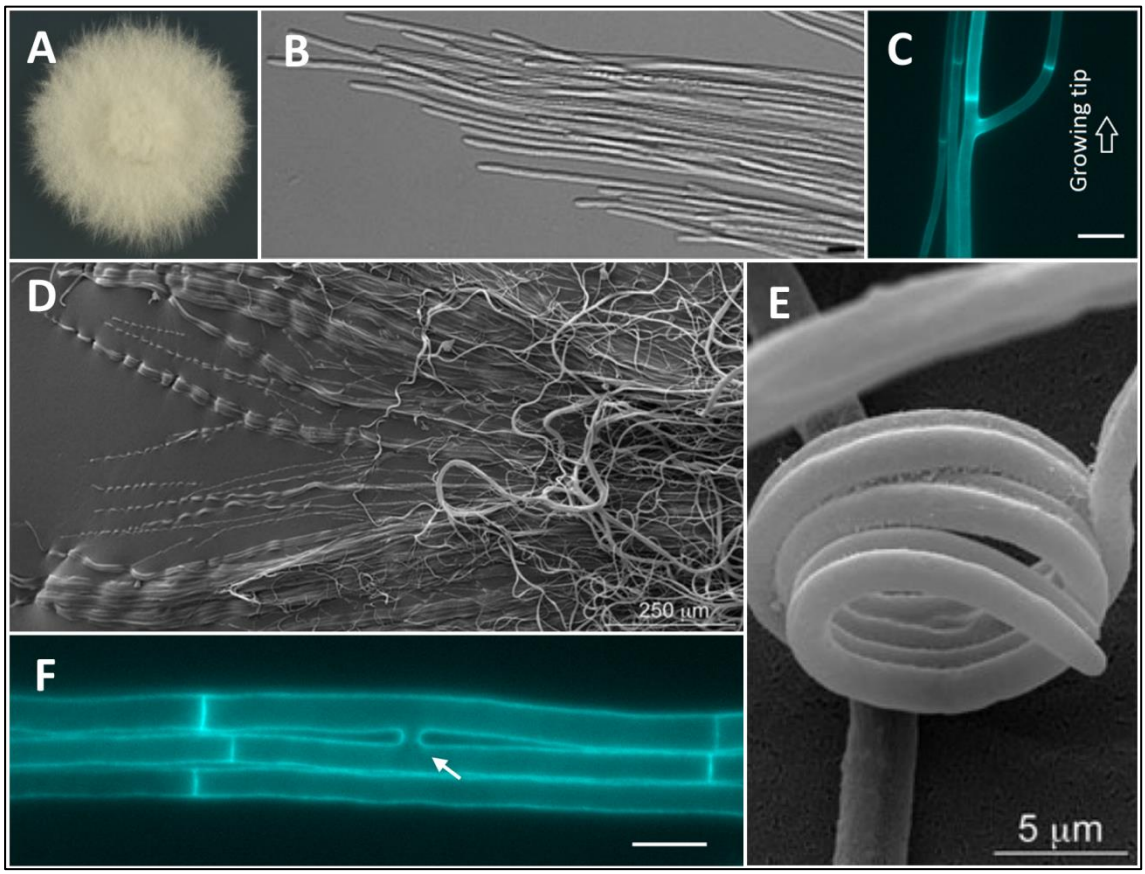

Figure 1.1 Culture and hyphal phenotypes of wild-type *E. festucae*. (A) Wild-type *E. festucae* strain Fl1 colony after 9 days of culture on 2.4% potato dextrose agar. (B) Light micrograph of hyphae at the colony edge. (C) Fluorescence micrograph of hyphae branching near the apical tip. (D) Scanning electron micrograph of hyphae at the edge and towards the middle of the colony. (E) Scanning electron micrograph of a coiled hyphal structure. (F) Fluorescence micrograph of fusion between hyphae, indicated by the arrow. Bar represents 10 µm unless otherwise indicated. Images in (B), (D) and (E) are adapted from Scott *et al.*, (2012).

1.3. Growth of *E. festucae* in the host grass

In the host, *E. festucae* grows within the apoplastic (intercellular) spaces of the plant tissues with hyphae aligned parallel to the leaf axes (Figure. 2A). The hyphae colonise the aerial tissues of the host, including leaf blade, sheath and pseudostem tissues; but not the roots. Unlike many other biotrophic fungi, *E. festucae* does not form specialised feeding structures, such as haustoria; rather, it obtains its nutrients directly from the apoplastic fluid of the host, and appears to possess complete sets of genes for the

biosynthesis and assimilation of these nutrients (e.g., of thiamine, nitrate and sulphate; Scott *et al*., 2012). As a sexual species, *E. festucae* is also capable of both vertical and horizontal transmission. In the vertical (asexual) life cycle, the endophyte maintains a restrictive growth in the plant, eventually colonising the host seeds; however, in the horizontal or sexual life cycle the fungus is capable of switching to a proliferative mode of growth, typically resulting in a diseased host condition known as 'choke' (Figure. 2B). This is due to the formation of a fungal reproductive structure (stroma) over the host flag leaf, preventing emergence of the host inflorescence (Kirby, 1961). To date, however, there has been no report of 'choke' in the association between *E. festucae* and *L. perenne* (Scott *et al*., 2012).

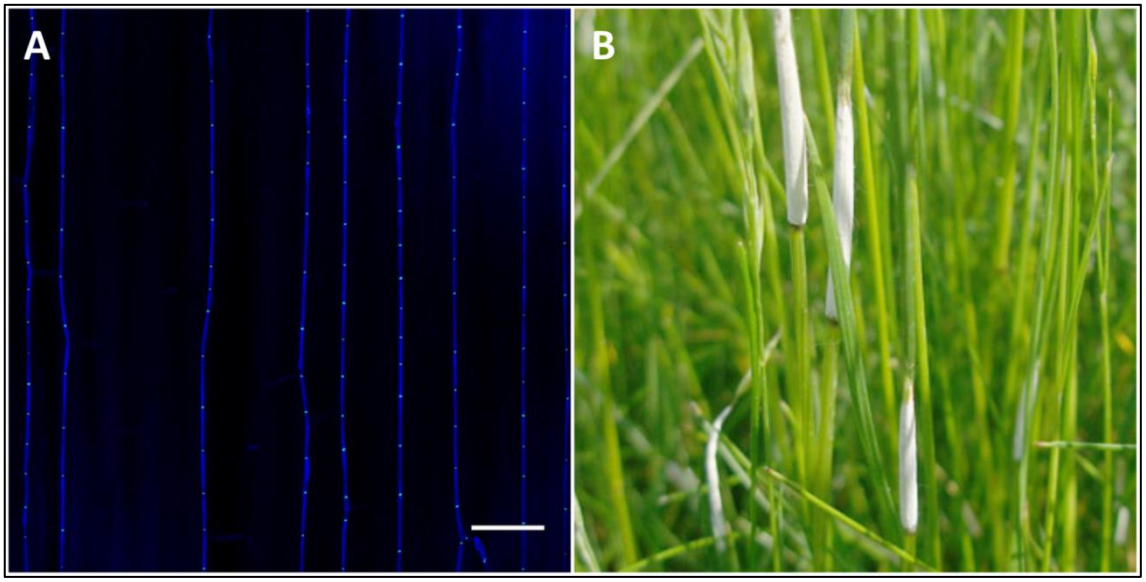

Figure 1.2. Growth of *E. festucae* in the plant and formation of *E. festucae* stromata. (A) Confocal image of the highly regulated hyphal growth of *E. festucae in planta*; hyphae grow within the intercellular spaces of the plant cells and seldom branch. Bar represents 50 µm. (B) Formation of *E. festucae* stromata on fine fescue. Image in (B) was reproduced from Scott *et al*., (2012).

Until recently, it was assumed that fungal hyphae grow solely by tip extension. Epichloë endophytes are also thought to initially spread by such tip growth, in the host shoot apical meristem (SAM). Hyphae in this region grow proliferatively and branch extensively, creating an interlinked hyphal network within the dividing plant cells. However in the leaf sheaths and blades, hyphal growth becomes substantially more restricted; only single hyphae are present between the plant cells, firmly attached to the leaf cell walls and infrequently branched. Here, the host cells grow by intercalary extension at a rate of over 10 mm per day; and if hyphae grew only by tip extension,

they would be sheared (Scott *et al.*, 2012). It was thus proposed and subsequently demonstrated by the use of EGFP-tagged endophytes that growth of *E. festucae* in these regions is through intercalary division and extension, along the length of the hypha and leaf axis, which allows cumulative growth of the hyphae in synchrony with the host plant (Christensen *et al.*, 2008). This model also explains the observed coordination of fungal hyphal growth to that of the plant; when the host leaf matures and growth of the host cells ceases, so does hyphal growth.

1.4. Molecular regulators of the symbiotic interaction in *E. festucae*

The interaction between the Epichloë and its host grass is so specialised, that it is likely the endophyte may have originally evolved as a pathogen of the grass and progressively turned into a mutualist (Clay & Schardl, 2002). The highly regulated interaction and the restrictive mode of growth of *E. festucae* in *L. perenne* imply the presence of some sort of communication between the host and endophyte that preserves the mutualistic interaction. Indeed, it has been shown that single genetic mutations in the fungus can lead to a breakdown in this highly regulated interaction, leading to the demise of the host due to a switch in the fungus from a mutualist to a pathogen (Takemoto *et al.*, 2006; Tanaka *et al.*, 2006; Eaton *et al.*, 2008; 2008; Charlton *et al.*, 2012; 2013).

The first attempt to look into the molecular regulators of this interaction employed a forward genetic screen in *E. festucae* to identify mutants with disrupted symbiotic phenotypes (Tanaka *et al.*, 2006). The study found that disruption of the *noxA* gene in *E. festucae*, encoding the catalytic subunit of the NADPH oxidase (Nox) enzyme complex (of which the mammalian gp91^{phox} is a homologue), disrupted the symbiotic interaction; giving rise to a stunted and prematurely-senescing host phenotype. Growth of the mutant endophyte in the plant was no longer restricted but proliferative, and hyphae invaded and colonised the host vascular bundles. It was subsequently found that deletion of two other genes encoding the NoxR and RacA subunits of the Nox enzyme complex similarly resulted in a disrupted host-endophyte interaction; the same was also found in a *noxR*-overexpressing mutant (Takemoto *et al.*, 2006; Tanaka *et al.*, 2008). NoxR and RacA are homologues of the mammalian p67phox and Rac2, respectively, which have been shown as necessary and sufficient for the activation of gp91phox (NoxA) under *in vitro* conditions (Diebold & Bokoch, 2001). These studies

altogether demonstrate that the Nox complex and subsequent generation of reactive oxygen species (ROS), such as O_2^-, are essential signalling components of the endophyte-host interaction. Given that these *E. festucae* mutants have an unrestricted growth in the plant, it was proposed that ROS production may be required for the endophyte to switch from tip to intercalary growth in the plant, in order to achieve a regulated and synchronised growth to that of the host (Eaton *et al.*, 2011). It is interesting that impairment in the ability of *E. festucae* to produce ROS leads to a switch to pathogenicity, whereas in other fungal species studied the inability to produce ROS results in a loss of pathogenicity (Egan *et al.*, 2007; Giesbert *et al.*, 2008; Rolke & Tudzynski, 2008; Segmuller *et al.*, 2008).

Following these studies, subsequent investigations further identified two other proteins; BemA and Cdc24, that interact with the NoxR subunit (Takemoto *et al.*, 2011). All three proteins were also found to preferentially localise to the fungal hyphal tips and septa. Deletion of *bemA* resulted in reduced hyphal fusion in the mutant, and disrupted the symbiotic interaction with the host (Takemoto *et al.*, 2011; Kayano *et al.*, 2013). Deletion of *cdc24* on the other hand is likely to be lethal as no Δ*cdc24* mutants could be isolated. Other important regulators of the interaction include an iron siderophore in *E. festucae*; SidN (Johnson *et al.*, 2007) and a regulator of hyphal fusion that is encoded by the *soft* (*so*) gene, deletion of which led to death of the host plant within 8 weeks (Charlton *et al.*, 2012). Interestingly, the Δ*so* mutant did not display an increased fungal mass *in planta*, indicating that proliferative growth of the endophyte may not be the only factor leading to a breakdown in symbiosis. A recent study additionally revealed a role for the *E. festucae* zinc-finger transcription factor, ProA in the symbiosis. Infection of ryegrass plants with the Δ*proA* mutant led to similar stunting and premature senescence of the host, with the endophyte growing unrestrictedly *in planta* (Tanaka *et al.*, 2013). In culture, hyphal fusion is absent in the Δ*proA*, as well as the Δ*noxA*, Δ*rac* and Δ*noxA*/Δ*noxB* mutants, indicating that the ability of the fungus to fuse may be important in the interaction with the host; however, experimental evidence for hyphal fusion *in planta* is still lacking.

Another important molecular regulator of the interaction is the fungal stress-activated mitogen-activated protein kinase (MAPK), SakA. Similar to the other symbiosis-defective mutants, the Δ*sakA* mutant of *E. festucae* showed an unrestricted growth in the plant and gives rise to a stunted and prematurely-senescing host phenotype (Eaton

et al., 2010). The compelling question following this finding is undoubtedly if there is any link between SakA, Nox and ROS. The answer is not entirely clear, as the Δ*sakA* mutant was found to have greater production of H_2O_2 in culture, and more H_2O_2 was also detected surrounding the mutant hyphae *in planta*; however, from expression analysis studies, SakA was shown not to regulate the expression of *noxA* and *noxR* in culture (Eaton *et al.*, 2008; 2010). The *sakA* study is also the first and only study to date in a grass-fungal system that employs high-throughput RNA sequencing to look at changes in plant and fungal gene expression between wild-type and mutant endophyte-infected plants. This has provided a wealth of information on the molecular basis underlying the mutualistic interaction, and on the changes in gene expression which accompanies the switch towards antagonism. Some of the significantly upregulated plant genes in the Δ*sakA*-infected samples included the archetypal plant defence genes; the nucleotide-binding leucine-rich repeat (NB-LRR) and pathogenicity response (PR) genes, as well as genes coding for antioxidant enzymes, such as peroxidases and catalases. The upregulation in NB-LRR and PR genes may indicate that the host is now recognising the fungus as a pathogen; while the upregulation of antioxidant enzymes may be a direct response to the increase in ROS levels. On the other hand, significantly upregulated fungal genes in the Δ*sakA* mutant included those coding for protein translation, nutrient transporters, and degradative enzymes; while significantly downregulated genes included virtually all of the secondary metabolite biosynthetic genes (Eaton *et al.*, 2010). These expression profiles are consistent with the proliferative mode of growth of the Δ*sakA* mutant in the plant, and its role as a pathogen rather than a symbiont. Also accompanying these changes was a significant upregulation of *pacC* in the Δ*sakA* mutant, which encodes a zinc-finger transcription factor that is activated by extracellular alkaline pH conditions. Alkalinisation of the apoplast is known to be an important plant defence response to pathogens, and PacC has also been shown to be a regulator of pathogenicity in several different fungi (discussed below).

These above studies have collectively shaped our understanding of the molecular interactions in the symbiosis between *E. festucae* and *L. perenne*; which involves at the least; an NADPH oxidase complex in the fungus and subsequent production of ROS as signalling molecules; cell polarity proteins (Cdc24 and BemA); a MAP kinase (SakA); a

zinc-finger transcription factor (ProA); an Fe^{3+} chelator (SidN); and possible regulators of hyphal fusion.

1.5. Fungal secondary metabolites

Fungal secondary metabolites are a group of small molecular-weight compounds produced by members of the phylum Ascomycota, many which have important biological activities. Clinically-relevant examples include the antibiotic penicillin (produced by *Penicillium chrysogenum*), the cholesterol-lowering agent lovastatin (*Aspergillus terreus*), and the carcinogenic compound aflatoxin (*Aspergillus flavus*). As the term implies, these secondary metabolites are produced during secondary metabolism, which is typically activated in the late exponential phase of growth; or when conditions of growth are less optimal, such as in a nutrient-low environment; or as a response to the presence of other competing organisms. The secondary metabolite pathways and the secondary metabolites themselves however, are not essential and are dispensable for the producing fungus (Keller & Hohn, 1997). In the agriculturally-important grass symbiont, *E. festucae*, the production and biological activities of these compounds are of particular interest due both to their desirable and undesirable effects on pasture grasses and livestock. Four main classes of secondary metabolites are produced by *E. festucae*: peramine, lolines, ergot alkaloids and the indole-diterpenes (Scott *et al.*, 2009; Schardl *et al.*, 2012).

1.5.1 Secondary metabolites of *E. festucae*

Resistance of ryegrass to the Argentine stem weevil (*Listronotus bonariensis*) was the first anti-insect benefit reported in an endophyte-grass association (Prestidge *et al.*, 1982). The responsible molecule, peramine, was first identified in the endophyte *Acremonium loliae* (Rowan, 1986) and later found to also be produced by *E. festucae* (Lane *et al.*, 1997). The Argentine stem weevil is a major ryegrass pest which would have otherwise caused severe damage to ryegrass pastures in New Zealand if not for the protection conferred by these endophytes (Rowan *et al.*, 1986). The second class of compounds, lolines, possess a broad-spectrum anti-insect activity and may protect against the aphid *Schizapus graminis* (Wilkinson *et al.*, 2000). Lolines also exhibit anti-nematode activities at higher concentrations (Bacetty *et al.*, 2009). The ergot alkaloids are complex molecules with cyclic ring structures that are toxic to both vertebrates and

invertebrates (Schardl *et al.*, 2004). These alkaloids are initially described in pathogenic fungi of the genus *Claviceps*, which have been notoriously recognised since the Middle Ages as contaminants of grain harvests, due to *Claviceps*-infected crops (Tudzynski & Scheffer, 2004). In humans, long-term ingestion of these alkaloids can lead to ergotoxicosis; a neurological disturbance accompanied by fever, dry gangrene, and in some cases death (van Dongen & de Groot, 1995). Livestock feeding on endophyte-infected fescues containing high levels of these alkaloids can develop similar symptoms including hyperthermia, convulsions and dry gangrene (Bacon, 1995). However, one of the ergot alkaloids, ergovaline is desirable for its activity against the black beetle (*Heteronychus arator*), a major ryegrass pest in the northern parts of New Zealand (Popay & Baltus, 2001). Lastly, the indole-diterpenes are a class of calcium-gated potassium channel inhibitors, the most relevant of which is lolitrem B, a neurotoxin that cause reversible tremors and ataxia (loss of muscular coordination) in grazing animals (Fletcher & Harvey, 1981; Wu *et al.*, 2010). This syndrome is also known as 'ryegrass staggers' due to the symptoms presented by the poisoned animals.

1.5.2 Genetic analysis of the *E. festucae* secondary metabolite genes

In fungi, genes for secondary metabolite biosynthesis are often organised in clusters and located close to telomeres. The telomeric and subtelomeric regions in the chromosome are regions where repetitive DNA elements are typically found and where heterochromatin forms. Consequently, heterochromatin formation can result in the epigenetic silencing of genes within these regions (Grewal & Jia, 2007). It is likely that the clustering and sub-telomeric placement of the secondary metabolite genes in fungi serve to facilitate the simultaneous regulation of these genes, e.g. by chromatin remodelling; as well as to ensure a complete inheritance of all genes in the pathway during sexual recombination (Keller & Hohn, 1997).

In *Aspergillus fumigatus* at least twenty such clusters are found sub-telomerically, with several located just 100 kb away from the telomeres (Perrin *et al.*, 2007). In *E. festucae*, the genes involved in the biosyntheses of lolitrem B, ergovaline and lolines are also organised in clusters; in the *LTM*, *EAS*, and *LOL* loci, respectively. An exception is peramine, which is synthesised by a single multidomain enzyme encoded by the *perA* gene. The *LTM* and *EAS* loci, but not *LOL*, are also located subtelomerically (Schardl *et al.*, 2012). In accordance with the postulated regulatory effects of the subtelomeric

placement of these clusters, it was recently shown that deletion of genes for the H3K9 or H3K27 methyltransferases in *E. festucae* resulted in the derepression of the *ltm* and *eas* genes in culture; while deletion of both methyltransferases in a double 'knockout' mutant led to an even greater derepression of the secondary metabolite genes (Chujo & Scott, 2014). Another interesting feature of these loci is the presence of repeat elements and transposon relics among the genes in the clusters which are thought to be footprints of earlier recombination events that led to the present arrangements of these clusters (Spiering *et al.*, 2005; Young *et al.*, 2006; Fleetwood *et al.*, 2007).

The *LTM*, *EAS* and *LOL* loci each contain 11 genes and span regions of about 90, 105, and 30 kb, respectively (Schardl *et al.*, 2012). All of the *ltm*, *eas*, and *lol* genes, as well as *perA*, have been characterised and shown to be highly expressed by the endophyte *in planta* but poorly expressed in culture (Fleetwood *et al.*, 2007; Tanaka *et al.*, 2005; Young *et al.*, 2005, 2006; Zhang *et al.*, 2009; this study) . Attempts to induce the production of the secondary metabolites in axenic culture have mostly been unsuccessful; although, Blankenship *et al.* (2001) were able to show that certain nutrient and pH conditions induce loline expression in *N. lolii*. This difficulty in inducing secondary metabolite production in culture but their high expression *in planta* suggests that plant-specific signalling may be required for the induction of secondary metabolite pathways in *E. festucae*. In support of this hypothesis, the expression of *ltmM*, an essential gene for lolitrem biosynthesis, was found to be spatially and temporally regulated in the plant (May *et al.*, 2008). By fusing the *ltmM* promoter to the *gusA* reporter gene, the authors demonstrated that *gusA* was expressed in all infected vegetative host tissues during pre-anthesis; but not at post-anthesis, the stage at which host flowers are fully opened. Expression of *gusA* during this stage of the host development was confined only to the gynoecium. This is fascinating as expression of *ltmM* in this region would ultimately mean the production of lolitrem B in the host seeds. The seed is the only non-pathogenic mode of dissemination for *E. festucae*, and the symbiosis appears to have evolved a means to protect it from animal herbivory.

1.6. Global regulators of secondary metabolism

Most of our understanding of how secondary metabolism is regulated in fungi comes primarily from studies in *Aspergillus*, and to a lesser extent in *Fusarium*, *Neurospora*, and other ascomycetes. The regulators of secondary metabolite biosynthetic pathways can

be divided into two classes; pathway specific and global acting regulators. Pathway specific regulators are usually transcription factors that regulate single secondary metabolite clusters, and genes for these regulators are often found within the particular clusters that they regulate. Examples include the $Zn(II)_2Cys_6$ zinc binuclear cluster transcription factor AflR, which controls the production of aflatoxin and sterigmatocystin in *Aspergillus nidulans* (Fernandes *et al.*, 1998) and the Cys_2His_2 zinc-finger transcription factor Tri6, which controls the production of trichothecene in *Fusarium graminearum* (Proctor *et al.*, 1995). The regulators discussed below fall under the group of global regulators which exert control over several secondary metabolite pathways. These proteins play key roles in regulating secondary metabolism in response to environmental signals such as light (VeA) and pH (PacC). Other regulators (not discussed) include CreA and AreA which respond to environmental carbon and nitrogen levels, respectively.

1.6.1 Regulation by light

The VeA protein in the velvet family (comprising VeA, VelB, VosA and VelC) was first found to be involved in the cellular response to light in *A. nidulans* by mutation of the *veA* gene which allowed the fungus to conidiate in the absence of light (Mooney & Yager, 1990). VeA was subsequently shown to regulate secondary metabolism in the fungus, by controlling penicillin and sterigmatocystin production (Kato *et al.*, 2003), and subsequent studies found similar roles for VeA in regulating biosynthesis of aflatoxin and its intermediate versicolorin in other *Aspergillus* species (Calvo *et al.*, 2004; Duran *et al.*, 2007). Homologs of VeA were later shown to regulate secondary metabolism in other filamentous fungi, including *Acremonium* (Dreyer *et al.*, 2007), *Fusarium* (Myung *et al.*, 2009) and *Penicillium* (Hoff *et al.*, 2010).

The VeA protein translocates into the nucleus in the absence of light and out of the nucleus in the presence of light, exactly how it responds to light is still unclear, but most likely through its interaction with the red-light sensing phytochrome, FphA in the nucleus (Stinnett *et al.*, 2007; Purschwitz *et al.*, 2008). It is also largely unknown how VeA regulates secondary metabolite pathways, as although it has a nuclear localisation signal (NLS) and a nuclear export signal (NES), the protein does not contain any DNA binding motifs (Purschwitz *et al.*, 2009). The velvet domains possessed by all four members of the family also have little resemblance to known protein motifs, but their

ability to form homo- and heterodimers suggests a possible protein-protein interaction role of the Velvet domain (Calvo, 2008; Sarikaya Bayram *et al.*, 2010; Bayram & Braus, 2012). In the nucleus, during the absence of light, VeA interacts with VelB and LaeA (described below) to form a heterotrimeric complex, designated as the Velvet complex (Bayram *et al.*, 2008; 2010).

1.6.2 Regulation by histone modifiers

LaeA (loss of aflR expression A) was first identified in a complementation screen of *Aspergillus* mutants with impaired expression of the *aflR* (aflatoxin) and *stc* (sterigmatocystin) gene clusters (Butchko *et al.*, 1999; Bok & Keller, 2004). Subsequent generation of a Δ*laeA* mutant showed that it regulates the expression of several secondary metabolites; including lovastatin, penicillin and sterigmatocystin; genes for all of which are organised in clusters in the genome (Bok & Keller, 2004). Placement of a gene normally unregulated by LaeA into the sterigmatocystin cluster, such as *argB*, a gene required for arginine metabolism, also results in it becoming LaeA regulated (Bok *et al.*, 2006). The later finding that LaeA is a nuclear protein and contains a putative protein methyltransferase (Bayram *et al.*, 2008) provide strong indication that it may act at the chromatin level; however, biochemical evidence for this hypothesis is still lacking. In a whole genome analysis of *A. fumigatus*, LaeA was shown to influence the expression of 9.5% (943 genes) of genes in the fungus, but positively regulate up to 40% of secondary metabolite genes (Perrin *et al.*, 2007). LaeA homologs in *Fusarium* and *Penicillium* have also been shown to regulate gibberellin and penicillin production, respectively (Hoff *et al.*, 2010; Wiemann *et al.*, 2010). Aside from LaeA, other histone modifiers such as the H3K9 histone methyltransferase ClrD (Reyes-Dominguez *et al.*, 2010) and the histone deacetylases, HdaA (Shwab *et al.*, 2007) also regulate the secondary metabolite pathways in *A. nidulans* including those for aflatoxin, isopenicillin and terrequinone biosyntheses.

1.6.3 Regulation by pH

In *A. nidulans*, sensing and response to extracellular pH by the fungus is mediated by the Pal pathway. Seven proteins are involved in this pathway: PalH, PalI, PalF, PalC, PalA, PalB, and PacC, all of which are essential and disruption to any of the genes for these proteins abolishes pH responsiveness in the fungus (Arst & Peñalva, 2003;

Peñalva *et al.*, 2008). The transcription factor PacC links the signal from this pH transduction pathway to downstream changes in gene expression. PacC and extracellular pH have been shown to regulate the expression of secondary metabolite genes in *A. nidulans* (Espeso *et al.*, 1993; 1996; Then Bergh & Brakhage, 1998), and in other filamentous fungi including *Fusarium* (Merhej *et al.*, 2011) and *Acremonium* (Schmitt *et al.*, 2001).

1.7. The Pal pathway as the main pH-response system

The Pal pathway in *A. nidulans* begins with a plasma membrane signalling complex consisting of PalH, hypothesised to be the pH sensor and two other proteins; PalF and PalI (Figure 1.3). PalH is a 7-trans-membrane domain (TMD) receptor with a cytosolic C-terminus that interacts with PalF (Herranz *et al.*, 2005). Proper localisation of PalH requires both PalF and PalI, as overexpressed PalH localises to the endosomal membrane but its co-overexpression with PalF (Calcagno-Pizarelli *et al.*, 2007) or PalI (Hervas-Aguilar *et al.*, 2010) results in proper localisation to the plasma membrane. PalF is an arrestin; and is found to be ubiquitinated and phosphorylated at ambient alkaline pH conditions in a process that is dependent on both PalH and PalI (Herranz *et al.*, 2005). Arrestins are a family of proteins that mediate the down-regulation of 7-TMD receptors through the endosomal pathway, and ubiquitination of membrane proteins is a signal for endosomal internalisation (Shenoy & Lefkowitz, 2011). This is in agreement with the findings of an initial study that suggested the involvement of the endosomal pathway in fungal pH-signalling (Xu *et al.*, 2004).

The endosomal sorting complex required for transport (ESCRT) is a complex cell apparatus important in endosomal trafficking. Four ESCRT complexes are found in fungi; ESCRT-0, ESCRT-I, ESCRT-II and ESCRT-III (Williams & Urbe, 2007). An initial study in *Saccharomyces cerevisiae* found that many subunits of the ESCRT complexes, except those of ESCRT-0, are required for the activation of Rim101p, the yeast homolog of PacC (Xu *et al.*, 2004). In *Aspergillus*, the remaining Pal proteins; PalC, PalA and PalB, have been shown to interact with ESCRT complexes. PalB, the cysteine protease which mediates the first pH-dependent cleavage of PacC, interacts with Vps24, a subunit of ESCRT-III (Denison *et al.*, 1995; Diez *et al.*, 2002). This interaction is necessary for the proper cleavage of PacC by PalB, and suggests some involvement of Vps24, possibly in activating the PalB protease (Rodríguez-Galán *et al.*, 2009). Yeast two-hybrid

experiments also showed the interaction of PalC and PalA with Vps32 of the ESCRT-III complex (Vincent *et al.*, 2003; Galindo *et al.*, 2007). Vps23, a component of ESCRT-I, was found to co-immunoprecipitate only with the ubiquitinated form of PalF, and is also recruited to the cell membrane. From the same GFP-fusion studies, PalA and PalC were found to localise to the cell membrane, probably by their known interactions with Vps32 (Galindo *et al.*, 2012). In addition, PalA recognises two YPXL/I motifs flanking the signalling protease cleavage site in the PacC protein, which suggests a possible role of PalA in the initial pH-dependent cleavage of PacC (Vincent *et al.*, 2003).

These results prompted a modification to earlier models of the Pal pathway, which proposed that the final complex assembles on the endosomal membrane (Peñalva *et al.*, 2008). Rather, the present model suggested by Galindo *et al.*, (2012) (Figure 1.3), proposes that ubiquitinated PalF recruits Vps23 (ESCRT-I), which in turn recruits Vps32 (ESCRT-III). More Vps32 proteins probably arrive on the cell membrane to form a polymer, as Vps32 proteins were observed to homopolymerise with other Vps32 proteins (Mayers & Audhya, 2012). Vps32 then recruits PalC, PalA, and another ESCRT-III protein, Vps24. PacC is then likely recruited through interaction of its YPXL/I motifs with PalA; and finally, the first cleavage of PacC is mediated by the cysteine protease PalB (Galindo *et al.*, 2012).

1.8. The PacC transcription factor

PacC is a Cys_2His_2 zinc-finger transcription factor that recognises the consensus sequence 5'-GCCAAG-3' (Espeso *et al.*, 1997; Schmitt *et al.*, 2001; Caracuel *et al.*, 2003b). In *A. nidulans*, three forms of PacC can be detected in cell extracts: PacC-72, PacC-53 and PacC-27, where the numbers refer to protein masses in kDa (Figure 1.4). The full length protein, PacC-72, is the predominant form when extracellular pH is acidic, but under extracellular alkaline pH conditions PacC becomes activated by two consecutive proteolytic cleavages (Orejas *et al.*, 1995). The initial pH-dependent cleavage of PacC-72 (678 residues) into PacC-53 (495 residues) is likely mediated by PalB, and takes place within a region of 24 conserved residues in the PacC protein, termed the 'signalling protease box' (Diez *et al.*, 2002). The second cleavage of PacC-53 to PacC-27 (250 residues) is performed by the proteasome, independent of a pH signal (Hervas-Aguilar *et al.*, 2007).

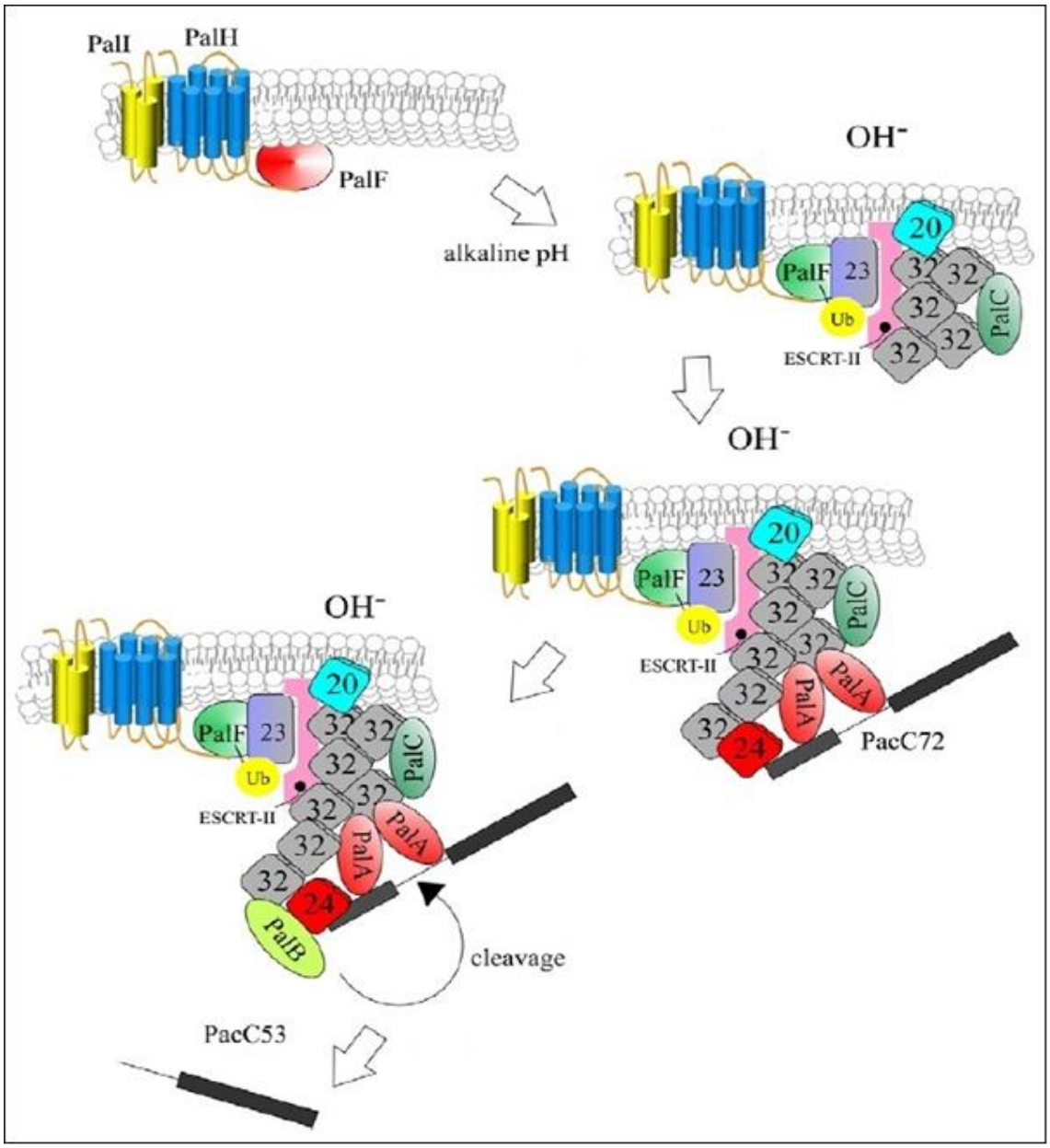

Figure 1.3. Current model for pH sensing through the Pal pathway. The plasma membrane pH-sensing complex comprises three proteins; PalH, PalI and PalF. Alkalinisation of extracellular pH leads to ubiquitination of PalF and subsequent recruitment of Vps23, Vps32, Vps24 and other ESCRT proteins to the cell membrane. Vps32 then recruits PalC and PalA, which in turn recruits PacC. PalB is recruited by Vps24 and mediates the first pH-dependent cleavage of PacC. Figure is reproduced and modified from Galindo *et al.*, (2012).

Three regions in the PacC protein; regions A, B and C (Figure 1.4), are thought to interact with each other and prevent the second proteasome-mediated cleavage of PacC by keeping the protein in a 'closed' state (Espeso *et al.*, 2000). Cleavage by PalB at the protease cleavage site is thought to release the C-terminus of the protein, including region C; and render the protein 'open', exposing its nuclear localisation signal (NLS), DNA binding domain, and processing cleavage site (reviewed in Arst & Peñalva,

2004). Both PacC-53 and PacC-27, but not PacC-72, localise to the nucleus; and the fully-cleaved form, PacC-27, remains in the nucleus regardless of extracellular pH conditions (Mingot *et al.*, 2001).

Two recent studies analysing the transcriptome of wild-type, *pacC*-deletion and *pacC*-constitutive-active mutants provide insights on the targets and extent of control that PacC has on the fungal genome. In *Colletotrichum gloeosporioides*, Alkan *et al.* (2013) observed that 5% (961 of 18,456) of genes in this fungus are under the control of PacC, i.e., down- or upregulated. On the other hand, Trushina *et al.* (2013) observed that only 1% (157) of the 12,427 genes in *Trichoderma virens* are under the control of PacC. These studies highlight the difference in the extent of influence that PacC can have in different fungal species. In line with this, the PacC homologue in *S. cerevisiae*, Rim101p, is currently known to have only gene-repressive functions (Lamb *et al.*, 2001; Peñalva *et al.*, 2008), although 150 of the ~5,000 genes in this fungus were found to be induced in response to alkaline pH (Serrano *et al.*, 2002). In this organism, other pH-regulatory systems, such as calcineurin and the Crz1/Tcn1 transcription factor, and others, also mediate the cellular response to alkaline pH (Viladevall *et al.*, 2004).

Some of the genes in *A. nidulans* that are under the control of PacC include those coding for proteases, permeases, transporters and siderophores, highlighting an important role that PacC has in the development of this fungus (reviewed in Peñalva *et al.*, 2008). PacC is also known to regulate other cellular processes in fungi including ion homeostasis (Lamb *et al.*, 2001; Caracuel *et al.*, 2003a), sporulation (Piccirillo *et al.*, 2010), and cell-wall dynamics (Moreno-Mateos *et al.*, 2007). The control of PacC over secondary metabolism has been well-studied across several fungal genera. PacC is known to positively regulate penicillin and cephalosporin biosyntheses in *A. nidulans* and *Acremonium chrysogenum*, respectively (Espeso *et al.*, 1993; Then Bergh & Brakhage, 1998; Schmitt *et al.*, 2001). However, PacC can also act to negatively regulate secondary metabolite pathways, even in the same fungus, such as that for sterigmatocystin biosynthesis in *A. nidulans* (Keller *et al.*, 1997). Similarly, PacC negatively regulates the biosyntheses of fumonisin in *F. verticillioides* (Flaherty *et al.*, 2003) and trichothecene *F. graminearum* (Merhej *et al.*, 2011).

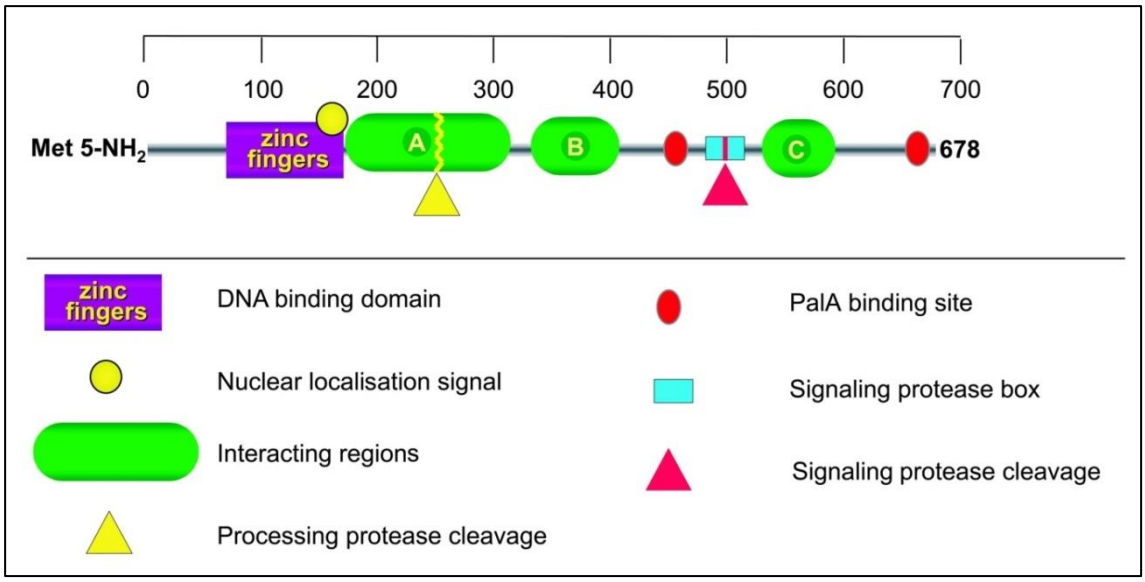

Figure 1.4. Relevant domains and regions of the PacC transcription factor in *A. nidulans*. In the absence of an alkaline pH signal, PacC is maintained in a 'closed' form by interaction of the three regions; A, B and C. Under alkaline conditions the protein is recruited by PalA to the cell membrane where the signalling protease PalB mediates the first cleavage of PacC at the signalling protease cleavage site. A second, pH-independent cleavage takes place at the processing cleavage site and is mediated by the proteasome. In the nucleus, the active PacC protein binds to promoter regions through the zinc-finger DNA-binding domain to either inhibit or promote gene transcription. Figure is reproduced and modified from Peñalva & Arst, (2004).

Another well-studied aspect is the regulation of PacC over fungal pathogenicity. This was first demonstrated in the pathogenic fungus *Candida albicans*, in which the *RIM101* (Pal) pathway and Rim101p (PacC) protein were found to be required for full pathogenicity of the fungus in mice (Davis *et al.*, 2000). Likewise, the *A. nidulans pacC* loss-of-function mutant has reduced virulence in mice, while the gain-of-function mutant was more virulent (Bignell *et al.*, 2005). Similar roles for PacC have been described in fungal pathogens of plants; PacC is essential for virulence of *Colletotrichum acutatum* on citrus (You *et al.*, 2007) and for virulence of *Sclerotinia sclerotiorum* on tomato and *Arabidopsis* (Rollins, 2003). However, a completely opposite role is played by PacC in *Fusarium oxysporum*; in this crop pathogen, *pacC* loss-of-function mutants were more virulent to tomato plants, while the constitutively-active *pacC* mutants showed significantly less virulence (Caracuel *et al.*, 2003b; Ortoneda *et al.*, 2004).

1.9. Aims of this study

The role of the PacC transcription factor in regulating fungal pathogenicity has been extensively demonstrated in host-pathogen interactions but not in a symbiotic relationship. PacC has also been shown to regulate secondary metabolite pathways in many fungal species; however, its role in regulating the production of agriculturally important secondary metabolites in *E. festucae* is not known. A recent RNAseq study showed that *pacC* is upregulated in a symbiotically-deficient mutant of *E. festucae*. In this mutant, secondary metabolite genes and many symbiotic genes are shut down (Eaton *et al.*, 2010).

The two main objectives of this study were to determine the effects of deletion (acid-mimicking) and constitutively active (alkaline-mimicking) *pacC* mutations on the symbiotic interaction of *E. festucae* with perennial ryegrass; and on the expression of secondary metabolite genes in the fungus. An additional aim was to observe the effects that these mutations have on the development of *E. festucae*; particularly under stress conditions which are known from studies in other fungi to require a functional PacC for tolerance. This includes conditions of salt, cell-wall and pH stress.

2. Materials and Methods

2. Materials and Methods

2.1 Biological material

Bacterial and fungal strains, plasmids, and plant material used this study are listed in Table 2.1.

Table 2.1. Organisms and plasmids used in this study

Organism/Strain	Characteristics	Reference
E. coli		
DH5α	F$^-$, φ80*lacZ*, ΔM15, Δ(*lacZYA-argF*), U169, *recA1*, *endA1*, *hsdR17* (r_k^-, m_k^-), *phoA*, *supE44*, λ$^-$, *thi-1*, *gyrA96*, *relA1*	Invitrogen
PN4244	DH5α; pYL1	This study
PN4245	DH5α; pYL2	This study
PN4246	DH5α; pYL3	This study
S. cerevisiae		
PN2735	MATa; his3Δ; leu2Δ; met15Δ; ura3Δ (BY4741; wild type)	Euroscarf, Frankfurt
E. festucae		
PN2278 (Fl1)	Wild-type	Young *et al*., 2005
PN3002 (Δ*pacC* #8)	Fl1/Δ*pacC*::P*trpC-nptII*-T*trpC*; Gen^R	This study
PN3003 (Δ*pacC* #11)	Fl1/Δ*pacC*::P*trpC-nptII*-T*trpC*; Gen^R	This study
PN3004 (Δ*pacC*/*pacC* #2)	Fl1/Δ*pacC*/*pacC*; pYL2; Gen^R, Hyg^R	This study
PN3005 (Δ*pacC*/*pacC* #7)	Fl1/Δ*pacC*/*pacC*; pYL2; Gen^R, Hyg^R	This study
PN3006 (Δ*pacC*/*pacC^{CA}* #1)	Fl1/Δ*pacC*/*pacC^{CA}*; pYL3; Gen^R, Hyg^R	This study
PN3007 (Δ*pacC*/*pacC^{CA}* #2)	Fl1/Δ*pacC*/*pacC^{CA}*; pYL3; Gen^R, Hyg^R	This study
PN3008 (Δ*pacC*/*pacC^{CA}* #6)	Fl1/Δ*pacC*/*pacC^{CA}*; pYL3; Gen^R, Hyg^R	This study
PN3009 (Δ*pacC*/*pacC^{CA}* #14)	Fl1/Δ*pacC*/*pacC^{CA}*; pYL3; Gen^R, Hyg^R	This study
PN3010 (Δ*pacC*/*pacC^{CA}* #19)	Fl1/Δ*pacC*/*pacC^{CA}*; pYL3; Gen^R, Hyg^R	This study
PN3011 (Δ*pacC*/*pacC^{CA}* #22)	Fl1/Δ*pacC*/*pacC^{CA}*; pYL3; Gen^R, Hyg^R	This study
L. perenne		
L. perenne cv. Samson	-	AgResearch

Plasmid	Characteristics	Reference
pCR™-Blunt II-TOPO®	Kan^R; Zeo^R; *LacZα-ccdB*	Invitrogen
pSF15.15 (PN1862)	pSP72 containing 1.4-kb *Hind*III P*trpC-hph* from pCB1004 cloned into *Sma*I site. Amp^R; Hyg^R; *Nco*I-free P*trpC-hph*	S. Foster
pSF17.1 (PN1865)	pSP72 containing 1.74-kb P*trpC-nptII*-T*trpC* PCR product (minus *Nco*I site) from pII99 cloned into *Sma*I site. Amp^R; Gen^R; *Nco*I-free P*trpC-nptII*-T*trpC*	S. Foster
pRS426 (PN4138)	Amp^R; *URA3*	Christianson *et al*., 1992
pPN114 (PN1992)	pPN94 containing 1.6-kb *Eco*RI/*Bam*HI *noxR* coding sequence	Takemoto *et al*., 2011
pYL1	pRS426 containing 5.5 kb *Eco*RI/*Xho*I insert of	This study

	5′ *pacC* region, *nptII*, and 3′ *pacC* region.	
pYL2	pSF15.15 containing 4.3 kb *Xba*I/*Pvu*II insert of native *pacC* locus	This study
pYL3	pSF15.15 containing 2.8 kb *Bam*HI/*Pst*I insert of P*tef*, *pacC*^{c}, T*trpC*	This study
pYLtopo1	pCR™-Blunt II-TOPO® containing 2.4 kb *pacC* cDNA	This study
pYLtopo2	pCR™-Blunt II-TOPO® containing 4.3 native *pacC* locus	This study
pYLtopo3	pCR™-Blunt II-TOPO® containing 1.4 kb *pacC*^{c}	This study
pYLtopo4	pCR™-Blunt II-TOPO® containing 0.8 kb P*tef*	This study
pYLtopo5	pCR™-Blunt II-TOPO® containing 0.6 kb T*trpC*	This study
pYLtopo6	pCR™-Blunt II-TOPO® containing 2.0 kb *pacC*^{c};T*trpC*	This study
pYLtopo7	pCR™-Blunt II-TOPO® containing 2.8 kb P*tef*,*pacC*^{c},T*trpC*	This study

2.2 Media and Growth Conditions

All media were prepared with Nanopure water and sterilised by autoclaving at 121°C for 20 min. Where not specified otherwise, solid media were prepared by addition of 1.5% (w/v) bacteriological agar.

2.2.1 *E. coli* growth conditions

E. coli strains were cultured overnight at 37°C on Luria-Bertani (LB) agar or in LB broth with shaking at 200 rpm. Where antibiotic selection was required, ampicillin or kanamycin was added to a concentration of 100 or 50 µg/mL, respectively. Cultures were kept at 4°C for short-term storage (<2 weeks) or in 50% (v/v) glycerol at -80°C for long-term storage.

2.2.2 *S. cerevisiae* growth conditions

S. cerevisiae strains were cultured on yeast-extract peptone dextrose (YPD) agar or synthetic defined uracil dropout (SD-Ura) agar at 30°C for 3-4 days. Cultures were kept at 4°C for short-term storage (<2 weeks) or in 20% (v/v) glycerol at -80°C for long-term storage.

2.2.3 *E. festucae* growth conditions

For regular culture of *E. festucae*, strains were grown at 22°C for 7-14 days on PD agar, or 3-5 days in PD broth with shaking at 200 rpm. Where antibiotic selection was required, hygromycin or geneticin was added to a concentration of 150 or 200 µg/mL, respectively. For temperature stress experiments, strains were cultured on PD agar at 30°C for 20 days. Cultures were kept at 4°C for short-term storage (<6 months) or in 15% (v/v) glycerol at -80°C for long-term storage. For transformation of *E. festucae*, protoplasts were regenerated in soft regeneration (RG) agar and overlaid with RG agar containing antibiotics and maintained for 2-3 weeks. Strains cultured on Blankenship media were maintained for 10-16 days.

2.2.4 *L. perenne* growth conditions

L. perenne seedlings were germinated on 3% (w/v) water agar at 22°C for 7 days in the dark, followed by another 7 days in the dark after inoculation with endophyte, and a further 7 days in the light before planting. Seedlings were then moved into root trainers containing commercial potting mix and maintained at a temperature (19°C) and light-controlled (16h/8h light/dark cycle) growth room. Plants were watered as necessary.

2.2.5 Luria-Bertani (LB) medium

LB medium (Miller, 1972) contained 1% (w/v) tryptone, 0.5% (w/v) yeast extract and 0.5% (w/v) NaCl, with pH of 7.0-7.5.

2.2.6 SOC medium

SOC medium (Dower *et al.*, 1988) contained 2% (w/v) tryptone, 0.5% (w/v) yeast extract, 20 mM glucose, 10 mM $MgSO_4.7H_2O$, 10 mM NaCl, 2.5 mM KCl and 10 mM $MgCl_2$.

2.2.7 Yeast-extract peptone dextrose (YPD) medium

YPD medium contained 2% (w/v) peptone and 0.5% (w/v) yeast extract, pH adjusted to 5.8. Glucose was added to a concentration of 2% (w/v) after autoclaving.

2.2.8 Synthetic defined uracil dropout (SD-Ura) medium

SD-Ura medium contained 1 M sorbitol, 0.67% (w/v) yeast nitrogen base without amino acids and 0.08% (w/v) uracil dropout supplement (Clontech #630416), pH adjusted to 5.8. Glucose was added to a concentration of 2% (w/v) after autoclaving.

2.2.9 Potato dextrose (PD) medium

PD medium contained 2.4% (w/v) potato dextrose. Where salts (NaCl, LiCl or KCl) were supplemented they were added to the medium and autoclaved together. Calcofluor (final concentration of 100 µg/mL), SDS (final concentration of 0.01% w/v) and H_2O_2 (final concentration of 6 mM) were made up separately in 10-100x stock solutions, filter-sterilised (0.2 µm) and added to autoclaved medium previously cooled to 50°C.

2.2.10 Regeneration (RG) medium

RG medium contained 2.4% (w/v) potato dextrose and 0.8 M sucrose, pH adjusted to 6.5. Base RG agar was made with 1.5% (w/v) bacteriological agar while soft RG agar used in overlays was made with 0.8% (w/v) bacteriological agar.

2.2.11 pH-defined Blankenship medium

Blankenship medium (Blankenship *et al*., 2001) contained 15 mM sucrose, 5 mM glutamine, 0.6 µM thiamine, 80 mM $MgSO_4$, trace elements, and buffered with 30 mM K_2HPO_4 and 30 mM KH_2PO_4. Trace elements solution was made up as a 1000x stock at the following final concentrations: 3.6 µM H_3BO_3, 1 µM $CuSO_4$, 0.7 µM KI, 0.8 µM FeNa-EDTA, 1 µM $MnSO_4$, 0.5 µM $NaMoO_4$ and $ZnSO_4$. The media was modified by adding basal salts K_2HPO_4 and KH_2PO_4 to a combined concentration of 60 mM. The amount of each proton donor and acceptor was calculated using the Henderson-Hasselbalch equation and pH was measured using the pH meter before autoclaving. Basal salts were made up as 20x stocks and autoclaved separately. $MgSO_4$ was also autoclaved separately to prevent precipitation of salt. Thiamine, glutamine and sucrose were made up as a 40x stock solutions and filter-sterilised (0.2 µm) together with the trace elements. Where solid Blankenship medium was made, the components were added separately to autoclaved agar previously cooled to 50°C.

2.2.12 pH-defined Caracuel medium

Caracuel medium (Caracuel *et al*., 2003b) contained 1% (w/v) glucose and 0.1% NH_4NO_3, buffered with 100 mM Na_2HPO_4 at pH 4; 50 mM Na_2HPO_4, 50 mM NaH_2PO_4 and 50 mM NaCl at pH 6; and 100 mM NaH_2PO_4 and 100 mM NaCl at pH 8.

2.2.13 Water agar (microscopy)

Water agar used in growing cultures for microscopy was made with a base layer (approx. 20 mL/petri dish) of 1.5% (w/v) low-melt agarose. A 1 mm-thick standard glass microscope slide was placed on the solidified agar base and overlaid with a thin layer of 1.5% (w/v) low- melt agarose (approx. 5 mL).

2.2.14 Water agar (seedling germination)

Water agar for seedling germination contained 3% (w/v) bacteriological agar.

2.3 DNA Isolation

2.3.1 Isolation of plasmid DNA from *E. coli*

A single *E. coli* colony was inoculated into 2 mL LB broth and grown overnight at 37°C with shaking at 200 rpm. Plasmid DNA was isolated using the High Pure Plasmid Isolation Kit (Roche) according to the manufacturer's instructions.

2.3.2 Isolation of DNA from *S. cerevisiae* (Yeast 'smash and grab'; Colot *et al*., 2006)

S. cerevisiae colonies were washed from plates twice with 1 mL YPD and pelleted by centrifugation at 25°C for 30 s at 6,000 rcf. The resulting supernatant was discarded and 100 µL of lysis buffer (2% (v/v) Triton X-100, 1% (w/v) SDS, 100 mM NaCl, 10 mM Tris HCl, pH 8, and 1mM EDTA, pH 8.5), 100 µL of chloroform, 100 µL of phenol and 100 µL of micro glass beads were added. The mixture was vortexed for 2 min and centrifugated at 25°C for 10 min at 16,000 rcf and 100 µL of the resulting supernatant was transferred to a fresh tube. DNA was precipitated by addition of 10 µL of 3 M NaOAc and 250 µL of 95% ethanol followed by incubation for 10 min at room temperature. The sample was centrifuged at 25°C for 5 min at 16,000 rcf and the

resulting DNA pellet was washed with 1 mL 70% ethanol and resuspended in 50 µL H_2O.

2.3.3 Isolation of DNA from *E. festucae*

The method for standard genomic DNA isolation from *E. festucae* was adapted from Byrd *et al.* (1990). Mycelia from liquid culture was filtered through nappy liners, washed with H_2O and freeze-dried. Approx. 20 mg of freeze-dried mycelia was ground to a fine powder with a mortar and pestle, in the presence of liquid nitrogen. 800 µL of extraction buffer (150 mM EDTA, 50 mM Tris-HCl and 1% (w/v) SLS, pH adjusted to 8.0) containing 2 mg/mL proteinase K was added and the mixture incubated for 30 min at 37°C, followed by centrifugation at 25°C for 10 min at 16,000 rcf. The supernatant was removed to a fresh tube and 0.5 vol of phenol and 0.5 vol of chloroform were added. The sample was then vortexed and centrifuged at 25°C for 10 min at 16,000 rcf. The phenol:chloroform extraction step was repeated two more times, followed by a final chloroform extraction. DNA was subsequently precipitated by addition of 1 vol of isopropanol and incubated at 25°C for 10 min. The DNA was pelleted by centrifugation, washed with 70% ethanol and resuspended in 100 µL H_2O. RNA was removed by addition of 1 µL of DNase-free RNase A (10 mg/mL) and incubated at 37°C for 15 min.

2.3.4 Isolation of DNA from *E. festucae* (small-scale)

The method above was modified for a rapid smaller-scale DNA extraction from *E. festucae* used in some circumstances, e.g., for obtaining DNA used in PCR screening of transformants. Mycelia were cultured in 200 µL PD broth for 3-4 days and pelleted by centrifugation at 25°C for 1 min at 6,000 rcf. The supernatant was discarded and 200 µL of extraction buffer was added. The sample was vortexed and incubated at 70°C for 30 min. The solution was neutralised with 200 µL of 5M potassium acetate and incubated on ice for 10 min. The sample was centrifugated at 4°C for 20 min at 16,000 rcf and the resulting supernatant was transferred to a new tube. DNA was precipitated with 0.7 vol of isopropanol, incubated on ice for 10 min and centrifuged at 4°C for 15 min at 16,000 rcf. The resulting DNA pellet was washed with 70% ethanol and resuspended in 20 µL H_2O.

2.4 DNA Manipulation

2.4.1 DNA quantification

DNA was quantified with the NanoPhotometer (Implen) according to the manufacturer's instructions. Estimation of genomic DNA concentration was done by visual comparison with 50-200 ng of the Lambda (λ) DNA mass standards (Fermentas).

2.4.2 Restriction endonuclease digestion

Restriction digests were performed using commercial restriction enzymes (Roche and NEB) with the appropriate buffers and incubation time and temperature. Digests for clone checking purposes were performed with 100-200 ng of DNA in a 10 µL volume with 2 units of enzyme/µg of DNA. Digests for DNA fragment preparation were performed with 0.5-1 µg of DNA in a 50 µL volume with 5 units of enzyme/µg of DNA, and digests for Southern analysis were performed with 1-3 µg of DNA in a 100 µL volume with 10 units of enzyme/µg of DNA. All digests were carried out in a water bath or thermocycler.

2.4.3 Agarose gel electrophoresis

DNA was separated on 0.7-2% agarose gels in 1x Tris/Borate/EDTA (TBE) buffer (89 mM Tris, 89 mM boric acid, 2 mM Na_2EDTA, pH adjusted to 8.2) with a voltage of 2-4 volts/cm. DNA solution was loaded onto gels diluted 1:4 with loading dye (0.2% (w/v) Bromophenol blue, 20% (w/v) sucrose, 1% (w/v) SDS and 5 mM EDTA). Gels were stained with ethidium bromide (1 µg/mL) for 10-30 min and bands were visualised with the Molecular Imager® Gel Doc™ XR+ System and the Image Lab™ Software (BioRad). 1kb Plus DNA Ladder (Invitrogen) was used as a DNA ladder.

2.4.4 Purification of DNA and PCR product

Ethidium bromide-stained DNA bands were visualised and excised on the Dark Reader™ Non-UV transilluminator DR-88M (400-500 nm). DNA was purified from agarose slices or from PCR reactions using the Wizard® SV Gel and PCR Clean-Up System (Promega).

2.4.5 Southern blotting

For Southern analysis (Southern, 1975), 2.5-5 µg genomic DNA was used in the initial restriction digest and ethanol precipitated. DNA was separated on 0.8% agarose gel at 30 V. Gels were soaked in 0.25 M HCl for 15 min (depurination step) followed by 0.5 M NaOH/0.5 M NaCl for 30 min (denaturation step), and 0.5 M Tris, pH 7.4, 2.0 M NaCl for 30 min (neutralisation step). Gels were subsequently washed in 2x saline-sodium citrate buffer (SSC; 0.3 M NaCl, 30 mM Na^+ citrate) for 2 min and placed on the blotting stand. Prewetted positively-charged nylon membrane (Roche) was placed over the gel, followed by three prewetted Whatman 3 MM filter paper. Paper towels were placed on top of the filter paper and weighted with approx. 500 g of weight on top of a flat piece of plastic plate. Gels were allowed to blot overnight and the resulting membrane washed in 2x SSC for 5 min and air-dried. DNA was crosslinked to the membrane by exposure to ultraviolet (254 nm; Cex-800 UV light cross-linker) for 2 min.

2.4.6 DIG labelling of DNA, hybridisation and visualisation

DNA probes were labelled with digoxigenin-dUTP and subsequently hybridised to the blotted membrane using the DIG High Prime kit (Roche), according to manufacturer's instructions. Hybridised probes were detected with alkaline phosphatase-conjugated anti digoxigenin Fab fragments and visualised with Nitro blue tetrazolium chloride.

2.4.7 TOPO cloning

Blunt-end PCR products (amplified by Phusion® DNA polymerase) were cloned with the Zero Blunt® TOPO® PCR Cloning Kit as per manufacturer's instructions. Reaction volumes of 3 µL were used containing 0.5 µL PCR product, 1 µL pCR®-Blunt II-TOPO®, 1 µL of salt solution and 0.5 µL H_2O. The reaction was incubated at 22°C for 30 min and transformed into competent *E. coli*. Transformants were selected using kanamycin.

2.4.8 Ligation

Standard ligation of DNA was performed with T4 DNA ligase (Promega) according to manufacturer's instructions. A 1:3 or 3:1 molar ratio of vector:insert DNA was used when vector and insert are of different sizes or when cloning into a plasmid vector. A

1:1 molar ratio of vector:insert was used when ligating DNA fragments of similar sizes. 100-500 µg vector DNA was used in a 10 µL reaction with 0.1-1 U of T4 DNA ligase. The reaction mixture was incubated for 16 h at 22°C.

2.4.9 DNA sequencing

DNA for sequencing was sent to the Massey Genome Service. The BigDye™ Terminator (version 3.1) Ready Reaction Cycle Sequencing Kit (Applied Biosystems) w was used. For sequencing of plasmids from Zero Blunt® TOPO® reactions, the manufacturer-supplied M13F/M13R primers were used. Samples were sent in a 20 µL total volume containing 4 pmol primers and 100-200 ng plasmid DNA, or 5-100 ng DNA from PCR reactions.

2.5 RNA isolation and manipulation

2.5.1 Isolation of RNA from fungal mycelia

RNA was isolated from mycelia with TRIzol® (Invitrogen) according to the manufacturer's instructions. Mycelia from liquid culture were filtered with nappy liners and washed three times with H_2O, then flash-frozen with liquid nitrogen and ground into a fine powder with mortar and pestle, pre-cooled with liquid nitrogen. 1.2 mL of TRIzol® reagent was added and mixed well. 1 mL of the resulting mixture was used for RNA extraction according to the manufacturer's protocol, with inclusion of the high-salt precipitation step for precipitation of RNA from high-polysaccharide-containing samples. The resulting RNA was resuspended in 1x RNAsecure™ solution (Ambion) and incubated at 60°C for 10 min to inactivate RNases.

2.5.2 Isolation of RNA from plant samples

Tillers of endophyte-infected ryegrass were cut close to the base and the outermost sheath layer was gently peeled and discarded. 1 cm sections of the pseudostem regions were cut and flash-frozen in liquid nitrogen. Samples were ground into a fine powder with a mortar and pestle pre-cooled with liquid nitrogen and RNA was isolated with TRIzol® (Invitrogen) according to the manufacturer's instructions. The high-salt precipitation step was included and RNA was resuspended in 1x RNAsecure™ solution (Ambion) and incubated at 60°C for 10 min to inactivate RNases.

2.5.3 DNase I treatment

RNA used for RT-PCR (section 2.6.3) using the SuperScript™ II Reverse Transcriptase kit (Invitrogen) was first treated with RNase-free DNase I (NEB). 5 µg RNA was treated with 1 U of DNase I in a 50 µL reaction volume with 1x DNase I Reaction Buffer and incubated at 37°C for 10 min. DNase I was subsequently inactivated by addition of 5 mM EDTA and incubated at 75°C for 10 min. RNA concentration was re-determined following the DNase I treatment.

2.6 Polymerase chain reaction (PCR)

PCR was performed using the Eppendorf Mastercycler® thermocycler. The primers used in standard PCR in this study are listed in Table 2.2.

Table 2.2. PCR primers used in this study.

Name	Sequence (5′-3′)	Purpose
TC161	GTAACGCCAGGGTTTTCCCAGTCACGACGGATCCAC CGTACAAGTGGGCAGTCT	Δ*pacC* 5' Fwd
TC162	AAGCCCAAAAAGTGCTCCTTCAATATCCCTGGAAGG AGAAGGGATTG	Δ*pacC* 5' Rev
TC163	TCGAAAATCATTCCTACTAAGATGGGTAGCAGATGG CTCAAAGCACAAA	Δ*pacC* 3' Fwd
TC164	GCGGATAACAATTTCACACAGGAAACAGCGAATTCA TCGACCTCGTGCAGCTAAT	Δ*pacC* 3' Rev
nptIIF	GATATTGAAGGAGCACTTTTTG	*nptII* Fwd
nptIIR	CTACCCATCTTAGTAGGAATG	*nptII* Rev
M13F	GTAAAACGACGGCCAG	Seq of TOPO inserts
M13R	CAGGAAACAGCTATGAC	Seq of TOPO inserts
YL1	CCATCTAGAGAACATCTGCCCAAGCTTTC	Δ*pacC/pacC* Fwd +*Xba*I
YL2	ACTCAGCTGCGTGTCTGAAATCCGTCGTA	Δ*pacC/pacC* Rev +*Pvu*II
YL3	CCTCCTCAGACTATTGTTCCTATAT	*pacC* mRNA Fwd (WT)
YL4	TCAACTGAGCATGCATTCATCCGTC	*pacC* mRNA Rev (WT)
YL9	GGACATATGGTGTCGTCTCACGTTCTGG	$pacC^{CA}$ Fwd
YL10	TATATCGATTCAGCGACGCTCGCTGCTGTC	$pacC^{CA}$ Rev (w/stop codon)
YL11	CAGCCGGTGGTTATGACCGTAAGCG	$pacC^{CA}$ seq1 Fwd
YL12	CAGTGAGCCGTGAAGGGGCAGCAGAG	$pacC^{CA}$ seq1 Rev
YL13	GCAATCGATGATCCACTTAACGTTACTG	$pacC^{CA}$ Fwd
YL14	CTTCTGCAGTACCCATCTTAGTAGGAATG	T*trpC* Rev
YL15	TTCCTGAAAGACGCAACACTTATCC	Δ*pacC* screen1 Fwd
YL16	ATGCATATCTCACACTAGTTTCCTG	Δ*pacC* screen1 Rev
YL17F	GTCCTGCGCGGGGAACCACAAGTGC	Δ*pacC/pacC* seq1 Fwd
YL17R	GTACTCACGCAGGGTCTCAATGACGC	Δ*pacC/pacC* seq1 Rev
YL18F	CTGCCGCTGGAACCATTGCCTCCAG	Δ*pacC/pacC* seq2 Fwd
YL18R	CCGTGGCAGCCATGGGACCGTTGGG	Δ*pacC/pacC* seq2 Rev
YL20F	GTATTTCTGGACCGACCATGCCTTGC	Δ*pacC* screen2 5' Fwd

YL20R	CGAAGTCGAGCTCGAGGGAGCAGGC	Δ*pacC* screen2 5' Rev
YL21F	GATGTGGATATGAAGAGCCCACCTCG	Δ*pacC* screen2 3' Fwd
YL21R	CATCAACAGTGCGAGTAGGCTTCCC	Δ*pacC* screen2 3' Rev
YL22F	CTGTTTCTTCCTTGAACTCTCAAGCC	Δ*pacC* screen2 *nptII* Fwd
YL22R	CCTGGACGACTAAACCAAAATAGGC	Δ*pacC screen2 nptII* Rev
YL23F	CCTCAACTATAGGACCCAAAGCTCC	Δ*pacC/pacC* seq3 Fwd
YL23R	AAACTAGGGCCAAGAGTTGCTGTGG	Δ*pacC/pacC* seq3 Rev
YL24F	GCTGGATCCGGTAGCAAACGGTGGTCAAAGGATGG	P*tef* Fwd
YL24R	ATTCATATGGTTTGACGGTGATGTATGGAAGATTGAG	P*tef* Rev
YL25F	CGCTCCCGATTCCGGAAGTGCTTG	*pacC*^{CA} screen1 5' Fwd
YL25R	CCGATGAGACCTGCGCAGCGTCCAG	*pacC*^{CA} screen1 5' Rev
YL26F	CCCTAGTTTTGACAGCAGCGAGCGTC	*pacC*^{CA} screen1 3' Fwd
YL26R	GGTCTGACAGTTACCAATGCTTAATC	*pacC*^{CA} screen1 3' Rev

2.6.1 Standard PCR

Standard PCR was performed with Taq DNA polymerase (Roche) in 20 or 50 µL reaction volumes containing 1x PCR reaction buffer, 200 µM of each dNTP, 0.2 µM of each primer, Taq DNA polymerase (0.2 U/20 µL reaction or 0.5 U/50 µL reaction) and template DNA (1 ng plasmid DNA or 50-200 ng genomic DNA per 50 µL reaction volume). The reaction conditions were: one cycle at 94°C for 2 min; 35-45 cycles at 94°C for 15-30 s, 50-65°C for 30-60 s, 72°C for 1 min/1 kb; one cycle at 72°C for 10 min.

2.6.2 High-fidelity PCR

Where proofreading DNA polymerase activity was required PCR was performed with Phusion® High-Fidelity DNA Polymerase (Thermo Scientific). PCR was performed in 20 or 50 µL reaction volumes containing 1x Phusion HF buffer, 200 µM of each dNTP, 0.5 µM of each primer, Phusion DNA polymerase (0.4 U/20 µL reaction or 1 U/50 µL reaction) and template DNA (1 ng plasmid DNA or 50-200 ng genomic DNA per 50 µL reaction volume). Two-step reaction conditions were: one cycle at 98°C for 30 s; 35 cycles at 98°C for 10 s and 72°C for 30 s/1 kb; one cycle at 72°C for 10 min. Three-step reaction conditions were: one cycle at 98°C for 30 s; 35 cycles at 98°C for 10 s, 50-68°C for 10-30 s, 72°C for 30 s/1 kb; one cycle at 72°C for 10 min.

2.6.3 Reverse-transcription PCR (RT-PCR)

Standard RT-PCR was performed using SuperScript™ II Reverse Transcriptase (Invitrogen) according to manufacturer's instructions. 1 µg of RNA (DNase I-treated) was used in a 20 µL reaction volume with Oligo(dT) primers.

For quantitative reverse transcription PCR (qRT-PCR) purposes, RT-PCR was performed with the QuantiTect Reverse Transcription Kit (Qiagen), according to the manufacturer's instructions. 1 µg of RNA was used in a 20 µL reaction volume. cDNA synthesised from RNA obtained from axenic culture was diluted 2-fold with autoclaved Nanopure H_2O prior to use in qRT-PCR reactions, and cDNA synthesised from RNA obtained from plant sample was diluted 5-fold with autoclaved Nanopure H_2O prior to use in qRT-PCR reactions.

2.7 Quantitative reverse transcription PCR (qRT-PCR)

qRT-PCR was performed in 384-well plates with the LightCycler® 480 Instrument II (Roche) and with two technical replicates in all experiments. The primers used in qRT-PCR in this study and the corresponding *E. festucae* Fl1 or E2368 models numbers of the target genes are listed in Table 2.3.

Table 2.3. qRT-PCR primers used in this study and model numbers of the target genes.

Name	Sequence (5'-3')	Purpose	Gene Model
YL28F	AGCGCATCACGTAATTGCTG	*pacC* Fwd	EfM2.068150
YL28R	ACGCAAAGGATTCGGGAATG	*pacC* Rev	
YL32F	GCCCTAGTTTTGACAGCAGC	$pacC^{CA}$ Fwd	N.A.
YL32R	CTGACATCGACACCAACGAT	$pacC^{CA}$ Rev	
YL41F	CAGCTGGTCTGCAGAAAGAGA	*cnaA* Fwd	EfM2.051620
YL41R	AACGTCATATTTTTCCATCACAGA	*cnaA* Rev	
YL43F	CGAGGAAGAGGAAGCACAAG	*CNH1* Fwd	EfM2.014050
YL43R	CGTTTGTGATTGTCGATTGG	*CNH1* Rev	
YL45F	CCGATCCTTGGTGAAAGATT	*ena2* Fwd	EfM2.113810
YL45R	CGCCCAGAAAAATCAAAAGA	*ena2* Rev	
YL46F	TTGATCCAATGCAATCCAAA	Cyt P450 Fwd	EfM2.084750
YL46R	CTGCGATGAATTTCGCTTC	Cyt P450 Rev	
YL52F	TCGTCCCAACACTAGCTGAA	alkaline phos Fwd	EfM2.057140
YL52R	CGCTAGGGTTACCACCTCTG	alkaline phos Rev	
YL53F	ATCCTGAATCAGCGCACTCT	acid phos Fwd	EfM2.003400
YL53R	GCCTTCCTGGATCTTGATGA	acid phos Rev	
TC119	AGTGAGCATGTACCGCAAAA	*ltmE* Fwd	Unannotated
TC120	AATGAACCGGCTCAATTCTG	*ltmE* Rev	
TC123	TTGCAGCGCTGTCGTATAAT	*ltmP* Fwd	EfM2.109790

TC124	CACAACTTTCGCTTGTGGAA	*ltmP* Rev	
TC137	TCTCTTCCCGTAGCAAGGAA	*ltmM* Fwd	Unannotated
TC138	GAGTTCTGCCTGCCTTCATC	*ltmM* Rev	
TC261	TGCATTCTTTTGGATTAGCC	*easA* Fwd	EfM3.049660
TC262	AACGAAATACAAAAGCCATACCA	*easA* Rev	
TC319	ATGCCGGCGAGATTTAACTT	*dmaW* Fwd	EfM3.065770
TC320	TCTCTTCATAATCTGCCTTACACG	*dmaW* Rev	
TC305	CAGCTCCCTTACGGTATTGAA	*lpsA* Fwd	EfM3.063200
TC306	GGACCATATCCCGGAACAG	*lpsA* Rev	
TC399	AAAAAGCAACCGAATGCAAG	*EF*-2 Fwd	EfM3.021210
TC400	CGAGACGACATAACTACATGTATCAAA	*EF*-2 Rev	
TC407	TAGCTGGCGTTATGGAAAGG	*RPS22* Fwd	EfM3.016650
TC408	CGATTGTGCGACTACTACCTCA	*RPS22* Rev	
TC259	GAGTGCGAAGCGTAGAGTCC	*perA* Fwd	EfM2.086340
TC260	GGGTCTTCTCCAGACCACTG	*perA* Rev	

2.7.1 Cycling conditions

qRT-PCR was performed using the SsoFast™ EvaGreen® Supermix (Bio-Rad). A reaction volume of 10 µL was used containing 1 µL cDNA template, 1x SsoFast™ EvaGreen® Supermix and 0.5 µM of each forward and reverse primer. Initial denaturation step was performed at 95°C for 30 s, followed by 40 cycles of denaturation at 95°C for 5 s and annealing/extension at 60°C for 10 s. A melt curve was performed at 65-95°C with a ramp of 0.4°C/s. Signal was acquired at the end of each extension step and during the melt curve.

2.7.2 Generation of standard curve

For absolute quantification, cDNA standards (80-120 bp) were prepared by PCR amplification with Phusion® High-Fidelity DNA Polymerase (Thermo Scientific), separated on 2% (w/v) agarose gel, excised and purified. For calculations in making the standard a molecular weight of 660 g/mol for a nucleotide pair was used. Serial dilutions were prepared and concentrations of 10 aM to 10 pM were used in generating the standard curve.

2.7.3 Data analysis

Relative cDNA amounts between target and reference genes were calculated by comparison of the two concentration values interpolated from the standard curves or by the $2^{(\Delta Cp)}$ method.

2.8 Preparation of constructs

The Phusion® High-Fidelity DNA Polymerase was used in all PCR amplification of fragments used in making of gene constructs.

2.8.1 *pacC* replacement construct (pYL1)

The *pacC* replacement construct, plasmid pYL1, was prepared by initial PCR amplifications of a 2.0 kb fragment 5′ of *pacC* using the primer pair TC161/TC162 and a 1.9 kb fragment 3′ of *pacC* using the primer pair TC163/TC164, from wild-type *E. festucae* genomic DNA; and a 1.7 kb *nptII* fragment using the primer pair *nptII*F/*nptII*R from plasmid pSF17.1. The three fragments were cloned into *Eco*RI/*Xho*I-linearised pRS426 vector by yeast recombinational cloning (Section 2.10.2). Crude DNA isolated from recombinant yeast colonies (ura-prototroph) was used to transform *E. coli* and subsequent plasmid DNA isolated from ampicillin-resistant (Amp^R) *E. coli* colonies was checked by *Xho*I, and *Nco*I/*Cla*I restriction endonuclease digestions. One of these plasmids showing the correct restriction patterns was designated as pYL1.

2.8.2 *pacC* complementation construct (pYL2)

The *pacC* complementation construct, pYL2, was prepared by initial PCR amplification of a 4.3 kb fragment of the *pacC* locus using the primer pair YL1/YL2. The fragment was cloned into PCR-Blunt II-TOPO® vector and transformed into *E. coli*. Plasmid DNA was isolated from 8 Amp^R transformants and checked with *Bam*HI/*Eco*RV double digestion. One of these was selected for sequencing with primer pairs M13For/M13Rev, YL17F/YL17R, YL18F/YL18R and YL23F/YL23R and the sequence checked against the database at the *E. festucae* Genome Project (http://www.endophyte.uky.edu/). The resulting plasmid was designated pYLtopo2. The 4.3 kb fragment was excised from pYLtopo2 by digestion with *Pvu*II/*Xba*I and ligated into an *PvuII/XbaI*-linearised pSF15.15, and cloned into *E. coli*. The resulting

plasmid showing the correct restriction patterns with *Hin*dIII and *Sph*I was designated pYL2.

2.8.3 *pacC* constitutive active (*pacC*^{CA}) construct (pYL3)

The *pacC*^{CA} constitutive active construct, pYL3, was prepared by initial PCR amplification of a 2.4 kb fragment of *pacC* using the primer pair YL3/YL4 and cDNA synthesised from total RNA from wild-type *E. festucae* as template. The fragment was gel excised, purified, cloned into PCR-Blunt II-TOPO® vector (pYLtopo1) and used as template for site-directed PCR mutagenesis with primer pair YL9/YL10. The fragment was gel excised and purified, cloned into PCR-Blunt II-TOPO® vector and sequenced with the primer pair M13For/M13Rev. One of these plasmids was designated pYLtopo3. A 0.8 kb P*tef* fragment was also amplified from plasmid pPN94 using the primer pair YL24F/YL24R and similarly cloned into PCR-Blunt II-TOPO® vector; the resulting plasmid was designated pYLtopo4 after sequence check. A 0.6 kb T*trpC* fragment was amplified from plasmid pSF17.1 using the primer pair YL11/YL12 and similarly cloned into PCR-Blunt II-TOPO® vector; the resulting plasmid was designated pYLtopo5 after sequence check. Finally, the T*trpC* fragment was excised from pYLtopo5 by digestion with *Cla*I/*Pst*I and ligated into *Cla*I/*Pst*I-linearised pYLtopo4 and cloned into *E. coli*. One of the plasmids was designated pYLtopo6. The P*tef* fragment was excised from pYLtopo3 by digestion with *Bam*HI/*Nde*I and ligated into *Bam*HI/*Nde*I-linearised pYLtopo6 in a similar way to make pYLtopo7, and the 2.8 kb P*tef*:*pacC*^{CA}:T*trpC* fragment was excised from pYLtopo7 by *Bam*HI/*Pst*I digestion and ligated into *Bam*HI/*Pst*I-linearised pSF15.15 to make the *pacC* constitutive active construct pYL3.

2.9 Preparation of protoplasts and competent cells

2.9.1 Chemically competent *E. coli*

50 mL of super optimal broth (SOB; 2% (w/v) tryptone, 0.5% (w/v) yeast extract, 0.05 % (w/v) NaCl, 2.5 mM KCl, 2 mM $MgCl_2$, pH adjusted to 7) was inoculated with a fresh overnight culture of *E. coli* and incubated at 18°C for 20-50 hours with shaking at 200 rpm until mid-log phase was reached (A_{600} = 0.4-0.8). The cells were chilled on ice for 10 min and centrifuged at 4°C for 10 min at 6,000 rcf then resuspended in 17 mL ice-

chilled transformation buffer (TB; 10 mM PIPES, 15 mM $CaCl_2$, 0.25 M KCl, pH adjusted to 6.7, and 0.18 M $MnCl_2$, 0.45 µm filter-sterilised) and incubated on ice for 10 min. The cells were again centrifuged at 4°C for 10 min at 6,000 rcf then resuspended in 4 mL ice-chilled TB. 300 mL of DMSO was added, mixed well, and 100 µL aliquots of cell suspension were flash-frozen in liquid nitrogen and stored at -80°C.

2.9.2 Electrocompetent *E. coli*

600 mL of LB broth was inoculated with 6 mL of fresh overnight culture of *E. coli* and incubated at 37°C for 5 h at 250 rpm until a mid-log phase was reached (A_{600} = 0.4-0.8). The culture was chilled on ice for 10 min and centrifuged at 4°C for 15 min at 6,000 rcf then resuspended in 600 mL ice-chilled sterile 10% (v/v) glycerol. The cells were pelleted by centrifugation at 4°C for 15 min at 6,000 rcf and resuspended in 300 mL, then 12 mL, and finally 1.2 mL of 10% (v/v) glycerol. 50 µL aliquots of cell suspension were aliquoted and flash-frozen in liquid nitrogen and stored at -80°C.

2.9.3 Protoplasts of *E. festucae*

150 ml of PD broth was inoculated with a fresh culture of *E. festucae* and incubated at 22°C for 4 days with shaking at 150 rpm. Mycelia were filtered with a sterilised nappy liner and washed with sterile H_2O, followed by OM buffer (100 mM Na_2HPO_4, 100 mM NaH_2PO_4, 1.2 M $MgSO_4$, 100 mM Na_2HPO_4). 40 mL of 0.2 µm filter-sterilised lysing enzymes (Sigma L1412) was added and incubated overnight at 22°C with shaking at 80 rpm. Protoplasts were filtered with a sterilised nappy liner and 5 mL aliquots of protoplasts were overlaid with 2 mL of ST buffer (0.6 M sorbitol, 1 M Tris-HCl, pH 8) in a Corex tube. The cell suspension was centrifuged at 4°C for 5 min at 5,000 rcf then the resulting middle layer of protoplasts was removed to a fresh tube. The protoplasts were resuspended in 5 mL of STC buffer (1 M sorbitol, 50 mM $CaCl_2$, 1 M Tris-HCl, pH 8) centrifuged at 4°C for 5 min at 5,000 rcf. This step was repeated 2 more times and the protoplasts resuspended in 500 µL of STC buffer. A cell count was performed using the haemocytometer and a concentration of 1.25 x 10^8 protoplasts/mL was made in STC buffer. 20 µL of 40% (w/v) PEG was added to 80 µL protoplast, flash-frozen and stored at -80°C.

2.10 Bacterial and fungal transformation

2.10.1 *E. coli* transformation

Chemically-competent *E. coli* was transformed by heat-shock. 5-10 µL of DNA was added to 100 µL of prepared cell suspension (Section 2.9.1) and incubated on ice for 20 min. The cells were heat-shocked by incubation in 42°C water bath for 30 s and immediately placed on ice for 2 min. 400 µL of SOC medium pre-warmed to 37°C was added and the sample incubated at 37°C for 1 h with shaking at 200 rpm. 50, 100 and 200 µL of the sample was spread on LB agar with or without antibiotic selection and incubated overnight at 37°C.

Electro-competent *E. coli* was transformed by electroporation. 1-5 µL of DNA was added to 100 µL of prepared cell suspension (Section 2.9.2), gently mixed and immediately pulsed at 2.0 kV, 200 Ω and 2.5 µF. 400 µL SOC medium pre-warmed to 37°C was added and the sample incubated at 37°C for 1 h with shaking at 200 rpm. 50, 100 and 200 µL of the sample was spread on LB agar with/without antibiotic selection and incubated overnight at 37°C.

2.10.2 *S. cerevisiae* transformation (yeast recombinational cloning)

A single yeast colony (*S. cerevisiae* strain FY834) was obtained from fresh culture on YPD plate for 2-3 days and inoculated into 5 mL YPD broth. The cells were cultured at 30°C with shaking at 200 rpm overnight. 1 mL of the culture was re-inoculated into 50 mL YPD broth, incubated at 30°C with shaking at 200 rpm for 5 h. Cells were pelleted by centrifugation at 25°C for 5 min at 1,000 rcf and washed with 25 mL sterile H_2O, followed by further washing and equilibration in 1 mL then 400 µL of 100 mM lithium acetate (LiAc). 50 µL aliquots of the cell suspension were pelleted by centrifugation at 4°C for 15 s at 6,000 rcf and 240 µL of 50% (w/v) PEG, 36 µL of 1M LiAc, 10 µL of 2 mg/mL of heat-denatured salmon sperm DNA were added. The mixture was mixed well and maintained on ice and 300 ng of each DNA fragments to be recombined was added. The mixture was incubated at 30°C for 30 min and heat-shocked at 42°C for 30 min. Cells were pelleted by centrifugation at 4°C for 15 s at 6,000 rcf and washed three times with sterile H_2O. The cell pellet was resuspended in 50 µL sterile H_2O and 30 µL aliquots were spread on SD-ura plates and incubated at 30°C for 3-4 days.

2.10.3 *E. festucae* transformation

E. festucae protoplasts were transformed using the method adapted from Itoh *et al.* (1994). 1-5 µg of DNA 2 µL of spermidine (50 mM) and 50 µL of heparin (5 mg/mL) were added to 100 µL prepared protoplast suspension (Section 2.9.3). The sample was incubated on ice for 30 min and 900 µL of 40% (w/v) PEG solution was added. The sample was mixed well gently and returned to ice for another 20 min. 50 µL of the cell suspension was added to 3.5 mL of soft RG agar pre-warmed to 50°C and poured onto pre-solidified RG agar (5 mL). The plates were incubated for 24 h at 22°C and overlaid with 15 mL of soft RG agar with antibiotic selection. The plates were incubated at 22°C for 2-3 weeks until resistant transformants grew through the overlay. These were nuclear-purified by subculturing mycelia from the colony edge onto PD media with the respective antibiotic selection, for three rounds.

2.11 Plant manipulation

2.11.1 Seed sterilisation

L. perenne seeds were surface sterilised by the method adapted from Latch and Christensen (1985). Seeds were soaked in 50% (v/v) H_2SO_4 for 30 min, rinsed in sterile H_2O and soaked in 50% (v/v) commercial bleach, rinsed well with sterile H_2O and air-dried in the laminar flow cabinet.

2.11.2 Seedling inoculation

L. perenne seedlings (7 d old germinated on water agar) were inoculated by the method adapted from Latch and Christensen (1985). *E. festucae* mycelia for inoculation experiments were grown on PD agar. A 2-3 mm longitudinal slit was made between the mesocotyl and coleoptile regions of the seedling and a small piece of cut mycelia was placed into the slit.

2.11.3 Immunoblot detection of endophyte

To screen for endophyte-infection, *L. perenne* tillers (8-9 weeks old post-inoculation) were cut close to the base of the pseudostem and printed on a nitrocellulose membrane (BDH). The membrane was incubated in blocking solution (20 mM Tris, 10 mM HCl, 50

mM NaCl, 0.5 % non-fat milk powder, pH adjusted to 7.5) for 2 h at 25°C with gentle shaking. The membrane was then incubated in blocking buffer containing 1:1000 dilution of rabbit polyclonal antibody raised to *N. lolii* Lp5 mycelium (Gwinn *et al.*, 1991) overnight at 4°C with gentle shaking. The membrane was then washed three times with fresh blocking buffer and incubated with blocking buffer containing 1:2000 dilution of anti-rabbit alkaline phosphatase-conjugated secondary antibody (Sigma) for 2 h at 25°C with gentle shaking. The membrane was developed with the Fast Red chromogen (Sigma) for 10-20 min.

2.11.4 Apoplast pH measurement

Apoplast fluid was extracted by the method adapted from van Hove *et al.* (2002). Approximately 5 g of plant pseudostem regions were placed in a 50 mL syringe barrel with distilled H_2O added up to 40 mL. The syringe tip was blocked with a stopper and pressure was applied manually for 30 seconds to cause the infiltration of water into the samples. The samples were subsequently blotted dry and placed in 5 mL pipette tips in a 50 mL falcon tube and centrifuged for 5 min at 2,000 rcf. pH of the apoplast fluid collected at the bottom of the tube was measured by the pH meter.

2.12 Microscopy

2.12.1 Light microscopy

For light microscopy of fungal hyphae, *E. festucae* cultures were grown on 1.5% (w/v) water agar (Section 2.2.12). The agar slice was excised and placed on a microscope, overlaid with 65% (w/v) glycerol and coverslip and examined under the Axiophot Compound Light Microscope (Zeiss).

2.12.2 Fluorescence microscopy

For fluorescence microscopy of fungal hyphae, *E. festucae* cultures were grown on 1.5% (w/v) water agar (Section 2.2.12). The agar slice was excised and placed on a microscope and a drop of 0.01% (w/v) calcofluor white, incubated for 5 min at 25°C and observed under the Stereomicroscope BX51 (Olympus) using with the U-MWU2 Ultraviolet excitation cube (wideband).

2.12.3 Confocal microscopy

For confocal microscopy of fungal hyphae *in planta*, approx. 0.5 x 1 cm sections were obtained from the pseudostem region of endophyte-infected *L. perenne* plants and soaked in ethanol for at least 24 h. The sample was then incubated in 10% (w/v) KOH for 16 h and in 500 µL staining solution (0.008% aniline blue (Sigma), 0.001% WGA-AlexaFluor488 (Molecular Probes) 0.02% (v/v) Tween®-20 (Invitrogen), 0.15 M NaCl, 2 mM KCl, 10 mM Na_2HPO_4, 2 mM KH_2PO_4, pH adjusted to 7.4). The samples were analysed under the Leica SP5 DM6000B confocal microscope (Leica Microsystems). An excitation wavelength of 405 nm and acquisition window of 449 nm to 555 nm was set for aniline blue and an excitation wavelength of 488 nm and acquisition window of 498 nm to 558 nm was set for WGA-AlexaFluor488. Images were obtained of 5-10 µm-thick z-distances with a step size of approx. half of each image thickness. Images were processed with ImageJ as a maximum projection (z-stack).

2.13 Bioinformatics

E. festucae genomic sequences were accessed from the *E. festucae* Genome Projects at the University of Kentucky (http://www.endophyte.uky.edu/; Schardl *et al*., 2013). Other fungal gene and protein sequences were retrieved from the NCBI databases (http://www.ncbi.nlm.nih.gov/). Multiple amino acid sequence alignments, were generated by ClustalW using the Gonnet matrix with an open gap penalty of 10.0, an extend gap penalty of 0.05 and a 40% delay divergent. Pairwise alignment identity and similarity scores were generated using the Gonnet matrix with an open gap penalty of 10.0 and an extend gap penalty of 0.1.

3. Results

3. Results

3.1 Identification and characterisation of the *E. festucae pacC* gene

The predicted homologue of *pacC* was identified in the *E. festucae* genome (http://www.endophyte.uky.edu/) by a tBLASTn search using the PacC amino acid sequence from *Fusarium graminearum* (Accession number ADO60821.1) as a query. The best hit with a score of 506 and an E-value of 0 was a putative gene on contig 117 (*E. festucae* Fl1 gene model EfM2.068150, *E. festucae* E2368 gene model EfM3.009480). Analysis of this sequence with the FGeneSH prediction model (Softberry Inc) and the MAKER annotation tool (Cantarel *et al.*, 2008) indicated that the predicted transcript contains 3 introns and codes for a 591 amino acid-containing protein, which shares 69%, 43%, and 42% amino acid sequence identity with PacC from *F. graminearum*, *Magnaporthe oryzae*, and *Neurospora crassa*, respectively (Figure 3.1). Also present are highly conserved sequences corresponding to regions A, B, and C of the PacC protein; the signalling protease box; and an N-terminal zinc-finger DNA-binding region.

To characterise the *E. festucae pacC* transcript, primers were designed to the 5' and 3' UTRs of the predicted transcript. PCR amplification with cDNA synthesised from total RNA showed the expected 2.3 kb instead of 2.7 kb band, which corresponds to a processed *pacC* transcript minus the introns (Appendix 6.1). Sequencing of this fragment confirmed the exon/intron boundaries as predicted by the FGeneSH algorithm and the positions of start and stop codons indicated that the predicted reading frame was correct.

3.2 Generation of Δ*pacC* and Δ*pacC*/ *pacC*^{CA} mutants

In order to investigate the role of PacC in the growth of *E. festucae* and symbiosis with the host grass, *pacC* deletion (Δ*pacC*) and constitutive active (Δ*pacC*/*pacC*^{CA}; henceforth called *pacC*^{CA}) mutants were generated to give acid- and alkaline-mimicking mutations, respectively.

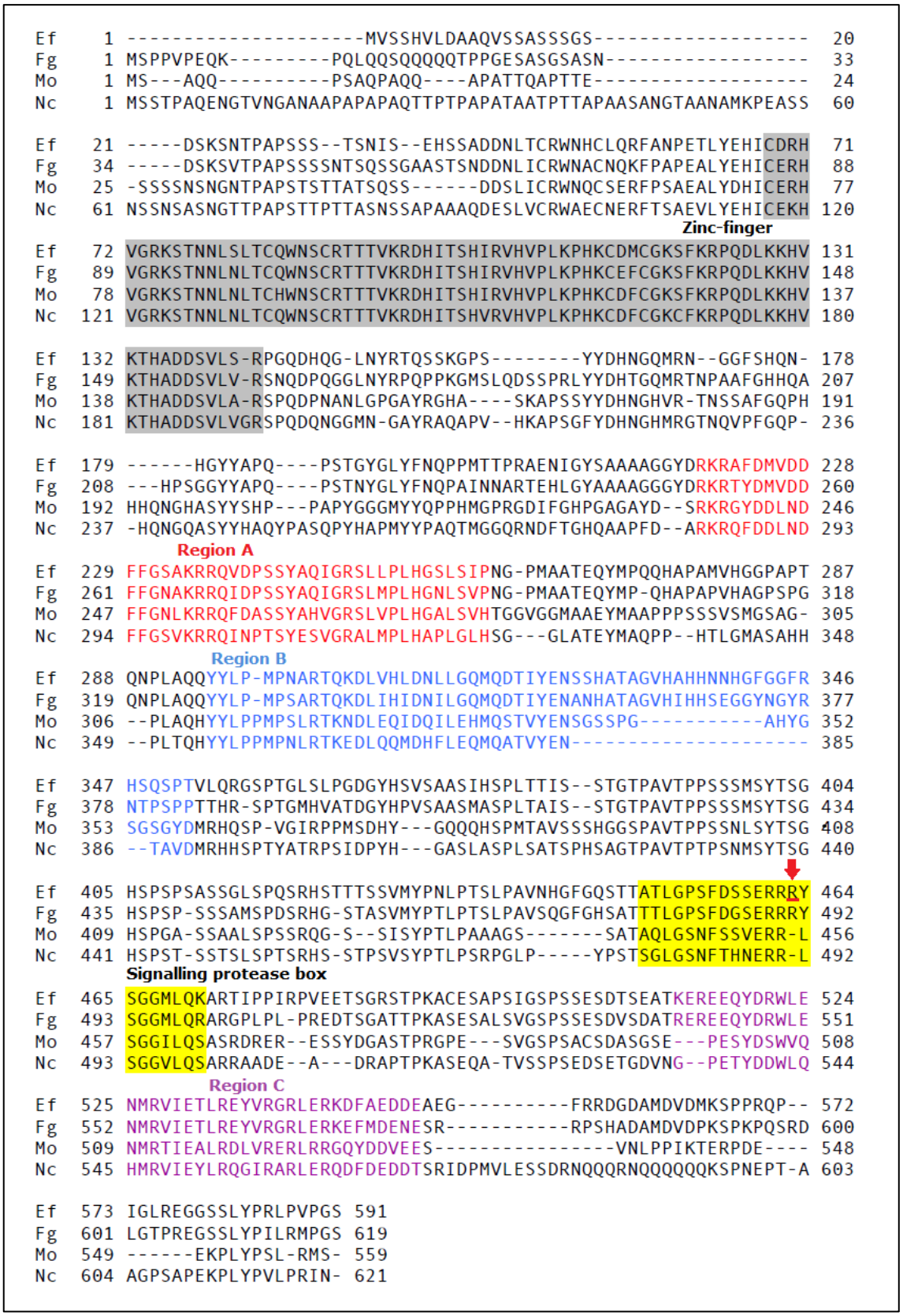

Figure 3.1. Multiple sequence alignment of *E. festucae* PacC with homologues from other fungi. Amino acid sequences from *F. graminearum* (ADO60821), *M. oryzae* (XP_003713788) and *N. crassa* (XP_957214) are shown in the alignment. The zinc finger regions are shaded in grey and the three interacting regions of the PacC protein; regions A, B and C are coloured in red,

blue and purple, respectively. The signalling protease box is highlighted in yellow, and the red arrow marks the arginine residue, the codon for which was mutated into a stop codon in the *pacC*^{CA} mutant.

The Δ*pacC* mutant was generated by transforming wild-type *E. festucae* protoplasts with a PCR-amplified fragment from the Δ*pacC* replacement construct, pYL1 (Section 2.8.1; Appendix 6.2.1). An initial PCR screen identified 12 out of 96 geneticin-resistant (Gen^{R}) transformants with patterns consistent with targeted replacement of the *pacC* locus (Figure 3.2A and B). A second PCR screen of 10 Δ*pacC* transformants further excluded transformant #29 from analysis (Figure 3.2C and D). Subsequently, Southern blot analysis was performed with *Nde*I/*Pst*I-digested genomic DNA from 5 Δ*pacC* transformants and probed with a DIG-labelled linear fragment amplified from pYL1. The results revealed that all 5 mutants had 'clean' single-copy replacement events (Figure 3.3).

The strategy employed to generate the constitutive active PacC mutant was to transform the Δ*pacC* mutant with a truncated version of the *pacC* gene (*pacC*^{CA}), lacking the 'C' interacting region of the protein (Tilburn *et al.*, 1995). The translated protein is expected to be in an 'open' state, accessible for cleavage by the processing protease and as a result activated independent of a pH-signal. To achieve this, the CGA codon coding for arginine 464 of the *E. festucae* PacC protein was altered to a stop codon (TGA) by site-directed PCR mutagenesis. To bypass the need for splicing of the transcript, the construct was also generated from the *pacC* cDNA sequence. The resulting *pacC*^{CA} sequence was placed under the control of the P*tef* promoter and inserted into a backbone vector to make the *pacC*^{CA} vector, pYL3 (Appendix 6.2.2; section 2.8.3). Transformation of Δ*pacC* mutant #8 with pYL3 resulted in 24 geneticin and hygromycin-resistant (Gen^{R}Hyg^{R}) transformants. An initial PCR screen was performed to interrogate the flanking regions of the integrated construct (Figure 3.4A to C) followed by another PCR screen to check the integrity of each element of the *pacC*^{CA} construct (Figure 3.4D to G). Results of the PCR screens revealed 8 transformants with patterns indicative of intact constructs (Figure 3.4). qRT-PCR analysis was subsequently performed using total RNA extracted from mycelia and showed that expression of the *pacC*^{CA} construct was variable among these 8 transformants, with *pacC*^{CA} #14 showing the highest expression level (Figure 3.5). Based on this result, *pacC*^{CA} #14 was selected for further experiments to test the

phenotype of the *pacC*^{CA} mutant. For other experiments, two additional *pacC*^{CA} mutants expressing high levels of the *pacC*^{CA} construct; #19 and #22 were included.

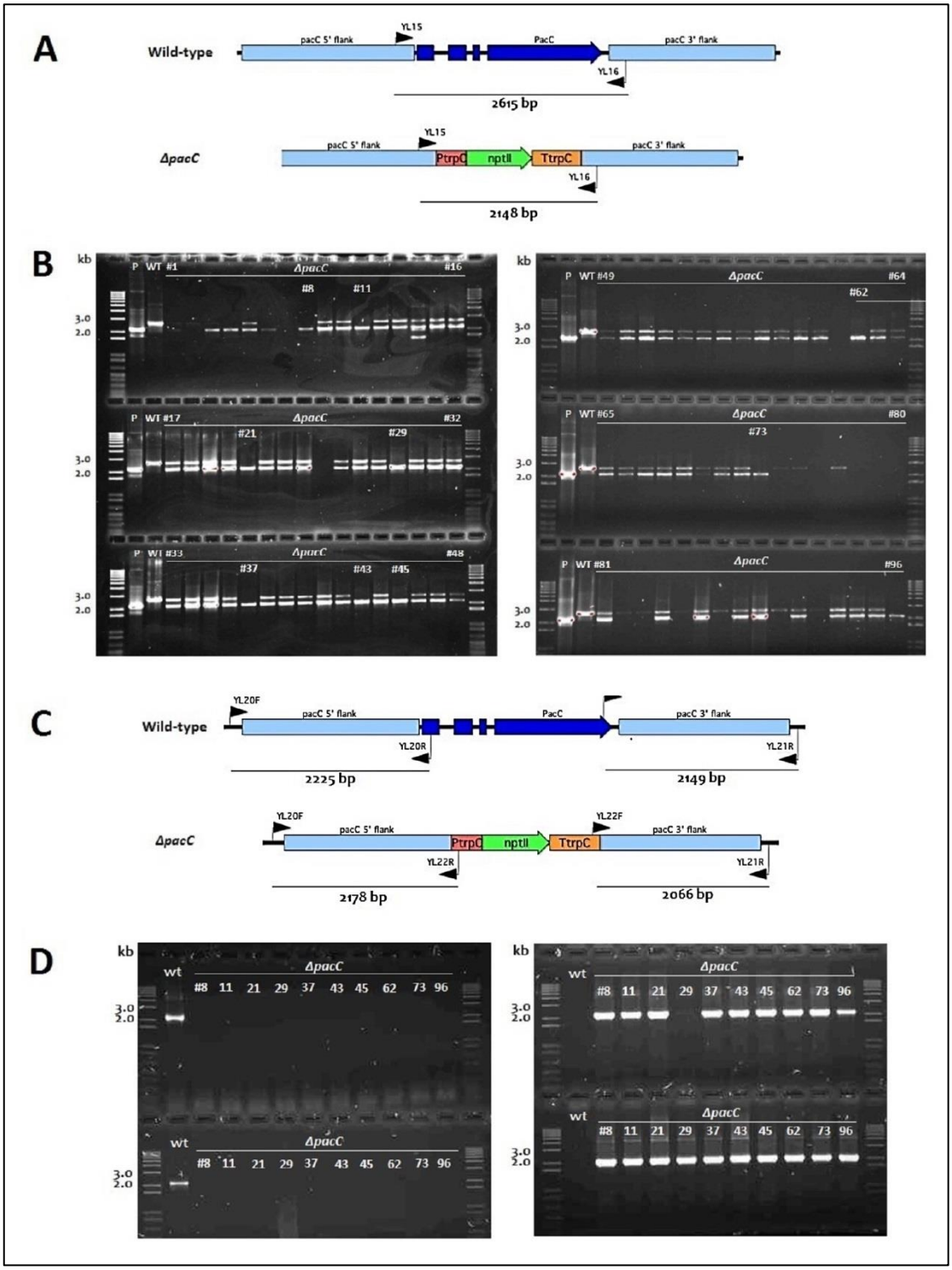

Figure 3.2. PCR screens of Δ*pacC* transformants. (A) Strategy of Δ*pacC* first PCR screen using primer pairs YL15/YL16 that generates a 2.6 kb fragment in wild-type, 2.1 kb fragment in Δ*pacC* and both fragments in ectopic mutants. (B) Gel showing bands amplified from 96 Δ*pacC* transformants using primers YL15/YL16. P: positive plasmid control pYL1. Δ*pacC* strains of interest; #8, 11, 37, 73 and 96 are indicated. (C) Strategy of Δ*pacC* second PCR screen using four

primer pairs; YL20F/YL20R and YL21F/ YL21R generate 2.2 kb and 2.1 kb fragments, respectively, in wild-type but none in Δ*pacC* transformants; YL20F/YL22R and YL22F/YL21R give 2.2 kb and 2.1 kb fragments in Δ*pacC* but none in wild-type. (D) Gel showing bands amplified from 10 Δ*pacC* transformants with primer pairs YL20F/YL20R (upper left panel), YL21F/YL21R (bottom left panel), YL20F/YL22R (upper right panel) and YL22F/YL21R (bottom right panel).

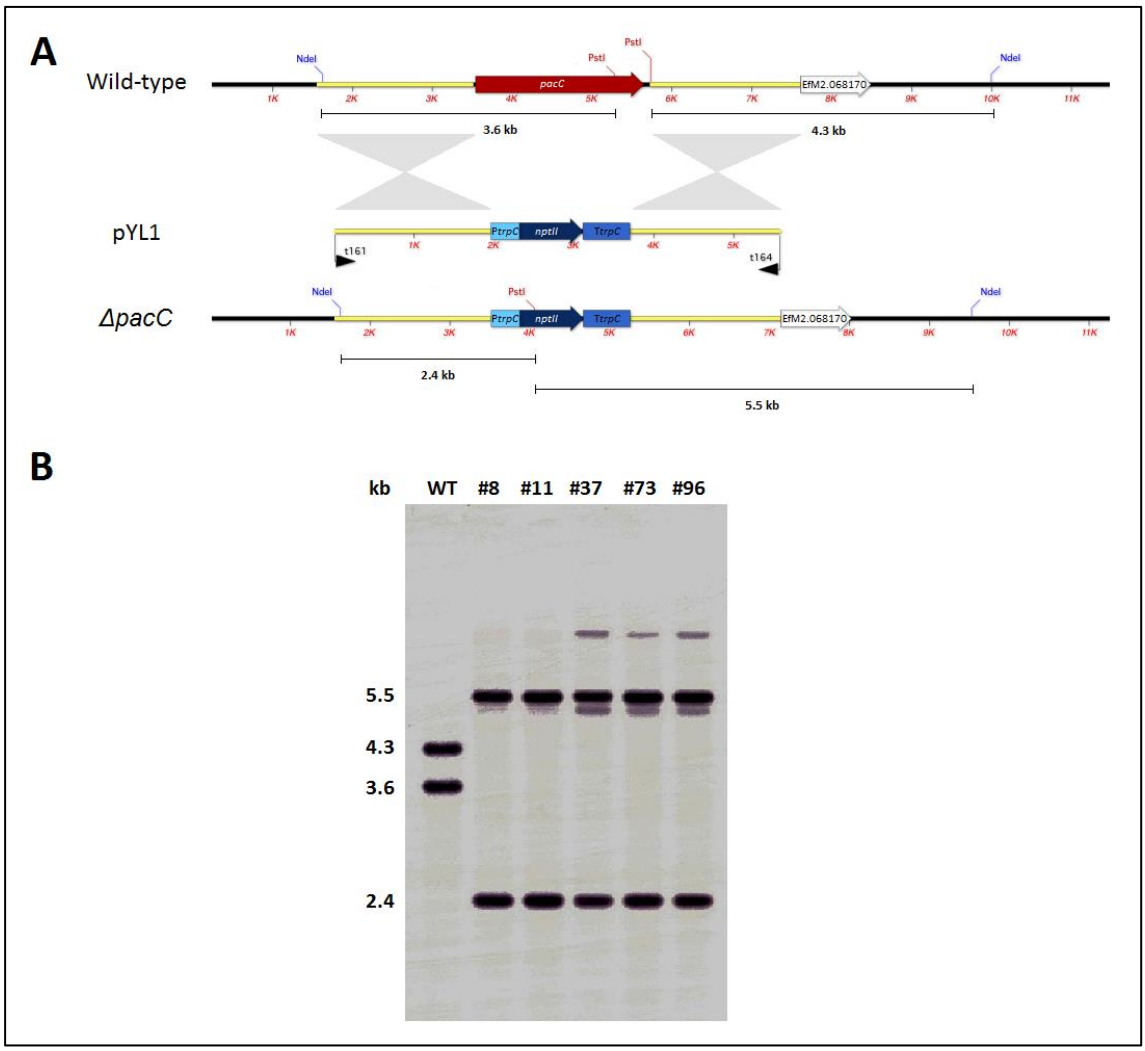

Figure 3.3. NBT/BCIP-stained Southern blot analysis of wild-type and Δ*pacC* transformants. (A) Schematics of wild-type *pacC* genomic locus; PCR-amplified linear transformation fragment from pYL1; and the *nptII*-replaced *pacC* locus in the Δ*pacC* mutant. Grey regions depict regions for double cross-over recombination events between the homologous sequences (in yellow). The cleavage sites of *Nde*I and *Pst*I restriction enzymes used in the genomic digest are indicated. A putative and uncharacterised gene downstream of *pacC*, EfM2.068170, as predicted by the MAKER gene prediction tool is indicated in the figure. (B) Southern blot of *Nde*I/*Pst*I digested genomic DNA from wild-type and Δ*pacC* transformants, probed with DIG-dUTP-labelled linear fragment from pYL1 and visualised with NBT/BCIP.

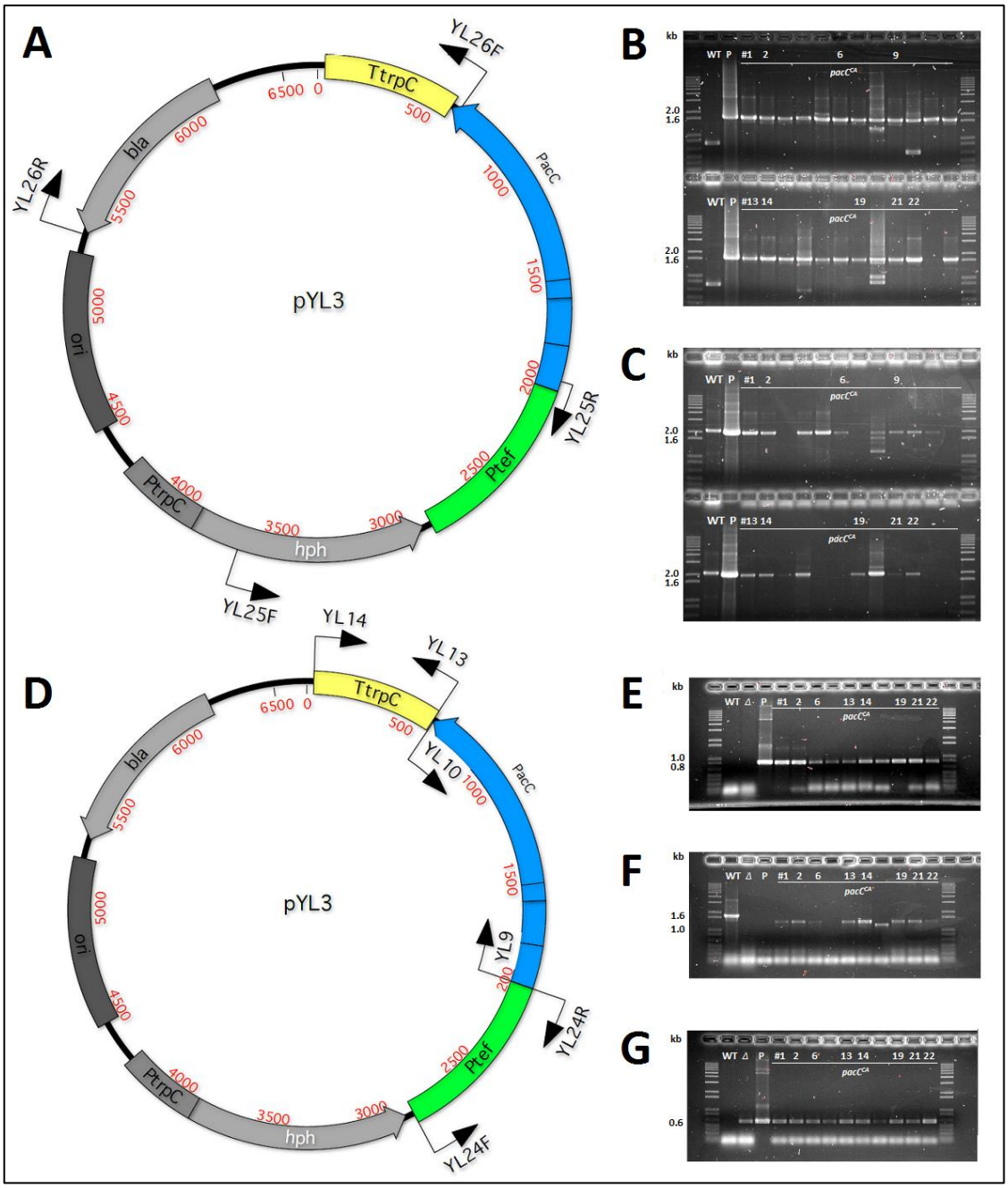

Figure 3.4. PCR screens of *pacC*^{CA} transformants. (A) Strategy of first PCR screen of *pacC*^{CA} transformants using primer pairs YL25F/YL25R and YL26F/YL26R that generate 1.7 kb and 2.0 kb fragments in *pacC*^{CA} transformants, respectively. (B and C) Gel of first PCR screen of 24 *pacC*^{CA} transformants using primer pairs YL25F/YL25R (B) and YL26F/YL26R (C). P: positive plasmid control pYL3. *pacC*^{CA} strains #1, 2, 6, 13, 14, 19 and 22 are indicated. (D) Strategy of second PCR screen of *pacC*^{CA} transformants using primer pairs YL24F/YL24R, YL9/YL10 and YL13/YL14 that give 0.8 kb, 1.4 kb and 0.6 kb fragments in *pacC*^{CA} transformants, respectively. (E to G) Gels of second PCR screen of 22 *pacC*^{CA} transformants with primer pairs YL24F/YL24R (E), YL9/YL10 (F) and YL13/YL14 (G). Δ: negative control using genomic DNA from Δ*pacC* as template. P: positive plasmid control pYL3. *pacC*^{CA} strains #1, 2, 6, 13, 14, 19 and 22 are indicated.

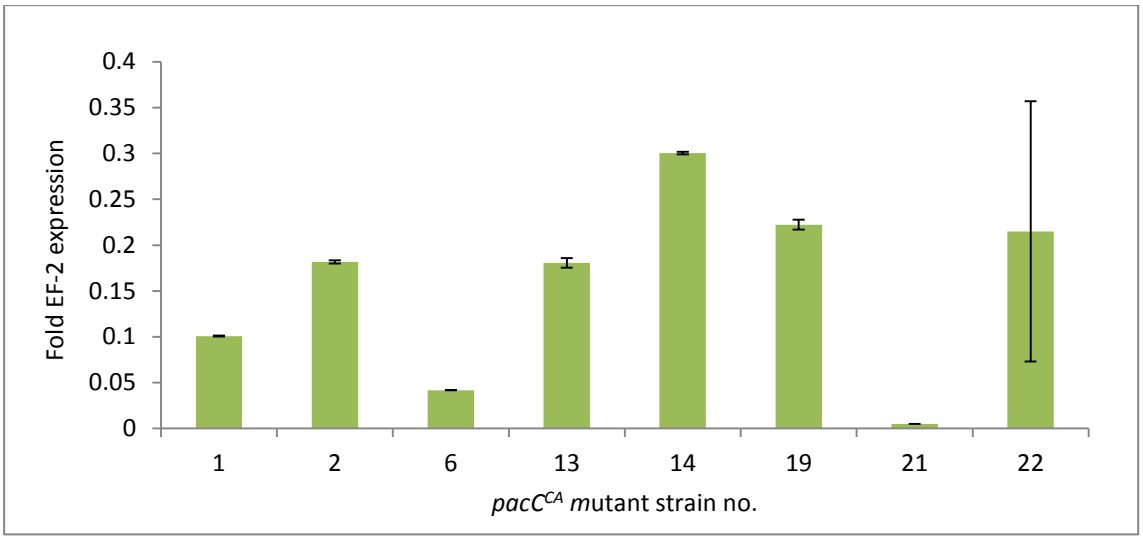

Figure 3.5. Expression of *pacC*^{CA} transcript in eight *pacC*^{CA} transformants. Mycelia were grown in 2.4% potato dextrose media for 3 days at 22°C and total RNA extracted from mycelia was used to synthesise cDNA and used for qRT-PCR analysis. Values were quantified by the $2^{(\Delta Cp)}$ method normalised to the expression levels of the *EF-2* reference gene. Data are representative of two technical replicates from a single biological replicate; Y-axis represents fold mRNA abundance to the *EF-2* gene, error bars represent standard deviation from two technical replicates.

3.3 Effects of *pacC* mutations on the development of *E. festucae*

3.3.1 PacC is required for normal senescence and tolerance to Na^+

The colony phenotypes of Δ*pacC* mutants (#8, 11, 37, 73 and 96) were initially compared to that of wild-type strain on PD agar (PDA). All five mutants displayed premature senescence which was evident at about day 9 (Figure 3.6). As a phenotype of increased salt sensitivity was reported in the Δ*pacC* mutant of *F. oxysporum* (Caracuel *et al.*, 2003a), growth of the three *E. festucae* Δ*pacC* mutants (#8, 11 and 73) was tested on high concentration-NaCl media. On both 0.5 M and 1 M NaCl-supplemented PDA, the Δ*pacC* mutant colonies showed reduced radial growth in comparison to wild-type (Figure 3.7). The Δ*pacC* colonies also displayed a premature senescence phenotype which was most noticeable in the centre, older region of the colonies. This phenotype was less evident under 1 M NaCl condition, most likely because radial growth of the colonies was dramatically reduced. As all three Δ*pacC* mutants displayed an invariant colony phenotype, Δ*pacC* mutant #8 was used for subsequent experiments.

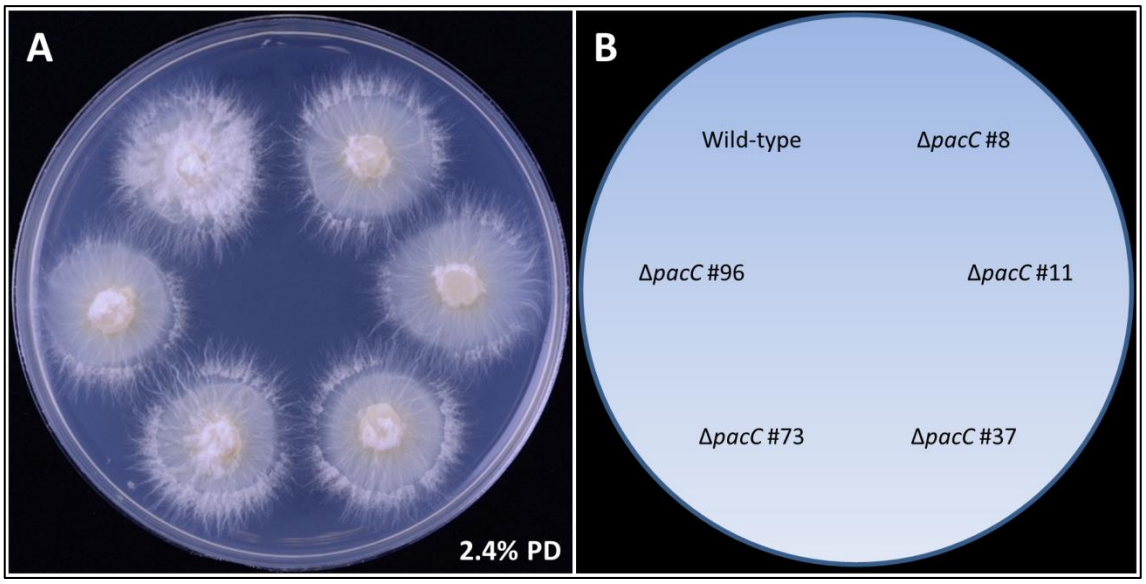

Figure 3.6. Premature senescence of Δ*pacC* mutant colonies on PDA. Wild-type and Δ*pacC* mycelial plugs 5 mm in diameter were inoculated onto 2.4% potato dextrose agar and cultured at 22°C for 11 days. The *E. festucae* colony strains are as labelled on the right.

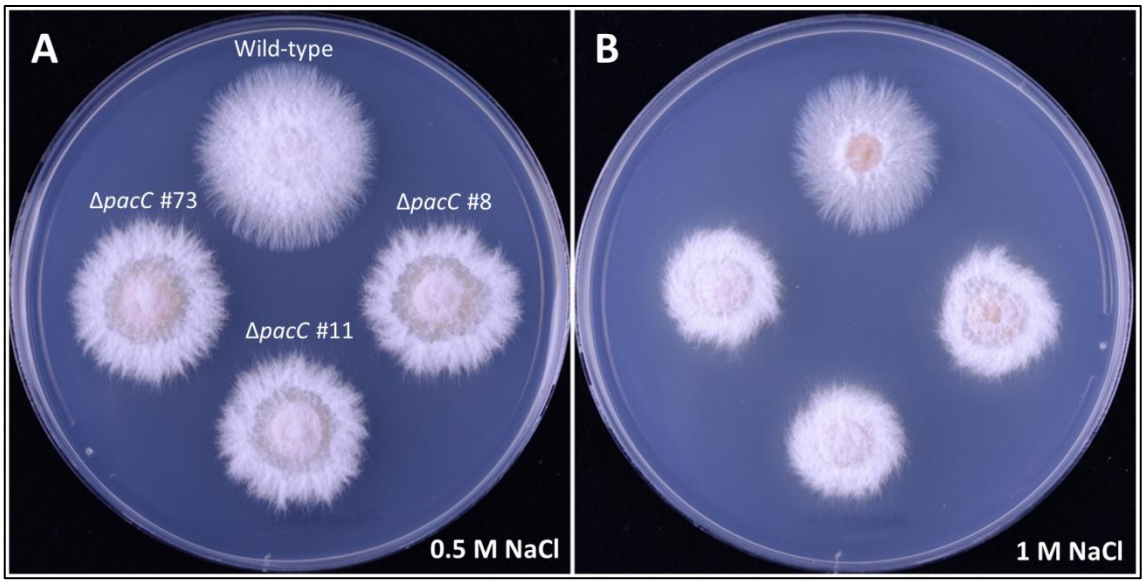

Figure 3.7. Sensitivity of Δ*pacC* mutants to high concentrations of NaCl. Colony morphology of wild-type and Δ*pacC* mutants on 2.4% potato dextrose agar supplemented with (A) 0.5 M, and (B) 1 M NaCl. Mycelial plugs 5 mm in diameter were inoculated onto the growth agar and cultured at 22°C for 14 days. Figures are representative of results from two biological replicates; colony labelling in (A) applies to both figures.

3.3.2 Complementation of Δ*pacC* mutant

To determine if the salt-sensitive and premature-senescence phenotype of the Δ*pacC* mutants was due to deletion of *pacC*, the native *pacC* gene was reintroduced into the Δ*pacC* #8 by transformation with the pYL2 *pacC* complementation vector (Section 2.8.2;

Appendix 6.2.3). 24 $Gen^{R}Hyg^{R}$ transformants were screened by PCR to interrogate the flanking regions of the construct (Figure 3.8A to C) and the *pacC* gene sequence (Figure 3.8D and E). The screen identified 17 transformants with patterns indicative of intact constructs. Subsequently, Δ*pacC*/*pacC* transformants #2 and #4 were selected for complementation tests. Reintroduction of the native *pacC* gene into Δ*pacC* complemented the salt sensitivity and senescence phenotypes (Figure 3.9). As both Δ*pacC*/*pacC* #2 and #4 transformants showed similar phenotypes, Δ*pacC*/*pacC* #2 was selected for use in further experiments.

3.3.3 PacC is required for tolerance to K^+ and Li^+

As a phenotype for K^+ and Li^+ sensitivity was also reported for Δ*pacC* mutant in *Fusarium* (Caracuel *et al*., 2003) the effects of these ions on the *pacC* mutants of *E. festucae* were tested. A reduction in colony radial growth of the Δ*pacC* mutant in comparison to wild-type was observed under 0.1 M and 0.2 M Li^+, 0.5 M and 1 M K^+; but not under 0.05 M Li^+-conditions (Figure 3.10A to F). Premature senescence of the Δ*pacC* colonies was evident under the lower salt concentrations of 0.05 M and 0.1 M Li^+; but not under 0.5 M Li^+ and K^+ conditions; and both the senescence and K^+/Li^+-sensitivity phenotypes of the Δ*pacC* mutant were rescued in the complementation strain (Figure 3.10). Growth tests on Na^+-supplemented PDA were also repeated with the inclusion of the $pacC^{CA}$ mutant. Under 0.5 M Na^+, a reduction of growth in the Δ*pacC* mutant was noticeable in comparison to wild-type; but under 1 M Na^+, growth of all strains were dramatically reduced (Figure 3.10H and I). In comparison to the previous Na^+ stress tests (Figure 3.7 and 3.9), the cultures were grown for 9 days instead of 14 days in this experiment, which accounts for the smaller colonies observed. The $pacC^{CA}$ mutant showed a reduced colony radial growth on PDA alone (Figure 3.10B), and the extent of growth reduction in comparison to wild-type was relatively similar on all of the conditions tested (Figure 3.10C to I), indicating that the $pacC^{CA}$ mutant is not sensitive to salt. A difference in hyphal morphology was also observed at the colony edge of the $pacC^{CA}$ mutant, with hyphae being less extended and more cottony in appearance (Figure 3.10B to F).

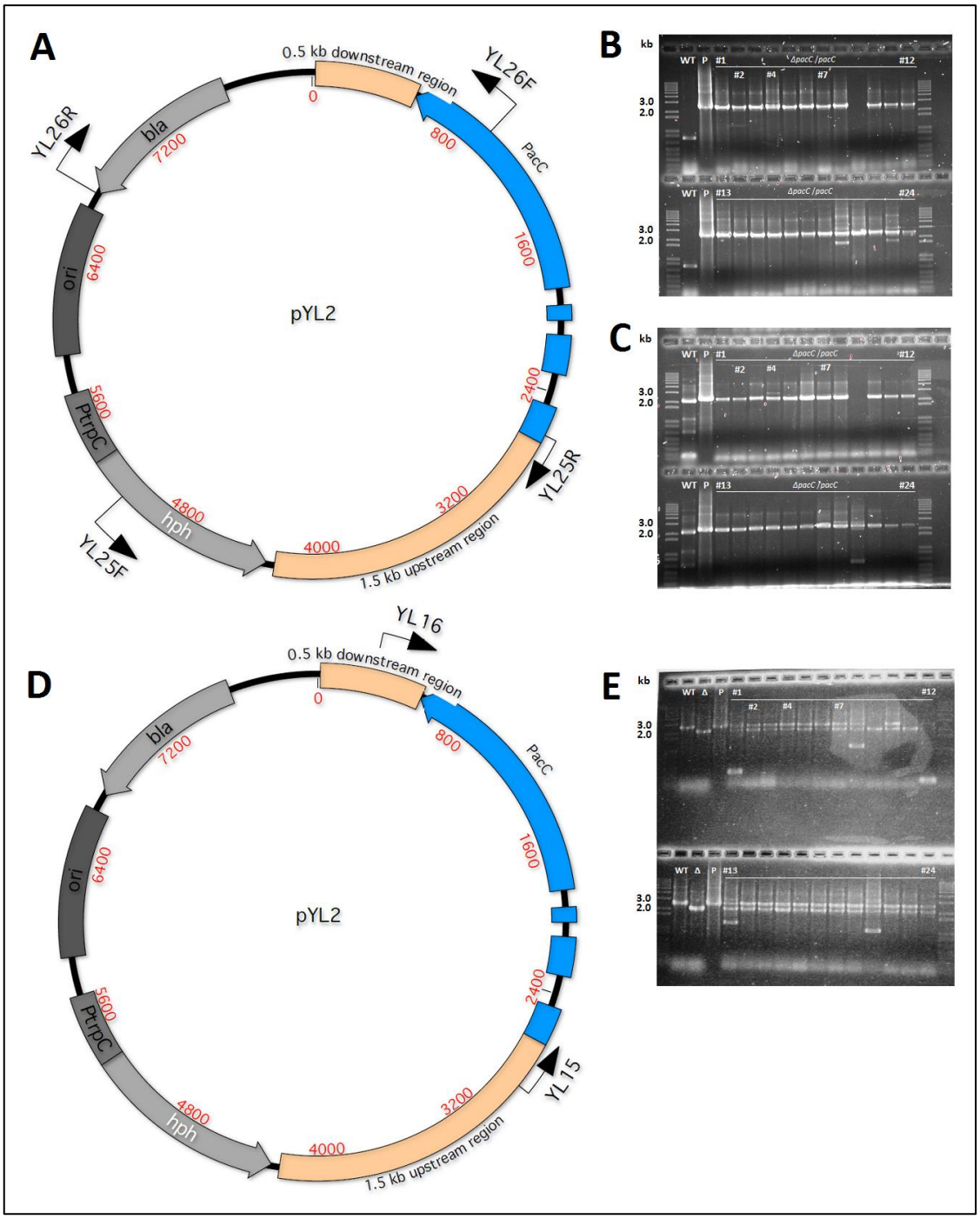

Figure 3.8. PCR screens of Δ*pacC/pacC* transformants. (A) Strategy of first PCR screen of Δ*pacC/pacC* transformants using primer pairs YL25F/YL25R and YL26F/YL26R that respectively generate 2.5 kb and 2.3 kb fragments in Δ*pacC/pacC* transformants. (B and C) Gels of first PCR screen of 24 Δ*pacC/pacC* transformants using primer pairs YL25F/YL25R (B) and YL26F/YL26R (C). P: positive plasmid control pYL2. (D) Strategy of second PCR screen of Δ*pacC/pacC* transformants using primer pair YL15/YL16 that generates a 2.6 kb fragment in wild-type, a 2.1 kb fragment in the Δ*pacC* mutant and a 2.6 kb fragment in Δ*pacC/pacC* transformants. (E) Gel of second PCR screen of 10 Δ*pacC/pacC* transformants with primer pair YL15/YL16. Δ: negative control using Δ*pacC* genomic DNA, P: positive plasmid control pYL2. Δ*pacC* strains #2, 4 and 7 are indicated.

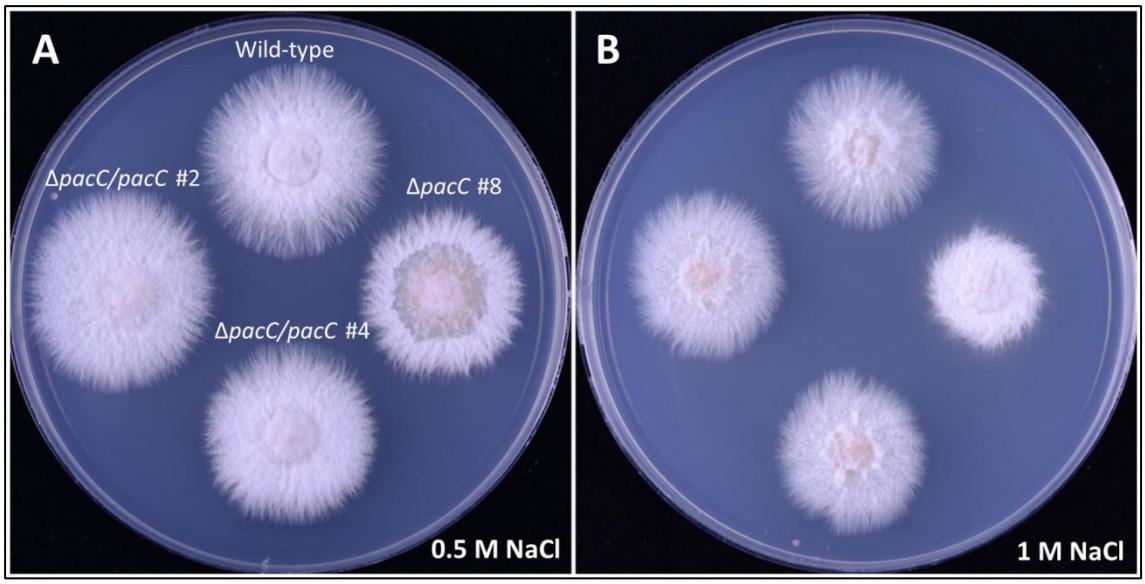

Figure 3.9. Complementation test of Δ*pacC* mutant on high concentration-NaCl media. Colony morphology of wild-type, Δ*pacC* and Δ*pacC*/*pacC* mutants on 2.4% potato dextrose agar supplemented with (A) 0.5 M NaCl and (B) 1 M NaCl. Mycelial plugs 5 mm in diameter were inoculated onto the growth agar and cultured at 22°C for 14 days. Figures are representative of results from two biological replicates; colony labelling in (A) applies to both figures.

3.3.4 The ENA family of P-type Na+-ATPases may regulate salt tolerance in *E. festucae*

In filamentous yeasts, the P-type Na^+-ATPase, ENA1, controls ion (Na^+, K^+ and Li^+) homeostasis (Haro *et al.*, 1991; Banuelos & Rodriguez-Navarro, 1998). The expression of *ena1* is also dependent on PacC and alkaline pH in *Fusarium* (Caracuel *et al.*, 2003a). A tBLASTn search was performed to identify the putative *ena1* gene in *E. festucae* using the amino acid sequence of the ENA1 protein from *F. oxysporum*. The search identified two genes in the *E. festucae* genome; one in contig 766 with a score of 701 and an E-value of 0, designated *ena1* (Fl1 gene model EfM2.084240); and another in contig 358 with a score of 603 and an E-value of 0, designated *ena2* (Fl1 gene model EfM2.113810). The predicted translated proteins of *ena1* and *ena2* share 44% and 38% amino acid identity with ENA1 from *F. graminearum*, respectively (Appendix 6.3.1). In addition, the 1 kb promoter regions of *ena1* and *ena2* each contains seven and two 5′-GCCAAG-3′ PacC binding consensus sequences, respectively.

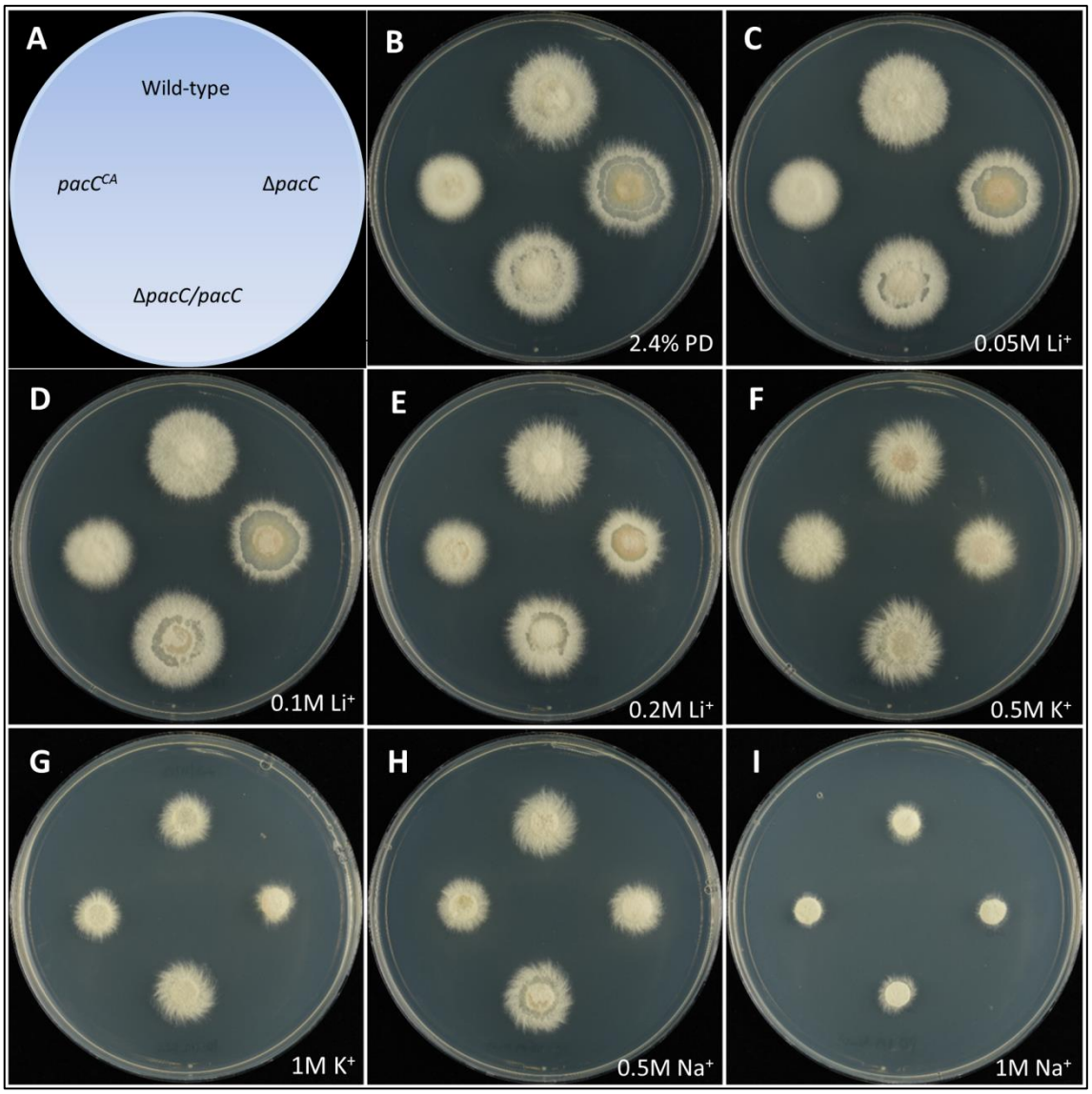

Figure 3.10. Colony morphology of *pacC* mutants on high concentration K^+ and Li^+ media. Colony morphology of wild-type and *pacC* mutants on 2.4% potato dextrose agar supplemented with the indicated ions. Mycelial plugs 5 mm in diameter were inoculated onto the growth agar and cultured at 22°C for 9 days. Figures are representative of results from two biological replicates and colony labelling in (A) applies to all figures.

To determine if the expression of *ena2* was dependent on pH and PacC, mycelia of wild-type and *pacC*-mutant strains were cultured in Blankenship media (Blankenship *et al*., 2001) buffered at pH 5, 6.5 and 8. The results showed that in wild-type strain the expression of *ena2* was slightly downregulated under neutral conditions, while in the Δ*pacC* mutant an alkaline pH-dependent upregulation of the gene was observed (Figure 3.11), suggesting a PacC-dependent upregulation of the gene at acidic pH. Given that potato dextrose used in the salt-stress tests has a pH of 5.1, the sensitivity of the Δ*pacC* mutant to Na^+, K^+ and Li^+ may be due to the decreased expression of *ena2* in

the mutant at acidic pH. The *pacC*^{CA} mutant showed a lower expression of *ena2* relative to wild-type under all pH conditions which suggests that over-activation of PacC may directly or indirectly inhibit the expression of this gene (Figure 3.11). The expression of *ena1* was not analysed in this study.

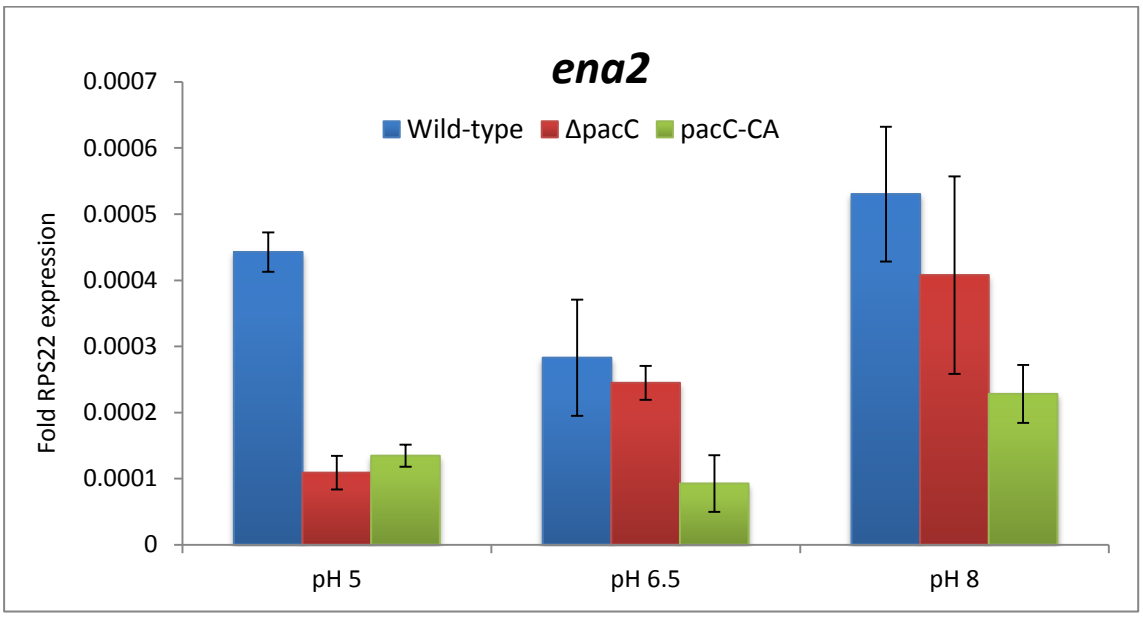

Figure 3.11. Expression of *ena2* in culture. Steady-state mRNA levels of *ena2* in wild-type and *pacC* mutants of *E. festucae*. Mycelia were cultured in Blankenship media buffered at pH 6.5 for 5 days, washed, and transferred to fresh Blankenship media buffered at pH 5, 6.5 or 8 and incubated for a further 2 hours before harvesting. Total RNA extracted from mycelia was used to synthesise cDNA. Primers used in the analysis are listed in Table 2.3. Values were calculated by the $2^{(\Delta Cp)}$ method and normalised to the expression levels of the 40S ribosomal protein S22 (*RPS22*) reference gene (y-axis). Bars represent standard error of the mean calculated from three biological replicates.

3.3.5 Effect of *pacC* mutations on tolerance to other cellular stresses

The effects of oxidative, cell-membrane, cell-wall and temperature stresses were tested on the *pacC* mutants by observing colony radial growth following the various stress conditions. Under conditions with H_2O_2, both wild-type and *pacC*-mutant strains displayed reduced colony radial growth compared to PDA alone (Figure 3.12A and B). However, there was no difference in the extent of growth reduction between the mutants and wild-type, indicating that deletion or over-activation of *pacC* (PacC) do not affect oxidative stress sensitivity in *E. festucae*. No difference in radial growth was observed in the presence of the lipid emulsifying agent SDS, indicating that mutations in *pacC* do not affect cell-membrane integrity (Figure 3.12C). Growth of wild-type and Δ*pacC* mutant was similar in the presence of calcofluor white; however, the *pacC*^{CA}

mutant showed a slight reduction in radial growth (Figure 3.12D). As calcofluor white binds to chitin with high affinity preventing the formation of chitin microfibrils in the fungal cell-wall (Herth, 1980), the result suggests that the *pacC*^{CA} mutant is sensitive to cell-wall stress caused by an interference in chitin polymerisation.

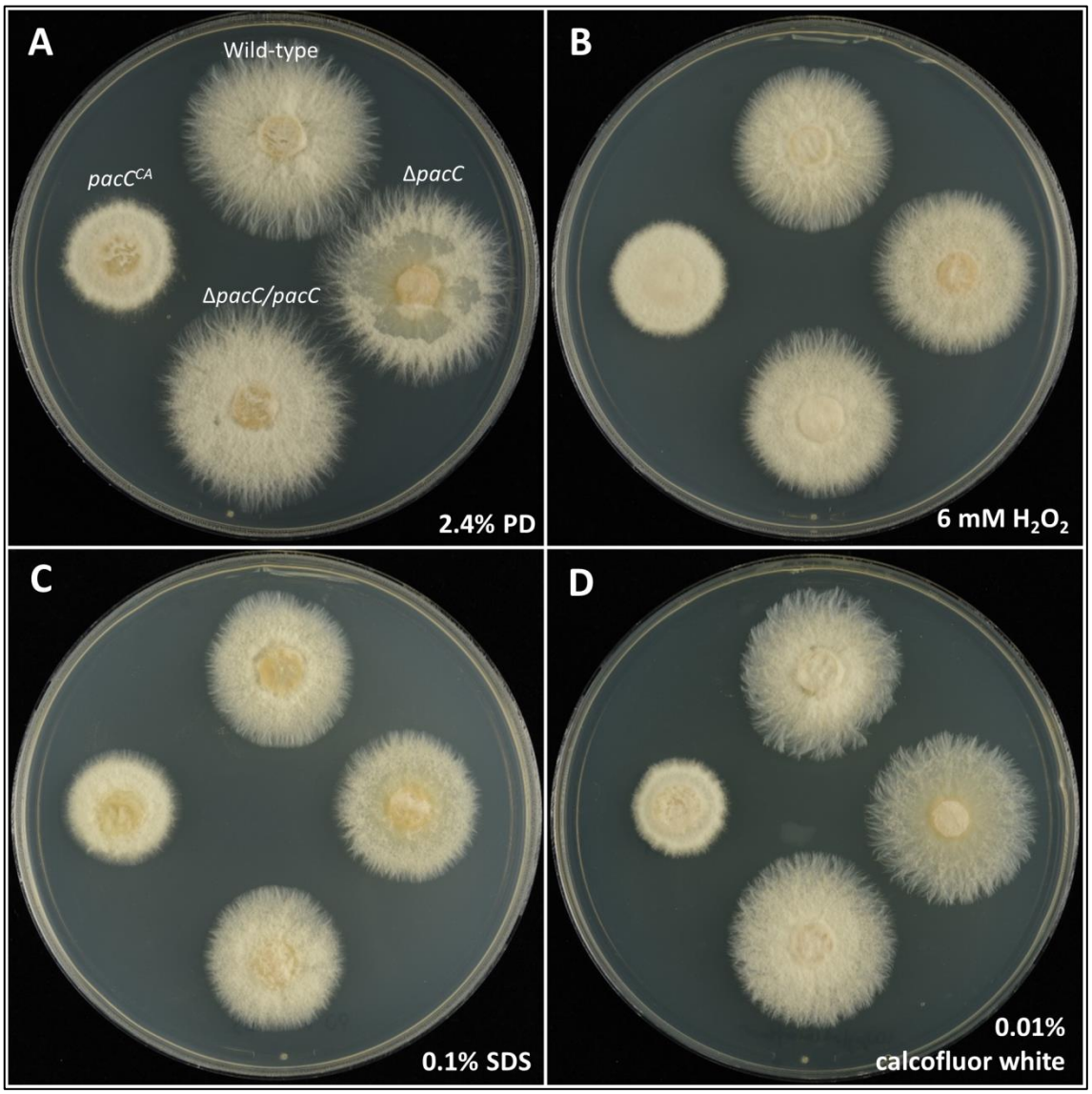

Figure 3.12. Effect of oxidative and cell-wall stresses on *pacC* mutants. Colony morphology of wild-type and *pac*C mutants on: (A) 2.4% potato dextrose agar, and on 2.4% potato dextrose agar supplemented with (B) 6 mM H_2O_2, (C) 0.01% SDS and (D) 0.01% calcofluor white. Mycelial plugs 5 mm in diameter were inoculated onto the growth agar and cultured at 22°C for 9 days. Figures are representative of results from two biological replicates and colony labelling in (A) applies to all figures.

All of the *E. festucae* strains displayed considerable reduction in radial growth rates when cultured at 30°C instead of 22°C (Figure 3.13). The *pacC*^{CA} mutant in particular grew very slowly at 30°C and had a desiccated-like colony morphology (Figure 3.13B).

Extended hyphae at the colony edge of this mutant were also almost non-existent. The Δ*pacC* mutant in comparison did not show a reduced radial growth compared to wild-type but developed distinctive fluffy colony morphology indicative of an increase in aerial hyphae formation. The wild-type and complemented strain showed reduced radial growth at 30°C, but did not exhibit any differences in colony morphology from culture at 22°C (Figure 3.13).

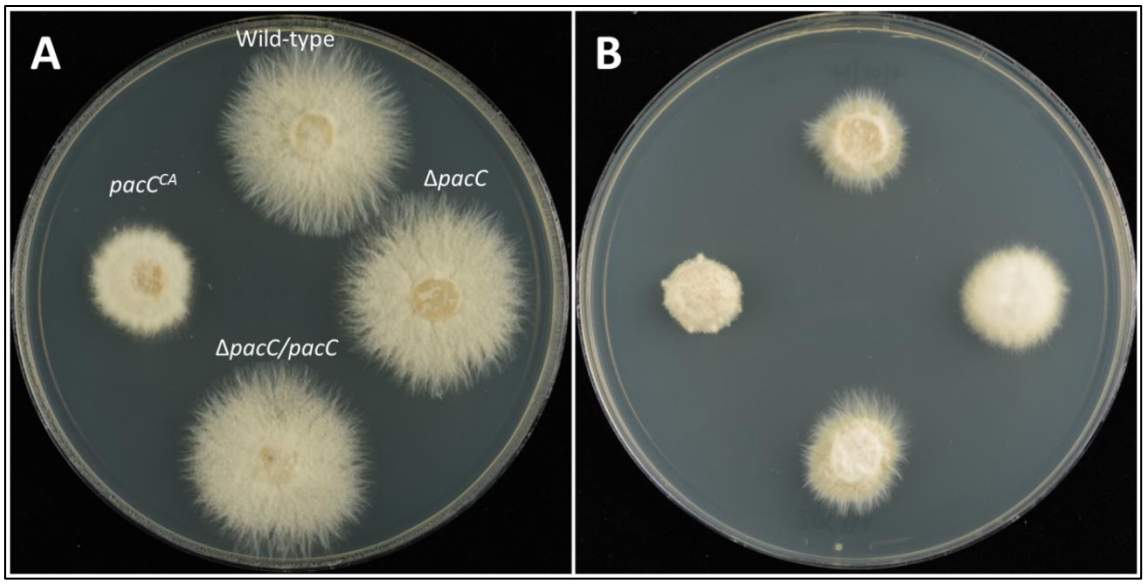

Figure 3.13. Effect of temperature stress on *pacC* mutants. Colony morphology of wild-type and *pacC* mutants on (A) 2.4% potato dextrose agar cultured at 22°C and (B) 2.4% potato dextrose cultured at 30°C. Mycelial plugs 5 mm in diameter were inoculated onto the growth agar and incubated at 22°C for 10 days or at 30°C for 20 days, as there was very minimal colony growth by day 10 on the plate incubated at 30°C. Figures are representative of results from two biological replicates and colony labelling in (A) applies to both figures.

3.3.6 PacC is not required for growth on acid or alkaline media

PacC is activated by extracellular alkaline pH and several studies in *Fusarium* (Caracuel *et al*., 2003b; Merhej *et al*, 2011) and *Trichoderma* (Trushina *et al*., 2013) reported a drastic reduction in growth of the Δ*pacC* mutant under alkaline conditions (pH 7 and above); and either similar or reduced growth of the *pacC*^{CA} mutant under acidic conditions. To test if the corresponding *pacC* mutations in *E. festucae* had similar growth effects, wild-type and *pacC* mutant strains were cultured on pH-defined Blankenship media. On these media, wild-type and complementation strains had comparable radial growth rates at pH 6.5 and pH 8, but a slightly reduced growth at pH 5 (Figure 3.14A to C). In contrast to other reports, the Δ*pacC* mutant did not show a reduction in radial growth under alkaline pH condition, indicating that PacC is not required for growth under

alkaline conditions in *E. festucae*. The *pacC*^{CA} mutant also grew surprisingly well on the Blankenship media, in particular under the alkaline pH condition; although the mutant showed reduced radial growth on other PD-based media (Figure 3.14A to C).

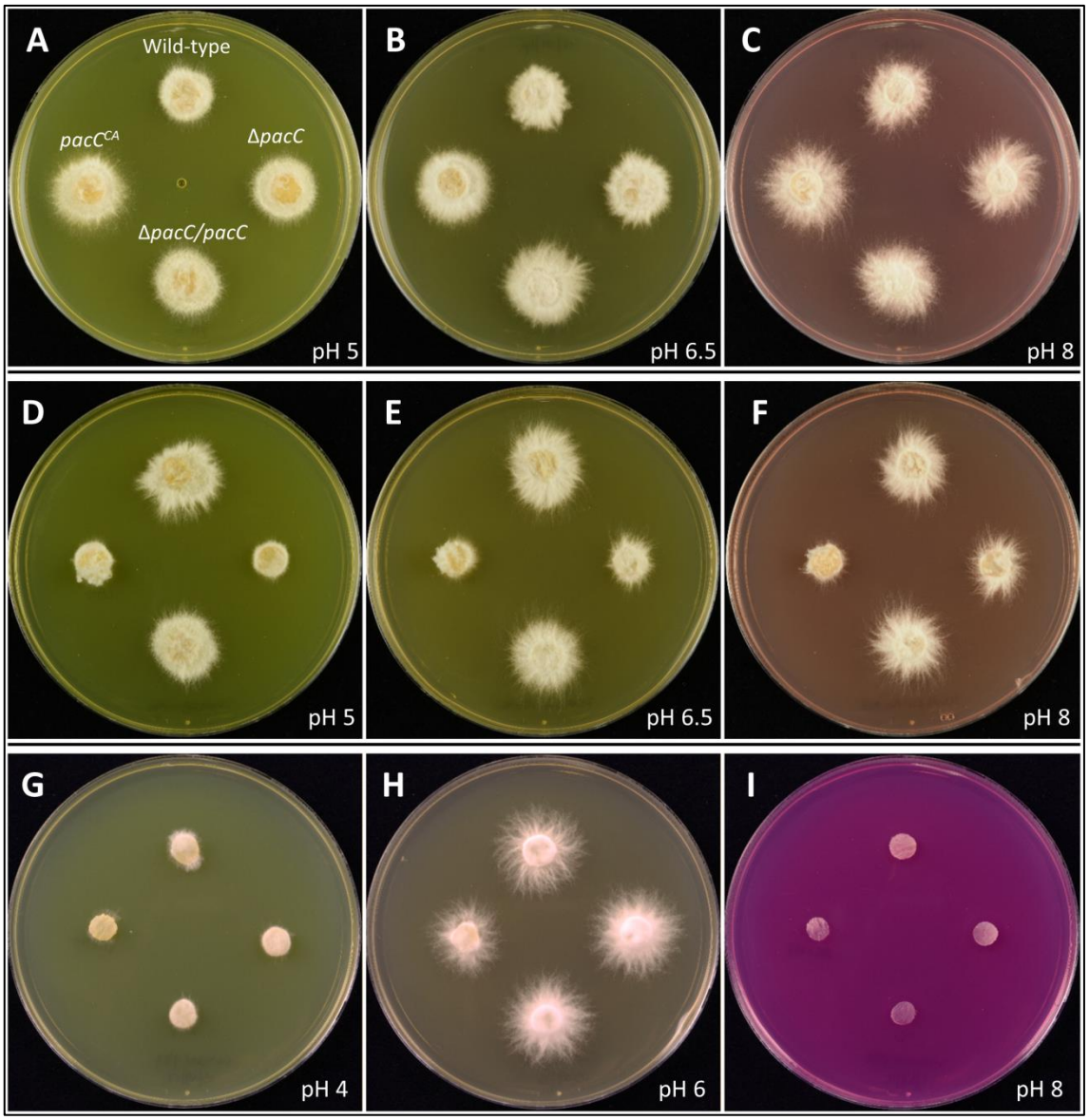

Figure 3.14. Colony morphology of *pacC* mutants on pH-defined media. Growth of wild-type and *pacC* mutant strains on (A to C) pH-defined Blankenship media, (D to F) pH-defined Blankenship media containing 100x trace elements, and (G to I) pH-defined synthetic media from Caracuel *et al*., (2003). 1.1 mg/mL phenol red was added to the media for visualisation of media pH. Mycelial plugs 5 mm in diameter were inoculated onto the growth agar and incubated at 22°C for 16 days (A to C) or for 14 days (D to I). Figures A to F are representative of results from two independent experiments with two biological replicates and figures G to I are representative of results from one experiment with two biological replicates. Labelling of the colony strains in (A) applies to all figures.

The above experiment was also performed inadvertently with 100x more trace elements (Section 2.2.11). These conditions did not seem to affect growth of wild-type and complemented strains (Figure 3.14D to F), but radial growth of the Δ*pacC* and *pacC*^{CA} mutants was reduced under these conditions, indicating that these mutations lead to an increased sensitivity to higher concentrations of trace elements. The Δ*pacC* mutant was also able to grow under the alkaline pH conditions, indicating that alkaline pH may affect expression of genes required for tolerance to the increased trace elements (Figure 3.14F). Finally, as these results differ from three previous studies (Caracuel *et al*., 2003b; Merhej *et al*, 2011; Trushina *et al*., 2013), all of which used a medium (synthetic medium) similar to that described in Caracuel *et al*., (2003b), growth of the *E. festucae* mutants was tested on this medium. All *E. festucae* strains were able to grow on pH 6 conditions of this medium, but not at pH 4 or 8 (Figure 3.14G to I).

3.3.7 Role of PacC in regulating PacC-dependent genes in *E. festucae*

The finding that PacC is not required for growth of *E. festucae* under alkaline conditions raises the question about the importance of this transcription factor in *E. festucae*. To address this question, the expression of genes which have been found to be pH- and PacC-dependent in other fungi were analysed in the *E. festucae pacC* mutants. The genes for acid phosphatase (upregulated under acidic conditions) and alkaline phosphatase (upregulated under alkaline conditions), which are pH- and PacC dependent in *Aspergillus* (Caddick *et al*., 1986; Peñalva *et al*., 2008) were analysed in *E. festucae*. Two other genes; *CNH1*, coding for a putative Na^+/H^+ antiporter; and a gene coding for a cytochrome P450, both of which are pH- and PacC-dependent in *T. virens* (Trushina *et al*., 2013) were also analysed in *E. festucae*.

Using amino acid sequence from the *A. nidulans* alkaline phosphatase, the putative gene in *E. festucae* (EfM2.057140) was identified in contig 720 with a score of 463 and an E-value of 0. One consensus PacC binding sequence was found in the 1 kb promoter region of this gene, and the predicted protein shares 61% and 75% amino acid identity with alkaline phosphatases from *A. nidulans* and *F. oxysporum*, respectively (Appendix 6.3.2). The putative acid phosphatase gene in *E. festucae* was also identified by a tBLASTn search using the amino acid sequence of the protein from *A. flavus*. A hit with a score of 181 and an E-value of 9e-72 was a gene in contig 160 (EfM2.003400). The 1 kb promoter region of this gene contains one PacC binding consensus sequence and the

predicted protein shares 38% and 24% amino acid identity with acid phosphatases from *M. oryzae* and *A. flavus*, respectively (Appendix 6.3.3). The gene was also likely to have been misannotated by the MAKER gene prediction algorithm, as the predicted protein contains a ~300 stretch of amino acid residues at its N-terminus which are not present in the other fungal homologues; however, qRT-PCR analysis should not be affected as primers were designed to the 3'-UTR region of the predicted transcript.

The putative *CNH1* gene in *E. festucae* was identified by a tBLASTn search using the amino acid sequence of CNH1 from *T. virens* (Protein ID 10799; *Trichoderma virens* v2.0, JGI, http://genome.jgi-psf.org/TriviGv29_8_2/TriviGv29_8_2.home.html). The search identified a hit (EfM2.014050) in contig 46 with a score of 1169 and an E-value of 0. Two consensus PacC binding sites are present in the 1 kb promoter region of the gene and the predicted translated protein of this gene shares 67% and 59% amino acid identity with CNH1 from *T. virens* and *N. crassa*, respectively (Appendix 6.3.4). The putative gene for cytochrome P450 in *E. festucae* was also identified by a tBLASTn search, using the amino acid sequence of cytochrome P450 from *T. virens* (Protein ID 86792). A hit (EfM2.084750) was identified in contig 461 with a score of 613 and an E-value of 1e-175. The 1 kb promoter region of this gene did not contain any consensus PacC binding sequence and the predicted translated protein of this gene shares 62% and 56% amino acid identity with cytochrome P450 from *T. virens* and *N. crassa*, respectively (Appendix 6.3.5).

The results of the expression analysis showed that the expression of alkaline phosphatase in *E. festucae* was slightly dependent on alkaline pH (Figure 3.15A). Interestingly, expression of this gene was lower in wild-type than in Δ*pacC*, and the difference was more evident at alkaline pH, indicating that PacC negatively regulates the expression of this gene in *E. festucae*; contrary to the findings in other fungi. The decreased expression of the gene in the *pacC*^{CA} mutant at pH 8 concurs with this hypothesis; however, the mutant also showed higher expression compared to wild-type under acidic and neutral conditions (Figure 3.15A). The expression of acid phosphatase was slightly dependence on alkaline pH in wild-type and Δ*pacC* mutant, suggesting that it is alkaline dependent but PacC-independent. The higher expression in the Δ*pacC* mutant and reduced expression in the *pacC*^{CA} mutant suggests a role for PacC in downregulating this gene (Figure 3.15B).

In contrast to the finding in *T. virens* in which *CNH1* expression was 9-fold higher in wild-type strain at pH 8 compared to wild-type strain at pH 4 or Δ*pacC* at pH 8 (Trushina *et al*., 2013), the expression of *CNH1* in *E. festucae* did not show a dependence on pH and PacC, although a slight downregulation of the gene at acidic pH in the Δ*pacC* mutant may indicate an active role of PacC at acidic pH in *E. festucae* (Figure 3.15C). In *T. virens*, the gene for cytochrome P450 is an acid-dependent and PacC-repressed gene whose expression was downregulated 9-fold in wild-type at pH 8 compared to wild-type at pH 4 or Δ*pacC* at pH 8 (Trushina *et al*., 2013). In *E. festucae*, the expression of this gene appeared to be slightly upregulated under both acidic and alkaline conditions, but did not show a dependence on PacC (Figure 3.15D). However, the small differences observed in the expression levels of *CNH1*, and in particular cytochrome P450, between the strains and treatments, and their low expression levels suggest that these differences may not be physiologically significant and may be the result of sample variability.

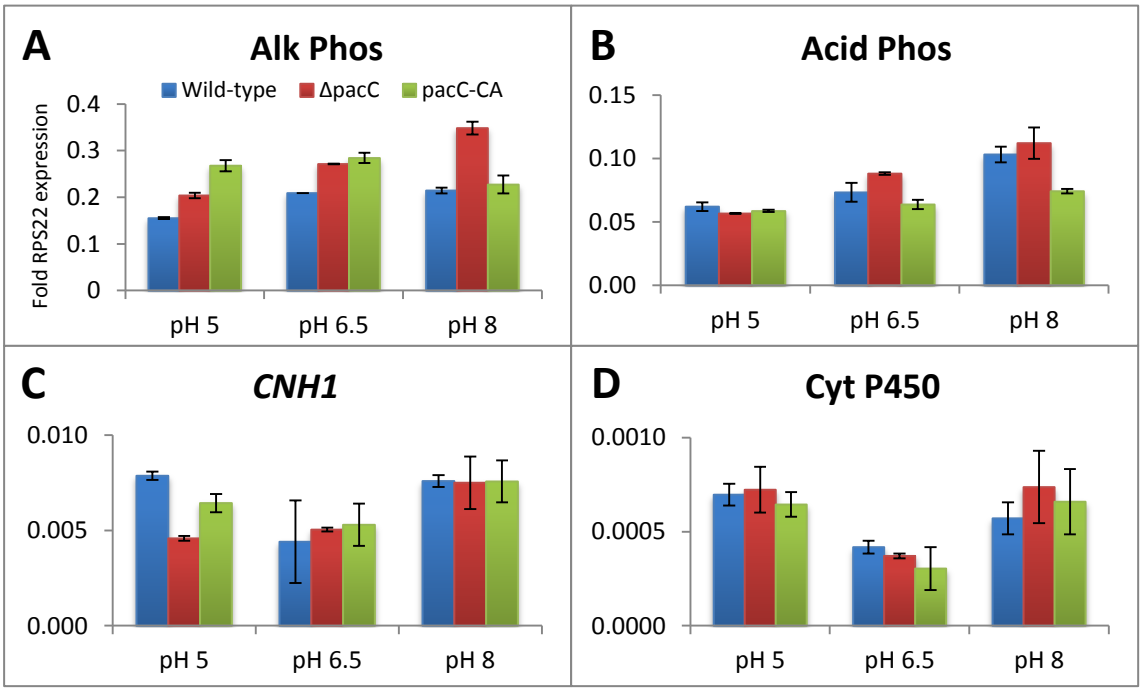

Figure 3.15. Relative expression of known pH- and PacC-dependent genes in *E. festucae*. Steady state transcript levels of the putative genes for (A) Alkaline phosphatase, (B) Acid phosphatase, (C) Na+/H+ antiporter CNH1 and (D) a cytochrome P450. Mycelia were cultured in Blankenship media buffered at pH 6.5 for 5 days, washed, and transferred to fresh Blankenship media buffered at pH 5, 6.5 or 8 and incubated for a further 2 hours before harvesting. Total RNA extracted from mycelia was used to synthesise cDNA and values were calculated by the $2^{(\Delta Cp)}$ method normalised to the expression levels of the *RPS22* reference gene (y-axes). Primers used in the analyses are listed in Table 2.3. Bars represent standard error of the mean calculated from three biological replicates.

3.3.8 Δ*pacC* mutant has reduced aerial hyphae development

Closer examination of mycelial colonies cultured on the high-concentration salt media (Section 3.3.3) revealed a reduction of aerial hyphae formation in the Δ*pac*C mutant. This observation was more evident in cultures growing on media containing K^+ ions, which seemed to induce aerial hyphae formation in wild-type, Δ*pacC*/*pacC*, and *pacC*^{CA} strains (Figure 3.16). A similar phenotype was observed on Δ*pac*C colonies cultured on Blankenship medium containing 100x trace elements (Figure 3.17). Blankenship medium was buffered with potassium phosphate buffer, to give a total of 60 mM K^+ ion in the media (Section 2.2.11).

3.3.9 Effect of *pacC*^{CA} mutation on hyphal growth and dynamics

The difference in hyphal morphology observed at the colony edge of the *pacC*^{CA} mutant (Section 3.3.3; Figure 3.10) was examined closer by light microscopy. Formation of hyphal bundles was clearly visible at the colony edges of wild-type, Δ*pac*C and complemented strains, but was less frequently observed in the *pacC*^{CA} mutant (Figure 3.18).

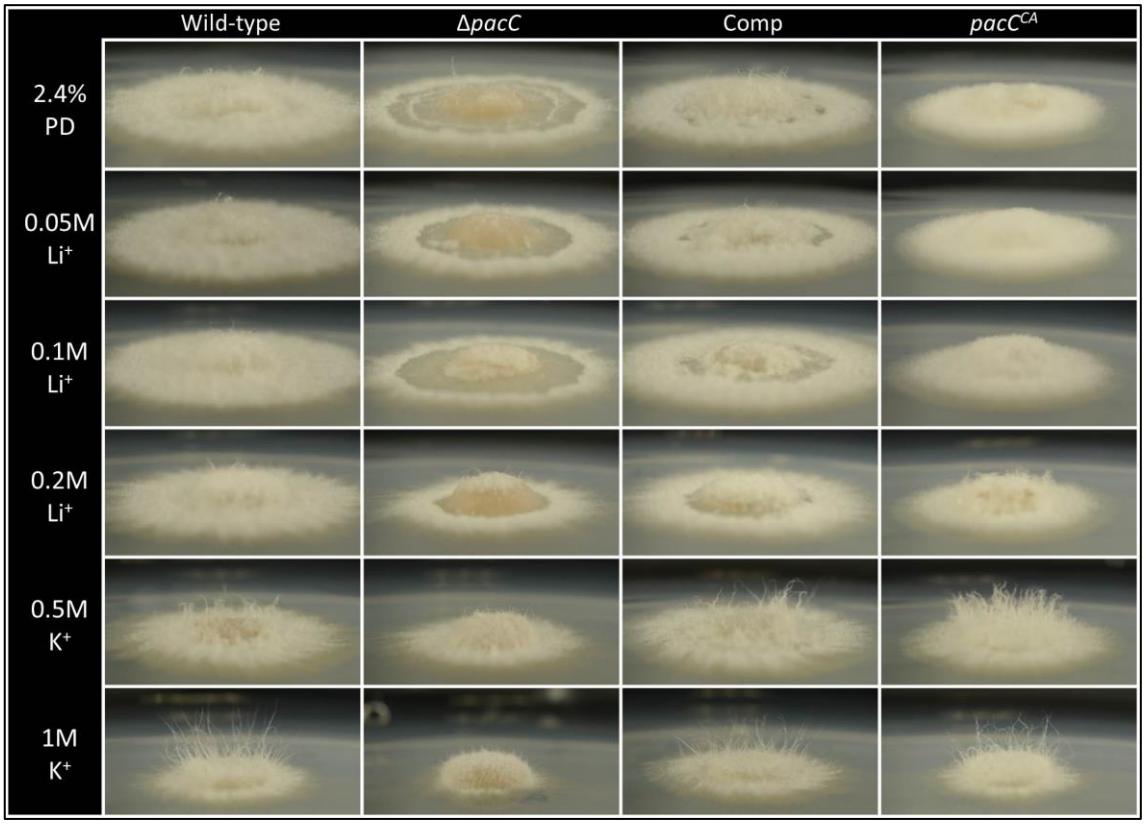

Figure 3.16. Aerial hyphae development in *pacC* mutants cultured under high salt-concentration conditions. Mycelial plugs 5 mm in diameter were inoculated onto 2.4% potato

dextrose agar supplemented with the indicated concentrations of LiCl or KCl and cultured at 22°C for 9 days. Figures are representative of results from two biological replicates.

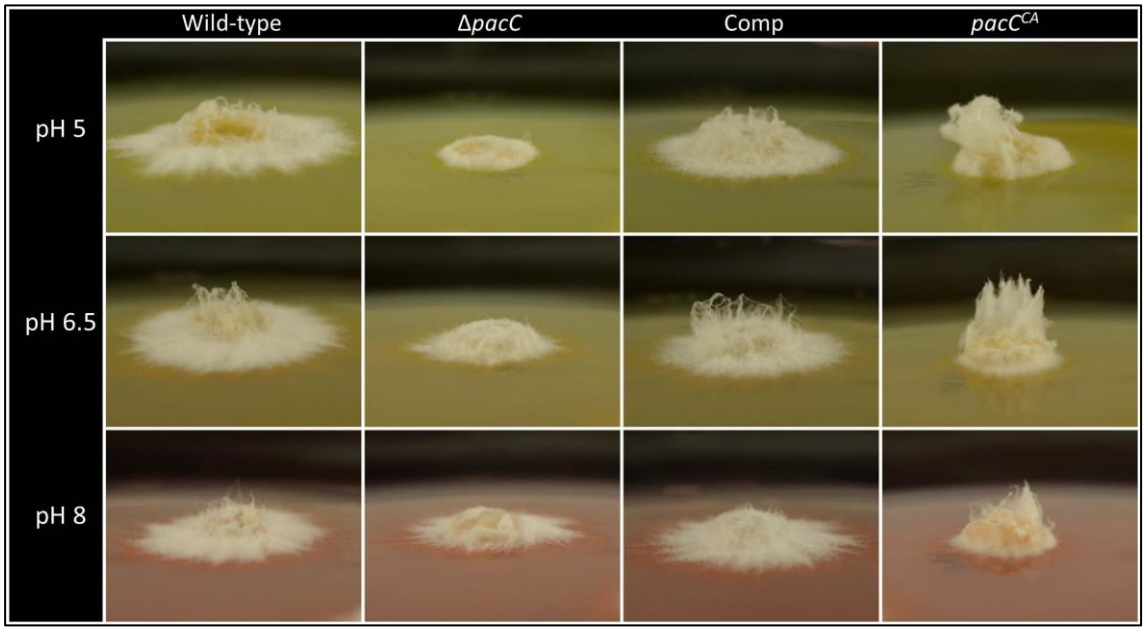

Figure 3.17. Aerial hyphae development in *pacC* mutants cultured on buffered Blankenship media. Mycelial plugs 5 mm in diameter were inoculated onto Blankenship media containing 100x trace elements and incubated at 22°C for 10 days. Figures are representative of results from three biological replicates.

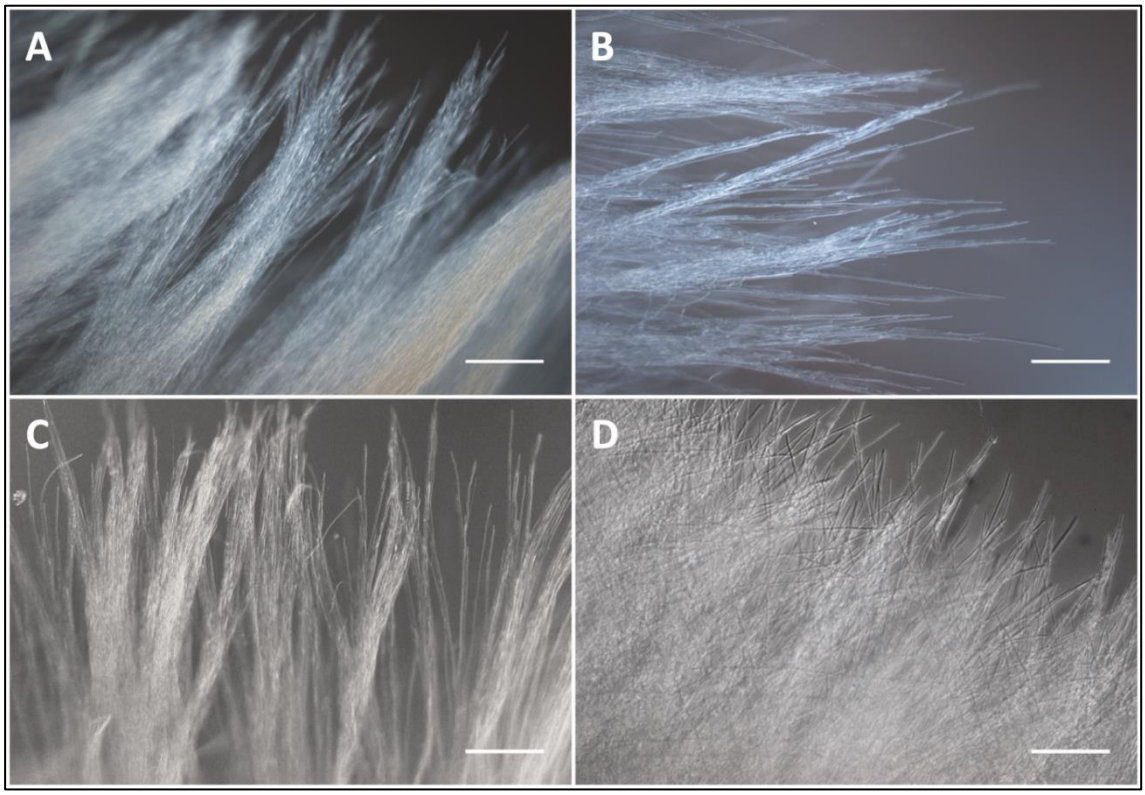

Figure 3.18. Hyphal morphology at the colony edge of wild-type and *pacC* mutants of *E. festucae*. (A) Wild-type, (B) Δ*pacC*, (C) Δ*pacC/pacC*, and (D) *pacC*^{CA} mutants. Mycelia were

grown on 2.4% potato dextrose agar for 19 days at 22°C. Images were taken of hyphae at the colony edge with a light microscope at 100x magnification. Bars = 200 µm.

When hyphae were stained with calcofluor white and examined under the fluorescence microscope, coiled aerial hyphal structures were regularly observed in the wild-type strain; these structures were about 25 µm across and occasionally contained a conidiophore (Figure 3.19A). Such structures are characteristically found on the aerial hyphal networks of a growing *E. festucae* colony (Scott *et al*., 2012); although, the Δ*pacC* mutant which had reduced aerial hyphae formation (Section 3.3.8) still formed these structures which were similar in size, morphology, and frequency of occurrence to wild-type (Figure 3.19B).

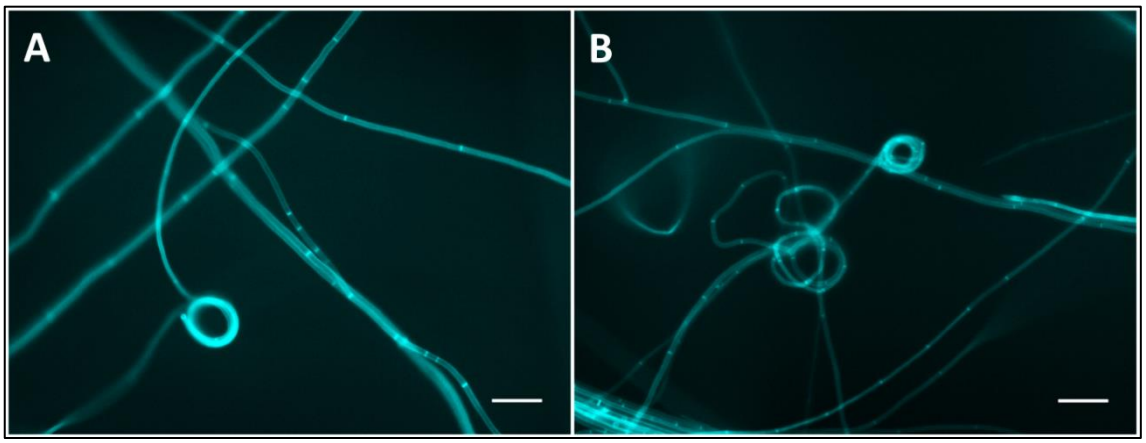

Figure 3.19. Formation of coiled hyphal structures in wild-type and Δ*pacC* mutant. Coiled hyphal structures in (A) Wild-type and (B) Δ*pacC* mutant. Mycelia were grown on water agar for 11 days at 22°C. Hyphae were stained with calcofluor white and imaged with the fluorescence microscope. Bars = 25 µm.

The coiled hyphal structures were similarly observed in the *pacC*^{CA} mutant at a rate of occurrence that was similar to wild-type. However, in comparison to the wild-type strain, these structures were noticeably larger, more intensely coiled, and had abundant conidia (Figure 3.20). Closer examination of individual hyphae in the *pacC*^{CA} mutants further revealed the widespread presence of intrahyphal hyphae; structures that were not observed in the wild-type strain (Figure 3.21). Given the links between hyphal conidiation and fusion, the latter phenotype was also examined in the *pacC* mutant strains. While hyphal fusion was reported to be absent in hyperconidiating mutants of *E. festucae* (Kayano *et al*., 2013; Tanaka *et al*., 2013), in both *pacC*^{CA} and Δ*pacC* mutants, fusions were observed at a similar rate to the wild-type (Figure 3.22).

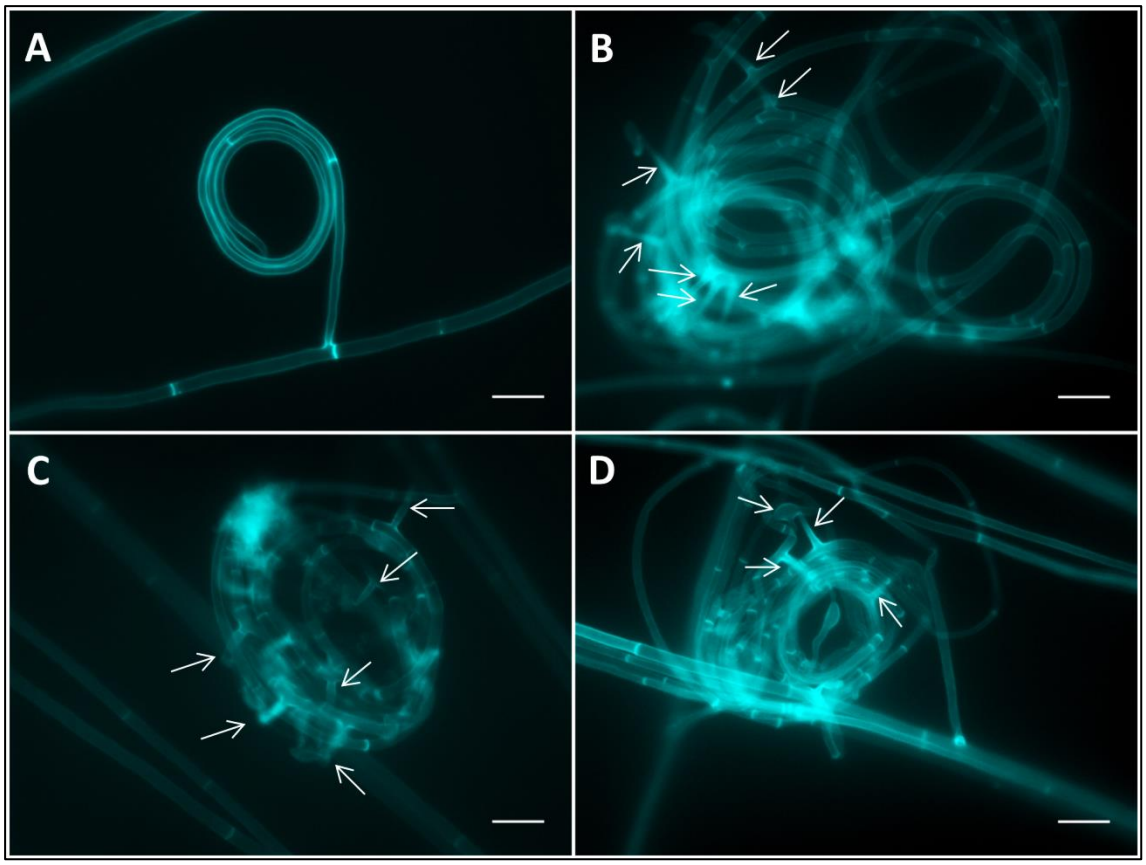

Figure 3.20. Coiled hyphal structures and conidiation in wild-type and *pacC*^{CA} mutants of *E. festucae*. Coiled hyphal structures in (A) Wild-type, and which were increasingly coiled with increased conidiation in (B) *pacC*^{CA} #14, (C) *pacC*^{CA} #19, and (D) *pacC*^{CA} #22 mutants. Mycelia were grown on water agar for 11 days at 22°C. Hyphae were stained with calcofluor white and imaged with the fluorescence microscope. Conidiophores are indicated by the white arrows. Bars = 10 µm.

3.3.10 Sensing and modification of extracellular pH in the *pacC* mutants

PacC is an important transcription factor that responds to ambient pH conditions, acting downstream of the Pal pathway following cleavage by the signaling protease PalB (Section 1.7). Homologues of the Pal proteins; PalH, PalI, PalF, PalC, PalA and PalB were identified in *E. festucae* (Appendix 6.3.6 to 6.3.11). Thus, in the Δ*pacC* mutant, the molecular signal(s) relayed through the Pal pathway in response to changes in extracellular pH should be partially or entirely disrupted; while the *pacC*^{CA} mutant on the other hand should have a constitutive activation of such signal(s).

Therefore, to test if the *pacC* deletion and constitutive active mutants are still able to sense as well as modify ambient pH, mycelia were incubated in pH-defined media and the media pH was measured before and after a set period of growth. Initial measurements using wild-type strain grown in Blankenship media buffered at

different pH(s) showed that changes in media pH were observed within 6 hours. After 24 hours of incubation, pH of the alkaline media dropped from 8.0 to 7.5, while pH of the acidic media rose from 5.2 to 5.9, and pH of the neutral media remained relatively unchanged at 6.7 (Figure 3.23). This experiment was subsequently repeated with wild-type, Δ*pacC*, Δ*pacC*/*pacC*, and *pacC*^{CA} strains using a time point of 6 hours. The results showed that in all *pacC* mutant strains, there was a change in media pH after 6 hours of culture (Figure 3.24). The extent of pH change in the *pacC* mutants was similar to wild-type and was observed to go in both directions; i.e., pH was lowered toward neutral in the alkaline media, and raised toward neutral in the acidic media, indicating that Δ*pacC* and *pacC*^{CA} mutants were able to sense and modify the extracellular pH. The result also suggests that *E. festucae* has a preference of growth under neutral pH conditions.

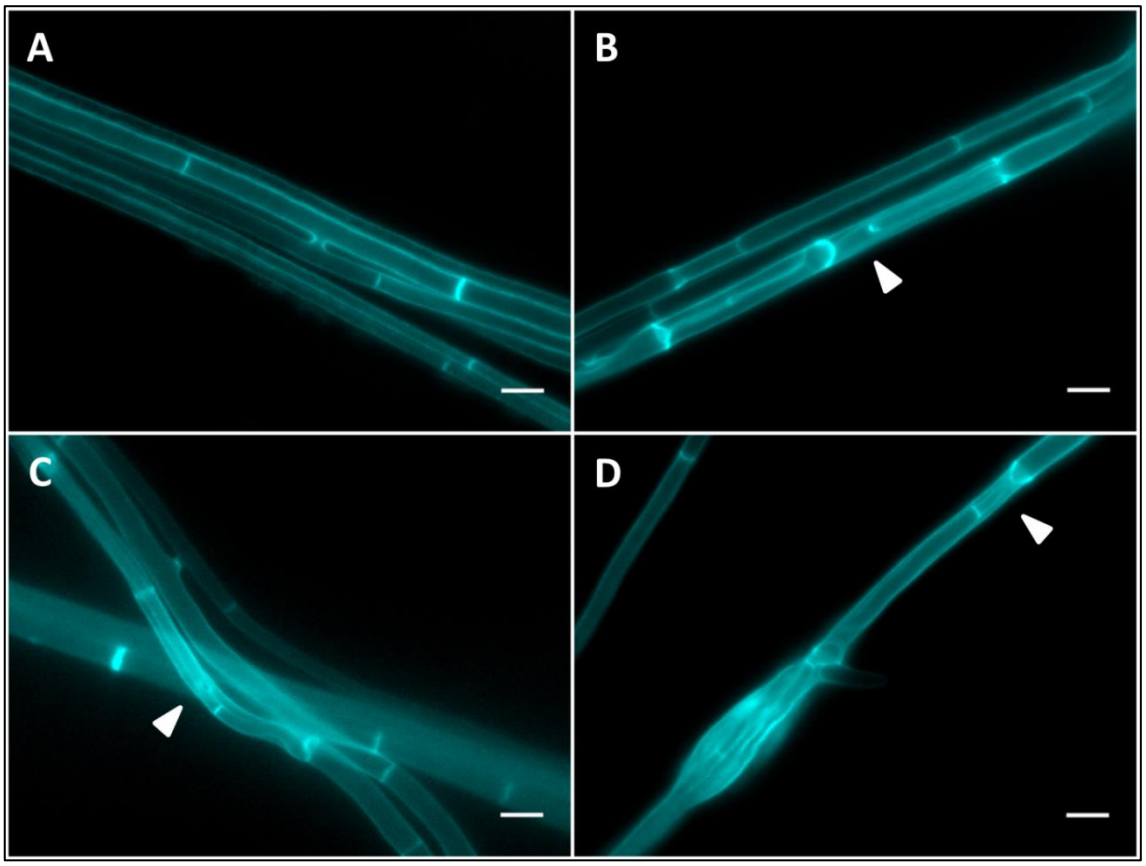

Figure 3.21. Development of normal and intrahyphal hyphae in wild-type and *pacC*^{CA} mutants of *E. festucae*. (A) Hyphal structure and morphology in wild-type strain. (B to D) Intrahyphal hyphae formation in (B) *pacC*^{CA} #14, (C) *pacC*^{CA} #19, and (D) *pacC*^{CA} #22 mutants. White arrows indicate the sites of intrahyphal hyphae formation. Mycelia were grown on water agar for 11 days at 22°C. Hyphae were stained with calcofluor white and imaged with the fluorescence microscope. Bars = 5 µm.

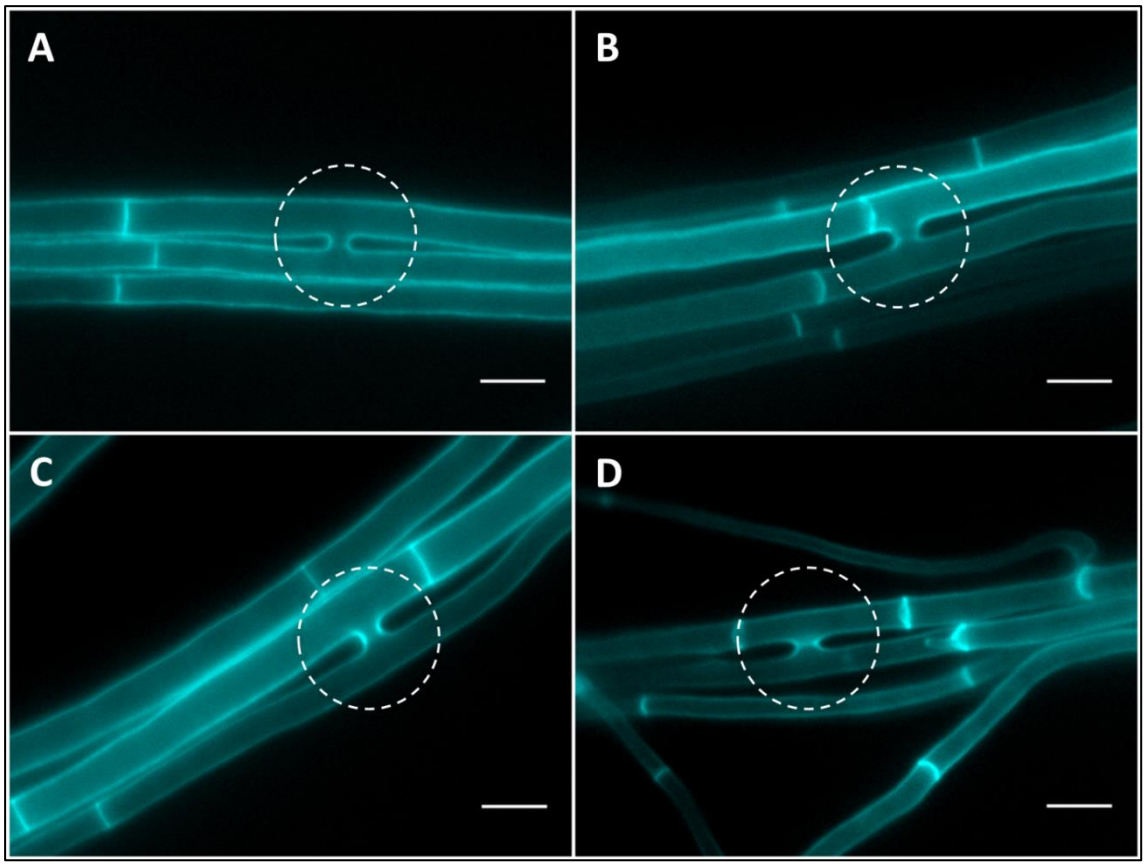

Figure 3.22. Hyphal fusion in wild-type and *pacC* mutants of *E. festucae*. Hyphal fusion in (A) Wild-type, (B) Δ*pacC*, (C) *pacC*^{CA} #14, and (D) *pacC*^{CA} #22. Circles indicate sites of hyphal fusion. Mycelia were grown on water agar for 11 days at 22°C. Hyphae were stained with calcofluor white and images were taken with the fluorescence microscope. Bars = 5 µm.

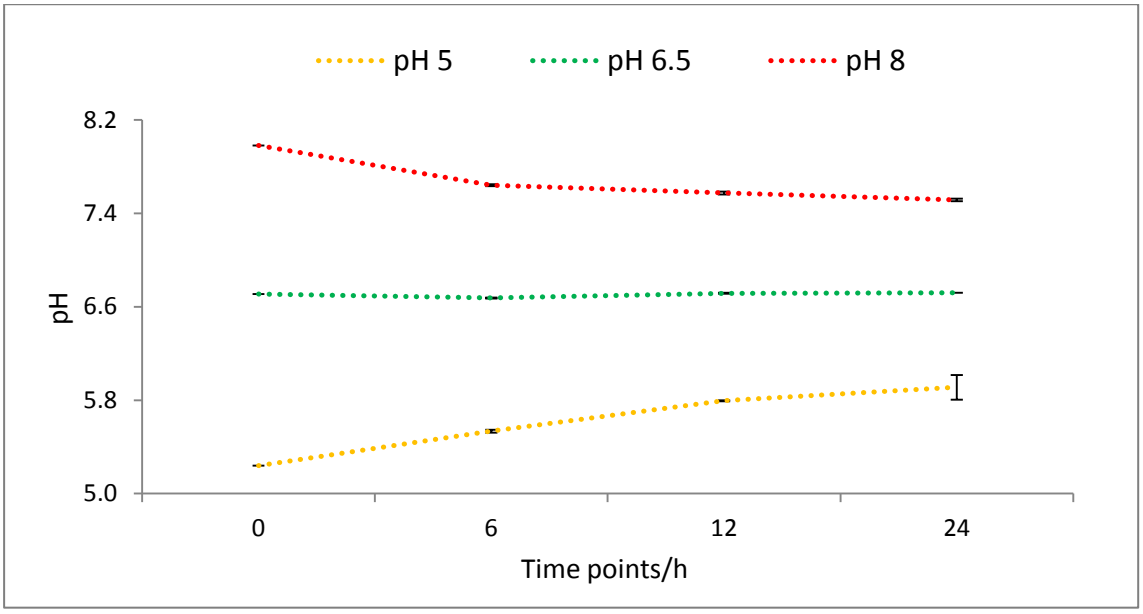

Figure 3.23. Modification of growth media pH by wild-type *E. festucae* strain. pH of media before and after 6, 12 and 24 hours of incubation with wild-type mycelia. Mycelia were grown in PD for 3 days, filtered and washed three times with sterile distilled water and transferred

into Blankenship media buffered at the indicated pH(s). Bars represent standard error of the mean calculated from three biological replicates.

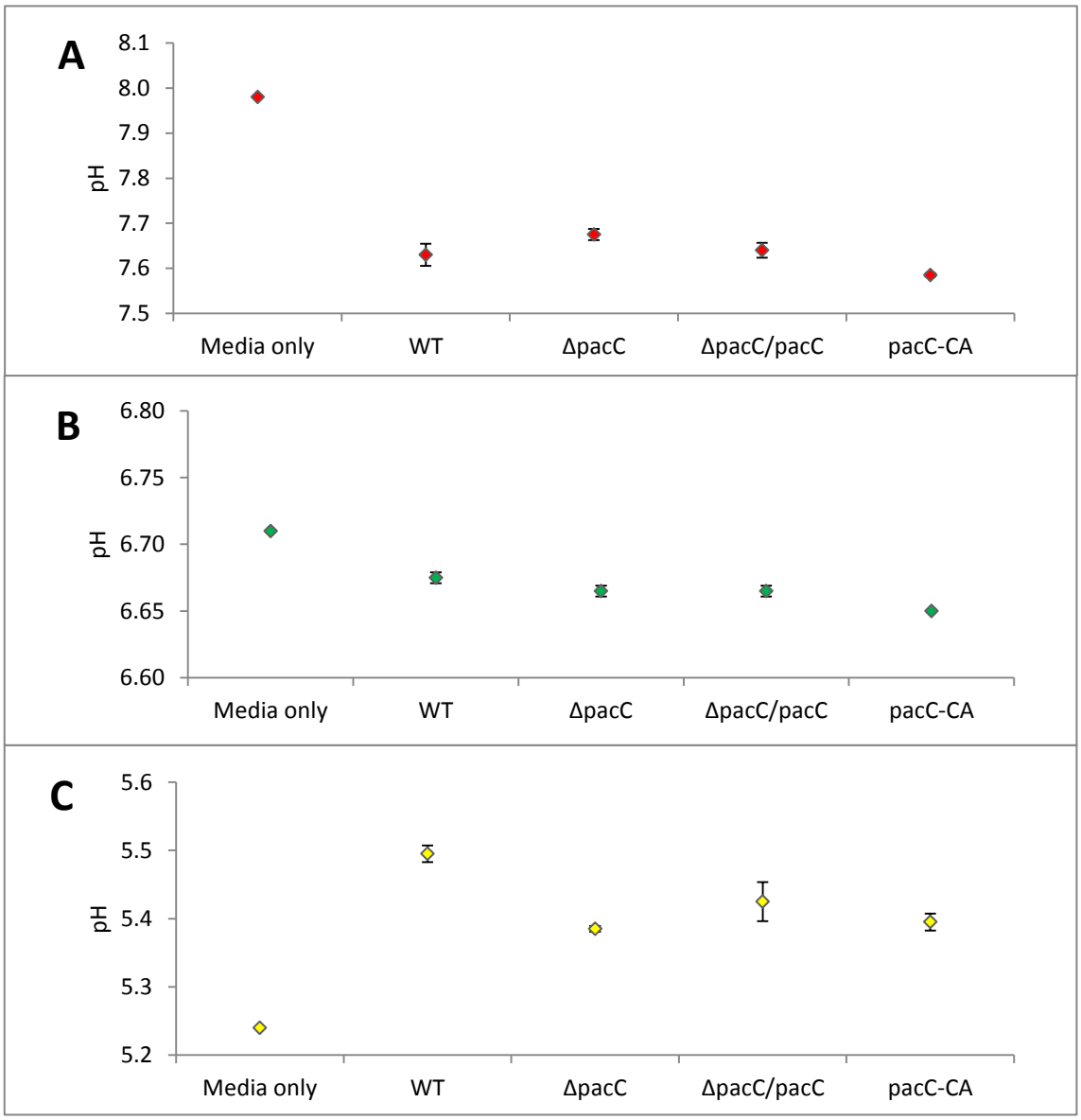

Figure 3.24. Modification of growth media pH by wild-type and *pacC* mutants of *E. festucae*. pH of media before and after 6 hours of incubation with wild-type Δ*pacC*, Δ*pacC*/*pacC*, and *pacC*^{CA} mycelia. Mycelia were grown in PD for 3 days, filtered and washed three times with sterile distilled water and transferred into Blankenship media buffered at the indicated pH(s): (A) pH 8, (B) pH 6.5 and (C) pH 5. Bars represent standard error of the mean calculated from three biological replicates.

3.4 Regulation of secondary metabolism in *E. festucae* by pH and PacC

As PacC is known to regulate secondary metabolism in several different fungi (Espeso *et al.*, 1993; Keller *et al.*, 1997; Merhej *et al.*, 2011; Schmitt *et al.*, 2011; Trushina *et al.*,

2013) the role of PacC in regulating expression of the three main classes of secondary metabolites in *E. festucae* was tested. To this end, seven genes; three from the *LTM* cluster (*ltmE*, *ltmP* and *ltmM*), three from the *EAS* cluster (*easA*, *dmaW* and *lpsA*), and a single gene, *perA*, which codes for a multi-domain protein responsible for peramine biosynthesis, were selected for representative analysis. Two 5'-GCCAAG-3' PacC consensus binding sequences were found in the promoter region of *ltmP*, one was found in the promoter region of *dmaW*, and no PacC binding sequences were found in the 1 kb promoter regions of the remaining five genes.

Standard curves were generated for each gene and primer efficiencies were found to range between 1.86 to 1.96 (Appendix 6.4.1 and 6.4.2). qRT-PCR was subsequently performed on total RNA extracted from wild-type mycelia grown in PD media and the results showed that only two genes; *lpsA*, and *perA*, were above the detection limit (Cp value <35; results not shown). In comparison, culture in the Blankenship medium, which has been shown to induce the expression of *lol* genes in *E. festucae* strain E2368 (Blankenship *et al*., 2001) resulted in detectable levels of *ltmE*, *easA*, *dmaW*, *lpsA* and *perA* (described in the next section). The expression levels of *ltmP* and *ltmM* remained undetectable in this medium. Interestingly, the expression levels of *lpsA* and *perA*, which were detectable in PD medium, were not upregulated in the Blankenship medium. Taking these results into consideration, the Blankenship medium was used in subsequent experiments to analyse the expression of secondary metabolite genes.

3.4.1 Role of pH and PacC in regulating secondary metabolism in *E. festucae*

The role of PacC in regulating secondary metabolism in *E. festucae* was subsequently investigated by incubating wild-type, Δ*pacC*, Δ*pacC*/*pacC* and *pacC*^{CA} mycelia in pH-defined Blankenship media. A pilot experiment was performed using wild-type strain and time points of 6, 12 and 24 hours of incubation in pH-defined Blankenship media. However, after 12 and 24 hours, the differences in the expression of secondary metabolite genes and *pacC* between the different pH conditions were less distinguishable from 6 hours (results not shown), perhaps due to neutralisation of the media (Section 3.3.10). The experiment was thus repeated with a shorter time point of 2 hours. In this experiment, data were normalised against the expression of the 40S ribosomal protein S22 (*RPS22*) and elongation factor-2 (*EF*-2) reference genes, and both

gave very similar results in all analyses. Consequently, just the data normalised to the *RPS22* reference gene are presented.

The expression of *pacC* was firstly considered, and found to be pH-dependent in the wild-type strain. The expression of *pacC* at pH 8 was 1.9-fold the expression in pH 6.5; and the expression at pH 6.5 was 1.8-fold the expression at pH 5 (Figure 3.25A). As anticipated, the *pacC* transcript was not detectable in the deletion mutant. The expression of *pacC*^{CA} construct, which product is expected to be activated independent of alkaline pH was stable across all pH conditions in the *pacC*^{CA} mutant at a level similar to the expression of *pacC* in the wild-type strain at pH 6.5 (Figure 3.25A).

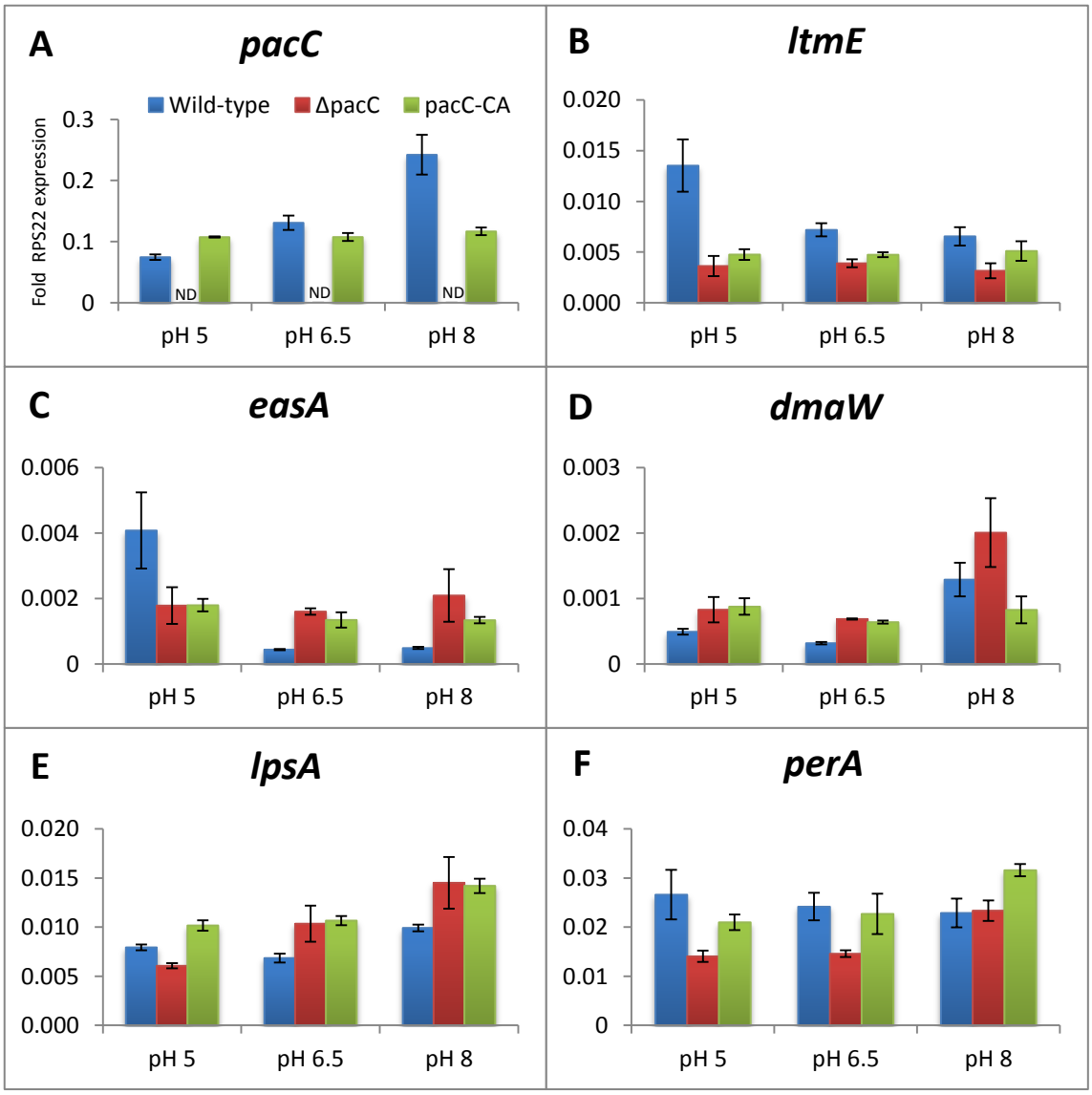

Figure 3.25. Effect of pH and *pacC* mutations on secondary metabolite gene expression in culture. (A to F) Steady-state mRNA levels of secondary metabolite genes in wild-type, Δ*pacC* #8 and *pacC*^{CA} #14 mutants of *E. festucae* grown in culture. The transcript analysed in the *pacC*^{CA} mutant in (A) refers to the *pacC*^{CA} transcript and not the endogenous *pacC* transcript. Mycelia

were cultured in Blankenship media buffered at pH 6.5 for 5 days, washed, and transferred to fresh Blankenship media buffered at pH 5, 6.5 or 8 and incubated for a further 2 hours before harvesting. Total RNA extracted from mycelia was used to synthesise cDNA. Primers used in the analyses are listed in Table 2.3. Absolute values were determined by interpolation from a standard curve and normalised to the expression levels of the 40S ribosomal protein S22 (*RPS22*) reference gene. Y-axes represent relative expression of the gene to that of *RPS22*. Bars represent standard error of the mean calculated from three biological replicates. N.D.; not detectable.

All of the secondary metabolite genes were minimally expressed in all strains under all pH conditions, indicating that pH alone is insufficient to turn on secondary metabolite gene expression in *E. festucae* (Figure 3.25). In the wild-type strain, expression of *ltmE* and *easA* was induced under acidic pH, but surprisingly, this induction was absent in the Δ*pacC* mutant, suggesting that PacC may be required for the induction of these genes under acidic pH conditions - a state in which PacC is thought to be inactive (Figure 3.25B and C). However, the indication that PacC is required for expression of these genes is complicated by the lack of induction of these genes in the *pacC*^{CA} mutant, suggesting that over-activation of PacC may in fact prevent the upregulation of these genes (Figure 3.25B and C). The expression of *easA* at neutral and alkaline pH was ~4 times lower in wild-type than in the Δ*pacC* mutant strain, suggesting that alkaline pH-activated PacC may act to repress the *easA* gene. However, the *pacC*^{CA} mutant did not show a greater repression of *easA* than wild-type, which would be expected if PacC was acting as a repressor (Figure 3.25B and C).

The expression of *dmaW* was upregulated in both wild-type and Δ*pacC* mutant under alkaline pH condition, indicating that this upregulation is alkaline pH- but not PacC-dependent (Figure 3.25D). This upregulation, however, was not seen in the *pacC*^{CA} mutant. In the case of *lpsA*, a general trend of increasing expression with increasing pH was observed in all three strains, suggesting that the upregulation of this gene may also be alkaline pH-dependent but PacC-independent (Figure 3.25E). Lastly, the expression of *perA* in wild-type and *pacC*^{CA} mutant remained relatively unchanged across the different pH conditions (Figure 3.25F). In the Δ*pacC* mutant, however, expression of *perA* in acidic and neutral pH was only half that of wild-type and *pacC*^{CA} strains, indicating a repressive role for PacC under acidic conditions (Figure 3.25F).

These results do not provide strong evidence for PacC regulation of secondary metabolite genes in *E. festucae*; but indicate that some genes can be alkaline pH-induced but PacC-independent, and also suggest some active role of PacC at acidic pH in *E.*

festucae. However, the genes were very lowly expressed and the differences observed between treatments and strains were small; thus it is possible that the differences were due to sample variability instead of a bona fide effect of pH or mutations in *pacC*.

3.4.2 Expression analysis of secondary metabolite genes *in planta*

The secondary metabolite genes in *E. festucae* are naturally repressed in axenic culture, due in part to global silencing effects such as heterochromatic repression of genes. Therefore, the role of PacC in regulating the secondary metabolite genes was also investigated *in planta*, where heterochromatic gene silencing effects are abolished (Chujo & Scott, 2014). To this end, *L. perenne* plants were artificially infected with wild-type and *pacC* mutant strains, and the expression of secondary metabolite genes was determined in the pseudostem regions of endophyte-infected plants.

In the wild-type strain, expression of all secondary metabolite genes was considerably higher *in planta* than *in vitro*, ranging from a 60-fold difference in the expression of *perA* to a 1000-fold difference in the expression of *easA* and *dmaW* (Figure 3.26). Analysis of the steady-state mRNA levels in this strain showed the expression of *pacC* to be 0.14-fold of *RPS22* in the plant, closely similar to the expression level *in vitro* which was 0.13-fold of *RPS22* at pH 6.5 (Figure 3.27A). A measurement of the apoplast fluid pH taken from pseudostem regions of a wild-type-infected plant revealed a pH of 6.12 (Section 3.5; Table 3.2). These results indicate that the apoplast environment where *E. festucae* grows in has a pH that is close to neutral. The expression of *pacC* in the complemented mutant was relatively similar at 0.16-fold of *RPS22* and some expression of *pacC* was detectable in the Δ*pacC* mutant, likely due to contamination of the plant samples (Figure 3.27A). The expression of $pacC^{CA}$ in the $pacC^{CA}$ mutant was also relatively similar *in planta* and *in vitro*, at about 0.08 and 0.10-fold the expression of *RPS22*, respectively (Figure 3.27A). The interpretation of these results, however, assumes that there is no difference in the expression levels of *RPS22* and *EF-2 in planta* and *in vitro*.

Analysis of the steady-state levels of the *ltm* genes (*ltmE*, *ltmP* and *ltmM*) showed that there was no difference in the expression of these genes among wild-type, Δ*pacC*, and $pacC^{CA}$-infected plants (Figure 3.27B to D). Analysis of *easA* and *dmaW* also showed no difference among the strains (Figure 3.27E and F). The expression of *lpsA* was slightly reduced in the *pacC* mutants compared to wild-type, however this reduction was also

present in the complemented strain (Figure 3.27G). Only one gene, *perA*, appeared to be differently expressed and downregulated in the *pacC*^{CA} mutant (Figure 3.27H). Taken together with results from the *in vitro* expression analyses, these findings do not support the hypothesis that PacC regulates secondary metabolite pathways in *E. festucae*.

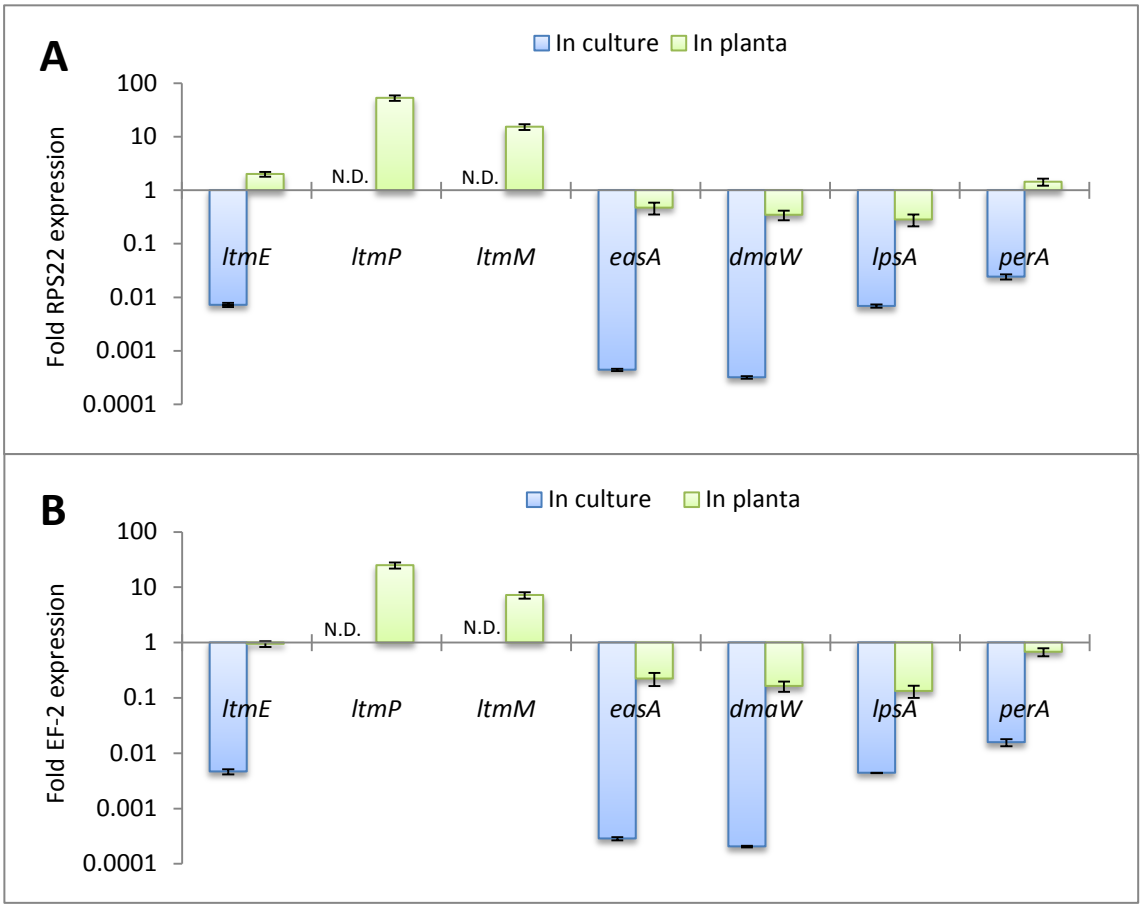

Figure 3.26. Expression of secondary metabolite genes in wild-type *E. festucae* in culture and *in planta*. Differences in the expression of secondary metabolite biosynthetic genes by wild-type *E. festucae* in axenic culture and *in planta*, shown relative to the levels of (A) *RPS22* and (B) *EF*-2 reference genes. Values were determined by interpolation from a standard curve, Y-axes represent relative mRNA abundance to the *RPS22* or *EF*-2 reference gene transcripts. Bars represent standard error of the mean calculated from three biological replicates. N.D.; not detectable.

3.5 Symbiotic phenotypes of *pacC* mutants of *E. festucae*

In several other pathogenic fungi studied, PacC has been shown to control virulence and pathogenicity of the fungi toward their hosts (Bignell *et al.*, 2005; Caracuel *et al.*, 2003b; Davis *et al.*, 2002; Ortoneda *et al.*, 2004). However no study has been done to date which looks at the role of PacC in a symbiotic interaction. To investigate the role

of PacC in the symbiosis of *E. festucae* with perennial ryegrass, *L. perenne* plants were infected with the acid-mimicking (Δ*pacC*) and alkaline-mimicking (*pacC*^{CA}) mutants of *E. festucae* and the resulting host phenotypes were observed.

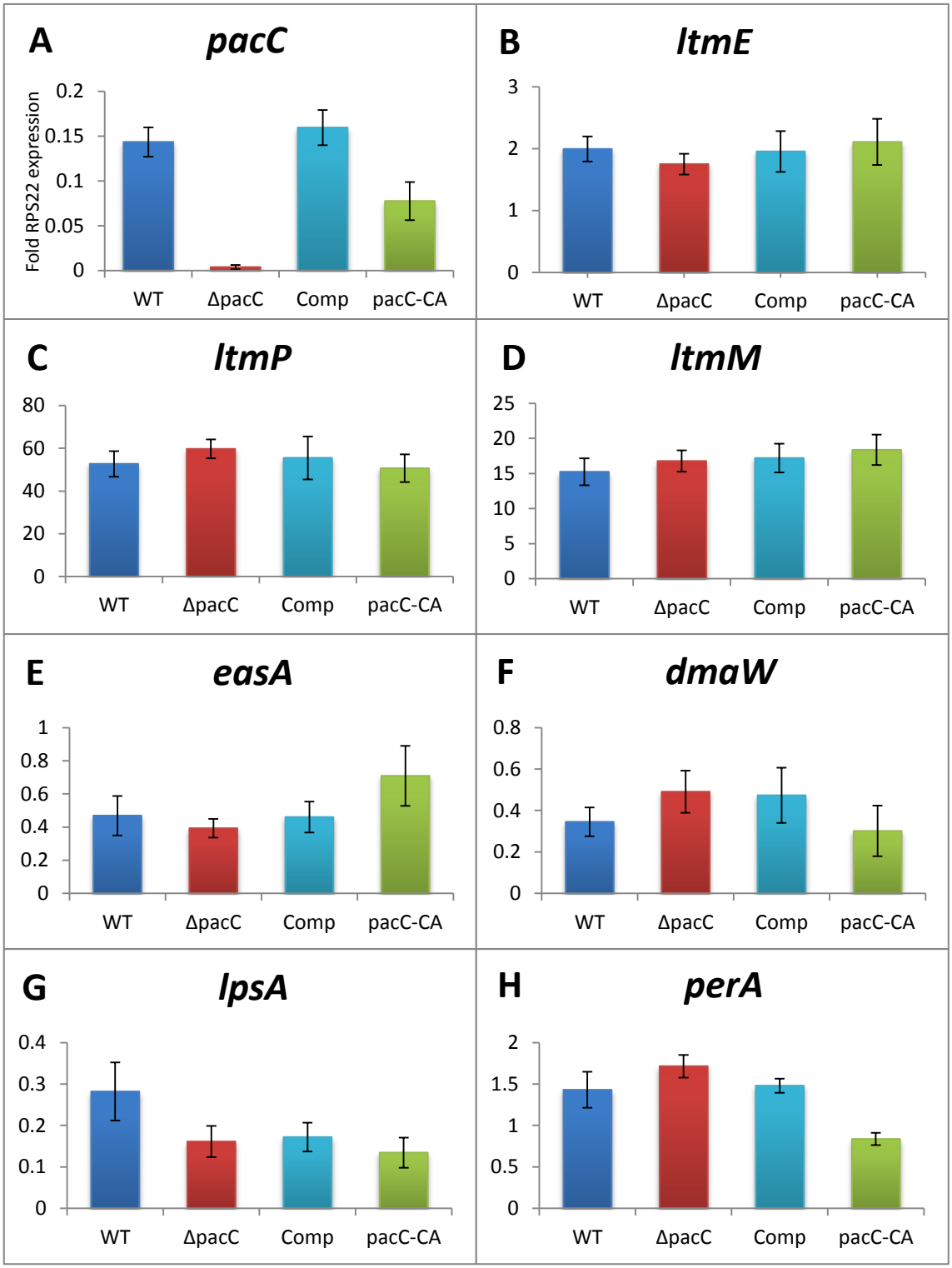

Figure 3.27. Expression of secondary metabolite genes in wild-type and *pacC* mutants *in planta*. Steady-state mRNA levels of (A) *pacC*, (B) *ltmE*, (C) *ltmP* and (D) *ltmM*, (E) *easA*, (F) *dmaW*, (G) *lpsA* and (H) *perA* in wild-type, Δ*pacC*, Δ*pacC*/*pacC*, and *pacC*^{CA} mutant-infected

ryegrass. Total RNA was isolated from pseudostems of endophyte-infected ryegrass at 10 weeks post inoculation and used for cDNA synthesis. Absolute values were determined by interpolation from a standard curve and normalised to the expression levels of the 40S ribosomal protein S22 (*RPS22*) reference gene (y-axes). In (A), the *pacC*^{CA} transcript was measured instead of *pacC* for *pacC*^{CA} mutant. Bars represent standard errors of the mean calculated from three biological replicates.

At 9 weeks post-inoculation, a tiller from each plant was immunoblotted in order to screen for infection-positive plants. Both Δ*pacC* and *pacC*^{CA} mutants gave vastly different infection rates in three experiments, ranging from about 60 to 80% for the Δ*pacC* mutant, and 45 to 95% for the *pacC*^{CA} mutants (Table 3.1). In some experiments, both Δ*pacC* and *pacC*^{CA} mutants showed lower infection rates of about 60%, compared to the 90% seen in the wild-type strain; however, a similar lower infection rate of about 60% was also seen in the complementation strain (Table 3.1). These results suggest that there is no significant difference in the infection rates of wild-type and *pacC* mutants but reveal a high variability in infection rates between experiments.

		Experiment 1			**Experiment 2**			**Experiment 3**		
Strain	Strain no.	Screened	Infected	**% infected**	Screened	Infected	**% infected**	Screened	Infected	**% infected**
Wild-type	Fl1	29	24	***82.8***	54	46	***85.2***	9	9	***100.0***
ΔpacC	#8	22	13	***59.1***	25	13	***52.0***	16	13	***81.3***
	#11				29	15	***51.7***	12	10	***83.3***
	#73	12	7	***58.3***						
ΔpacC/pacC	#2	21	13	***61.9***	31	21	***67.7***	11	7	***63.6***
	#7				33	20	***60.6***			
pacC-CA	#14	20	16	***80.0***	21	11	***52.4***	39	17	***43.6***
	#19	15	10	***66.7***	19	10	***52.6***	18	17	***94.4***
	#22							27	12	***44.4***

Table 3.1. Ryegrass infectivity rates of wild-type and *pacC* mutants. Table showing number of plants screened and those that were positive for infection by the indicated *E. festucae* strains. Results from three independent experiments are shown. Percent infectivity was calculated from [(no of plants infected/no of plants screened) x 100%].

To investigate if mutations in *pacC* lead to a change in the host apoplast pH, apoplast fluid was extracted from wild-type and *pacC*-mutant-infected ryegrass and the pH were measured (Section 2.11.4). Apoplast fluid extracted from wild-type and *pacC* mutant-infected pseudostem had comparable pH of about 6.3 to 6.4 (Table 3.2A). Interestingly, the pH of the blade regions of the plants were slightly more acidic with values of 6.1 to 6.2, but were not significantly different between wild-type and *pacC*-mutant infected plants (Table 3.2B).

A				B			
Pseudostem	WT	ΔpacC #11	pacC-CA #14	**Blade**	WT	ΔpacC #11	pacC-CA #14
	6.32	6.59	6.41		6.12	6.19	6.28
		6.41	6.38			6.02	6.13
		6.20				6.04	
Average	6.32	6.40	6.40	Average	6.12	6.08	6.21
S.D.	N.A.	0.20	0.02	S.D.	N.A.	0.09	0.11

Table 3.2. Apoplast pH of endophyte-infected ryegrass plants. (A) pH of pseudostem regions of wild-type, Δ*pacC* #11 and *pacC*^{CA} #14-infected ryegrass. (B) pH of blade regions of wild-type, Δ*pacC* #11 and *pacC*^{CA} #14-infected ryegrass. S.D. = standard deviation of mean calculated from two or three biological replicates.

3.5.1 *pacC*^{CA} mutant-infected ryegrass plants are mildly hypertillered

Whole-plant phenotype analyses indicated that perennial ryegrass infected with the Δ*pacC* mutants had similar leaf, stem and root morphologies to wild-type-infected plants (Figure 3.28). On the other hand, ryegrass plants infected with the *pacC*^{CA} mutants had slightly larger root systems and a mild hypertillering phenotype compared to wild-type infected plants (Figure 3.29A). This phenotype was most noticeable in plants infected with *pacC*^{CA} mutant #14 which had the highest expression level of the *pacC*^{CA} construct (Figure 3.29B). A tiller count performed on these plants revealed that plants infected with the *pacC*^{CA} mutants, in particular with *pacC*^{CA} #14 had a slight increase in tiller number (Figure 3.30). Although the difference in expression of *pacC*^{CA} transcript in *pacC*^{CA} #14 was only 1.6-fold more than the expression in *pacC*^{CA} #19 and 1.4-fold more than the expression in *pacC*^{CA} #22 (Figure 3.28B), the expression of *pacC* in wild-type strain at pH 8 was also greater than pH 6.5 by only 1.8-fold. Thus, while the increase in *pacC*^{CA} expression in mutant #14 was relatively small, it is likely to be responsible for the increased host hypertillering phenotype seen in plants infected with this mutant. Given that a number of symbiotic mutants induce premature senescence of the host plants (Eaton *et al*., 2010; Takemoto *et al*., 2006; Tanaka *et al*., 2006, 2013), these plants were maintained up till 17 weeks post-inoculation but no indication of premature senescence was observed (results not shown).

3.5.2 Aberrant hyphal morphology of the *pacC*^{CA} mutants *in planta*

The difference in the hypertillered phenotype of *pacC*^{CA} mutant-infected plants was examined more closely by confocal microscopy to visualise the growth of the

endophyte *in planta*. Wheat germ agglutinin (WGA) conjugated to the AlexaFluor488 fluorophore was used to stain chitin-rich septa and aniline blue was used to visualise the fungal cytoplasm.

Figure 3.28. Phenotype of perennial ryegrass plants infected with wild-type and Δ*pacC* mutants. Plants were infected with the indicated endophyte strains. Image was taken at 10 weeks post-inoculation.

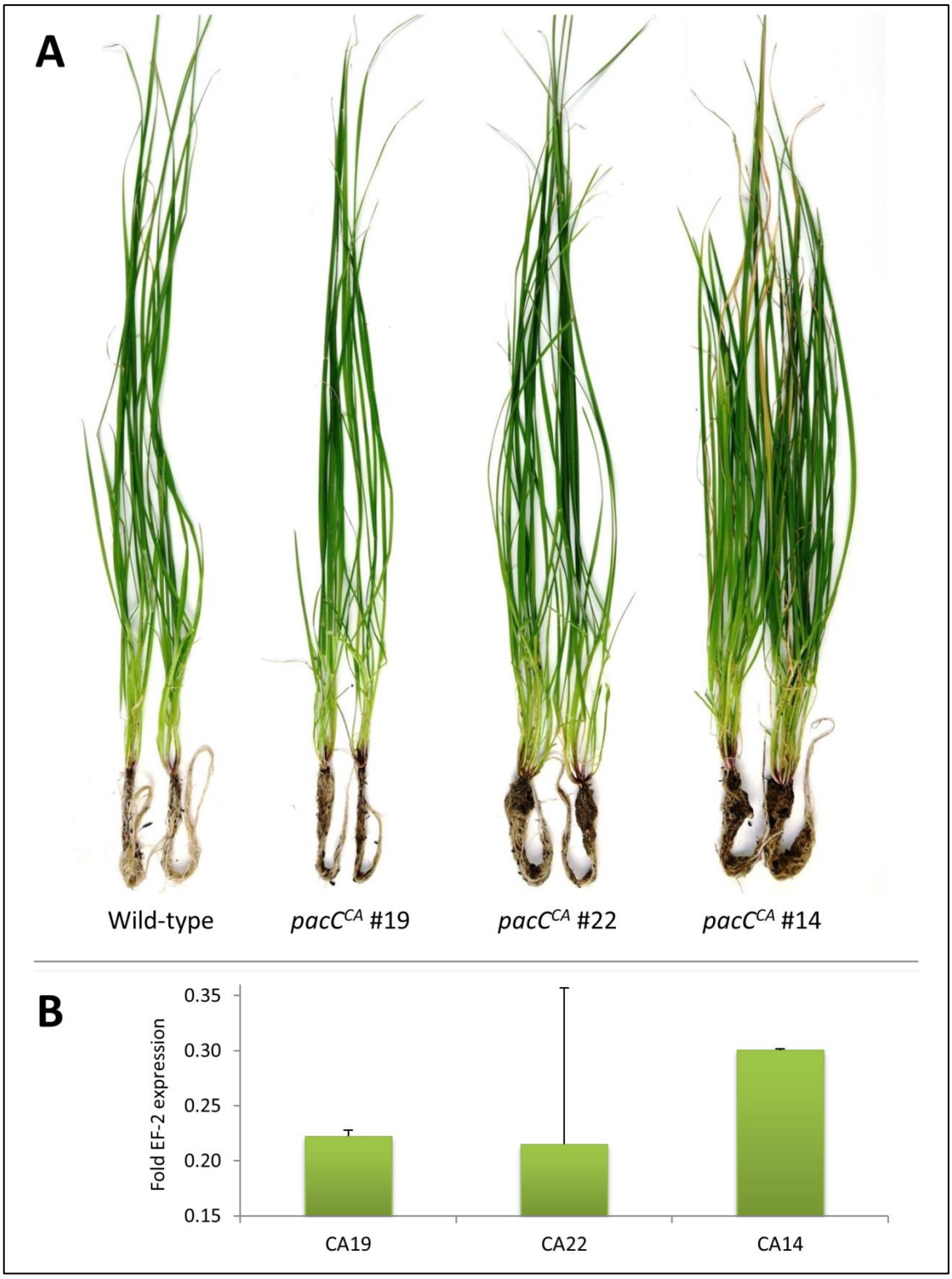

Figure 3.29. Phenotype of ryegrass plants infected with wild-type and *pacC*^{CA} mutants. (A) Image of ryegrass plants taken at 10 weeks post-inoculation. (B) Expression levels of *pacC*^{CA} in the indicated *pacC*^{CA} mutants in culture. Mycelia were cultured in PD media for 3 days at 22°C and total RNA was used for cDNA synthesis. Values were normalised against the *EF*-2 reference gene. Bars represent standard deviation of the mean calculated from two technical replicates.

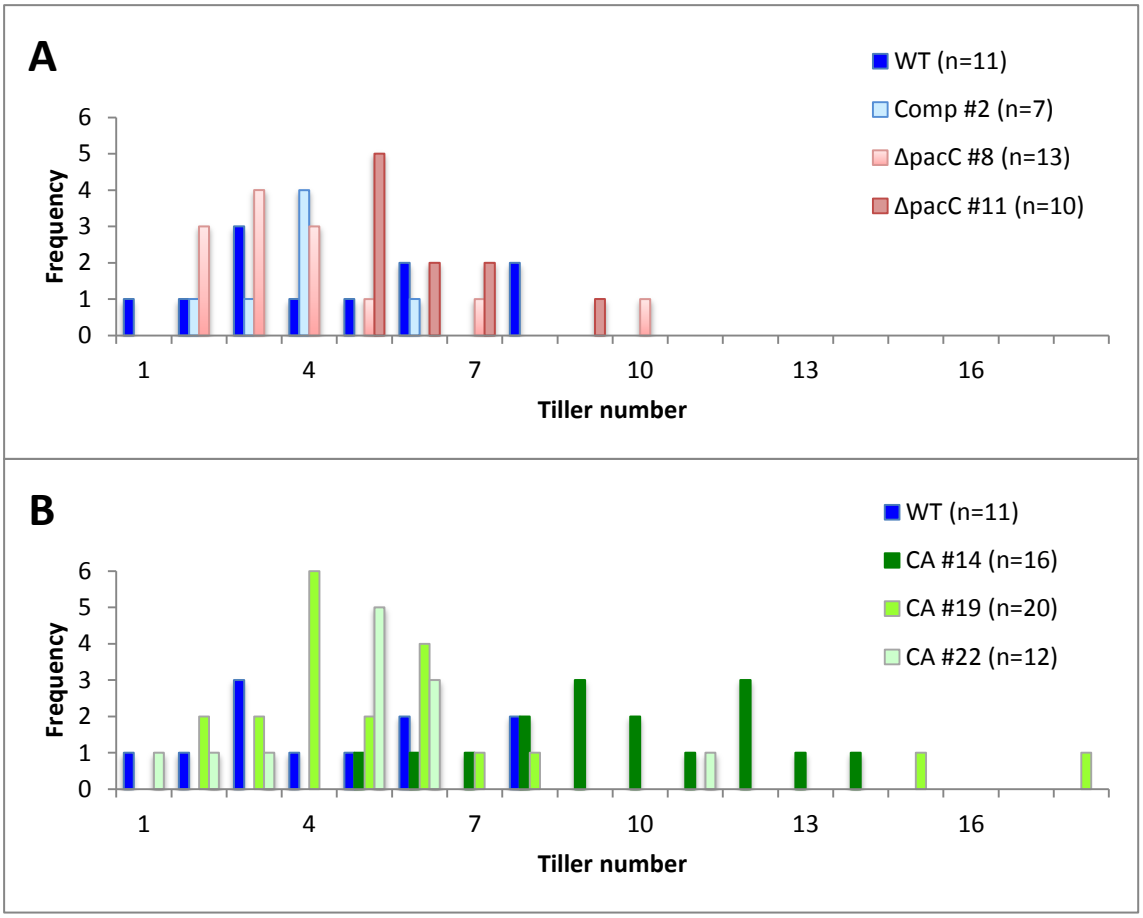

Figure 3.30. Effects of *pacC* mutants on tiller number of perennial ryegrass. Tiller number of *L. perenne* plants infected with (A) wild-type, Δ*pacC* and complemented strains, and (B) wild-type and *pacC*^{CA} mutants of *E. festucae* counted at 10 weeks post inoculation. The numbers of infected plants used in the count are indicated in the legend.

Growth of the Δ*pacC* mutants (Δ*pacC* #8 and #11; results not shown for Δ*pacC* #11) in the plant was similar to the wild-type strain; hyphae grew in a restricted pattern between plant cells parallel to the leaf axis, seldom branched and had regularly-spaced septa (Figure 3.31A and B). A similar restricted growth pattern was seen in plants infected with the *pacC*^{CA} mutants #14, #19 and #22 (Figure 3.31C and D; results not shown for *pacC*^{CA} #19). However in *pacC*^{CA} #14-infected samples, hyphae were also frequently observed to aggregate close to host vascular bundles (Figure 3.31C). These aggregations were typically accompanied by the absence of hyphae throughout the adjacent leaf areas; indicating that the hyphal networks surrounding the host vascular bundle may be chemotactically attracted to grow near, or possibly in, the nutrient-rich transport system of the host. These hyphal aggregations and preference of growth near host vascular bundles were not observed in *pacC*^{CA} #19 and #22, which indicates that

the abnormal hyphal behaviour in *pacC*^{CA} #14 may be due to the higher expression of *pacC*^{CA} construct in the mutant.

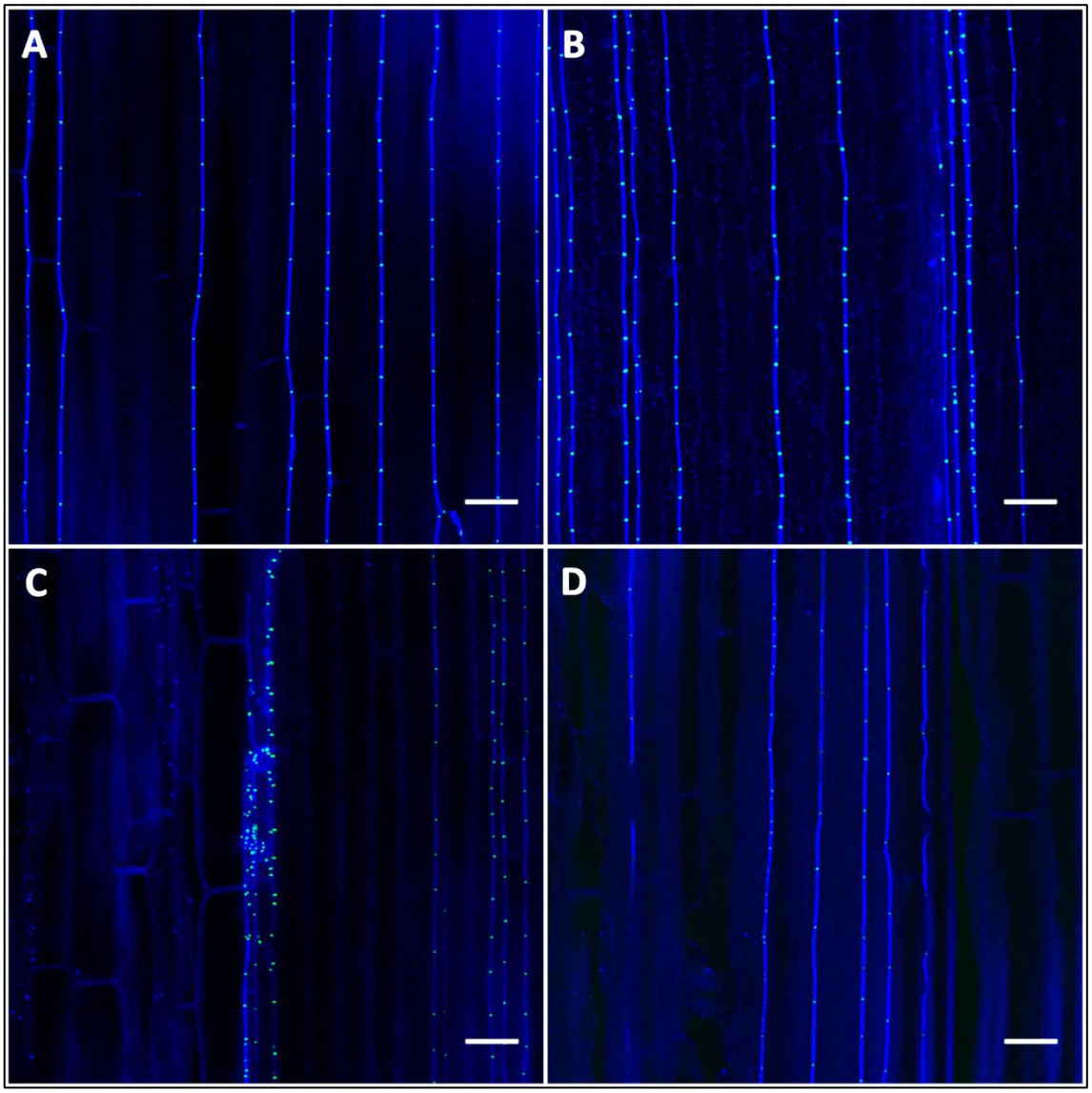

Figure 3.31. Growth of wild-type and *pacC* mutants in the ryegrass host. Confocal depth series images of longitudinal pseudostem sections of plants infected with (A) wild-type, (B) Δ*pacC* #8, (C) *pacC*^{CA} #14, and (D) *pacC*^{CA} #22 mutants of *E. festucae*. Images are 10 µm maximum intensity projections (Z-stacks) of composite images. Aniline blue was used to stain fungal cytoplasm, visualised in blue; and WGA/AlexaFluor488 was used to stain fungal septa, visualised in green. Bars represent 50 µm.

Closer examination of these aggregations in the *pacC*^{CA} #14-infected samples revealed that hyphae within the aggregations were intricately convoluted, had extensive ramifications, and where septa occurred they were at irregular distances (Figure 3.32A and B). Despite the absence of hyphal aggregations and preferential growth near host vascular bundles, such convoluted structures were also observed in *pacC*^{CA} #22 (Figure

3.32C). These hyphal convolutions were similarly formed in *pacC*^{CA} #19, but were less frequently observed (results not shown). In contrast, these aggregations were not observed in the wild-type strain, even after careful analysis of at least 2 samples each from 3 biological replicates (Figure 3.32D). Hyphal breakages were also frequently observed in the *pacC*^{CA} mutant-infected samples; whereas in the wild-type-infected plants, hyphal breakages were a very rare occurrence (Figure 3.33).

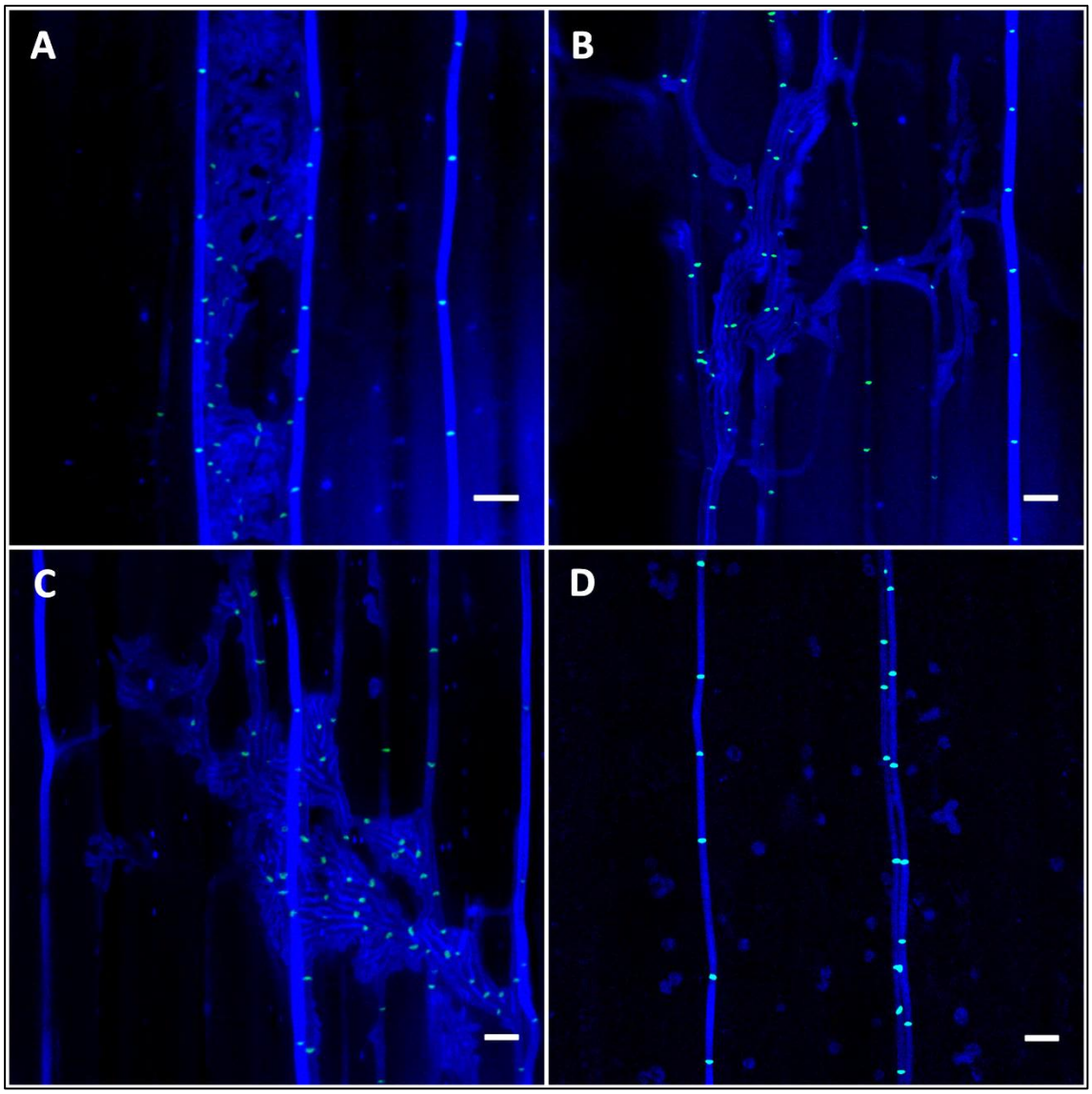

Figure 3.32. Hyphal morphology of wild-type and *pacC*^{CA} mutants *in planta*. Confocal depth series images of longitudinal pseudostem sections of plants infected with (A) wild-type, (B and C) *pacC*^{CA} #14, and (D) *pacC*^{CA} #22 mutants of *E. festucae*. Images are 10 µm maximum intensity projections (Z-stacks) of composite images. Aniline blue was used to stain fungal cytoplasm, visualised in blue; and WGA/AlexaFluor488 was used to stain fungal septa, visualised in green. Bars represent 10 µm.

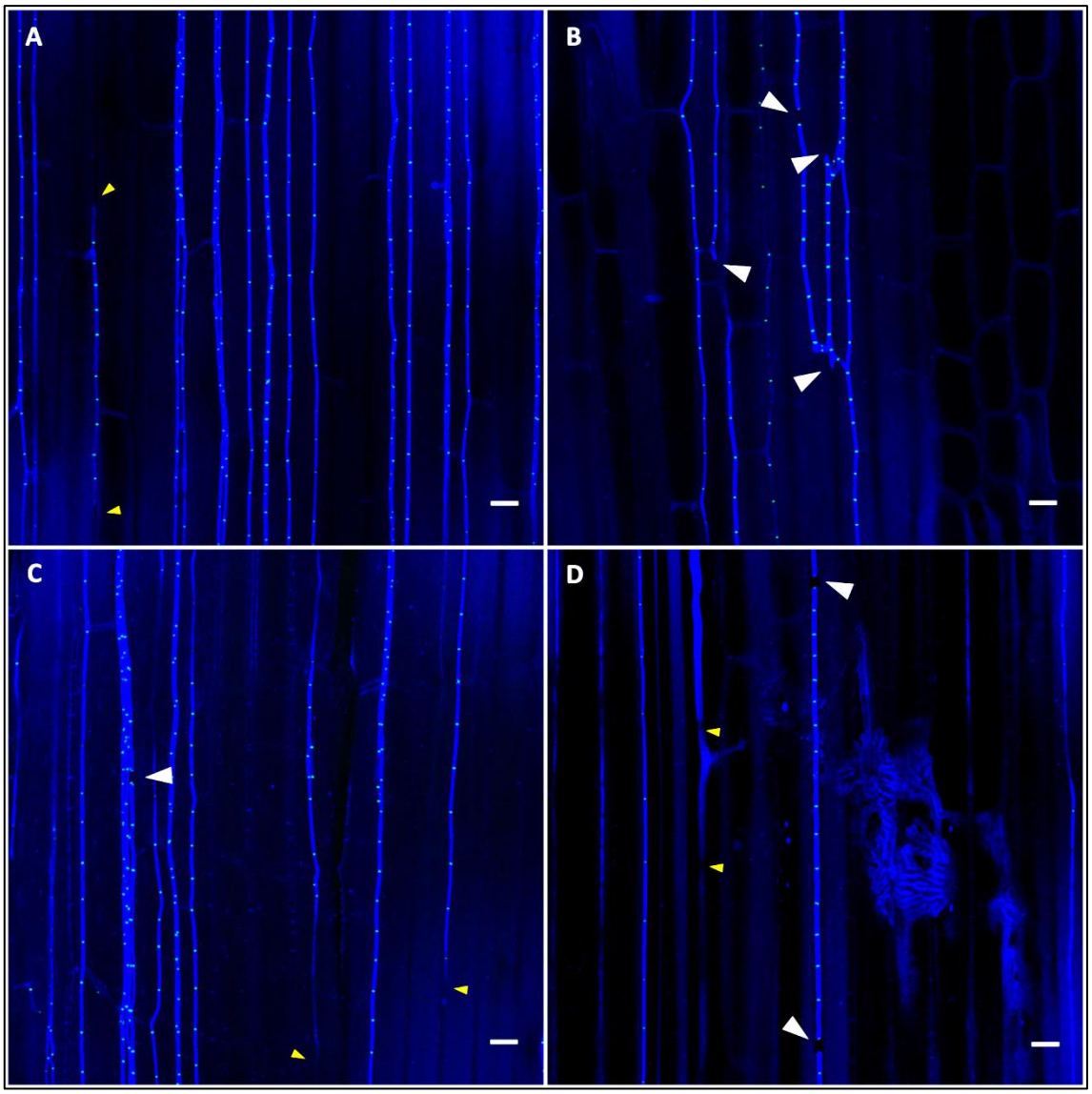

Figure 3.33. Hyphal breakage in *pacC*^{CA} mutants. Confocal depth series images of longitudinal pseudostem sections of plants infected with (A) wild-type, (B) *pacC*^{CA} #14 (C), *pacC*^{CA} #19, and (D) *pacC*^{CA} #22 mutants of *E. festucae*. Images are 10 µm maximum intensity projections (Z-stacks) of composite images. Aniline blue was used to stain fungal cytoplasm, visualised in blue; and WGA/AlexaFluor488 was used to stain fungal septa, visualised in green. Sites of hyphal breakages are indicated by white arrows, and sites where hyphae interweave through the plant layers are indicated by smaller yellow arrows. Bars represent 10 µm.

4. Discussion

4. Discussion

The aim of this study was to characterise the cellular roles of the PacC transcription factor in the plant symbiont *Epichloë festucae* and in the symbiotic association of the fungus with perennial ryegrass. PacC (Rim101p) is activated under extracellular alkaline pH conditions by the Pal (RIM101) pathway, one of the main pH-responsive signaling pathways in filamentous fungi. In various fungal species studied, the PacC transcription factor was found to regulate important cellular processes, particularly fungal pathogenicity and secondary metabolism. The finding in the recent RNAseq study (Eaton *et al*., 2010) that *pacC* was upregulated in a symbiotically-defective *E. festucae* mutant implicates a role for PacC in the *E. festucae*-*L. perenne* symbiosis. The decreased expression of secondary metabolite biosynthetic genes in the mutant additionally indicates a role for PacC in regulating secondary metabolism in *E. festucae*.

Using a range of bioinformatics tools, a putative *pacC* gene was identified in the *E. festucae* genome and shown to code for a protein containing several known and conserved domains characteristic of PacC. The corresponding transcript of this gene could be detected in cell extracts and its expression was found to be dependent on alkaline pH. This is in accordance with findings in other fungi where alkaline pH-activated PacC acts to induce its own transcription in an auto-regulatory manner (Tilburn *et al*., 1995; Caracuel *et al*., 2003b). A Δ*pacC* mutant was generated and shown to have reduced salt tolerance, a phenotype similar to results obtained for Δ*pacC* mutants in other fungi (Caracuel *et al*., 2003a; Lamb & Mitchell, 2003). Taken together, these results indicate that the gene identified in *E. festucae* is a true homologue of *pacC*.

4.1. Phenotypes of the Δ*pacC* mutant

The premature senescence phenotype of the Δ*pacC* mutant in *E. festucae* has not been reported so far in other fungi. In *E. festucae*, colony senescence is typically marked by the onset of a 'wet' appearance which indicates a loss of colony hydrophobicity. Fungal senescence is a complex process that is primarily caused by mitochondrial dysfunction as a result of the accumulation of mutant mitochondrial DNA or plasmids (Bertrand, 2000). The transmission of this genetic material between cells and throughout the whole organism is made possible in filamentous fungi by the formation of septa and hyphal anastomoses. Although the Δ*pacC* mutant was observed to fuse normally, it

would be interesting to test if fusion-defective mutants of *E. festucae*, such as Δ*proA* and Δ*noxA*, are less susceptible to senescence. Disruptions to mitochondrial functions that lead to senescence can also be caused by changes in the activity of other cellular proteins such as cytochromes a, b and c, as observed in *Neurospora* and *Podospora* (Pittenger, 1956; Begel *et al*., 1999). It is unknown if changes in these proteins are responsible for the senescence phenotype seen in the Δ*pacC* mutant, or if the corresponding genes are under PacC regulation in *E. festucae*; but given that PacC is a transcription factor, it is conceivable that its absence in the deletion mutant results in differential regulation of genes that regulate mitochondrial functionality.

The increased sensitivity to Na^+, K^+ and Li^+ ions in the Δ*pacC* mutant indicates a role for PacC in regulating salt tolerance in *E. festucae*. K^+ is the major intracellular cation and is regarded as 'non-toxic'; while Na^+ being the major extracellular cation, and Li^+, a trace element, are regarded as 'toxic' (Caracuel *et al*., 2003a). In *F. oxysporum*, deletion of *pacC* affected growth in the presence of Na^+ and Li^+, but not K^+ and sorbitol; indicating that PacC regulates the cellular response to salt but not osmotic stress in this fungus (Caracuel *et al*., 2003a). In comparison, PacC in *E. festucae* appears to be involved in regulating both salt and osmotic stress responses, as high concentrations of K^+, Na^+ and Li^+ ions affected growth of the Δ*pacC* mutant.

All living cells are subjected to a concentration gradient of salts between the intra- and extracellular environments. In eukaryotes with cell walls, such as fungi, the membrane potential is maintained partly by the P-type ATPases, which mediate Na^+, K^+, and Li^+ effluxes in *S. cerevisiae* (Haro *et al*., 1991). Expression of the ENA family of Na^+-ATPases is also dependent on alkaline pH in *Schwanniomyces*, and is additionally dependent on PacC in *Fusarium* (Banuelos & Rodriguez-Navarro, 1998; Caracuel *et al*., 2003a). While the expression of *ena1* was not analysed in this study, expression of *ena2* was found to be PacC-dependent; but surprisingly only under acidic conditions, indicating that PacC activity is still present at acidic pH in *E. festucae*. Growth of the Δ*pacC* and *pacC*^{CA} mutants was also tested under other stress conditions, including both oxidative (H_2O_2) and cell-membrane (SDS) stresses, but was not sensitive to either. In contrast, the *pacC* deletion mutant of *F. oxysporum* is sensitive to H_2O_2 whereas the dominant active mutation in *pacC* in this fungus led to increased tolerance to this form of oxidative stress (Caracuel *et al*., 2003b).

Surprisingly, deletion of *pacC* has no effect on the growth of *E. festucae* at alkaline pH. PacC is a transcription factor activated by extracellular alkaline pH, in order to upregulate the expression of genes required for growth at such pH (Peñalva & Arst, 2004). Deletion of *pacC* in *Aspergillus* (Galindo *et al*., 2007), *Fusarium* (Caracuel *et al*., 2003b; Merhej *et al*., 2011), *Cryptococcus* (O'Meara *et al*., 2010), *Saccharomyces* (Xu & Mitchell, 2001) and *Trichoderma* (Trushina *et al*., 2013) all adversely affected the ability of these organisms to grow under alkaline conditions. The finding that PacC is not required for growth under alkaline pH in *E. festucae* suggests that the transcription factor may play a less important role in the response of *E. festucae* to alkaline pH than in other fungi. In line with this hypothesis, the expression of *pacC* in *Trichoderma* is 27-fold higher at pH 8 than at pH 4 (Trushina *et al*., 2013), whereas in *E. festucae* it is only 3-fold higher at pH 8 than at pH 5.

However, the pH experiments described above with *E. festucae* could additionally be conducted using other pH-defined media, as Caracuel *et al*., (2003a) showed that *pacC* expression can vary depending on the carbon source used. Cultures of *F. oxysporum* grown in 1% sucrose had decreased expression of *pacC* at pH 5.6 compared to pH 7.0, and detectable *pacC* levels at pH 4.5. However, when *F. oxysporum* was cultured in 1% citrus pectin the expression levels of *pacC* were comparable at pH 5.6 and pH 7.0, and was not detectable at pH 4.5. The carbon source used in the Blankenship media is sucrose, but the extent of activity of the PacC protein in acidic and alkaline pH conditions of these media is however unclear. Although the activation of PacC induces the expression of the *pacC* gene as a result of the auto-regulatory mechanism of the transcription factor (Tilburn *et al*., 1995), the increased expression of *pacC* does not necessary imply the subsequent processing and activation of the translated protein. A Western blot analysis performed using antibodies from *A. nidulans* against full-length PacC-72, and the processed forms PacC-53 and PacC-27 could provide insights into the activation of *E. festucae* PacC under the Blankenship media conditions.

4.2. PacC regulation of hyphal development in *E. festucae*

This study provides strong evidence that over-activation of PacC leads to abnormal hyphal growth and development in *E. festucae*. In all three independent $pacC^{CA}$ mutants, intrahyphal hyphae and aberrantly coiled and conidiated hyphal structures

were observed in culture; and hyphal convolutions and hyphal breakage were observed *in planta*.

Intrahyphal hypha, the abnormal formation of a new intracellular hypha within an existing hypha that was observed in the *pacC*^{CA} mutant of *E. festucae*, has also been reported in other fungal genera including *Aspergillus* (Miller & Anderson, 1961), *Neurospora* (Lowry & Sussman, 1966), *Linderina* (Chan & Stephen, 1967) and *Sclerotinia* (Calonge, 1968). Several possible causes for the formation of these aberrant hyphae have been proposed; among them anaerobic growth conditions, accumulation of toxic metabolites, and injury to the mycelium (Calonge, 1968). Horiuchi *et al.* (1999) also reported for the first time, in *A. nidulans*, that deletion of a single gene, *csmA*, directly induces the formation of intrahyphal hyphae in this fungus. The multidomain protein encoded by this gene contains a chitin synthase domain, which plays a role in maintaining cell-wall integrity; and expression of only this domain in the Δ*csmA* mutant was sufficient to rescue the intrahyphal hyphae phenotype. The correlation of a chitin synthase with intrahyphal hyphae formation and the increased sensitivity of the *pacC*^{CA} mutant to cell-wall stress induced by calcofluor white suggest that overactivation of PacC in *E. festucae* may induce intrahyphal hyphae formation through the misregulation of chitin dynamics.

The hyperconidiation observed in the *pacC*^{CA} mutant is confined only to the coiled, spiral-like hyphal structures. In contrast, hyperconidiation in the *E. festucae* Δ*proA* mutant occurs throughout the colony, and single conidia develop along the length of a hypha (Tanaka *et al*., 2013). These differences suggest that there may be spatial regulation of conidiation in *E. festucae*. In addition, the ChsA chitin synthase in *Colletotrichum graminicola* preferentially localises to the plasma membrane of developing conidiophores (Amnuaykanjanasin & Epstein, 2006), suggesting that chitin synthases may also be involved in the abnormal conidiation of the *E. festucae pacC*^{CA} mutant. On the other hand, hyperconidiation may also be due to a direct upregulation of conidiation genes by PacC in *E. festucae*, as the PacC homologue in *S. cerevisiae*, Rim101p, is known to be a positive regulator of sporulation in this fungus (Peñalva *et al*., 2008).

It is presently unknown what causes the *pacC*^{CA} mutant to have increased hyphal breakage *in planta*, although it is possible that hyphae of the mutant are rendered more susceptible to shearing during intercalary growth due to disruption in cell-wall or

chitin dynamics. The ChsA chitin synthase in *C. graminicola* also preferentially localises to the plasma membrane at sites of hyphal breakage and seems to be involved in cell-wall repair (Amnuaykanjanasin & Epstein, 2006). This finding suggests that misregulation of chitin synthases may cause the abnormal hyphal development as observed for the *pacC*^{CA} mutant. In addition, chitin is in itself a potent elicitor of plant defence responses and it may be crucial for *E. festucae* to successfully regulate chitin dynamics in order to maintain the symbiosis. Some symbiotic-deficient mutants of *E. festucae*, such as Δ*irlA*, also display an unmasking of chitin *in planta* (Berry D, pers comm).

E. festucae mutants disrupted in cell-wall specific MAPKs such as Δ*mpkA* and Δ*mkkB* also form intrahyphal hyphae in culture and convoluted hyphal structures *in planta* (Becker Y, pers comm). These findings suggest a link between the formation of these abnormal structures and cell-wall dynamics in *E. festucae*. In both of these mutants, the formation of intrahyphal hyphae and convoluted hyphal structures may be explained by the inability of the mutants to fuse, leading to one hypha subsequently proliferating intracellularly inside another; or when in the plant, to form the convoluted hyphal structures. However, hyphal fusion was regularly observed in the *pacC*^{CA} mutant, indicating that formation of these abnormal structures is triggered by a change other than a defect in hyphal fusion alone. Nevertheless, the similarity in these findings suggests that disruption in cell-wall integrity and dynamics, probably involving chitin synthases, as chitin is a major component of fungal cell-wall, leads to an abnormal development of hyphae in *E. festucae*. As the *pacC*^{CA} mutants are presumed to have a constitutive activation of PacC, it would be interesting to see if similar abnormal hyphal developments are induced in wild-type *E. festucae* strain cultured under alkaline pH conditions.

In this study, the *pacC*^{CA} mutant was generated by expressing a truncated form of PacC (*pacC*^{CA}) that lacks the inhibitory 'C' region in a Δ*pacC* mutant background. Although a similar strategy has been used with success in other studies (Caracuel *et al*., 2003a, 2003b; Merhej *et al*., 2011; Tilburn *et al*., 1995), there is the assumption here that the translated protein is recognised and successfully cleaved by the processing protease into its fully active form, PacC-27, in *E. festucae*. To confirm if this was the case, a Western blot analysis of cellular extracts from the *pacC*^{CA} mutants could be performed to detect PacC-27 in the *pacC*^{CA} mutant, or by expressing a GFP-*pacC*^{CA} fusion construct

to determine the cellular localisation of the protein; PacC-27 is nuclear regardless of extracellular pH conditions whereas PacC-72 is cytosolic under acidic condition (Diez *et al*., 2002; Mingot *et al*., 2001).

The only hyphal abnormalities observed in the Δ*pacC* mutant appeared to be a reduction in aerial hyphal development and premature senescence leading to a 'wet' appearance of the colony. It is likely that both of these phenotypes are interconnected, as deletion of the *hypA* gene, coding for a hydrophobin, produced similar 'wettable' mycelia resulting from a loss of surface hydrophobicity in *Arthroderma* colonies (Heddergott *et al*., 2012). Disruption of the *SC3* hydrophobin gene in *Schizophyllum* also showed that hydrophobins are necessary for aerial hyphae formation in this fungus (van Wetter *et al*., 1996). Hydrophobins are small, secreted proteins produced by filamentous fungi that confer hydrophobicity to the fungal mycelium (Wosten, 2001). Given that the Δ*pacC* mutant colonies displayed an analogous phenotype, it is possible that hydrophobin genes, under the control of PacC, may be downregulated in this mutant. However, other hydrophobins than HypA and SC3 are likely operating in *E. festucae*, as homologues of these proteins could not be identified in the genome sequence of the fungus.

4.3. Role of PacC in the endophyte-ryegrass symbiosis

The requirement for PacC for fungal virulence has been demonstrated in several pathogenic fungi including *C. albicans* (Davis *et al*., 2000), *A. nidulans* (Bignell *et al*., 2005), *C. acutatum* (You *et al*., 2007) and *S. sclerotiorum* (Rollins, 2003). In *F. oxysporum*, PacC performs the opposite function by negatively regulating virulence (Caracuel *et al*., 2003b). Deletion of *pacC* in *E. festucae* did not lead to a change in the symbiotic interaction phenotype, with plants developing the same as wild-type infected plants. No noticeable difference was also observed in the growth of the Δ*pacC* mutants at the cellular level *in planta*. On the other hand, plants infected with the *pacC*^{CA} mutants were mildly hypertillered but showed no signs of senescence even at 19 weeks post-inoculation. At the cellular level, the *pacC*^{CA} mutant had increased hyphal breakage and formed highly convoluted hyphal structures in the host. It is unclear what induces the formation of these structures, as no pattern was observed with regard to the sites of formation of these structures was observed.

Hypertillering is often seen in ryegrass infected with symbiotically-defective *E. festucae* mutants, including Δ*noxA* (Tanaka *et al*., 2006), Δ*noxR* (Takemoto *et al*., 2006), Δ*racA* (Tanaka *et al*., 2008) and Δ*sakA* (Eaton *et al*., 2010), and may signify a loss of apical dominance in the host (Chujo and Scott, 2014). As apical dominance is regulated by levels of host hormones including auxin, cytokinin and others (Harrison & Kaufman, 1980; Murphy & Briske, 1992), it is likely that some sort of molecular communication is present between the endophyte and host which affects this process, and which is disrupted by the above gene mutations. Hypertillering of the *pacC*^{CA} mutant-infected plants may also be triggered by the preferential growth of the mutant near host vascular bundles, thereby depleting the host of nutrients. However, this tendency of hyphae to grow close to host vascular bundles was observed only in the *pacC*^{CA} #14 mutant, which also induced hypertillering most strongly in the host compared to the other two *pacC*^{CA} mutants. Nonetheless, all *pacC* mutants still grew in a restricted pattern in the host and showed no signs of increased hyphal biomass. Taking into consideration the absence of any significant change in the host phenotype, these results indicate that PacC is not essential for the symbiosis of *E. festucae* with perennial ryegrass.

4.4. PacC regulation of secondary metabolite pathways in *E. festucae*

PacC has been shown to be a positive regulator of secondary metabolite pathways in many other fungal species. However, in most of these species the secondary metabolites or their biosynthetic genes are either adequately expressed at detectable levels, or the optimal conditions for their expression have been elucidated. In contrast, the expression of three secondary metabolites of *E. festucae* strain Fl1; lolitrem B, ergovaline and peramine, are extremely low in culture as the genes encoding the enzymes for these pathways are transcriptionally silent (Chujo and Scott, 2014). Whether the genes required for these pathways can be activated *ex planta* remains to be determined.

Gene expression analyses performed using axenic culture samples indicated that the *dmaW* gene involved in ergovaline synthesis was slightly upregulated in alkaline pH in a PacC-independent manner, whereas *ltmE* and *easA* were slightly upregulated in a PacC-dependent manner under acidic pH conditions. These results imply that PacC may still be active under extracellular acidic pH conditions in *E. festucae*. The extent of

gene upregulation observed in these experiments was also very small (<10-fold) compared to the enhanced expression (several hundred to a thousand-fold) observed in mutants lacking a functional H3K9 (Δ*clrD*), or H3K27 (Δ*ezhB)* methyltransferase or in the Δ*clrD*/Δ*ezhB* double-deletion mutant, compared to wild-type (Chujo and Scott, 2014). These results suggest that a gene silencing mechanism may still be in place in the *pac*C mutants, such that heterochromatic silencing prevents the PacC transcription factor from accessing gene promoter elements. To analyse the role of PacC in regulating these genes in an 'open', euchromatic state, the expression of the secondary metabolite genes could be analysed in Δ*pacC* and *pacC*^{CA} mutants generated in a Δ*clrD* or Δ*ezhB* background.

Nonetheless, results of the *in planta* expression analyses in this study do not indicate a regulation of PacC over secondary metabolite genes in *E. festucae* in the plant. Expression of all of the secondary metabolite genes analysed was similar in wild-type and *pac*C mutants, with only *lpsA* showing a 0.5-fold decrease in expression in the *pac*C mutants compared to wild-type; however, this downregulation was also observed in the complemented strain. The expression of secondary metabolite genes in *E. festucae* is high *in planta* as most of the gene regulatory switches are likely already turned on for expression. Thus, it is possible that PacC does regulate these genes but that its effects are masked due to the experimental conditions used. Until the effects of *pac*C mutations on secondary metabolism are analysed in a Δ*clrD* or Δ*ezhB* background, the present data indicate that PacC does not regulate secondary metabolite gene expression in *E. festucae*.

4.5 Presence of other pH-regulatory pathways in *E. festucae*

Both Δ*pacC* and *pacC*^{CA} mutants of *E. festucae* appear to be able to modify extracellular pH, as pH of both alkaline (pH 8) and acidic (pH 5) growth media were altered towards neutral (pH 6.5) after a period of incubation in these media. Assuming that this change in pH was not due to secretion of waste products with a neutral pKa, these mutants appear to still be able to sense and modify the environmental pH. In support of this hypothesis, pH of minimal synthetic media 3 (MSM3) after 9 days of culture with wild-type *E. festucae* mycelia was at an acidic value of about 5 (Chujo T, pers comm), indicating that waste products produced by *E. festucae* have an acidic, and not a neutral pKa.

Adaptation of a fungus to environmental pH conditions is crucial for survival, and the ability to influence ambient pH is not unique to *E. festucae*. Similar experiments were performed by Vylkova *et al.* (2011), in which *C. albicans* mycelia were cultured in YPD media to obtain sufficient biomass and washed with water before being transferred to pH-adjusted media. The authors found that *C. albicans* actively modified alkaline and acidic pH environments towards neutral, and was able to raise the pH of the growth media from 4 to 7 within a time span of 12 hours. Interestingly, this alkalinisation was not dependent on Rim101p (PacC) in the fungus, a result similar to the findings reported in this thesis. The insect pathogen *Metarhizium anisopliae* also actively modifies extracellular pH by adjusting the secretion of the highly basic compound ammonia in order to create conditions that allow activity of its secreted proteases (St Leger *et al.*, 1999).

Based on the results of this study, it is proposed that additional molecular pathways exist in *E. festucae* which respond to extracellular pH changes and enable the Δ*pacC* mutant to grow under alkaline conditions. The upregulation of *ena2*, *ltmE* and *easA* in the wild-type strain under acidic condition suggests the presence of regulatory mechanism(s) that either act to induce the expression of these genes at acidic pH or repress their expression at alkaline pH. The finding that this upregulation was absent in the Δ*pacC* mutant also suggests that this putative regulatory mechanism may act in concert with the PacC transcription factor.

The Ca^{2+}/calmodulin-dependent protein phosphatase calcineurin is a highly conserved protein in eukaryotes that is activated by a rise in Ca^{2+} levels in the cytoplasm and acts to dephosphorylate the transcription factor Crz1. Once dephosphorylated, the activated Crz1 transcription factor then enters the nucleus to regulate gene expression (Cunningham & Fink, 1994; Rusnak & Mertz, 2000). In *C. albicans*, Rim101p, Crz1, and calcineurin are all required for growth at alkaline pH. Importantly, Crz1, via calcineurin, acts in a parallel manner with Rim101 to regulate the expression of certain genes, such as *ENA21* which codes for a P-type Na^{+}-ATPase in this fungus (Kullas *et al.*, 2007). Interestingly, ryegrass plants infected with Δ*cnaA* (calcineurin) mutants of *E. festucae* developed a strong hypersensitivity response, indicating that calcineurin is essential for proper establishment of the symbiosis between *E. festucae* and perennial ryegrass (Mitić, 2011).

The cyclic AMP (cAMP)-dependent protein kinase A (PKA) negatively regulates Crz1 in *S. cerevisiae* by phosphorylation of the transcription factor and inhibits its translocation into the nucleus (Kafadar & Cyert, 2004). The cellular levels of the PKA-activating molecule, cAMP, is in turn decreased under alkaline growth conditions, thereby preventing PKA activation. Correspondingly, mutations that lead to constitutive PKA activation result in a heightened sensitivity of the fungus to alkaline pH (Casado *et al.*, 2011). PKA may therefore be involved in the cellular response to ambient pH conditions in *S. cerevisiae* by acting in an opposite manner to calcineurin. Interestingly, PKA in *Cryptococcus neoformans* is required for the nuclear localisation and activation of Rim101 (O'meara *et al.*, 2010). The authors also reported for the first time an integration between the PKA and Rim pathways, as well as a novel mechanism of Rim101p activation via PKA phosphorylation. It is conceivable that in addition to PacC; calcineurin and PKA pathways also mediate the cellular response to pH in *E. festucae*.

4.6 Conclusions

This study represents the first investigation into the role of PacC in the interaction of a fungal symbiont and its host. In other fungal species studied, PacC can act as a positive regulator of virulence and pathogenicity in one species; yet as a negative regulator in another. The effects of both loss-of-function (Δ*pacC*) and gain-of-function (*pacC*^{CA}) mutations of PacC were examined in this study and the results conclude that PacC is dispensable for the establishment and maintenance of the symbiosis. However, the *pacC*^{CA} mutant forms aberrant hyphal structures *in planta*. Elucidating the molecular basis for, and the mechanisms involved in the formation of these structures may contribute to our understanding of the symbiosis.

Overactivation of PacC in *E. festucae* additionally leads to abnormal conidiation and formation of intrahyphal hyphae in culture but does not interfere with the ability of the fungus to fuse. This is in contrast to the hyperconidiating mutants of *E. festucae* such as Δ*proA*, Δ*noxA* and Δ*noxA*/*noxB*, or mutants that form aberrant intrahyphal hyphae such as Δ*mpkA* and Δ*mkkB*, all of which are defective in hyphal fusion. The *pacC*^{CA} mutant also showed increased sensitivity to chitin-related cell-wall stress, indicating that the abnormal hyphal development observed in these mutants, both in culture and *in planta* may be due to a disruption in cell-wall repair or synthesis that may involve

regulators of chitin dynamics. The Δ*pacC* mutant on the other hand did not show any abnormality under these conditions.

Contrary to studies which report to date a requirement for PacC for fungal growth under alkaline conditions, deletion of *pacC* in *E. festucae* did not affect its ability to grow under alkaline conditions. Both Δ*pacC* and *pacC*^{CA} mutants were also able to sense and modify both acidic and alkaline extracellular pH, and archetypal genes that are pH- and PacC-dependent in other fungi were unaffected by pH conditions and *pacC* mutations in *E. festucae*.

These results indicate that important cellular processes regulated by PacC in other fungi; such as growth under alkaline conditions, secondary metabolism, and pathogenesis, are not under the control of PacC in *E. festucae*. The change in the transcript levels of *pacC* in *E. festucae* in response to pH changes is also lower than would be expected for a major transcription factor. As alkalinisation of the apoplast is a major plant defence response to pathogens (Dixon & Harrison, 1994; Vera-Estrella *et al.*, 1994; Granado *et al.*, 1995; Felle *et al.*, 2005), it is tempting to speculate that these functions of PacC in responding to alkaline pH conditions have been lost in *E. festucae*, perhaps as a requirement in the course of its evolution in switching from a pathogen to a symbiont of its host perennial ryegrass.

5. Bibliography

5. Bibliography

Alkan, N., X. Meng, G. Friedlander, E. Reuveni, S. Sukno, A. Sherman, M. Thon, R. Fluhr & D. Prusky, (2013) Global aspects of PacC regulation of pathogenicity genes in *Colletotrichum gloeosporioides* as revealed by transcriptome analysis. *Molecular plant-microbe interactions : MPMI* **26**: 1345-1358.

Amnuaykanjanasin, A. & L. Epstein, (2006) A class Vb chitin synthase in *Colletotrichum graminicola* is localized in the growing tips of multiple cell types, in nascent septa, and during septum conversion to an end wall after hyphal breakage. *Protoplasma* **227**: 155-164.

Arst, H.N., Jr. & A.M. Peñalva, (2003) pH regulation in *Aspergillus* and parallels with higher eukaryotic regulatory systems. *Trends in Genetics* **19**: 224-231.

Bacetty, A.A., M.E. Snook, A.E. Glenn, J.P. Noe, P. Nagabhyru & C.W. Bacon, (2009) Chemotaxis disruption in *Pratylenchus scribneri* by tall fescue root extracts and alkaloids. *Journal of chemical ecology* **35**: 844-850.

Bacon, C.W., (1995) Toxic endophyte-infected tall fescue and range grasses: historic perspectives. *Journal of animal science* **73**: 861-870.

Banuelos, M.A. & A. Rodriguez-Navarro, (1998) P-type ATPases mediate sodium and potassium effluxes in *Schwanniomyces occidentalis*. *Journal of Biological Chemistry* **273**: 1640-1646.

Bayram, O. & G.H. Braus, (2012) Coordination of secondary metabolism and development in fungi: the velvet family of regulatory proteins. *FEMS microbiology reviews* **36**: 1-24.

Bayram, O., G.H. Braus, R. Fischer & J. Rodriguez-Romero, (2010) Spotlight on *Aspergillus nidulans* photosensory systems. *Fungal genetics and biology : FG & B* **47**: 900-908.

Bayram, O., S. Krappmann, M. Ni, J.W. Bok, K. Helmstaedt, O. Valerius, S. Braus-Stromeyer, N.J. Kwon, N.P. Keller, J.H. Yu & G.H. Braus, (2008) VelB/VeA/LaeA complex coordinates light signal with fungal development and secondary metabolism. *Science* **320**: 1504-1506.

Begel, O., J. Boulay, B. Albert, E. Dufour & A. Sainsard-Chanet, (1999) Mitochondrial group II introns, cytochrome c oxidase, and senescence in *Podospora anserina*. *Molecular and cellular biology* **19**: 4093-4100.

Bertrand, H., (2000) Role of mitochondrial DNA in the senescence and hypovirulence of fungi and potential for plant disease control. *Annual review of phytopathology* **38**: 397-422.

Bignell, E., S. Negrete-Urtasun, A.M. Calcagno, K. Haynes, H.N. Arst, Jr. & T. Rogers, (2005) The *Aspergillus* pH-responsive transcription factor PacC regulates virulence. *Molecular microbiology* **55**: 1072-1084.

Blankenship, J.D., M.J. Spiering, H.H. Wilkinson, F.F. Fannin, L.P. Bush & C.L. Schardl, (2001) Production of loline alkaloids by the grass endophyte, *Neotyphodium uncinatum*, in defined media. *Phytochemistry* **58**: 395-401.

Bok, J.W. & N.P. Keller, (2004) LaeA, a regulator of secondary metabolism in *Aspergillus* spp. *Eukaryot Cell* **3**: 527-535.

Bok, J.W., D. Noordermeer, S.P. Kale & N.P. Keller, (2006) Secondary metabolic gene cluster silencing in *Aspergillus nidulans*. *Molecular microbiology* **61**: 1636-1645.

Butchko, R.A., T.H. Adams & N.P. Keller, (1999) *Aspergillus nidulans* mutants defective in *stc* gene cluster regulation. *Genetics* **153**: 715-720.

Byrd, A.D., C.L. Schardl, P.J. Songlin, K.L. Mogen & M.R. Siegel, (1990) The beta-tubulin gene of *Epichloe typhina* from perennial ryegrass (*Lolium perenne*). *Current genetics* **18**: 347-354.

Caddick, M.X., A.G. Brownlee & H.N. Arst, Jr., (1986) Regulation of gene expression by pH of the growth medium in *Aspergillus nidulans*. *Molecular & general genetics : MGG* **203**: 346-353.

Calcagno-Pizarelli, A.M., S. Negrete-Urtasun, S.H. Denison, J.D. Rudnicka, H.J. Bussink, T. Munera-Huertas, L. Stanton, A. Hervas-Aguilar, E.A. Espeso, J. Tilburn, H.N. Arst, Jr. & M.A. Penalva, (2007) Establishment of the ambient pH signaling complex in *Aspergillus nidulans*: PalI assists plasma membrane localization of PalH. *Eukaryot Cell* **6**: 2365-2375.

Calonge, F.D., (1968) Origin and development of intrahyphal hyphae in *Sclerotinia fructigena*. *Mycologia* **60**: 932-942.

Calvo, A.M., (2008) The VeA regulatory system and its role in morphological and chemical development in fungi. *Fungal genetics and biology : FG & B* **45**: 1053-1061.

Calvo, A.M., J. Bok, W. Brooks & N.P. Keller, (2004) *veA* is required for toxin and sclerotial production in *Aspergillus parasiticus*. *Applied and environmental microbiology* **70**: 4733-4739.

Cantarel, B.L., I. Korf, S.M. Robb, G. Parra, E. Ross, B. Moore, C. Holt, A. Sanchez Alvarado & M. Yandell, (2008) MAKER: an easy-to-use annotation pipeline designed for emerging model organism genomes. *Genome research* **18**: 188-196.

Caracuel, Z., C. Casanova, M.I. Roncero, A. Di Pietro & J. Ramos, (2003a) pH response transcription factor PacC controls salt stress tolerance and expression of the P-Type Na+ -ATPase Ena1 in *Fusarium oxysporum*. *Eukaryot Cell* **2**: 1246-1252.

Caracuel, Z., M.I. Roncero, E.A. Espeso, C.I. Gonzalez-Verdejo, F.I. Garcia-Maceira & A. Di Pietro, (2003b) The pH signalling transcription factor PacC controls virulence in the plant pathogen *Fusarium oxysporum*. *Molecular microbiology* **48**: 765-779.

Casado, C., A. Gonzalez, M. Platara, A. Ruiz & J. Arino, (2011) The role of the protein kinase A pathway in the response to alkaline pH stress in yeast. *The Biochemical journal* **438**: 523-533.

Chan, C. & R.C. Stephen, (1967) Intrahyphal hyphae in the genus *Linderina*. *Canadian Journal of Botany* **45**: 1995-1998.

Charlton, D. (2012, 13-06-2012). 'Pastures - Ryegrasses', Te Ara - the Encyclopedia of New Zealand. Retrieved 12-03, 2014, from http://www.teara.govt.nz/en/pastures/page-3

Charlton, N.D., J.Y. Shoji, S.R. Ghimire, J. Nakashima & K.D. Craven, (2012) Deletion of the fungal gene soft disrupts mutualistic symbiosis between the grass endophyte *Epichloe festucae* and the host plant. *Eukaryot Cell* **11**: 1463-1471.

Christensen, M.J., J.R. Bennett, A.H. Ansari, H. Koga, R.D. Johnson, G.T. Bryan, R.W. Simpson, P.J. Koolard, M.E. Nickless & C.R. Voisey, (2008) Epichloe endophytes grow by intercalary hyphal extension in elongating grass leaves. *Fungal genetics and biology : FG & B* **45**: 84-93.

Christensen, M.J., J.R. Bennett & J. Schmidt, (2006) Growth of *Epichloe/Neotyphodium* and p-endophytes in leaves of *Lolium* and *Festuca* grasses. *Mycological Research* **106**: 93–106.

Christianson, T.W., R.S. Sikorski, M. Dante, J.H. Shero & P. Hieter, (1992) Multifunctional yeast high-copy-number shuttle vectors. *Gene* **110**: 119-122.

Chujo, T. & B. Scott, (2014) Histone H3K9 and H3K27 methylation regulates fungal alkaloid biosynthesis in a fungal endophyte-plant symbiosis. *Molecular microbiology*: (In press).

Clay, K. & C.L. Schardl, (2002) Evolutionary Origins and Ecological Consequences of Endophyte Symbiosis with Grasses. *The American Naturalist* **160**: S99-S127.

Colot, H.V., G. Park, G.E. Turner, C. Ringelberg, C.M. Crew, L. Litvinkova, R.L. Weiss, K.A. Borkovich & J.C. Dunlap, (2006) A high-throughput gene knockout procedure for *Neurospora* reveals functions for multiple transcription factors. *Proceedings of the National Academy of Sciences of the United States of America* **103**: 10352-10357.

Cunningham, K.W. & G.R. Fink, (1994) Ca2+ transport in Saccharomyces cerevisiae. *The Journal of experimental biology* **196**: 157-166.

Davis, D., J.E. Edwards, Jr., A.P. Mitchell & A.S. Ibrahim, (2000) *Candida albicans* RIM101 pH response pathway is required for host-pathogen interactions. *Infect Immun* **68**: 5953-5959.

Denison, S.H., M. Orejas & H.N. Arst, Jr., (1995) Signaling of ambient pH in *Aspergillus* involves a cysteine protease. *The Journal of biological chemistry* **270**: 28519-28522.

Diebold, A.B. & G.M. Bokoch, (2001) Molecular basis for Rac2 eegulation of phagocyte NADPH oxidase. *Nat Immunol* **2**: 211-215.

Diez, E., J. Alvaro, E.A. Espeso, L. Rainbow, T. Suarez, J. Tilburn, H.N. Arst, Jr. & M.A. Penalva, (2002) Activation of the *Aspergillus* PacC zinc finger transcription factor requires two proteolytic steps. *The EMBO journal* **21**: 1350-1359.

Dixon, R.A. & M.J. Harrison, (1994) Early events in the activation of plant defense responses. *Annual review of phytopathology* **32**: 479-501.

Dower, W.J., J.F. Miller & C.W. Ragsdale, (1988) High efficiency transformation of E. coli by high voltage electroporation. *Nucleic acids research* **16**: 6127-6145.

Dreyer, J., H. Eichhorn, E. Friedlin, H. Kurnsteiner & U. Kuck, (2007) A homologue of the *Aspergillus* velvet gene regulates both cephalosporin C biosynthesis and hyphal fragmentation in *Acremonium chrysogenum*. *Applied and environmental microbiology* **73**: 3412-3422.

Duran, R.M., J.W. Cary & A.M. Calvo, (2007) Production of cyclopiazonic acid, aflatrem, and aflatoxin by *Aspergillus flavus* is regulated by *veA*, a gene necessary for sclerotial formation. *Applied microbiology and biotechnology* **73**: 1158-1168.

Eaton, C.J., M.P. Cox, B. Ambrose, M. Becker, U. Hesse, C.L. Schardl & B. Scott, (2010) Disruption of signaling in a fungal-grass symbiosis leads to pathogenesis. *Plant physiology* **153**: 1780-1794.

Eaton, C.J., M.P. Cox & B. Scott, (2011) What triggers grass endophytes to switch from mutualism to pathogenism? *Plant science : an international journal of experimental plant biology* **180**: 190-195.

Eaton, C.J., I. Jourdain, S.J. Foster, J.S. Hyams & B. Scott, (2008) Functional analysis of a fungal endophyte stress-activated MAP kinase. *Current genetics* **53**: 163-174.

Egan, M.J., Z.Y. Wang, M.A. Jones, N. Smirnoff & N.J. Talbot, (2007) Generation of reactive oxygen species by fungal NADPH oxidases is required for rice blast disease. *Proceedings of the National Academy of Sciences of the United States of America* **104**: 11772-11777.

Espeso, E.A. & M.A. Penalva, (1996) Three binding sites for the *Aspergillus nidulans* PacC zinc-finger transcription factor are necessary and sufficient for regulation by ambient pH of the isopenicillin N synthase gene promoter. *The Journal of biological chemistry* **271**: 28825-28830.

Espeso, E.A., T. Roncal, E. Diez, L. Rainbow, E. Bignell, J. Alvaro, T. Suarez, S.H. Denison, J. Tilburn, H.N. Arst, Jr. & M.A. Penalva, (2000) On how a transcription factor can avoid its proteolytic activation in the absence of signal transduction. *The EMBO journal* **19**: 719-728.

Espeso, E.A., J. Tilburn, H.N. Arst, Jr. & M.A. Penalva, (1993) pH regulation is a major determinant in expression of a fungal penicillin biosynthetic gene. *The EMBO journal* **12**: 3947-3956.

Espeso, E.A., J. Tilburn, L. Sanchez-Pulido, C.V. Brown, A. Valencia, H.N. Arst, Jr. & M.A. Penalva, (1997) Specific DNA recognition by the *Aspergillus nidulans* three zinc finger transcription factor PacC. *J Mol Biol* **274**: 466-480.

Felle, H.H., A. Herrmann, R. Huckelhoven & K.H. Kogel, (2005) Root-to-shoot signalling: apoplastic alkalinization, a general stress response and defence factor in barley (Hordeum vulgare). *Protoplasma* **227**: 17-24.

Fernandes, M., N.P. Keller & T.H. Adams, (1998) Sequence-specific binding by *Aspergillus nidulans* AflR, a C6 zinc cluster protein regulating mycotoxin biosynthesis. *Molecular microbiology* **28**: 1355-1365.

Flaherty, J.E., A.M. Pirttila, B.H. Bluhm & C.P. Woloshuk, (2003) PAC1, a pH-Regulatory Gene from *Fusarium verticillioides*. *Applied and environmental microbiology* **69**: 5222-5227.

Fleetwood, D.J., B. Scott, G.A. Lane, A. Tanaka & R.D. Johnson, (2007) A complex ergovaline gene cluster in *Epichloë* endophytes of grasses. *Applied and environmental microbiology* **73**: 2571-2579.

Fletcher, L.R. & I.C. Harvey, (1981) An association of a *Lolium* endophyte with ryegrass staggers. *New Zealand veterinary journal* **29**: 185-186.

Florea, S., K. Andreeva, C. Machado, P.M. Mirabito & C.L. Schardl, (2009) Elimination of marker genes from transformed filamentous fungi by unselected transient transfection with a Cre-expressing plasmid. *Fungal genetics and biology : FG & B* **46**: 721-730.

Galindo, A., A.M. Calcagno-Pizarelli, H.N. Arst, Jr. & M.A. Penalva, (2012) An ordered pathway for the assembly of fungal ESCRT-containing ambient pH signalling complexes at the plasma membrane. *Journal of cell science* **125**: 1784-1795.

Galindo, A., A. Hervas-Aguilar, O. Rodriguez-Galan, O. Vincent, H.N. Arst, Jr., J. Tilburn & M.A. Penalva, (2007) PalC, one of two Bro1 domain proteins in the fungal pH signalling pathway, localizes to cortical structures and binds Vps32. *Traffic* **8**: 1346-1364.

Giesbert, S., T. Schurg, S. Scheele & P. Tudzynski, (2008) The NADPH oxidase Cpnox1 is required for full pathogenicity of the ergot fungus *Claviceps purpurea*. *Molecular plant pathology* **9**: 317-327.

Glass, N.L., C. Rasmussen, M.G. Roca & N.D. Read, (2004) Hyphal homing, fusion and mycelial interconnectedness. *Trends in microbiology* **12**: 135-141.

Granado, J., G. Felix & T. Boller, (1995) Perception of fungal sterols in plants. *Plant physiology* **107**: 485-490.

Grewal, S.I. & S. Jia, (2007) Heterochromatin revisited. *Nature reviews. Genetics* **8**: 35-46.

Gwinn, K.D., M.H. Collins-Shepard & B.B. Reddick, (1991) Tissue print-immunoblot, an accurate method for the detection of *Acremonium coenophialum* in tall fescue. *Phytopathology* **81**: 747-748.

Haro, R., B. Garciadeblas & A. Rodriguez-Navarro, (1991) A novel P-type ATPase from yeast involved in sodium transport. *FEBS letters* **291**: 189-191.

Harrison, M.A. & P.B. Kaufman, (1980) Hormonal regulation of lateral bud (tiller) release in oats (*Avena sativa* L.). *Plant physiology* **66**: 1123-1127.

Heddergott, C., S. Bruns, S. Nietzsche, I. Leonhardt, O. Kurzai, O. Kniemeyer & A.A. Brakhage, (2012) The *Arthroderma benhamiae* hydrophobin HypA mediates hydrophobicity and influences recognition by human immune effector cells. *Eukaryot Cell* **11**: 673-682.

Herranz, S., J.M. Rodriguez, H.J. Bussink, J.C. Sanchez-Ferrero, H.N. Arst, Jr., M.A. Penalva & O. Vincent, (2005) Arrestin-related proteins mediate pH signaling in fungi. *Proceedings of the National Academy of Sciences of the United States of America* **102**: 12141-12146.

Herth, W., (1980) Calcofluor white and Congo red inhibit chitin microfibril assembly of *Poterioochromonas*: evidence for a gap between polymerization and microfibril formation. *The Journal of cell biology* **87**: 442-450.

Hervas-Aguilar, A., A. Galindo & M.A. Penalva, (2010) Receptor-independent Ambient pH signaling by ubiquitin attachment to fungal arrestin-like PalF. *The Journal of biological chemistry* **285**: 18095-18102.

Hervas-Aguilar, A., J.M. Rodriguez, J. Tilburn, H.N. Arst, Jr. & M.A. Penalva, (2007) Evidence for the direct involvement of the proteasome in the proteolytic processing of the *Aspergillus nidulans* zinc finger transcription factor PacC. *The Journal of biological chemistry* **282**: 34735-34747.

Hoff, B., J. Kamerewerd, C. Sigl, R. Mitterbauer, I. Zadra, H. Kurnsteiner & U. Kuck, (2010) Two components of a velvet-like complex control hyphal morphogenesis, conidiophore development, and penicillin biosynthesis in *Penicillium chrysogenum*. *Eukaryot Cell* **9**: 1236-1250.

Horiuchi, H., M. Fujiwara, S. Yamashita, A. Ohta & M. Takagi, (1999) Proliferation of intrahyphal hyphae caused by disruption of csmA, which encodes a class V chitin synthase with a myosin motor-like domain in Aspergillus nidulans. *Journal of bacteriology* **181**: 3721-3729.

Itoh, Y., R. Johnson & B. Scott, (1994) Integrative transformation of the mycotoxin-producing fungus, *Penicillium paxilli*. *Current genetics* **25**: 508-513.

Johnson, L., M. Steringa, A. Koulman, M.J. Christensen, R.D. Johnson, C.R. Voisey, G.T. Bryan, I. Lamont & S. Rasmussen, (2007) Biosynthesis of an extracellular siderophore is essential for maintenance of mutualistic endophyte-ryegrass symbioses. In: Proceedings of the Sixth International Symposium on Fungal Endophytes of Grasses. A. Popay & E. Thom (eds). Dunedin, pp. 177-179.

Kafadar, K.A. & M.S. Cyert, (2004) Integration of stress responses: modulation of calcineurin signaling in *Saccharomyces cerevisiae* by protein kinase A. *Eukaryot Cell* **3**: 1147-1153.

Kato, N., W. Brooks & A.M. Calvo, (2003) The expression of sterigmatocystin and penicillin genes in *Aspergillus nidulans* is controlled by *veA*, a gene required for sexual development. *Eukaryot Cell* **2**: 1178-1186.

Kayano, Y., A. Tanaka, F. Akano, B. Scott & D. Takemoto, (2013) Differential roles of NADPH oxidases and associated regulators in polarized growth, conidiation and hyphal fusion in the symbiotic fungus *Epichloe festucae*. *Fungal genetics and biology : FG & B* **56**: 87-97.

Keller, N.P. & T.M. Hohn, (1997) Metabolic pathway gene clusters in filamentous fungi. *Fungal genetics and biology : FG & B* **21**: 17-29.

Keller, N.P., C. Nesbitt, B. Sarr, T.D. Phillips & G.B. Burow, (1997) pH regulation of sterigmatocystin and aflatoxin biosynthesis in *Aspergillus* spp. *Phytopathology* **87**: 643-648.

Kirby, E.J.M., (1961) Host-parasite eelations in the choke disease of grasses. *Trans. Brit. mycol. Soc.* **44**: 493-503.

Kullas, A.L., S.J. Martin & D. Davis, (2007) Adaptation to environmental pH: integrating the Rim101 and calcineurin signal transduction pathways. *Molecular microbiology* **66**: 858-871.

Lamb, T.M. & A.P. Mitchell, (2003) The transcription factor Rim101p governs ion tolerance and cell differentiation by direct repression of the regulatory genes *NRG1* and *SMP1* in *Saccharomyces cerevisiae*. *Molecular and cellular biology* **23**: 677-686.

Lamb, T.M., W. Xu, A. Diamond & A.P. Mitchell, (2001) Alkaline response genes of *Saccharomyces cerevisiae* and their relationship to the RIM101 pathway. *The Journal of biological chemistry* **276**: 1850-1856.

Lane, G.A., B.A. Tapper, E. Davies, M.J. Christensen & G.C.M. Latch, (1997) Occurrence of extreme alkaloid levels in endophyte-infected perennial ryegrass, tall fescue, and meadow fescue. *Neotyphodium/Grass Interactions*: 433-436.

Latch, G.C.M. & M.J. Christensen, (1985) Artificial infection of grasses with endophytes. *Ann. appl. Biol* **107**: 17-24.

Lowry, R.J. & A.S. Sussman, (1966) Intra-hyphal hyphae in "clock" mutants of *Neurospora*. *Mycologia* **58**: 541-548.

May, K.J., M.K. Bryant, X. Zhang, B. Ambrose & B. Scott, (2008) Patterns of expression of a lolitrem biosynthetic gene in the *Epichloë festucae*-perennial ryegrass symbiosis. *Molecular plant-microbe interactions : MPMI* **21**: 188-197.

Mayers, J.R. & A. Audhya, (2012) Vesicle formation within endosomes: An ESCRT marks the spot. *Communicative & integrative biology* **5**: 50-56.

Merhej, J., F. Richard-Forget & C. Barreau, (2011) The pH regulatory factor Pac1 regulates *Tri* gene expression and trichothecene production *in Fusarium graminearum*. *Fungal genetics and biology : FG & B* **48**: 275-284.

Miller, C.W. & N.A. Anderson, (1961) Proliferation of conidiophores and intrahyphal hyphae in *Aspergillus niger*. *Mycologia* **53**: 433-436.

Mingot, J.M., E.A. Espeso, E. Diez & M.A. Penalva, (2001) Ambient pH signaling regulates nuclear localization of the *Aspergillus nidulans* PacC transcription factor. *Molecular and cellular biology* **21**: 1688-1699.

Mitić, M. (2011). Investigation of the molecular basis of symbiosis between *Epichloë festucae* and perennial ryegrass. (Ph.D), Massey University, New Zealand.

Moon, C.D., B. Scott, C.L. Schardl & M.J. Christensen, (2000) The evolutionary origins of *Epichloë e*ndophytes from annual ryegrasses. *Mycologia* **92**: 1103-1118.

Mooney, J.L. & L.N. Yager, (1990) Light is required for conidiation in *Aspergillus nidulans*. *Genes & Development* **4**: 1473-1482.

Moreno-Mateos, M.A., J. Delgado-Jarana, A.C. Codon & T. Benitez, (2007) pH and Pac1 control development and antifungal activity in *Trichoderma harzianum*. *Fungal genetics and biology : FG & B* **44**: 1355-1367.

Murphy, S.J. & D.D. Briske, (1992) Regulation of tillering by apical dominance: chronology, interpretivevalue, and current perspectives. *J Range Manage* **45**: 419-429.

Myung, K., S. Li, R.A. Butchko, M. Busman, R.H. Proctor, H.K. Abbas & A.M. Calvo, (2009) *FvVE1* regulates biosynthesis of the mycotoxins fumonisins and fusarins in *Fusarium verticillioides*. *Journal of agricultural and food chemistry* **57**: 5089-5094.

O'Meara, T.R., D. Norton, M.S. Price, C. Hay, M.F. Clements, C.B. Nichols & J.A. Alspaugh, (2010) Interaction of *Cryptococcus neoformans* Rim101 and protein kinase A regulates capsule. *PLoS pathogens* **6**: e1000776.

Orejas, M., E.A. Espeso, J. Tilburn, S. Sarkar, H.N. Arst & M.A. Penalva, (1995) Activation of the *Aspergillus* PacC transcription factor in response to alkaline

ambient pH requires proteolysis of the carboxy-terminal moiety. *Genes & Development* **9**: 1622-1632.

Ortoneda, M., J. Guarro, M.P. Madrid, Z. Caracuel, M.I.G. Roncero, E. Mayayo & A. Di Pietro, (2004) *Fusarium oxysporum* as a multihost model for the genetic dissection of fungal virulence in plants and mammals. *Infection and Immunity* **72**: 1760-1766.

Parniske, M., (2008) Arbuscular mycorrhiza: the mother of plant root endosymbioses. *Nature reviews. Microbiology* **6**: 763-775.

Peñalva, M.A. & H.N. Arst, Jr., (2004) Recent advances in the characterization of ambient pH regulation of gene expression in filamentous fungi and yeasts. *Annual review of microbiology* **58**: 425-451.

Peñalva, M.A., J. Tilburn, E. Bignell & H.N. Arst, Jr., (2008) Ambient pH gene regulation in fungi: making connections. *Trends in microbiology* **16**: 291-300.

Perrin, R.M., N.D. Fedorova, J.W. Bok, R.A. Cramer, J.R. Wortman, H.S. Kim, W.C. Nierman & N.P. Keller, (2007) Transcriptional regulation of chemical diversity in *Aspergillus fumigatus* by LaeA. *PLoS pathogens* **3**: e50.

Piccirillo, S., M.G. White, J.C. Murphy, D.J. Law & S.M. Honigberg, (2010) The Rim101p/PacC pathway and alkaline pH regulate pattern formation in yeast colonies. *Genetics* **184**: 707-716.

Pittenger, T.H., (1956) Synergism of two cytoplasmically inherited mutants in *Neurospora crassa*. *Proceedings of the National Academy of Sciences of the United States of America* **42**: 747-752.

Popay, A.J. & J.G. Baltus, (2001) Black beetle damage to perennial ryegrass infected with AR1 endophyte. *Proceedings of the New Zealand Grassland Association* **63**: 267-271.

Prestidge, R.A., R.P. Pottinger & G.M. Barker, (1982) An association of *Lolium* endophyte with ryegrass resistance to Argentine stem weevil. In: Proc. NZ Weed Pest Control Conf. pp. 119-122.

Proctor, R.H., T.M. Hohn & S.P. McCormick, (1995) Reduced virulence of *Gibberella zeae* caused by disruption of a trichothecene toxin biosynthetic gene. *Molecular plant-microbe interactions : MPMI* **8**: 593-601.

Purschwitz, J., S. Muller & R. Fischer, (2009) Mapping the interaction sites of *Aspergillus nidulans* phytochrome FphA with the global regulator VeA and the White Collar protein LreB. *Molecular genetics and genomics : MGG* **281**: 35-42.

Purschwitz, J., S. Muller, C. Kastner, M. Schoser, H. Haas, E.A. Espeso, A. Atoui, A.M. Calvo & R. Fischer, (2008) Functional and physical interaction of blue- and red-light sensors in *Aspergillus nidulans*. *Current biology : CB* **18**: 255-259.

Reyes-Dominguez, Y., J.W. Bok, H. Berger, E.K. Shwab, A. Basheer, A. Gallmetzer, C. Scazzocchio, N. Keller & J. Strauss, (2010) Heterochromatic marks are associated with the repression of secondary metabolism clusters in *Aspergillus nidulans*. *Molecular microbiology* **76**: 1376-1386.

Rodríguez-Galán, O., A. Galindo, A. Hervas-Aguilar, H.N. Arst, Jr. & M.A. Penalva, (2009) Physiological involvement in pH signaling of Vps24-mediated recruitment of *Aspergillus* PalB cysteine protease to ESCRT-III. *The Journal of biological chemistry* **284**: 4404-4412.

Rolke, Y. & P. Tudzynski, (2008) The small GTPase Rac and the p21-activated kinase Cla4 in *Claviceps purpurea*: interaction and impact on polarity, development and pathogenicity. *Molecular microbiology* **68**: 405-423.

Rollins, J.A., (2003) The *Sclerotinia sclerotiorum pac1* gene is required for sclerotial development and virulence. *Molecular plant-microbe interactions : MPMI* **16**: 785-795.

Rowan, D.D., M.B. Hunt & D.L. Gaynor, (1986) Peramine, a novel insect deeding deterrent from eyegrass infected with the endophyte *Acremonium loliae*. *J. Chem. Soc., Chem. Commun.*: 935-936.

Rusnak, F. & P. Mertz, (2000) Calcineurin: form and function. *Physiological reviews* **80**: 1483-1521.

Sarikaya Bayram, O., O. Bayram, O. Valerius, H.S. Park, S. Irniger, J. Gerke, M. Ni, K.H. Han, J.H. Yu & G.H. Braus, (2010) LaeA control of velvet family regulatory proteins for light-dependent development and fungal cell-type specificity. *PLoS genetics* **6**: e1001226.

Schardl, C.L., A. Leuchtmann & M.J. Spiering, (2004) Symbioses of grasses with seedborne fungal endophytes. *Annual review of plant biology* **55**: 315-340.

Schardl, C.L., B. Scott, S. Florea & D.X. Zhang, (2009) Epichloë endophytes: clavicipitaceous symbionts of grasses. In: Plant Relationships, 2nd Edition. H. Deising (ed). Springer-Verlag Berlin Heidelberg, pp. 275-306.

Schardl, C.L., C.A. Young, J.R. Faulkner, S. Florea & J. Pan, (2012) Chemotypic diversity of epichloae, fungal symbionts of grasses. *Fungal Ecology* **5**: 331-344.

Schardl, C.L., C.A. Young, U. Hesse, S.G. Amyotte, K. Andreeva, P.J. Calie, D.J. Fleetwood, D.C. Haws, N. Moore, B. Oeser, D.G. Panaccione, K.K. Schweri, C.R. Voisey, M.L. Farman, J.W. Jaromczyk, B.A. Roe, D.M. O'Sullivan, B. Scott, P. Tudzynski, Z. An, E.G. Arnaoudova, C.T. Bullock, N.D. Charlton, L. Chen, M. Cox, R.D. Dinkins, S. Florea, A.E. Glenn, A. Gordon, U. Guldener, D.R. Harris, W. Hollin, J. Jaromczyk, R.D. Johnson, A.K. Khan, E. Leistner, A. Leuchtmann, C. Li, J. Liu, J. Liu, M. Liu, W. Mace, C. Machado, P. Nagabhyru, J. Pan, J. Schmid, K. Sugawara, U. Steiner, J.E. Takach, E. Tanaka, J.S. Webb, E.V. Wilson, J.L. Wiseman, R. Yoshida & Z. Zeng, (2013) Plant-symbiotic fungi as chemical engineers: multi-genome analysis of the Clavicipitaceae reveals dynamics of alkaloid loci. *PLoS genetics* **9**: e1003323.

Schmitt, E.K., R. Kempken & U. Kuck, (2001) Functional analysis of promoter sequences of cephalosporin C biosynthesis genes from *Acremonium chrysogenum*: specific DNA-protein interactions and characterization of the transcription factor PacC. *Molecular genetics and genomics : MGG* **265**: 508-518.

Scott, B., Y. Becker, M. Becker & G.M. Cartwright, (2012) Morphogenesis, growth, and development of the grass symbiont *Epichlöe festucae*. **22**: 243-264.

Scott, B., D. Takemoto, A. Tanaka, C.A. Young, M.K. Bryant & K. May, (2007) Functional analysis of the *Epichloe festucae*-perennial ryegrass symbiosis. In: 6th international symposium on fungal endophytes of grasses grasslands research and practice series no 13. A. Popay & E.R. Thom (eds). New Zealand Grassland Association, pp. 433–441.

Scott, B., R. Wrenn, K. May, D. Takemoto, C.A. Young, A. Tanaka, D.J. Fleetwood & R.D. Johnson, (2009) Regulation and functional analysis of bioprotective metabolite genes from the grass symbiont *Epichloe festucae*. In: Recent Developments in Management of Plant Diseases, Plant Pathology in the 21st Century. U*.e.a.* Gisi (ed). Springer Science, pp. 199-213.

Segmuller, N., L. Kokkelink, S. Giesbert, D. Odinius, J. van Kan & P. Tudzynski, (2008) NADPH oxidases are involved in differentiation and pathogenicity in *Botrytis cinerea*. *Molecular plant-microbe interactions : MPMI* **21**: 808-819.

Serrano, R., A. Ruiz, D. Bernal, J.R. Chambers & J. Arino, (2002) The transcriptional response to alkaline pH in *Saccharomyces cerevisiae*: evidence for calcium-mediated signalling. *Molecular microbiology* **46**: 1319-1333.

Shenoy, S.K. & R.J. Lefkowitz, (2011) β-Arrestin-mediated receptor trafficking and signal transduction. *Trends in pharmacological sciences* **32**: 521-533.

Shwab, E.K., J.W. Bok, M. Tribus, J. Galehr, S. Graessle & N.P. Keller, (2007) Histone deacetylase activity regulates chemical diversity in *Aspergillus*. *Eukaryotic Cell* **6**: 1656-1664.

Southern, E.M., (1975) Detection of specific sequences among DNA fragments separated by gel electrophoresis. *J Mol Biol* **98**: 503-517.

Spiering, M.J., C.D. Moon, H.H. Wilkinson & C.L. Schardl, (2005) Gene clusters for insecticidal loline alkaloids in the grass-endophytic fungus *Neotyphodium uncinatum*. *Genetics* **169**: 1403-1414.

St Leger, R.J., J.O. Nelson & S.E. Screen, (1999) The entomopathogenic fungus *Metarhizium anisopliae* alters ambient pH, allowing extracellular protease production and activity. *Microbiology* **145 (Pt 10)**: 2691-2699.

Stinnett, S.M., E.A. Espeso, L. Cobeno, L. Araujo-Bazan & A.M. Calvo, (2007) *Aspergillus nidulans* VeA subcellular localization is dependent on the importin alpha carrier and on light. *Molecular microbiology* **63**: 242-255.

Takemoto, D., S. Kamakura, S. Saikia, Y. Becker, R. Wrenn, A. Tanaka, H. Sumimoto & B. Scott, (2011) Polarity proteins Bem1 and Cdc24 are components of the filamentous fungal NADPH oxidase complex. *Proceedings of the National Academy of Sciences of the United States of America* **108**: 2861-2866.

Takemoto, D., A. Tanaka & B. Scott, (2006) A p67Phox-like regulator is recruited to control hyphal branching in a fungal–grass mutualistic symbiosis. *The Plant cell* **18**: 2807–2821.

Tanaka, A., G.M. Cartwright, S. Saikia, Y. Kayano, D. Takemoto, M. Kato, T. Tsuge & B. Scott, (2013) ProA, a transcriptional regulator of fungal fruiting body development, regulates leaf hyphal network development in the *Epichloe festucae-Lolium perenne* symbiosis. *Molecular microbiology* **90**: 551-568.

Tanaka, A., M.J. Christensen, D. Takemoto, P. Park & B. Scott, (2006) Reactive oxygen species play a role in regulating a fungus-perennial ryegrass mutualistic interaction. *The Plant cell* **18**: 1052-1066.

Tanaka, A., D. Takemoto, T. Chujo & B. Scott, (2012) Fungal endophytes of grasses. *Current opinion in plant biology* **15**: 1-7.

Tanaka, A., D. Takemoto, G.S. Hyon, P. Park & B. Scott, (2008) NoxA activation by the small GTPase RacA is required to maintain a mutualistic symbiotic association between *Epichloe festucae* and perennial ryegrass. *Molecular microbiology* **68**: 1165-1178.

Tanaka, A., B.A. Tapper, A. Popay, E.J. Parker & B. Scott, (2005) A symbiosis expressed non-ribosomal peptide synthetase from a mutualistic fungal endophyte of perennial ryegrass confers protection to the symbiotum from insect herbivory. *Molecular microbiology* **57**: 1036-1050.

Then Bergh, K. & A.A. Brakhage, (1998) Regulation of the *Aspergillus nidulans* penicillin biosynthesis gene *acvA* (*pcbAB*) by amino acids: implication for involvement of transcription factor PacC. *Applied and environmental microbiology* **64**: 843-849.

Tilburn, J., S. Sarkar, D.A. Widdick, E.A. Espeso, M. Orejas, J. Mungroo, M.A. Penalva & H.N. Arst, Jr., (1995) The *Aspergillus* PacC zinc finger transcription factor mediates regulation of both acid- and alkaline-expressed genes by ambient pH. *The EMBO journal* **14**: 779-790.

Trushina, N., M. Levin, P.K. Mukherjee & B.A. Horwitz, (2013) PacC and pH-dependent transcriptome of the mycotrophic fungus *Trichoderma virens*. *BMC genomics* **14**: 138.

Tsai, H., J. Liu, C. Staben, M.J. Christensen, G.C.M. Latch, M.R. Siegel & C.L. Schardl, (1994) Evolutionary diversification of fungal endophytes of tall fescue grass by

hybridization with Epichloe species. *Proceedings of the National Academy of Sciences of the United States of America* **91**: 2542-2546.
Tudzynski, P. & J. Scheffer, (2004) *Claviceps purpurea*: molecular aspects of a unique pathogenic lifestyle. *Molecular plant pathology* **5**: 377-388.
van Dongen, P.W.J. & A.N.J.A. de Groot, (1995) History of ergot alkaloids from ergotism to ergometrine. *European Journal of Obstretics & Gynaecology and Reproductive Biology* **60**: 109-116.
van Hove, L.W.A., P. Heeres & M.E. Bossen, (2002) The annual variation in stomatal ammonia compensation point of rye grass *Lolium perenne* leaves in an intensively managed grassland. *Atmospheric Environment* **36**: 2965-2977.
van Wetter, M., F.H.J. Schuren, T.A. Schuurs & J.G.H. Wessels, (1996) Targeted mutation of the SC3 hydrophobin gene of *Schizophyllum commune* affects formation of aerial hyphae. *FEMS microbiology letters* **140**: 265-269.
Vera-Estrella, R., B.J. Barkla, V.J. Higgins & E. Blumwald, (1994) Plant defense response to fungal pathogens (activation of host-plasma membrane H+-ATPase by elicitor-induced enzyme dephosphorylation). *Plant physiology* **104**: 209-215.
Viladevall, L., R. Serrano, A. Ruiz, G. Domenech, J. Giraldo, A. Barcelo & J. Arino, (2004) Characterization of the calcium-mediated response to alkaline stress in *Saccharomyces cerevisiae*. *The Journal of biological chemistry* **279**: 43614-43624.
Vincent, O., L. Rainbow, J. Tilburn, H.N. Arst & M.A. Penalva, (2003) YPXL/I is a protein interaction motif recognized by *Aspergillus* PalA and its human homologue, AIP1/Alix. *Molecular and cellular biology* **23**: 1647-1655.
Vylkova, S., A.J. Carman, H.A. Danhof, J.R. Collette, H. Zhou & M.C. Lorenz, (2011) The fungal pathogen *Candida albicans* autoinduces hyphal morphogenesis by raising extracellular pH. *mBio* **2**: e00055-00011.
Wiemann, P., D.W. Brown, K. Kleigrewe, J.W. Bok, N.P. Keller, H.U. Humpf & B. Tudzynski, (2010) FfVel1 and FfLae1, components of a velvet-like complex in *Fusarium fujikuroi*, affect differentiation, secondary metabolism and virulence. *Molecular microbiology* **77**: 972-944.
Wilkinson, H.H., M.R. Siegel, J.D. Blankenship, A.C. Mallory, L.P. Bush & C.L. Schardl, (2000) Contribution of fungal loline alkaloids to protection from aphids in a grass-endophyte mutualism. *Molecular plant-microbe interactions : MPMI* **13**: 1027-1033.
Williams, R.L. & S. Urbe, (2007) The emerging shape of the ESCRT machinery. *Nature reviews. Molecular cell biology* **8**: 355-368.
Wosten, H.A., (2001) Hydrophobins: multipurpose proteins. *Annual review of microbiology* **55**: 625-646.
Wu, Y., Y. Yang, S. Ye & Y. Jiang, (2010) Structure of the gating ring from the human large-conductance Ca(2+)-gated K(+) channel. *Nature* **466**: 393-397.
Xu, W. & A.P. Mitchell, (2001) Yeast PalA/AIP1/Alix homolog Rim20p associates with a PEST-like region and is required for its proteolytic cleavage. *Journal of bacteriology* **183**: 6917-6923.
Xu, W., F.J. Smith, Jr., R. Subaran & A.P. Mitchell, (2004) Multivesicular body-ESCRT components function in pH response regulation in *Saccharomyces cerevisiae* and *Candida albicans*. *Molecular biology of the cell* **15**: 5528-5537.
You, B.J., M. Choquer & K.R. Chung, (2007) The *Colletotrichum acutatum* gene encoding a putative pH-responsive transcription regulator is a key virulence determinant during fungal pathogenesis on citrus. *Molecular plant-microbe interactions : MPMI* **20**: 1149-1160.
Young, C.A., M.K. Bryant, M.J. Christensen, B.A. Tapper, G.T. Bryan & B. Scott, (2005) Molecular cloning and genetic analysis of a symbiosis-expressed gene cluster

for lolitrem biosynthesis from a mutualistic endophyte of perennial ryegrass. *Molecular genetics and genomics : MGG* **274**: 13-29.

Young, C.A., S. Felitti, K. Shields, G. Spangenberg, R.D. Johnson, G.T. Bryan, S. Saikia & B. Scott, (2006) A complex gene cluster for indole-diterpene biosynthesis in the grass endophyte *Neotyphodium lolii*. *Fungal genetics and biology : FG & B* **43**: 679-693.

Zhang, D.X., A.J. Stromberg, M.J. Spiering & C.L. Schardl, (2009) Coregulated expression of loline alkaloid-biosynthesis genes in *Neotyphodium uncinatum* cultures. *Fungal genetics and biology : FG & B* **46**: 517-530.

6. Appendices

6. Appendices

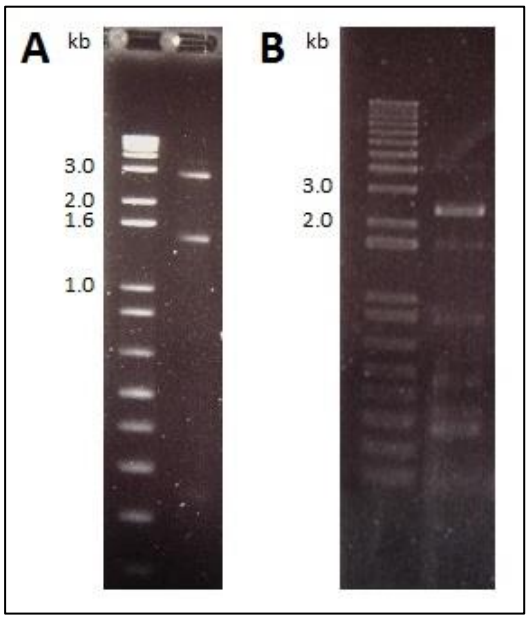

Appendix 6.1. PCR amplification of *pacC* transcript. (A) SDS-denaturing agarose gel of crude RNA extracted from wild-type *E. festucae* Fl1 showing the two ribosomal RNA bands. (B) Gel showing a 2.3 kb pacC fragment (2.7 genomic sequence minus 0.3 kb intronic sequence) amplified from cDNA synthesised from total RNA shown in (A) with primers YL3/YL4.

Appendix 6.2. Vector maps

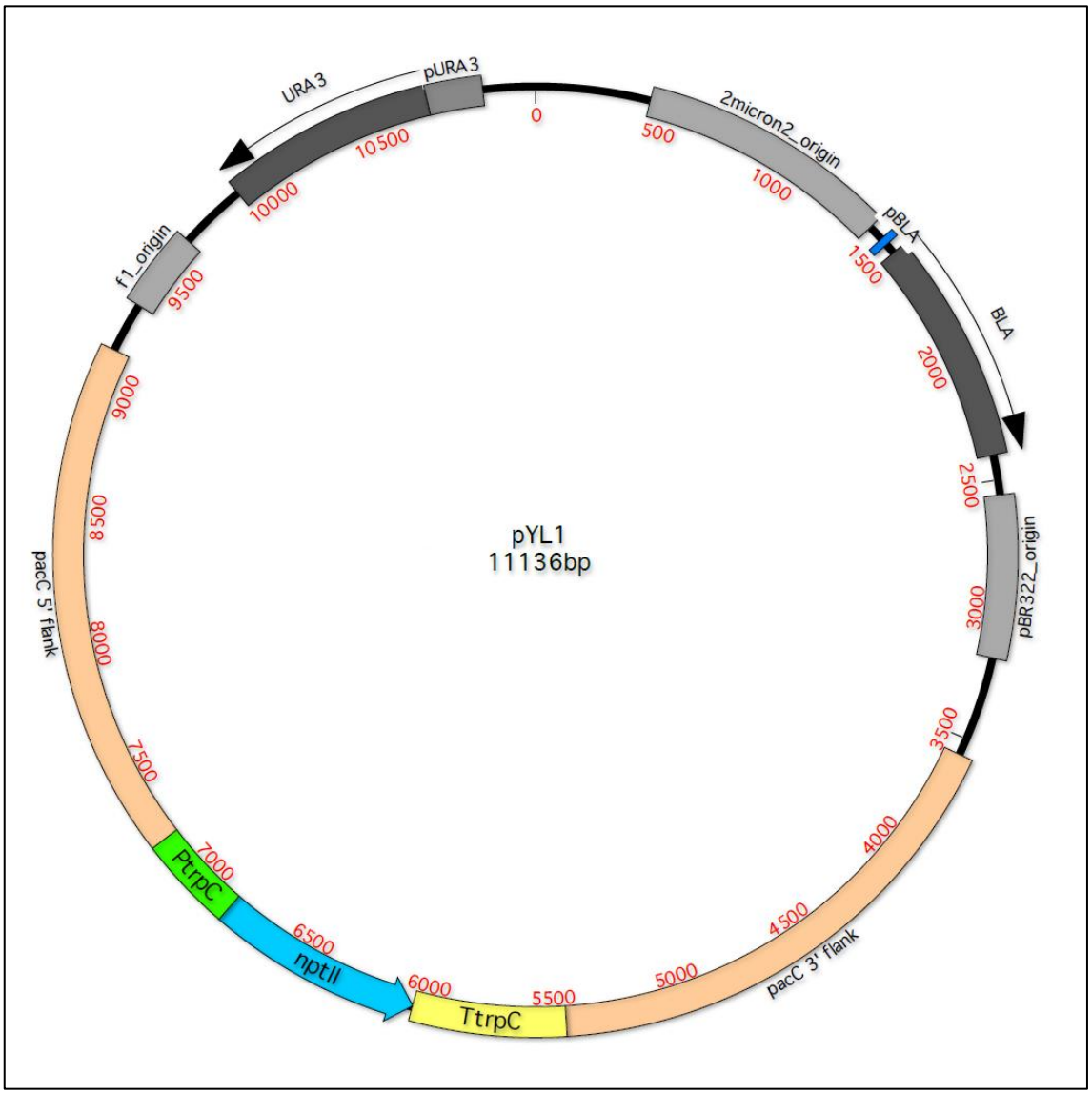

Appendix 6.2.1. pYL1 vector

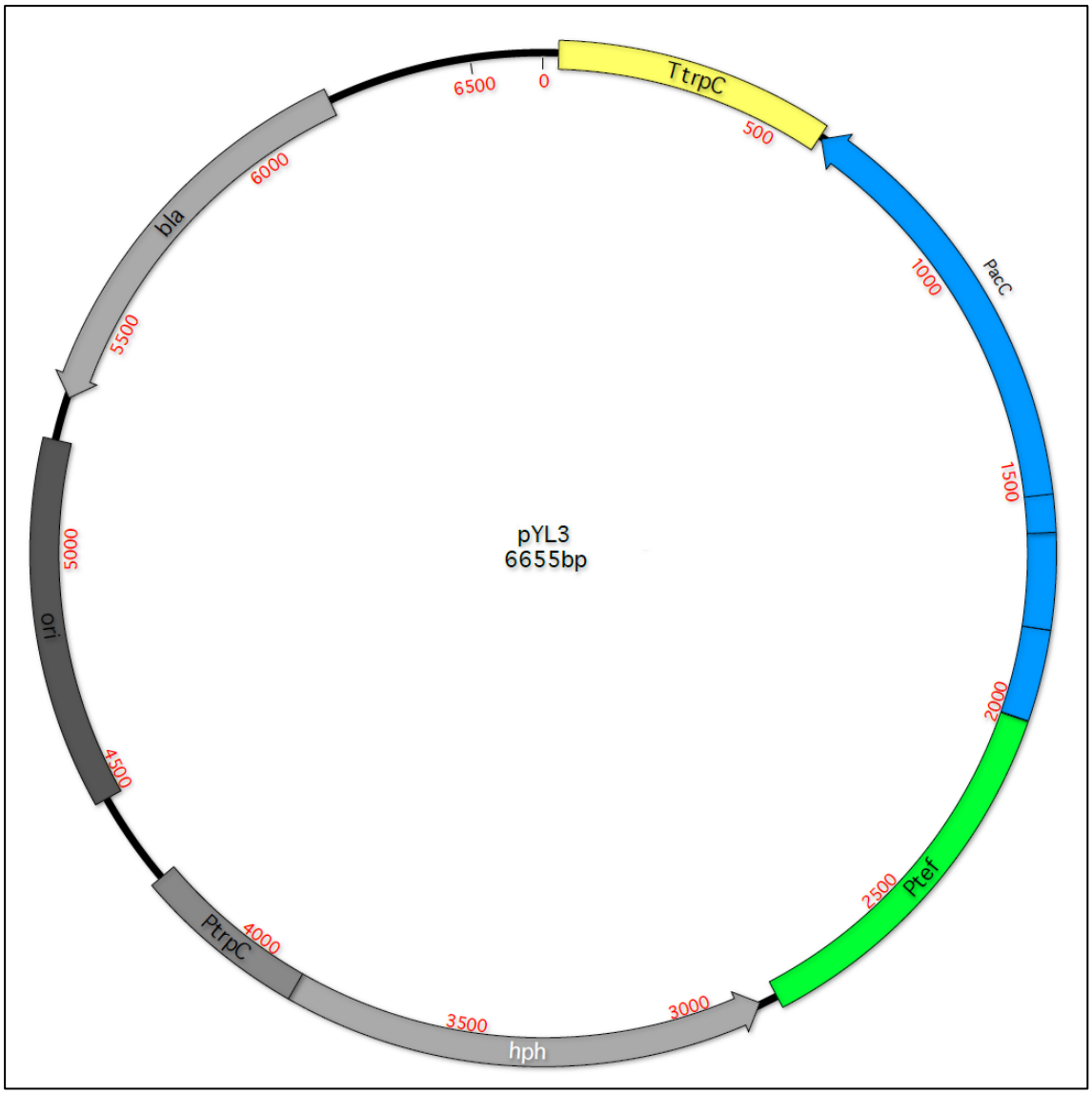

Appendix 6.2.2. pYL3 vector.

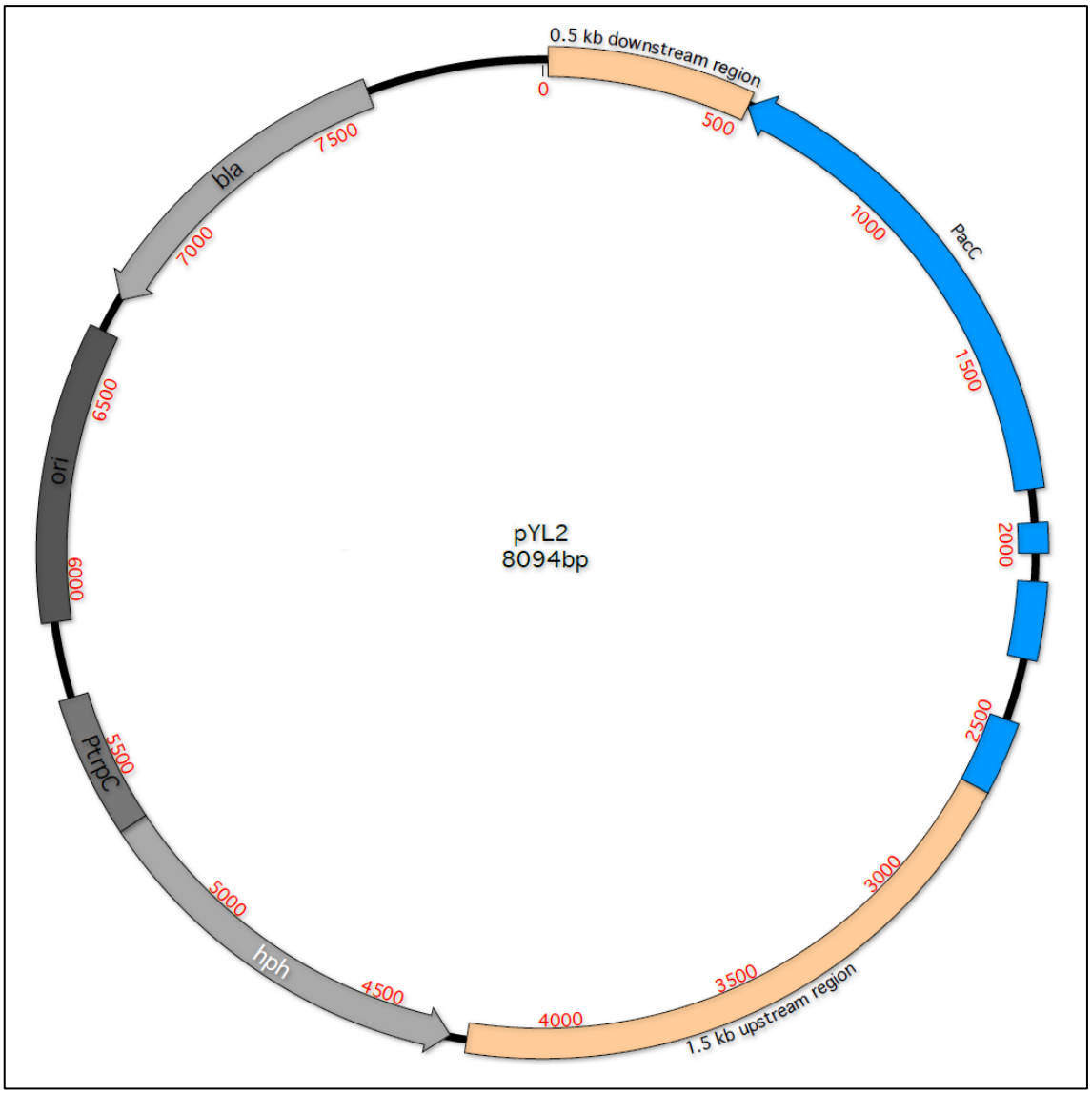

Appendix 6.2.3. pYL2 vector.

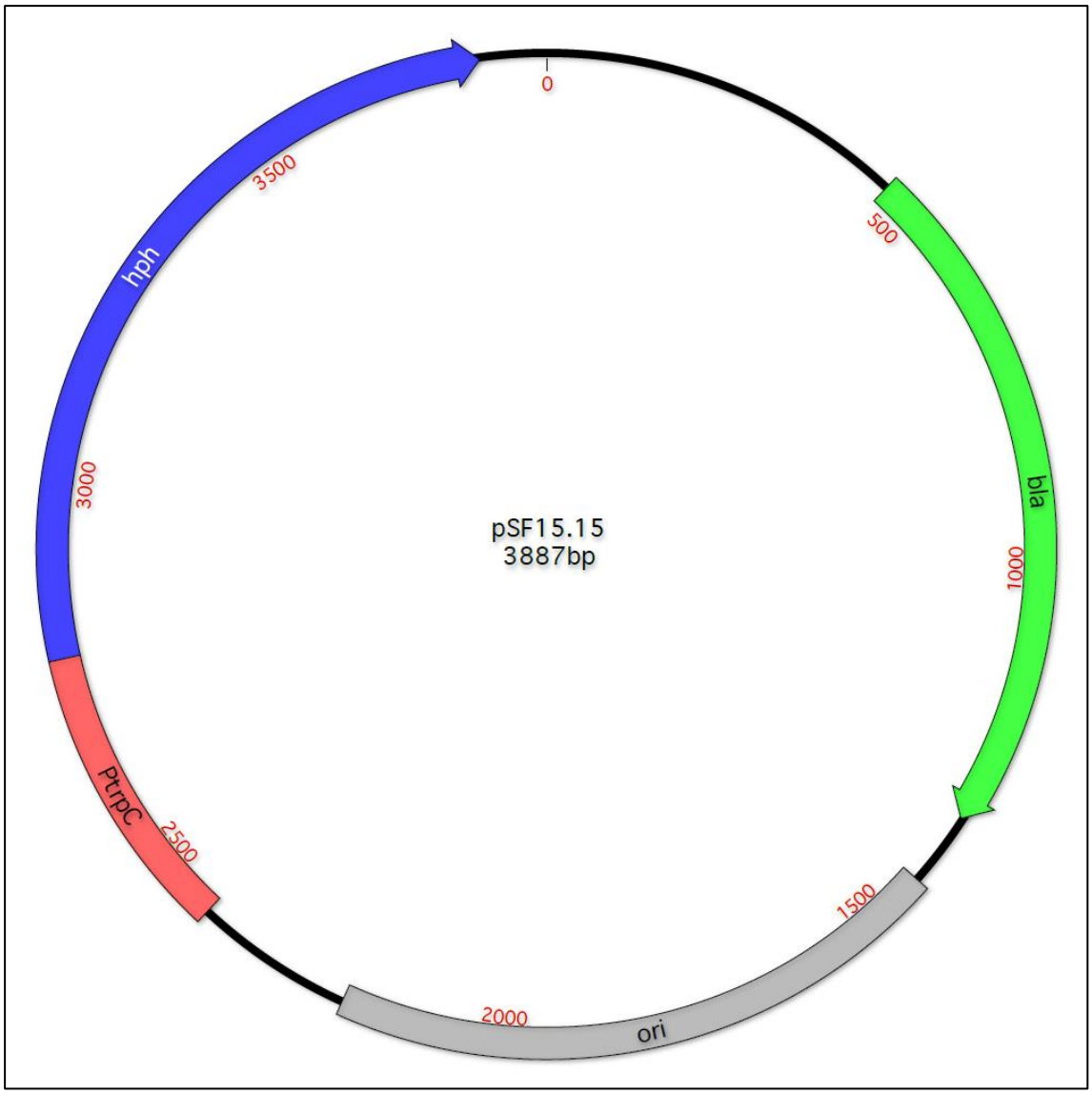

Appendix 6.2.4. pSF15.15 vector.

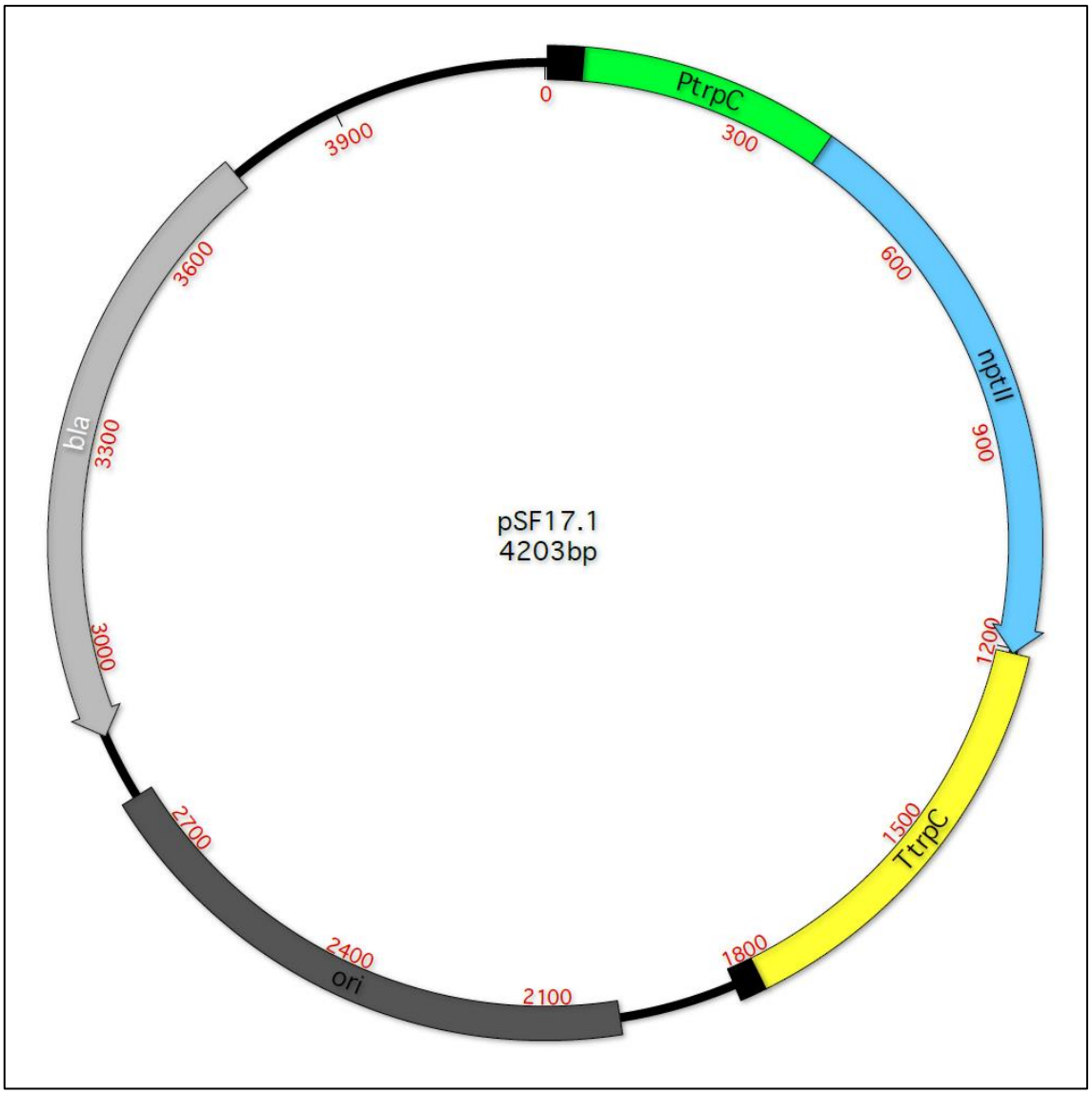

Appendix 6.2.5. pSF17.1 vector.

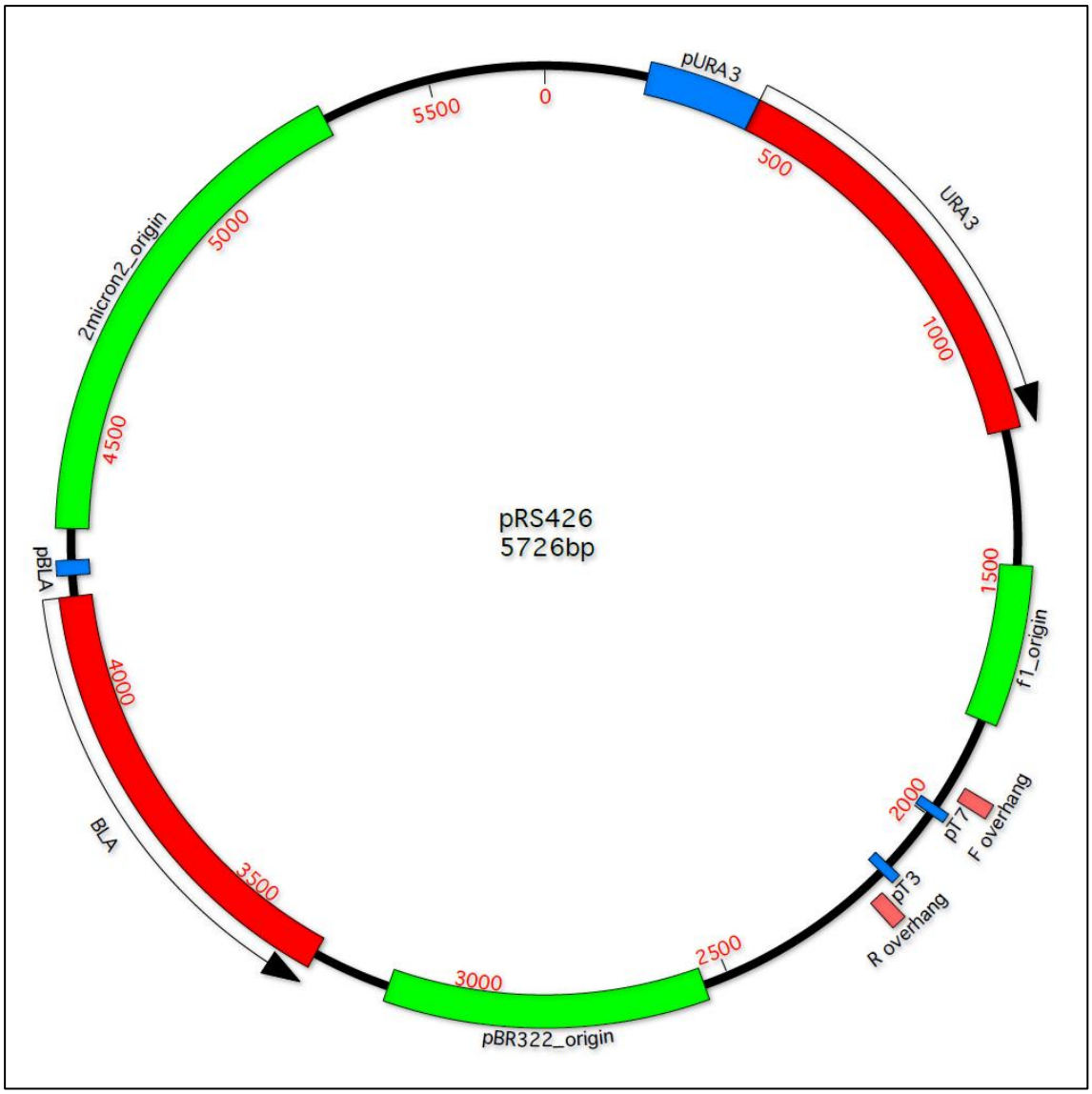

Appendix 6.2.6. pRS426 vector.

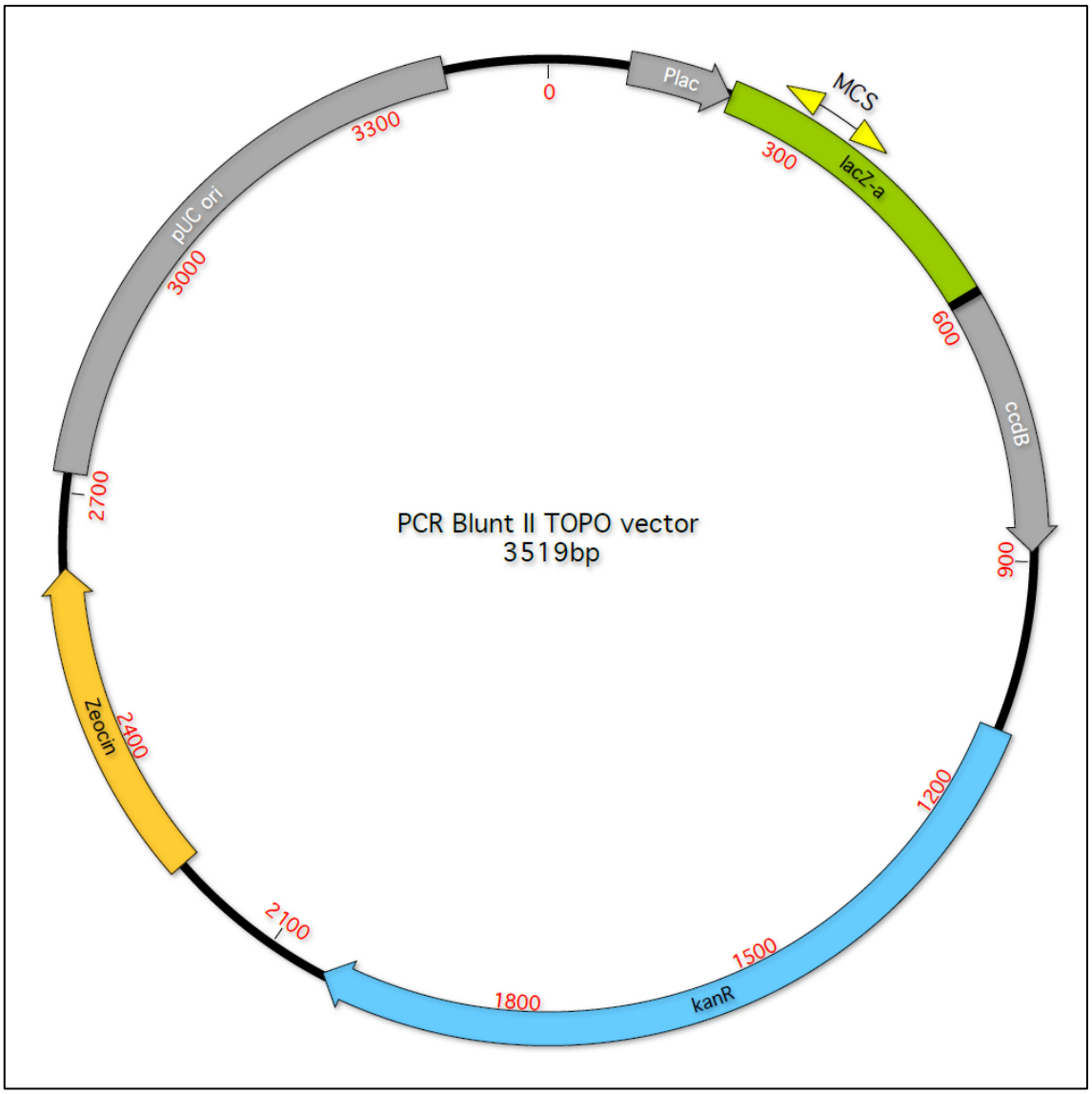

Appendix 6.2.7. pCR®-Blunt II-TOPO® vector.

Appendix 6.3. Multiple sequence alignments

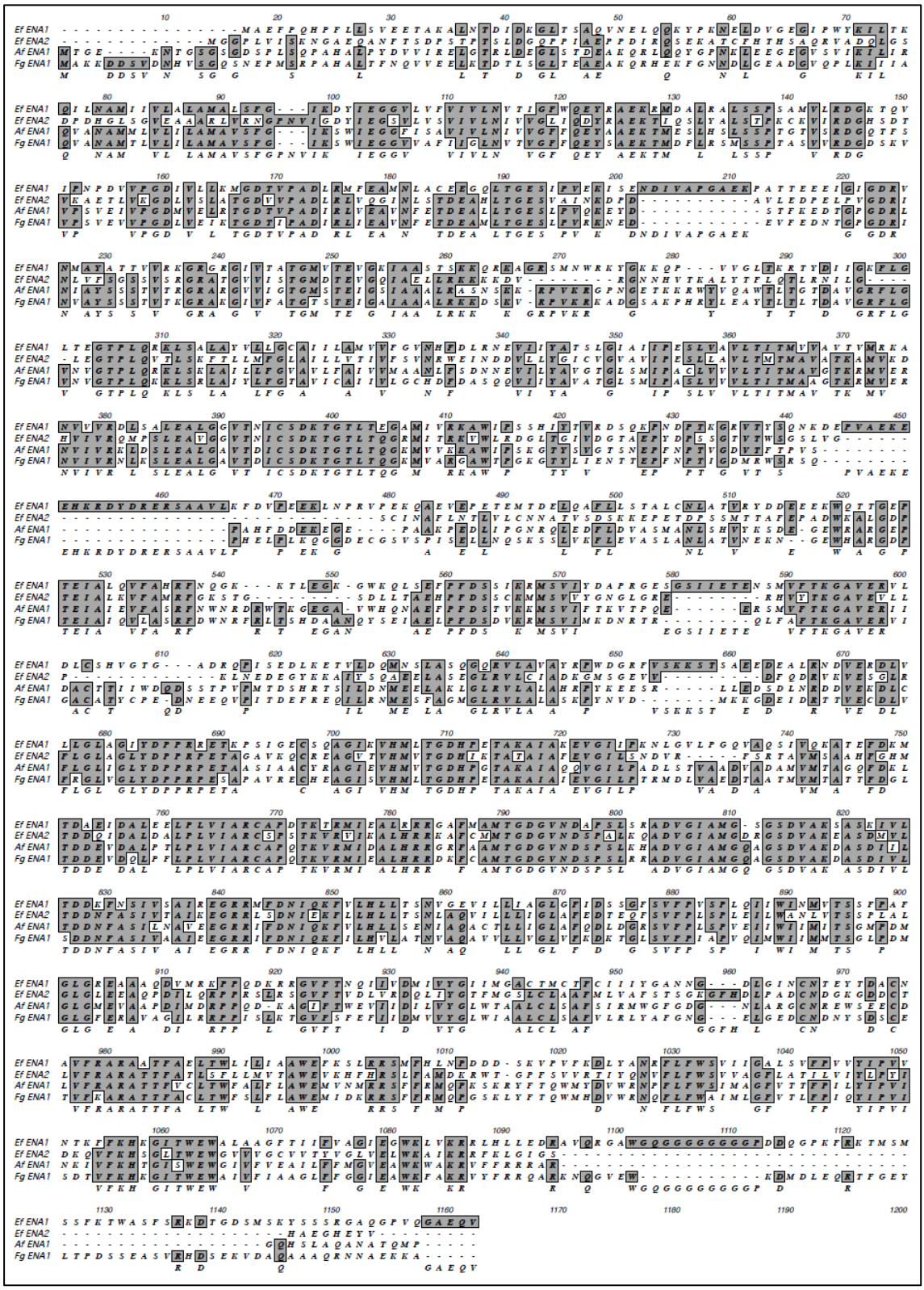

Appendix 6.3.1. Multiple sequence alignment of *E. festucae* ENA proteins with homologues from other fungi. Amino acid sequences are shown of *E. festucae* ENA1 (predicted from the putative gene EfM2.084240), *E. festucae* ENA2 (predicted from the putative gene EfM2.113810), ENA1 from *A. flavus* (XP_002376874.1) and ENA1 from *F. graminearum* (AAR01872.1).

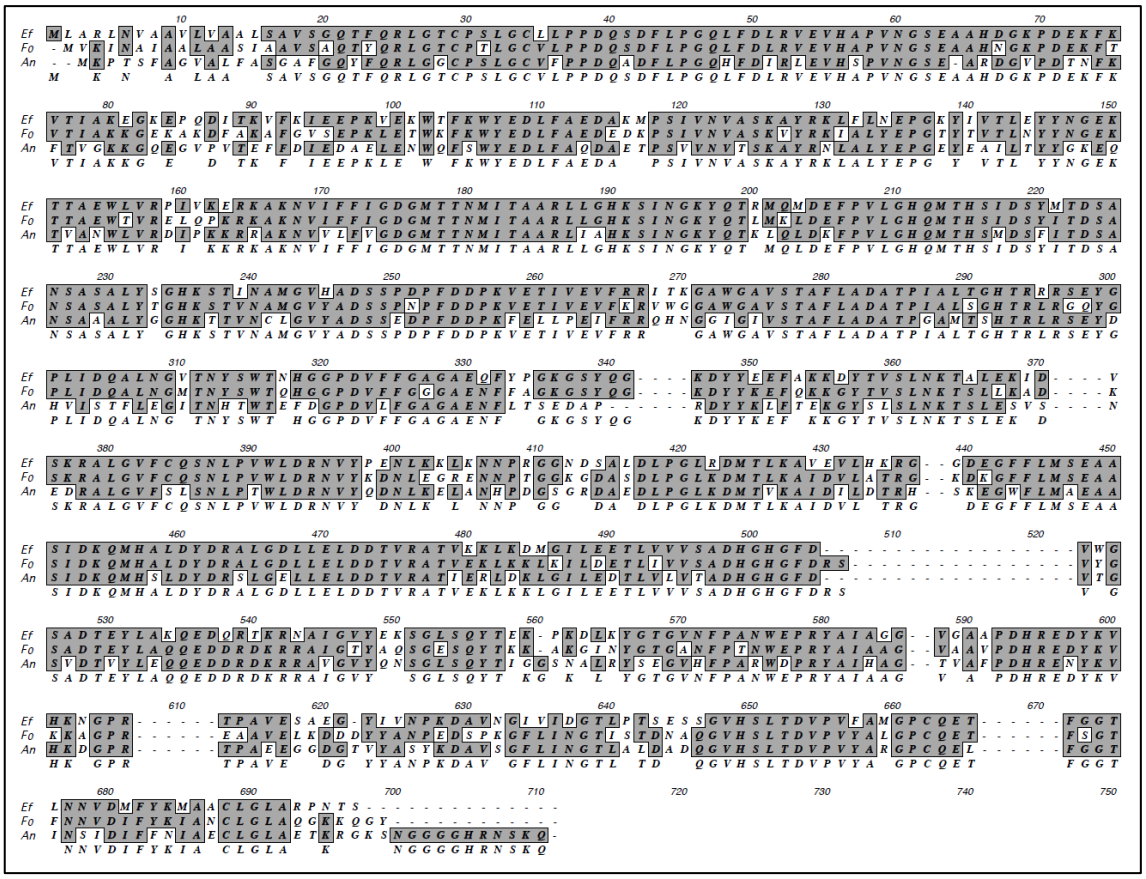

Appendix 6.3.2. Multiple sequence alignment of *E. festucae* alkaline phosphatase with other fungal homologues. Amino acid sequences of alkaline phosphatases from *F. oxysporum* (EMT65064.1) and *A. nidulans* (XP_660097.1) are shown. *E. festucae* alkaline phosphatase is the predicted translated product of the putative gene EfM2.057140.

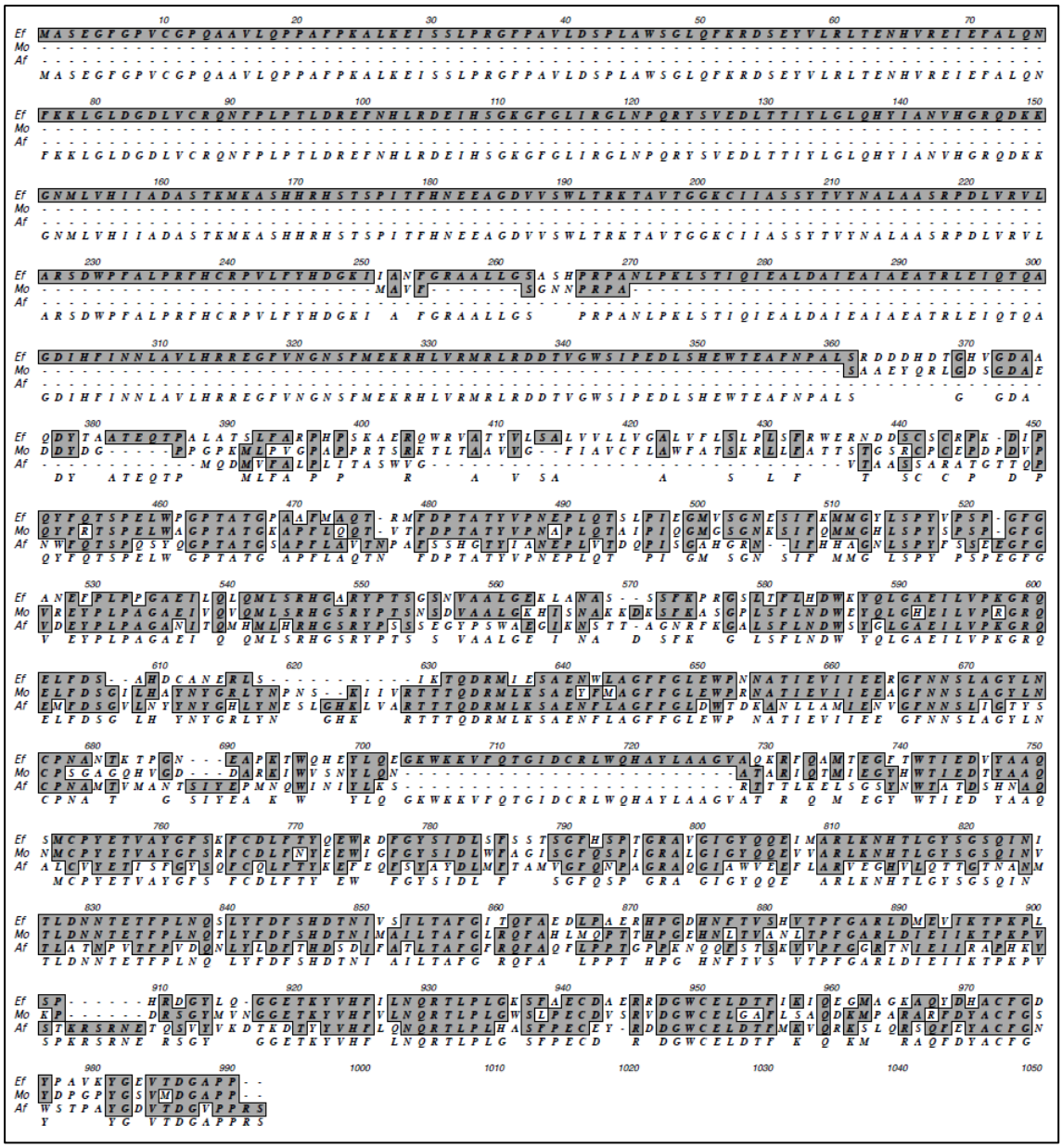

Appendix 6.3.3. Multiple sequence alignment of *E. festucae* acid phosphatase with other fungal homologues. Amino acid sequences of *M. oryzae* (EHA48929.1) and *A. flavus* (XP_002373082.1) acid phosphatases are shown. The *E. festucae* acid phosphatase is the predicted translated product of the putative gene EfM2.003400.

Appendix 6.3.4. Multiple sequence alignment of *E. festucae* CNH1 with other fungal homologues. Amino acid sequences of CNH1 from *T. virens* (JGI protein ID 10799) and *N. crassa* (CAF05976.1) are shown. The *E. festucae* CNH1 protein is the predicted translated product of the putative gene EfM2.014050.

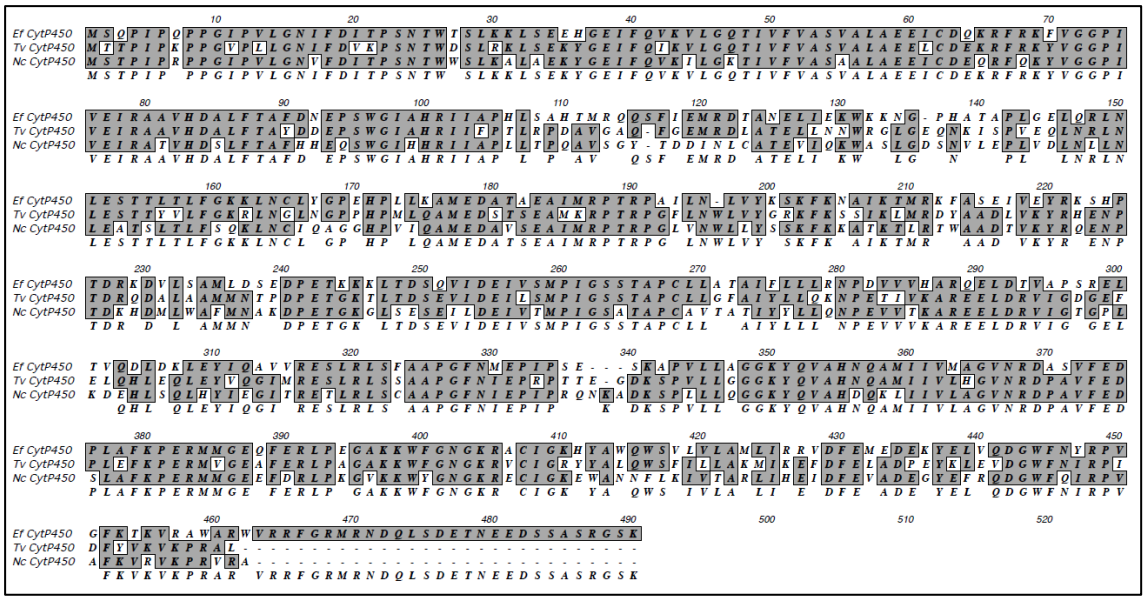

Appendix 6.3.5. Multiple sequence alignment of cytochrome P450 proteins from *E. festucae* and other fungal homologues. Amino acid sequences of cytochrome P450 from *T. virens* (JGI protein ID 86792) and *N. crassa* (XP_955933.1) are shown. The *E. festucae* cytochrome P450 protein is the predicted translated product of the putative gene EfM2.084750.

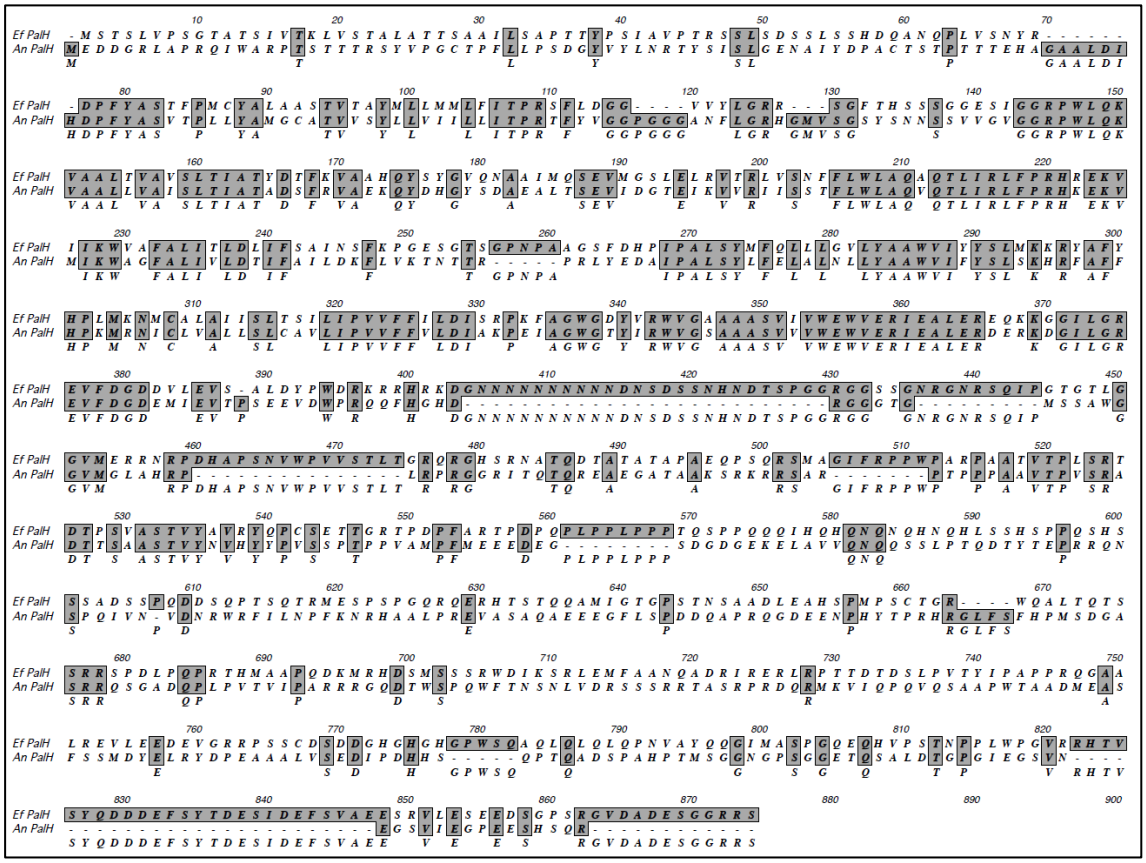

Appendix 6.3.6. Multiple sequence alignment of PalH from *E. festucae* and *A. nidulans*. Amino acid sequence of PalH from *E. festucae* and *A. nidulans* (AAF70858.1) are shown. The putative *E. festucae* gene (EfM2.074620) in contig 674 was identified by a tBLASTn search using

A. nidulans PalH protein with a score of 287 and an E-value of 3e-77. The proteins share 31% amino acid identity.

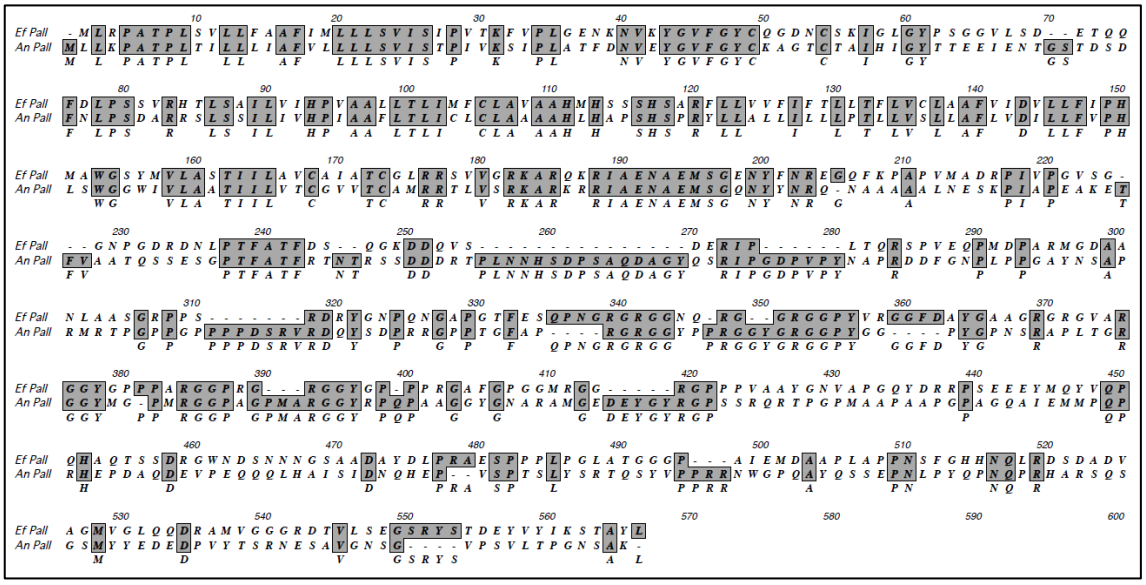

Appendix 6.3.7. Multiple sequence alignment of PalI from *E. festucae* and *A. nidulans*. Amino acid sequence of PalI from *E. festucae* and *A. nidulans* (CAA07588.2) are shown. The putative *E. festucae* gene (EfM2.064340) in contig 263 was identified by a tBLASTn search using *A. nidulans* PalI protein with a score of 127 and an E-value of 7e-41. The proteins share 36% amino acid identity.

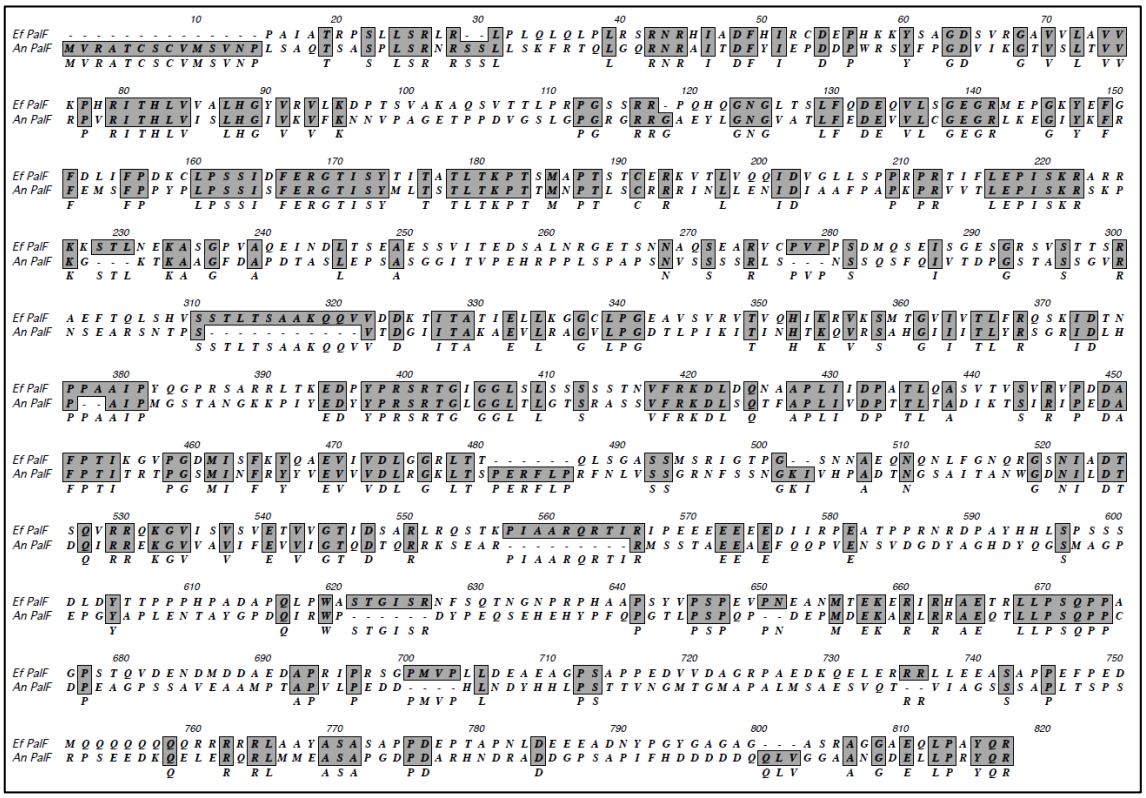

Appendix 6.3.8. Multiple sequence alignment of PalF from *E. festucae* and *A. nidulans*. Amino acid sequence of PalF from *E. festucae* and *A. nidulans* (AAC49808.1) are shown. The

putative *E. festucae* gene (no gene model assigned) in contig 568 was identified by a tBLASTn search using *A. nidulans* PalF protein with a score of 384 and an E-value of 1e-106. The proteins share 34% amino acid identity.

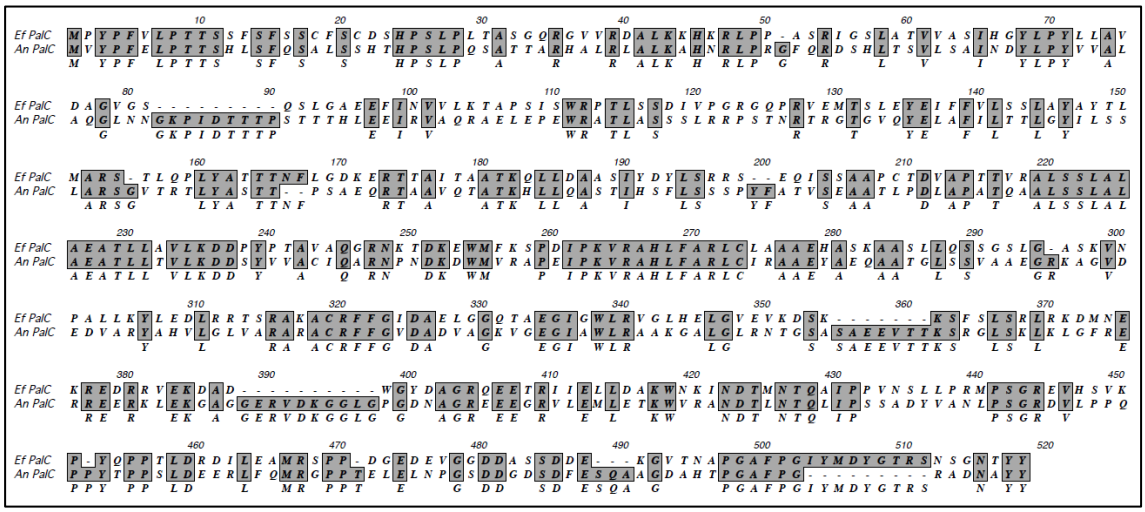

Appendix 6.3.9. Multiple sequence alignment of PalC from *E. festucae* and *A. nidulans*. Amino acid sequence of PalC from *E. festucae* and *A. nidulans* (AAF70857.1) are shown. The putative *E. festucae* gene (EfM2.108790) in contig 754 was identified by a tBLASTn search using *A. nidulans* PalC protein with a score of 222 and an E-value of 7e-65. The proteins share 42% amino acid identity.

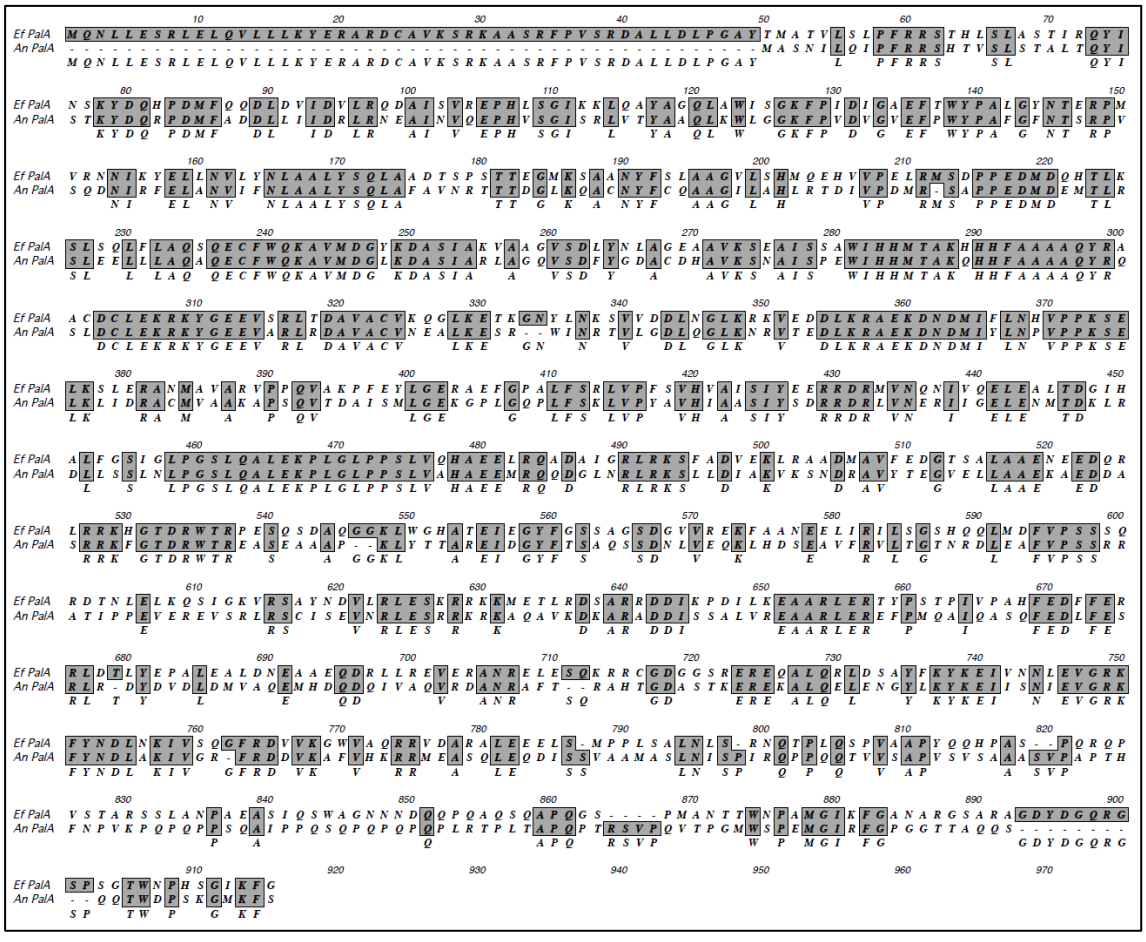

Appendix 6.3.10. Multiple sequence alignment of PalA from *E. festucae* and *A. nidulans*. Amino acid sequence of PalA from *E. festucae* and *A. nidulans* (CAB05920.3) are shown. The putative *E. festucae* gene (EfM2.035980) in contig 657 was identified by a tBLASTn search using *A. nidulans* PalA protein with a score of 654 and an E-value of 0. The proteins share 47% amino acid identity.

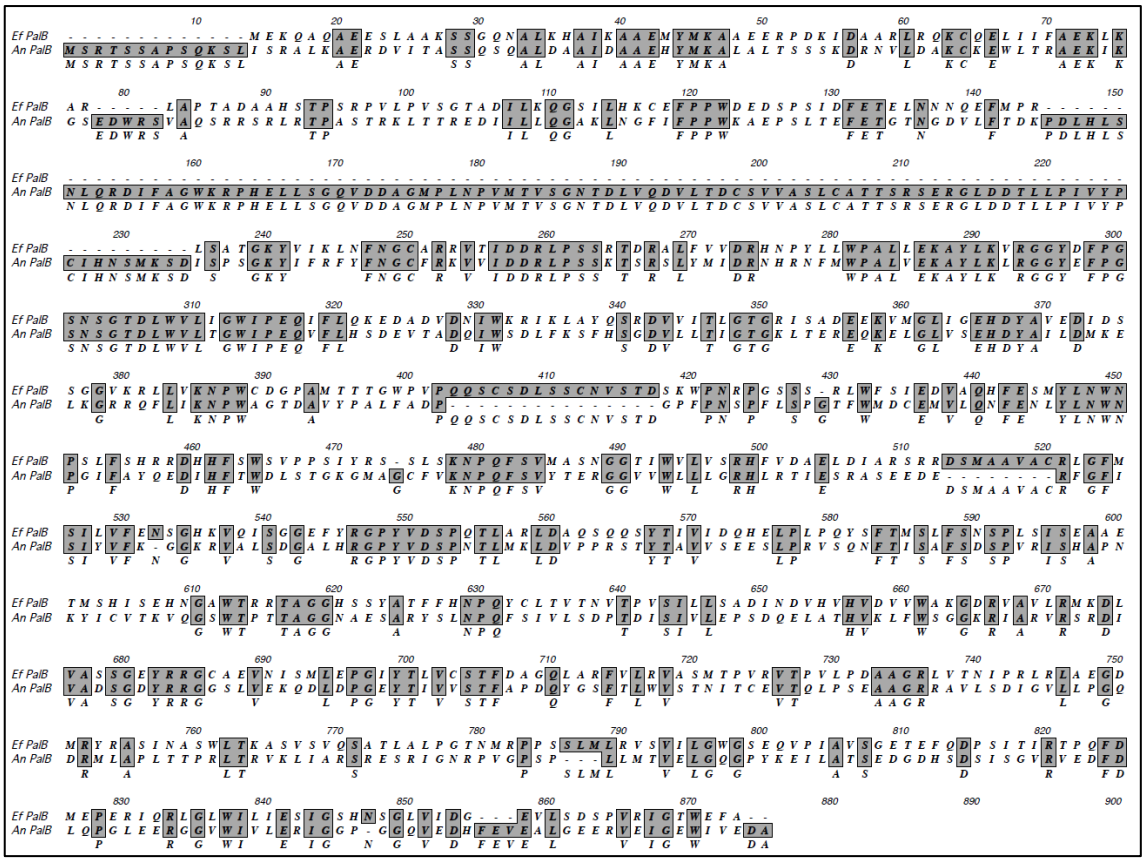

Appendix 6.3.11. Multiple sequence alignment of PalB from *E. festucae* and *A. nidulans*. Amino acid sequence of PalB from E. festucae and A. nidulans (CAA91013.2) are shown. The putative *E. festucae* gene (EfM2.017470) in contig 239 was identified by a tBLASTn search using *A. nidulans* PalB protein with a score of 319 and an E-value of e-131. The proteins share 33% amino acid identity.

Appendix 6.4. qRT-PCR standard curves

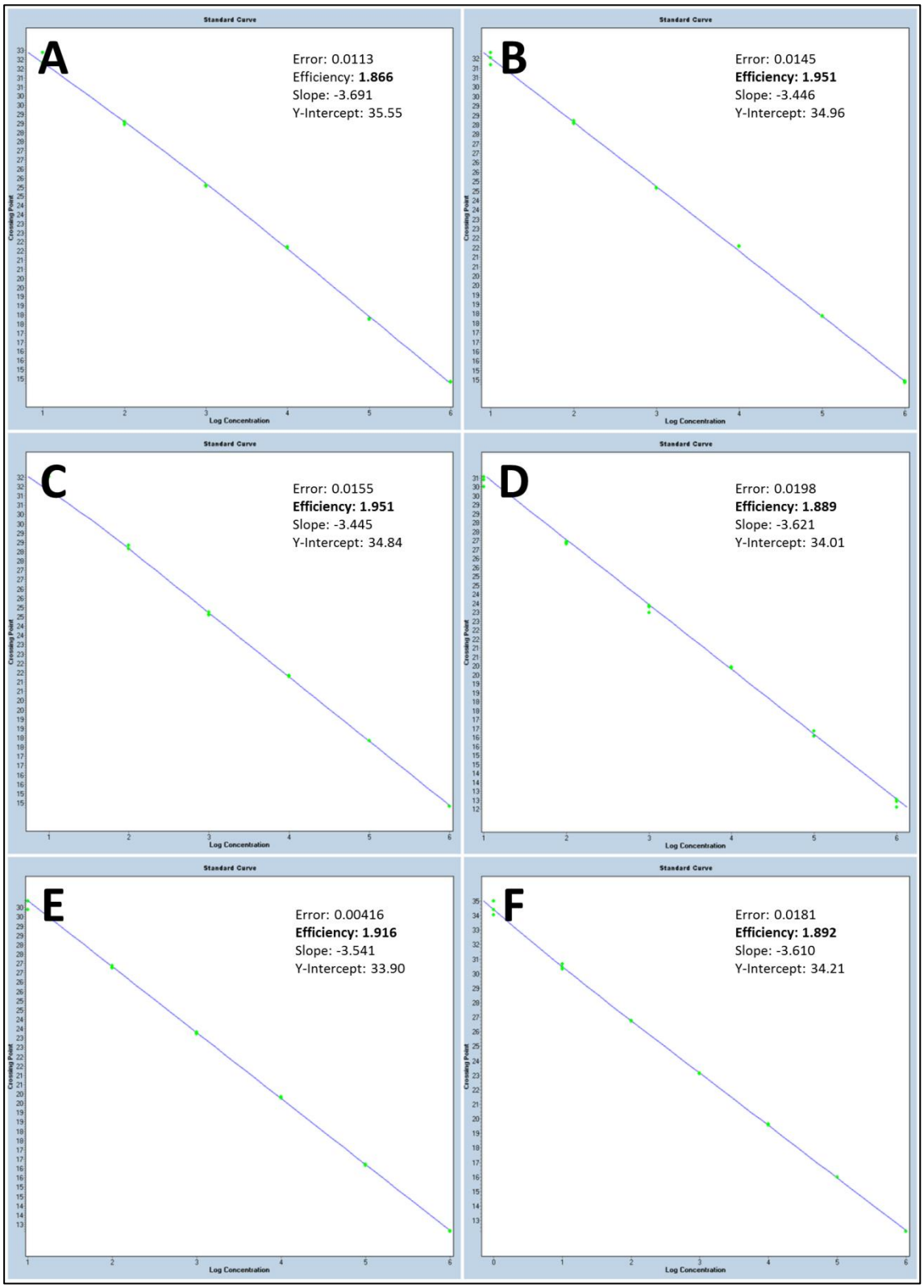

Appendix 6.4.1. qRT-PCR standard curves. (A) *EF*-2, (B) *RPS22*, (C) *plectin*, (D) *pacC*, (E), *pacC*^{CA} and (F) *perA*. The calculated primer efficiencies are indicated. Standards were prepared of 10 aM (assigned a value of '0' log-concentration on the y-axis) to 10 pM (assigned a value of '6' log-concentration on the y-axis) concentrations and analysed with three technical replicates.

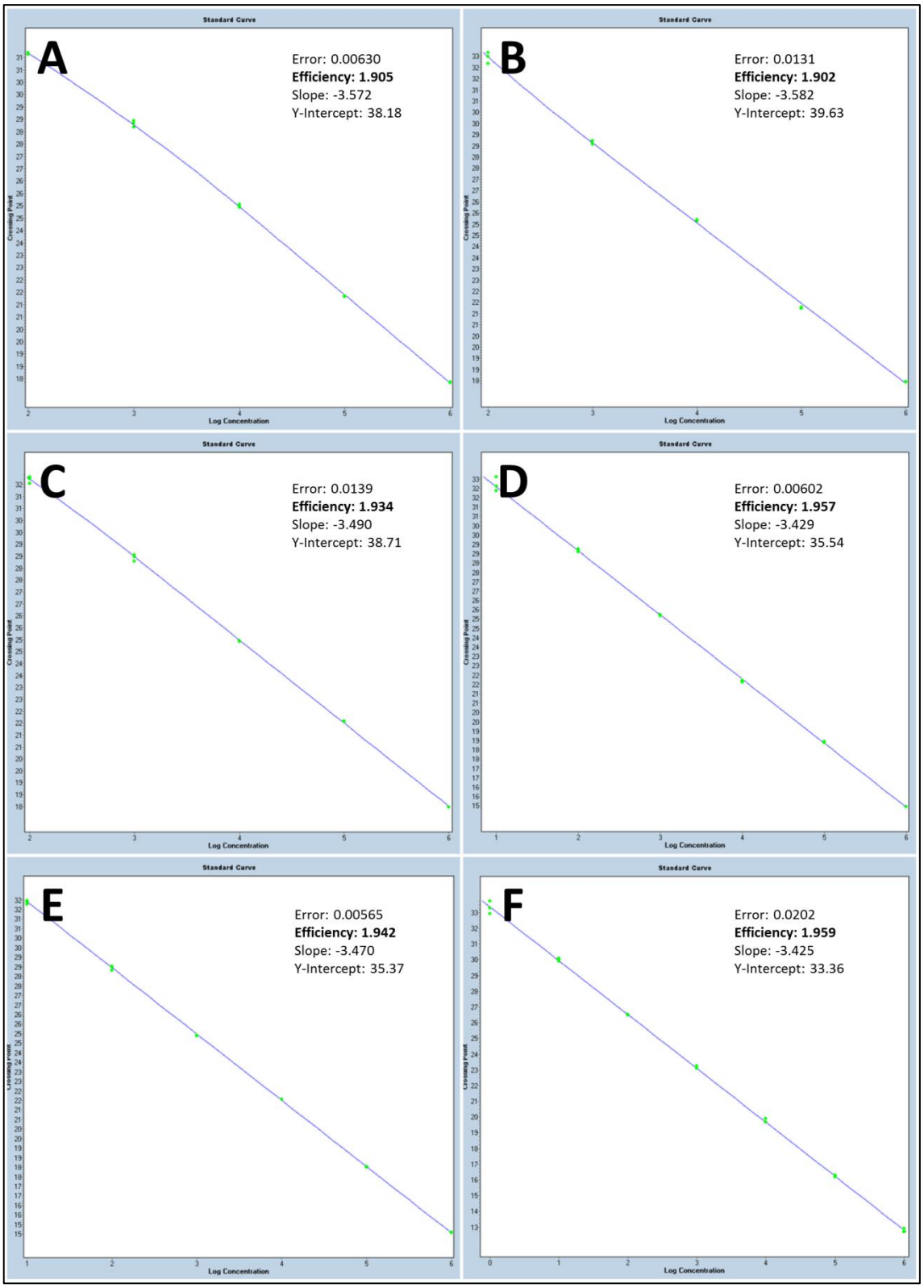

Appendix 6.4.2. qRT-PCR standard curves. (A) *ltmE*, (B) *ltmP*, (C) *ltmM*, (D) *easA*, (E), *dmaW* and (F) *lpsA*. The calculated primer efficiencies are indicated. Standards were prepared of 10 aM (assigned a value of '0' log-concentration on the y-axis) to 10 pM (assigned a value of '6' log-concentration on the y-axis) concentrations and analysed with three technical replicates.

Appendix 6.5. qRT-PCR data

	EF-2		pacC			
Name	Cp	Avg	Cp	2^(ΔCp)	Avg	Stdev
CA 1	19.23	19.165	22.47	0.1012	0.1008	0.0005
CA 1	19.1		22.48	0.1005		
CA 2	18.15	18.15	20.62	0.1805	0.1818	0.0018
CA 2	18.15		20.6	0.1830		
CA 6	18.19	18.185	22.77	0.0417	0.0418	0.0002
CA 6	18.18		22.76	0.0420		
CA 13	18.47	18.48	20.98	0.1768	0.1805	0.0053
CA 13	18.49		20.92	0.1843		
CA 14	18.44	18.41	20.14	0.3015	0.3004	0.0015
CA 14	18.38		20.15	0.2994		
CA 19	18.37	18.355	20.55	0.2184	0.2222	0.0054
CA 19	18.34		20.5	0.2261		
CA 21	17.68	17.68	25.32	0.0050	0.0050	0.0000
CA 21	17.68		25.3	0.0051		
CA 22	18.62	18.615	21.74	0.1146	0.2150	0.1419
CA 22	18.61		20.28	0.3153		

Appendix 6.5.1. qRT-PCR data of Figure 3.5: Expression of *pacC*^{CA} transcript in eight *pacC*^{CA} transformants.

	ENA2		EF-2		x / EF-2				RPS22		x / RPS22			
Sample	Cp	Avg	Cp	Avg	2^(ΔCp)	Avg	Stdev	S.E.	Cp	Avg		Avg	Stdev	S.E.
WT pH 5 - 1	31.66	31.61	19.22	19.225	0.00019	0.00020	0.00001	0.00000	20.28	20.285	0.00039	0.00044	0.00005	0.00003
WT pH 5 - 1	31.56		19.23						20.29					
WT pH 5 - 2	31.41	31.445	19.15	19.16	0.00020				20.3	20.31	0.00044			
WT pH 5 - 2	31.48		19.17						20.32					
WT pH 5 - 3	30.85	30.925	18.64	18.645	0.00020				19.94	19.94	0.00049			
WT pH 5 - 3	31		18.65						19.94					
WT pH 6.5 - 1	31.65	31.765	18.32	18.34	0.00009	0.00012	0.00005	0.00003	19.38	19.415	0.00019	0.00028	0.00015	0.00009
WT pH 6.5 - 1	31.88		18.36						19.45					
WT pH 6.5 - 2	31.9	31.865	18.48	18.475	0.00009				19.54	19.565	0.00020			
WT pH 6.5 - 2	31.83		18.47						19.59					
WT pH 6.5 - 3	30.6	30.835	18.36	18.355	0.00018				19.75	19.745	0.00046			
WT pH 6.5 - 3	31.07		18.35						19.74					
WT pH 8 - 1	31.04	31.005	18.58	18.585	0.00018	0.00022	0.00008	0.00004	19.74	19.75	0.00041	0.00053	0.00018	0.00010
WT pH 8 - 1	30.97		18.59						19.76					
WT pH 8 - 2	30.13	30.485	18.85	18.83	0.00031				20.08	20.07	0.00073			
WT pH 8 - 2	30.84		18.81						20.06					
WT pH 8 - 3	30.78	30.635	18.18	18.165	0.00018				19.51	19.515	0.00045			
WT pH 8 - 3	30.49		18.15						19.52					
	ENA2		EF-2		x / EF-2				RPS22		x / RPS22			
Sample	Cp	Avg	Cp	Avg	2^(ΔCp)	Avg	Stdev	S.E.	Cp	Avg		Avg	Stdev	S.E.
ΔpacC pH 5 - 1	33.48	33.53	19.2	19.2	0.00005	0.00007	0.00002	0.00001	19.91	19.925	0.00008	0.00011	0.00004	0.00003
ΔpacC pH 5 - 1	33.58		19.2						19.94					
ΔpacC pH 5 - 2	33.56	33.495	19.4	19.43	0.00006				20.01	20.01	0.00009			
ΔpacC pH 5 - 2	33.43		19.46						20.01					
ΔpacC pH 5 - 3	32.49	32.62	19.19	19.19	0.00009				20.01	20.005	0.00016			
ΔpacC pH 5 - 3	32.75		19.19						20					
ΔpacC pH 6.5 - 1	31.94	32.05	18.68	18.685	0.00009	0.00011	0.00002	0.00001	19.8	19.805	0.00021	0.00024	0.00004	0.00003
ΔpacC pH 6.5 - 1	32.16		18.69						19.81					
ΔpacC pH 6.5 - 2	31.77	31.795	18.97	18.965	0.00014				20.07	20.06	0.00029			
ΔpacC pH 6.5 - 2	31.82		18.96						20.05					
ΔpacC pH 6.5 - 3	31.89	31.995	18.81	18.8	0.00011				19.93	19.94	0.00024			
ΔpacC pH 6.5 - 3	32.1		18.79						19.95					
ΔpacC pH 8 - 1	31.56	31.51	19.32	19.31	0.00021	0.00020	0.00012	0.00007	20.36	20.36	0.00044	0.00041	0.00026	0.00015
ΔpacC pH 8 - 1	31.46		19.3						20.36					
ΔpacC pH 8 - 2	32.85	32.88	19.21	19.205	0.00008				20.01	20.02	0.00013			
ΔpacC pH 8 - 2	32.91		19.2						20.03					
ΔpacC pH 8 - 3	31.09	31.06	19.46	19.47	0.00032				20.47	20.47	0.00065			
ΔpacC pH 8 - 3	31.03		19.48						20.47					
	ENA2		EF-2		x / EF-2				RPS22		x / RPS22			
Sample	Cp	Avg	Cp	Avg	2^(ΔCp)	Avg	Stdev	S.E.	Cp	Avg		Avg	Stdev	S.E.
CA pH 5 - 1	32.22	32.255	18.87	18.85	0.00009	0.00008	0.00002	0.00001	19.61	19.605	0.00016	0.00013	0.00003	0.00002
CA pH 5 - 1	32.29		18.83						19.6					
CA pH 5 - 2	32.72	32.74	18.69	18.7	0.00006				19.47	19.475	0.00010			
CA pH 5 - 2	32.76		18.71						19.48					
CA pH 5 - 3	32.34	32.415	18.73	18.735	0.00008				19.68	19.68	0.00015			
CA pH 5 - 3	32.49		18.74						19.68					
CA pH 6.5 - 1	32.19	32.335	18.8	18.815	0.00009	0.00005	0.00004	0.00002	19.76	19.77	0.00017	0.00009	0.00007	0.00004
CA pH 6.5 - 1	32.48		18.83						19.78					
CA pH 6.5 - 2	33.22	33.135	18.65	18.645	0.00004				19.8	19.795	0.00010			
CA pH 6.5 - 2	33.05		18.64						19.79					
CA pH 6.5 - 3	35	35	18.23	18.265	0.00001				19.11	19.105	0.00002			
CA pH 6.5 - 3	35		18.3						19.1					
CA pH 8 - 1	32.69	32.675	19.08	19.1	0.00008	0.00012	0.00005	0.00003	19.93	19.935	0.00015	0.00023	0.00008	0.00004
CA pH 8 - 1	32.66		19.12						19.94					
CA pH 8 - 2	32.07	31.99	18.82	18.805	0.00011				19.97	19.975	0.00024			
CA pH 8 - 2	31.91		18.79						19.98					
CA pH 8 - 3	31.58	31.515	19.02	19.035	0.00018				19.8	19.795	0.00030			
CA pH 8 - 3	31.45		19.05						19.79					

Appendix 6.5.2. qRT-PCR data of Figure 3.11. Expression of *ena2* in wild-type, Δ*pacC* and *pacC*^{CA} mutant in culture.

	Alkphos		EF-2		x / EF-2				RPS22		x / RPS22			
Sample	Cp	Avg	Cp	Avg	2^(ΔCp)	Avg	Stdev	S.E.	Cp	Avg		Avg	Stdev	S.E.
WT pH 5 - 1	22.97	22.96	19.22	19.225	0.07510	0.06917	0.00549	0.00317	20.28	20.285	0.15658	0.15517	0.00344	0.00198
WT pH 5 - 1	22.95		19.23						20.29					
WT pH 5 - 2	23.01	23.035	19.15	19.16	0.06816				20.3	20.31	0.15125			
WT pH 5 - 2	23.06		19.17						20.32					
WT pH 5 - 3	22.62	22.605	18.64	18.645	0.06426				19.94	19.94	0.15767			
WT pH 5 - 3	22.59		18.65						19.94					
WT pH 6.5 - 1	21.67	21.675	18.32	18.34	0.09910	0.09239	0.01103	0.00637	19.38	19.415	0.20877	0.20901	0.00042	0.00024
WT pH 6.5 - 1	21.68		18.36						19.45					
WT pH 6.5 - 2	21.84	21.82	18.48	18.475	0.09841				19.54	19.565	0.20950			
WT pH 6.5 - 2	21.8		18.47						19.59					
WT pH 6.5 - 3	22	22.005	18.36	18.355	0.07966				19.75	19.745	0.20877			
WT pH 6.5 - 3	22.01		18.35						19.74					
WT pH 8 - 1	22	22	18.58	18.585	0.09375	0.09008	0.00327	0.00189	19.74	19.75	0.21022	0.21457	0.01081	0.00624
WT pH 8 - 1	22		18.59						19.76					
WT pH 8 - 2	22.33	22.345	18.85	18.83	0.08747				20.08	20.07	0.20661			
WT pH 8 - 2	22.36		18.81						20.06					
WT pH 8 - 3	21.65	21.655	18.18	18.165	0.08900				19.51	19.515	0.22688			
WT pH 8 - 3	21.66		18.15						19.52					
	Alkphos		EF-2		x / EF-2				RPS22		x / RPS22			
Sample	Cp	Avg	Cp	Avg	2^(ΔCp)	Avg	Stdev	S.E.	Cp	Avg		Avg	Stdev	S.E.
ΔpacC pH 5 - 1	22.26	22.265	19.2	19.2	0.11949	0.12554	0.01638	0.00946	19.91	19.925	0.19751	0.20393	0.00995	0.00574
ΔpacC pH 5 - 1	22.27		19.2						19.94					
ΔpacC pH 5 - 2	22.22	22.225	19.4	19.43	0.14409				20.01	20.01	0.21539			
ΔpacC pH 5 - 2	22.23		19.46						20.01					
ΔpacC pH 5 - 3	22.34	22.335	19.19	19.19	0.11305				20.01	20.005	0.19888			
ΔpacC pH 5 - 3	22.33		19.19						20					
ΔpacC pH 6.5 - 1	21.68	21.685	18.68	18.685	0.12500	0.12502	0.00260	0.00150	19.8	19.805	0.27168	0.27137	0.00144	0.00083
ΔpacC pH 6.5 - 1	21.69		18.69						19.81					
ΔpacC pH 6.5 - 2	21.95	21.935	18.97	18.965	0.12763				20.07	20.06	0.27263			
ΔpacC pH 6.5 - 2	21.92		18.96						20.05					
ΔpacC pH 6.5 - 3	21.84	21.83	18.81	18.8	0.12243				19.93	19.94	0.26981			
ΔpacC pH 6.5 - 3	21.82		18.79						19.95					
ΔpacC pH 8 - 1	21.98	22	19.32	19.31	0.15496	0.18072	0.02619	0.01512	20.36	20.36	0.32086	0.34845	0.02403	0.01387
ΔpacC pH 8 - 1	22.02		19.3						20.36					
ΔpacC pH 8 - 2	21.47	21.475	19.21	19.205	0.20733				20.01	20.02	0.36476			
ΔpacC pH 8 - 2	21.48		19.2						20.03					
ΔpacC pH 8 - 3	21.93	21.945	19.46	19.47	0.17987				20.47	20.47	0.35973			
ΔpacC pH 8 - 3	21.96		19.48						20.47					
	Alkphos		EF-2		x / EF-2				RPS22		x / RPS22			
Sample	Cp	Avg	Cp	Avg	2^(ΔCp)	Avg	Stdev	S.E.	Cp	Avg		Avg	Stdev	S.E.
CA pH 5 - 1	21.53	21.525	18.87	18.85	0.15658	0.15186	0.02050	0.01183	19.61	19.605	0.26425	0.26786	0.02076	0.01198
CA pH 5 - 1	21.52		18.83						19.6					
CA pH 5 - 2	21.27	21.26	18.69	18.7	0.16958				19.47	19.475	0.29018			
CA pH 5 - 2	21.25		18.71						19.48					
CA pH 5 - 3	21.68	21.685	18.73	18.735	0.12941				19.68	19.68	0.24914			
CA pH 5 - 3	21.69		18.74						19.68					
CA pH 6.5 - 1	21.52	21.505	18.8	18.815	0.15496	0.14506	0.02309	0.01333	19.76	19.77	0.30041	0.28431	0.01901	0.01097
CA pH 6.5 - 1	21.49		18.83						19.78					
CA pH 6.5 - 2	21.72	21.72	18.65	18.645	0.11867				19.8	19.795	0.26334			
CA pH 6.5 - 2	21.72		18.64						19.79					
CA pH 6.5 - 3	20.9	20.895	18.23	18.265	0.16154				19.11	19.105	0.28917			
CA pH 6.5 - 3	20.89		18.3						19.1					
CA pH 8 - 1	21.96	21.98	19.08	19.1	0.13584	0.12263	0.03409	0.01968	19.93	19.935	0.24232	0.22733	0.03364	0.01942
CA pH 8 - 1	22		19.12						19.94					
CA pH 8 - 2	22.38	22.38	18.82	18.805	0.08391				19.97	19.975	0.18881			
CA pH 8 - 2	22.38		18.79						19.98					
CA pH 8 - 3	21.79	21.79	19.02	19.035	0.14814				19.8	19.795	0.25087			
CA pH 8 - 3	21.79		19.05						19.79					

Appendix 6.5.3. qRT-PCR data of Figure 3.15A. Expression of alkaline phosphatase in wild-type, Δ*pacC* and *pacC*^{CA} mutant in culture.

	Acidphos		EF-2		x / EF-2				RPS22		x / RPS22			
Sample	Cp	Avg	Cp	Avg	2^(ΔCp)	Avg	Stdev	S.E.	Cp	Avg		Avg	Stdev	S.E.
WT pH 5 - 1	24.31	24.305	19.22	19.225	0.02956	0.02757	0.00210	0.00121	20.28	20.285	0.06164	0.06204	0.00592	0.00342
WT pH 5 - 1	24.3		19.23						20.29					
WT pH 5 - 2	24.46	24.46	19.15	19.16	0.02538				20.3	20.31	0.05633			
WT pH 5 - 2	24.46		19.17						20.32					
WT pH 5 - 3	23.81	23.815	18.64	18.645	0.02778				19.94	19.94	0.06816			
WT pH 5 - 3	23.82		18.65						19.94					
WT pH 6.5 - 1	23.34	23.32	18.32	18.34	0.03169	0.03193	0.00157	0.00091	19.38	19.415	0.06675	0.07326	0.01287	0.00743
WT pH 6.5 - 1	23.3		18.36						19.45					
WT pH 6.5 - 2	23.51	23.51	18.48	18.475	0.03050				19.54	19.565	0.06493			
WT pH 6.5 - 2	23.51		18.47						19.59					
WT pH 6.5 - 3	23.25	23.25	18.36	18.355	0.03361				19.75	19.745	0.08808			
WT pH 6.5 - 3	23.25		18.35						19.74					
WT pH 8 - 1	23.1	23.09	18.58	18.585	0.04404	0.04324	0.00254	0.00147	19.74	19.75	0.09876	0.10319	0.01073	0.00619
WT pH 8 - 1	23.08		18.59						19.76					
WT pH 8 - 2	23.45	23.46	18.85	18.83	0.04039				20.08	20.07	0.09539			
WT pH 8 - 2	23.47		18.81						20.06					
WT pH 8 - 3	22.64	22.63	18.18	18.165	0.04528				19.51	19.515	0.11542			
WT pH 8 - 3	22.62		18.15						19.52					
	Acidphos		EF-2		x / EF-2				RPS22		x / RPS22			
Sample	Cp	Avg	Cp	Avg	2^(ΔCp)	Avg	Stdev	S.E.	Cp	Avg		Avg	Stdev	S.E.
ΔpacC pH 5 - 1	24.05	24.06	19.2	19.2	0.03443	0.03473	0.00243	0.00140	19.91	19.925	0.05692	0.05659	0.00074	0.00043
ΔpacC pH 5 - 1	24.07		19.2						19.94					
ΔpacC pH 5 - 2	24.17	24.175	19.4	19.43	0.03729				20.01	20.01	0.05575			
ΔpacC pH 5 - 2	24.18		19.46						20.01					
ΔpacC pH 5 - 3	24.13	24.135	19.19	19.19	0.03246				20.01	20.005	0.05711			
ΔpacC pH 5 - 3	24.14		19.19						20					
ΔpacC pH 6.5 - 1	23.24	23.315	18.68	18.685	0.04039	0.04059	0.00142	0.00082	19.8	19.805	0.08778	0.08809	0.00170	0.00098
ΔpacC pH 6.5 - 1	23.39		18.69						19.81					
ΔpacC pH 6.5 - 2	23.5	23.535	18.97	18.965	0.04210				20.07	20.06	0.08993			
ΔpacC pH 6.5 - 2	23.57		18.96						20.05					
ΔpacC pH 6.5 - 3	23.48	23.47	18.81	18.8	0.03928				19.93	19.94	0.08657			
ΔpacC pH 6.5 - 3	23.46		18.79						19.95					
ΔpacC pH 8 - 1	23.28	23.285	19.32	19.31	0.06359	0.05736	0.00642	0.00371	20.36	20.36	0.13167	0.11214	0.02137	0.01234
ΔpacC pH 8 - 1	23.29		19.3						20.36					
ΔpacC pH 8 - 2	23.49	23.505	19.21	19.205	0.05077				20.01	20.02	0.08931			
ΔpacC pH 8 - 2	23.52		19.2						20.03					
ΔpacC pH 8 - 3	23.59	23.585	19.46	19.47	0.05771				20.47	20.47	0.11542			
ΔpacC pH 8 - 3	23.58		19.48						20.47					
	Acidphos		EF-2		x / EF-2				RPS22		x / RPS22			
Sample	Cp	Avg	Cp	Avg	2^(ΔCp)	Avg	Stdev	S.E.	Cp	Avg		Avg	Stdev	S.E.
CA pH 5 - 1	23.61	23.665	18.87	18.85	0.03553	0.03314	0.00315	0.00182	19.61	19.605	0.05995	0.05853	0.00153	0.00088
CA pH 5 - 1	23.72		18.83						19.6					
CA pH 5 - 2	23.57	23.565	18.69	18.7	0.03432				19.47	19.475	0.05872			
CA pH 5 - 2	23.56		18.71						19.48					
CA pH 5 - 3	23.84	23.815	18.73	18.735	0.02956				19.68	19.68	0.05692			
CA pH 5 - 3	23.79		18.74						19.68					
CA pH 6.5 - 1	23.66	23.61	18.8	18.815	0.03602	0.03230	0.00364	0.00210	19.76	19.77	0.06983	0.06372	0.00616	0.00356
CA pH 6.5 - 1	23.56		18.83						19.78					
CA pH 6.5 - 2	23.8	23.765	18.65	18.645	0.02876				19.8	19.795	0.06381			
CA pH 6.5 - 2	23.73		18.64						19.79					
CA pH 6.5 - 3	23.24	23.225	18.23	18.265	0.03213				19.11	19.105	0.05751			
CA pH 6.5 - 3	23.21		18.3						19.1					
CA pH 8 - 1	23.71	23.69	19.08	19.1	0.04152	0.03931	0.00434	0.00250	19.93	19.935	0.07407	0.07419	0.00296	0.00171
CA pH 8 - 1	23.67		19.12						19.94					
CA pH 8 - 2	23.66	23.67	18.82	18.805	0.03432				19.97	19.975	0.07721			
CA pH 8 - 2	23.68		18.79						19.98					
CA pH 8 - 3	23.59	23.605	19.02	19.035	0.04210				19.8	19.795	0.07130			
CA pH 8 - 3	23.62		19.05						19.79					

Appendix 6.5.4. qRT-PCR data of Figure 3.15B. Expression of acid phosphatase in wild-type, Δ*pacC* and *pacC*^{CA} mutant in culture.

	Acidphos		EF-2		x / EF-2				RPS22		x / RPS22			
Sample	Cp	Avg	Cp	Avg	2^(ΔCp)	Avg	Stdev	S.E.	Cp	Avg		Avg	Stdev	S.E.
WT pH 5 - 1	24.31	24.305	19.22	19.225	0.02956	0.02757	0.00210	0.00121	20.28	20.285	0.06164	0.06204	0.00592	0.00342
WT pH 5 - 1	24.3		19.23						20.29					
WT pH 5 - 2	24.46	24.46	19.15	19.16	0.02538				20.3	20.31	0.05633			
WT pH 5 - 2	24.46		19.17						20.32					
WT pH 5 - 3	23.81	23.815	18.64	18.645	0.02778				19.94	19.94	0.06816			
WT pH 5 - 3	23.82		18.65						19.94					
WT pH 6.5 - 1	23.34	23.32	18.32	18.34	0.03169	0.03193	0.00157	0.00091	19.38	19.415	0.06675	0.07326	0.01287	0.00743
WT pH 6.5 - 1	23.3		18.36						19.45					
WT pH 6.5 - 2	23.51	23.51	18.48	18.475	0.03050				19.54	19.565	0.06493			
WT pH 6.5 - 2	23.51		18.47						19.59					
WT pH 6.5 - 3	23.25	23.25	18.36	18.355	0.03361				19.75	19.745	0.08808			
WT pH 6.5 - 3	23.25		18.35						19.74					
WT pH 8 - 1	23.1	23.09	18.58	18.585	0.04404	0.04324	0.00254	0.00147	19.74	19.75	0.09876	0.10319	0.01073	0.00619
WT pH 8 - 1	23.08		18.59						19.76					
WT pH 8 - 2	23.45	23.46	18.85	18.83	0.04039				20.08	20.07	0.09539			
WT pH 8 - 2	23.47		18.81						20.06					
WT pH 8 - 3	22.64	22.63	18.18	18.165	0.04528				19.51	19.515	0.11542			
WT pH 8 - 3	22.62		18.15						19.52					
	Acidphos		EF-2		x / EF-2				RPS22		x / RPS22			
Sample	Cp	Avg	Cp	Avg	2^(ΔCp)	Avg	Stdev	S.E.	Cp	Avg		Avg	Stdev	S.E.
ΔpacC pH 5 - 1	24.05	24.06	19.2	19.2	0.03443	0.03473	0.00243	0.00140	19.91	19.925	0.05692	0.05659	0.00074	0.00043
ΔpacC pH 5 - 1	24.07		19.2						19.94					
ΔpacC pH 5 - 2	24.17	24.175	19.4	19.43	0.03729				20.01	20.01	0.05575			
ΔpacC pH 5 - 2	24.18		19.46						20.01					
ΔpacC pH 5 - 3	24.13	24.135	19.19	19.19	0.03246				20.01	20.005	0.05711			
ΔpacC pH 5 - 3	24.14		19.19						20					
ΔpacC pH 6.5 - 1	23.24	23.315	18.68	18.685	0.04039	0.04059	0.00142	0.00082	19.8	19.805	0.08778	0.08809	0.00170	0.00098
ΔpacC pH 6.5 - 1	23.39		18.69						19.81					
ΔpacC pH 6.5 - 2	23.5	23.535	18.97	18.965	0.04210				20.07	20.06	0.08993			
ΔpacC pH 6.5 - 2	23.57		18.96						20.05					
ΔpacC pH 6.5 - 3	23.48	23.47	18.81	18.8	0.03928				19.93	19.94	0.08657			
ΔpacC pH 6.5 - 3	23.46		18.79						19.95					
ΔpacC pH 8 - 1	23.28	23.285	19.32	19.31	0.06359	0.05736	0.00642	0.00371	20.36	20.36	0.13167	0.11214	0.02137	0.01234
ΔpacC pH 8 - 1	23.29		19.3						20.36					
ΔpacC pH 8 - 2	23.49	23.505	19.21	19.205	0.05077				20.01	20.02	0.08931			
ΔpacC pH 8 - 2	23.52		19.2						20.03					
ΔpacC pH 8 - 3	23.59	23.585	19.46	19.47	0.05771				20.47	20.47	0.11542			
ΔpacC pH 8 - 3	23.58		19.48						20.47					
	Acidphos		EF-2		x / EF-2				RPS22		x / RPS22			
Sample	Cp	Avg	Cp	Avg	2^(ΔCp)	Avg	Stdev	S.E.	Cp	Avg		Avg	Stdev	S.E.
CA pH 5 - 1	23.61	23.665	18.87	18.85	0.03553	0.03314	0.00315	0.00182	19.61	19.605	0.05995	0.05853	0.00153	0.00088
CA pH 5 - 1	23.72		18.83						19.6					
CA pH 5 - 2	23.57	23.565	18.69	18.7	0.03432				19.47	19.475	0.05872			
CA pH 5 - 2	23.56		18.71						19.48					
CA pH 5 - 3	23.84	23.815	18.73	18.735	0.02956				19.68	19.68	0.05692			
CA pH 5 - 3	23.79		18.74						19.68					
CA pH 6.5 - 1	23.66	23.61	18.8	18.815	0.03602	0.03230	0.00364	0.00210	19.76	19.77	0.06983	0.06372	0.00616	0.00356
CA pH 6.5 - 1	23.56		18.83						19.78					
CA pH 6.5 - 2	23.8	23.765	18.65	18.645	0.02876				19.8	19.795	0.06381			
CA pH 6.5 - 2	23.73		18.64						19.79					
CA pH 6.5 - 3	23.24	23.225	18.23	18.265	0.03213				19.11	19.105	0.05751			
CA pH 6.5 - 3	23.21		18.3						19.1					
CA pH 8 - 1	23.71	23.69	19.08	19.1	0.04152	0.03931	0.00434	0.00250	19.93	19.935	0.07407	0.07419	0.00296	0.00171
CA pH 8 - 1	23.67		19.12						19.94					
CA pH 8 - 2	23.66	23.67	18.82	18.805	0.03432				19.97	19.975	0.07721			
CA pH 8 - 2	23.68		18.79						19.98					
CA pH 8 - 3	23.59	23.605	19.02	19.035	0.04210				19.8	19.795	0.07130			
CA pH 8 - 3	23.62		19.05						19.79					

Appendix 6.5.5. qRT-PCR data of Figure 3.15C. Expression of *CNH1* in wild-type, Δ*pacC* and *pacC*^{CA} mutant in culture.

	CytP450		EF-2		x / EF-2				RPS22		x / RPS22			
Sample	Cp	Avg	Cp	Avg	2^(ΔCp)	Avg	Stdev	S.E.	Cp	Avg		Avg	Stdev	S.E.
WT pH 5 - 1	30.91	30.885	19.22	19.225	0.00031	0.00031	0.00005	0.00003	20.28	20.285	0.00064	0.00070	0.00010	0.00006
WT pH 5 - 1	30.86		19.23						20.29					
WT pH 5 - 2	30.65	30.575	19.15	19.16	0.00037				20.3	20.31	0.00081			
WT pH 5 - 2	30.5		19.17						20.32					
WT pH 5 - 3	30.47	30.565	18.64	18.645	0.00026				19.94	19.94	0.00063			
WT pH 5 - 3	30.66		18.65						19.94					
WT pH 6.5 - 1	30.56	30.64	18.32	18.34	0.00020	0.00018	0.00001	0.00001	19.38	19.415	0.00042	0.00042	0.00006	0.00003
WT pH 6.5 - 1	30.72		18.36						19.45					
WT pH 6.5 - 2	31.01	31.01	18.48	18.475	0.00017				19.54	19.565	0.00036			
WT pH 6.5 - 2	31.01		18.47						19.59					
WT pH 6.5 - 3	30.71	30.78	18.36	18.355	0.00018				19.75	19.745	0.00048			
WT pH 6.5 - 3	30.85		18.35						19.74					
WT pH 8 - 1	30.77	30.2	18.58	18.585	0.00032	0.00024	0.00008	0.00004	19.74	19.75	0.00071	0.00057	0.00015	0.00009
WT pH 8 - 1	29.63		18.59						19.76					
WT pH 8 - 2	30.86	30.825	18.85	18.83	0.00024				20.08	20.07	0.00058			
WT pH 8 - 2	30.79		18.81						20.06					
WT pH 8 - 3	30.88	30.735	18.18	18.165	0.00016				19.51	19.515	0.00042			
WT pH 8 - 3	30.59		18.15						19.52					
	CytP450		EF-2		x / EF-2				RPS22		x / RPS22			
Sample	Cp	Avg	Cp	Avg	2^(ΔCp)	Avg	Stdev	S.E.	Cp	Avg		Avg	Stdev	S.E.
ΔpacC pH 5 - 1	30.58	30.55	19.2	19.2	0.00038	0.00045	0.00017	0.00010	19.91	19.925	0.00063	0.00072	0.00021	0.00012
ΔpacC pH 5 - 1	30.52		19.2						19.94					
ΔpacC pH 5 - 2	30.01	30.03	19.4	19.43	0.00064				20.01	20.01	0.00096			
ΔpacC pH 5 - 2	30.05		19.46						20.01					
ΔpacC pH 5 - 3	30.61	30.775	19.19	19.19	0.00033				20.01	20.005	0.00057			
ΔpacC pH 5 - 3	30.94		19.19						20					
ΔpacC pH 6.5 - 1	31.06	31.23	18.68	18.685	0.00017	0.00017	0.00001	0.00001	19.8	19.805	0.00036	0.00037	0.00002	0.00001
ΔpacC pH 6.5 - 1	31.4		18.69						19.81					
ΔpacC pH 6.5 - 2	31.26	31.36	18.97	18.965	0.00019				20.07	20.06	0.00040			
ΔpacC pH 6.5 - 2	31.46		18.96						20.05					
ΔpacC pH 6.5 - 3	31.4	31.41	18.81	18.8	0.00016				19.93	19.94	0.00035			
ΔpacC pH 6.5 - 3	31.42		18.79						19.95					
ΔpacC pH 8 - 1	31.02	31.03	19.32	19.31	0.00030	0.00038	0.00016	0.00009	20.36	20.36	0.00061	0.00074	0.00033	0.00019
ΔpacC pH 8 - 1	31.04		19.3						20.36					
ΔpacC pH 8 - 2	31.07	31.035	19.21	19.205	0.00027				20.01	20.02	0.00048			
ΔpacC pH 8 - 2	31		19.2						20.03					
ΔpacC pH 8 - 3	30.2	30.28	19.46	19.47	0.00056				20.47	20.47	0.00111			
ΔpacC pH 8 - 3	30.36		19.48						20.47					
	CytP450		EF-2		x / EF-2				RPS22		x / RPS22			
Sample	Cp	Avg	Cp	Avg	2^(ΔCp)	Avg	Stdev	S.E.	Cp	Avg		Avg	Stdev	S.E.
CA pH 5 - 1	29.82	29.97	18.87	18.85	0.00045	0.00037	0.00009	0.00005	19.61	19.605	0.00076	0.00064	0.00011	0.00007
CA pH 5 - 1	30.12		18.83						19.6					
CA pH 5 - 2	30.03	30.075	18.69	18.7	0.00038				19.47	19.475	0.00064			
CA pH 5 - 2	30.12		18.71						19.48					
CA pH 5 - 3	30.6	30.56	18.73	18.735	0.00028				19.68	19.68	0.00053			
CA pH 5 - 3	30.52		18.74						19.68					
CA pH 6.5 - 1	30.49	30.675	18.8	18.815	0.00027	0.00015	0.00010	0.00006	19.76	19.77	0.00052	0.00030	0.00020	0.00011
CA pH 6.5 - 1	30.86		18.83						19.78					
CA pH 6.5 - 2	31.53	31.74	18.65	18.645	0.00011				19.8	19.795	0.00025			
CA pH 6.5 - 2	31.95		18.64						19.79					
CA pH 6.5 - 3	31.76	31.945	18.23	18.265	0.00008				19.11	19.105	0.00014			
CA pH 6.5 - 3	32.13		18.3						19.1					
CA pH 8 - 1	30.74	30.815	19.08	19.1	0.00030	0.00036	0.00021	0.00012	19.93	19.935	0.00053	0.00066	0.00030	0.00017
CA pH 8 - 1	30.89		19.12						19.94					
CA pH 8 - 2	31.16	31.115	18.82	18.805	0.00020				19.97	19.975	0.00044			
CA pH 8 - 2	31.07		18.79						19.98					
CA pH 8 - 3	29.99	29.755	19.02	19.035	0.00059				19.8	19.795	0.00100			
CA pH 8 - 3	29.52		19.05						19.79					

Appendix 6.5.6. qRT-PCR data of Figure 3.15D. Expression of cytochrome P450 in wild-type, Δ*pacC* and *pacC*^{CA} mutant in culture.

	pacC		EF-2		x / EF-2				RPS22		x / RPS22			
Sample	Value	Avg	Value	Avg	Value	Avg	Stdev	S.E.	Value	Avg	Value	Avg	Stdev	S.E.
WT pH 5 - 1	3.83E+03	3830	87600	90200	0.04246	0.04209	0.00202	0.00116	53500	53850	0.07112	0.07468	0.00452	0.00261
WT pH 5 - 1	3.83E+03		92800						54200					
WT pH 5 - 2	4.34E+03	4330	112000	108500	0.03991				57600	59200	0.07314			
WT pH 5 - 2	4.32E+03		105000						60800					
WT pH 5 - 3	5.75E+03	5815	134000	132500	0.04389				72800	72900	0.07977			
WT pH 5 - 3	5.88E+03		131000						73000					
WT pH 6.5 - 1	1.34E+04	13200	156000	153000	0.08627	0.08432	0.00216	0.00125	104000	103500	0.12754	0.13092	0.01171	0.00676
WT pH 6.5 - 1	1.30E+04		150000						103000					
WT pH 6.5 - 2	1.16E+04	11600	136000	137000	0.08467				95100	95650	0.12128			
WT pH 6.5 - 2	1.16E+04		138000						96200					
WT pH 6.5 - 3	1.23E+04	12300	152000	150000	0.08200				85800	85450	0.14394			
WT pH 6.5 - 3	1.23E+04		148000						85100					
WT pH 8 - 1	2.09E+04	21100	134000	133500	0.15805	0.14784	0.01228	0.00709	80700	80750	0.26130	0.24213	0.03242	0.01872
WT pH 8 - 1	2.13E+04		133000						80800					
WT pH 8 - 2	1.84E+04	18150	121000	120000	0.15125				70200	69700	0.26040			
WT pH 8 - 2	1.79E+04		119000						69200					
WT pH 8 - 3	1.81E+04	17850	132000	133000	0.13421				88000	87200	0.20470			
WT pH 8 - 3	1.76E+04		134000						86400					

	pacC		EF-2		x / EF-2				RPS22		x / RPS22			
Sample	Value	Avg	Value	Avg	Value	Avg	Stdev	S.E.	Value	Avg	Value	Avg	Stdev	S.E.
ΔpacC pH 5 - 1	2.71E+00	2.71	110000	109500	0.00002	0.00001	0.00001	0.00001	81900	81450	0.00003	0.00001	0.00002	0.00001
ΔpacC pH 5 - 1	2.71E+00		109000						81000					
ΔpacC pH 5 - 2	0.00E+00	0	98300	98050	0.00000				76900	77700	0.00000			
ΔpacC pH 5 - 2	0.00E+00		97800						78500					
ΔpacC pH 5 - 3	0.00E+00	0	116000	115500	0.00000				78100	78050	0.00000			
ΔpacC pH 5 - 3	0.00E+00		115000						78000					
ΔpacC pH 6.5 - 1	2.71E+00	2.71	155000	154500	0.00002	0.00001	0.00001	0.00001	88800	88650	0.00003	0.00001	0.00002	0.00001
ΔpacC pH 6.5 - 1	2.71E+00		154000						88500					
ΔpacC pH 6.5 - 2	0.00E+00	0	124000	129000	0.00000				76400	76900	0.00000			
ΔpacC pH 6.5 - 2	0.00E+00		134000						77400					
ΔpacC pH 6.5 - 3	0.00E+00	0	145000	145000	0.00000				80100	81000	0.00000			
ΔpacC pH 6.5 - 3	0.00E+00		145000						81900					
ΔpacC pH 8 - 1	0.00E+00	0	100000	101500	0.00000	0.00001	0.00001	0.00000	62800	62350	0.00000	0.00001	0.00001	0.00001
ΔpacC pH 8 - 1	0.00E+00		103000						61900					
ΔpacC pH 8 - 2	0.00E+00	1.355	111000	109500	0.00001				76500	76250	0.00002			
ΔpacC pH 8 - 2	2.71E+00		108000						76000					
ΔpacC pH 8 - 3	0.00E+00	1.355	94300	94450	0.00001				54600	55000	0.00002			
ΔpacC pH 8 - 3	2.71E+00		94600						55400					

	pacC		EF-2		x / EF-2				RPS22		x / RPS22			
Sample	Value	Avg	Value	Avg	Value	Avg	Stdev	S.E.	Value	Avg	Value	Avg	Stdev	S.E.
CA pH 5 - 1	1.23E+04	12450	154000	155000	0.08032	0.07503	0.00697	0.00403	119000	118000	0.10551	0.10749	0.00172	0.00099
CA pH 5 - 1	1.26E+04		156000						117000					
CA pH 5 - 2	1.35E+04	13550	174000	174500	0.07765				124000	125000	0.10840			
CA pH 5 - 2	1.36E+04		175000						126000					
CA pH 5 - 3	1.22E+04	12050	182000	179500	0.06713				111000	111000	0.10856			
CA pH 5 - 3	1.19E+04		177000						111000					
CA pH 6.5 - 1	1.21E+04	11950	157000	159000	0.07516	0.07734	0.00631	0.00364	107000	106000	0.11274	0.10760	0.01151	0.00665
CA pH 6.5 - 1	1.18E+04		161000						105000					
CA pH 6.5 - 2	1.20E+04	12200	165000	168500	0.07240				105000	105500	0.11564			
CA pH 6.5 - 2	1.24E+04		172000						106000					
CA pH 6.5 - 3	1.54E+04	15200	181000	180000	0.08444				161000	161000	0.09441			
CA pH 6.5 - 3	1.50E+04		179000						161000					
CA pH 8 - 1	1.11E+04	11000	144000	135000	0.08148	0.08167	0.00410	0.00237	98300	98500	0.11168	0.11682	0.01064	0.00614
CA pH 8 - 1	1.09E+04		126000						98700					
CA pH 8 - 2	1.25E+04	12350	160000	159000	0.07767				96400	95700	0.12905			
CA pH 8 - 2	1.22E+04		158000						95000					
CA pH 8 - 3	1.18E+04	11850	137000	138000	0.08587				108000	108000	0.10972			
CA pH 8 - 3	1.19E+04		139000						108000					

Appendix 6.5.7. qRT-PCR data of Figure 3.25A. Expression of *pacC* in wild-type, Δ*pacC* and *pacC*^{CA} mutant in culture.

	ltmE		EF-2		x / EF-2				RPS22		x / RPS22			
Sample	Value	Avg	Value	Avg	Value	Avg	Stdev	S.E.	Value	Avg	Value	Avg	Stdev	S.E.
WT pH 5 - 1	7.22E+02	601	87600	90200	0.00666	0.00759	0.00228	0.00132	53500	53850	0.01116	0.01352	0.00446	0.00257
WT pH 5 - 1	4.80E+02		92800						54200					
WT pH 5 - 2	1.03E+03	1105	112000	108500	0.01018				57600	59200	0.01867			
WT pH 5 - 2	1.18E+03		105000						60800					
WT pH 5 - 3	8.04E+02	783.5	134000	132500	0.00591				72800	72900	0.01075			
WT pH 5 - 3	7.63E+02		131000						73000					
WT pH 6.5 - 1	7.71E+02	612	156000	153000	0.00400	0.00465	0.00086	0.00050	104000	103500	0.00591	0.00719	0.00113	0.00065
WT pH 6.5 - 1	4.53E+02		150000						103000					
WT pH 6.5 - 2	7.09E+02	770.5	136000	137000	0.00562				95100	95650	0.00806			
WT pH 6.5 - 2	8.32E+02		138000						96200					
WT pH 6.5 - 3	6.20E+02	649.5	152000	150000	0.00433				85800	85450	0.00760			
WT pH 6.5 - 3	6.79E+02		148000						85100					
WT pH 8 - 1	6.94E+02	632	134000	133500	0.00473	0.00399	0.00080	0.00046	80700	80750	0.00783	0.00656	0.00157	0.00091
WT pH 8 - 1	5.70E+02		133000						80800					
WT pH 8 - 2	5.16E+02	491	121000	120000	0.00409				70200	69700	0.00704			
WT pH 8 - 2	4.66E+02		119000						69200					
WT pH 8 - 3	5.57E+02	418.5	132000	133000	0.00315				88000	87200	0.00480			
WT pH 8 - 3	2.80E+02		134000						86400					
	ltmE		EF-2		x / EF-2				RPS22		x / RPS22			
Sample	Value	Avg	Value	Avg	Value	Avg	Stdev	S.E.	Value	Avg	Value	Avg	Stdev	S.E.
ΔpacC pH 5 - 1	4.09E+02	380	110000	109500	0.00347	0.00262	0.00115	0.00066	81900	81450	0.00467	0.00363	0.00171	0.00099
ΔpacC pH 5 - 1	3.51E+02		109000						81000					
ΔpacC pH 5 - 2	9.37E+01	128.85	98300	98050	0.00131				76900	77700	0.00166			
ΔpacC pH 5 - 2	1.64E+02		97800						78500					
ΔpacC pH 5 - 3	3.61E+02	356.5	116000	115500	0.00309				78100	78050	0.00457			
ΔpacC pH 5 - 3	3.52E+02		115000						78000					
ΔpacC pH 6.5 - 1	2.50E+02	307.5	155000	154500	0.00199	0.00224	0.00034	0.00019	88800	88650	0.00347	0.00390	0.00069	0.00040
ΔpacC pH 6.5 - 1	3.65E+02		154000						88500					
ΔpacC pH 6.5 - 2	3.29E+02	272	124000	129000	0.00211				76400	76900	0.00354			
ΔpacC pH 6.5 - 2	2.15E+02		134000						77400					
ΔpacC pH 6.5 - 3	3.62E+02	380	145000	145000	0.00262				80100	81000	0.00469			
ΔpacC pH 6.5 - 3	3.98E+02		145000						81900					
ΔpacC pH 8 - 1	1.27E+02	141	100000	101500	0.00139	0.00196	0.00066	0.00038	62800	62350	0.00226	0.00316	0.00127	0.00074
ΔpacC pH 8 - 1	1.55E+02		103000						61900					
ΔpacC pH 8 - 2	2.39E+02	198	111000	109500	0.00181				76500	76250	0.00260			
ΔpacC pH 8 - 2	1.57E+02		108000						76000					
ΔpacC pH 8 - 3	2.83E+02	254	94300	94450	0.00269				54600	55000	0.00462			
ΔpacC pH 8 - 3	2.25E+02		94600						55400					
	ltmE		EF-2		x / EF-2				RPS22		x / RPS22			
Sample	Value	Avg	Value	Avg	Value	Avg	Stdev	S.E.	Value	Avg	Value	Avg	Stdev	S.E.
CA pH 5 - 1	3.74E+02	478	154000	155000	0.00308	0.00328	0.00025	0.00015	119000	118000	0.00405	0.00476	0.00090	0.00052
CA pH 5 - 1	5.82E+02		156000						117000					
CA pH 5 - 2	5.48E+02	557.5	174000	174500	0.00319				124000	125000	0.00446			
CA pH 5 - 2	5.67E+02		175000						126000					
CA pH 5 - 3	5.67E+02	640.5	182000	179500	0.00357				111000	111000	0.00577			
CA pH 5 - 3	7.14E+02		177000						111000					
CA pH 6.5 - 1	4.56E+02	471	157000	159000	0.00296	0.00344	0.00059	0.00034	107000	106000	0.00444	0.00474	0.00040	0.00023
CA pH 6.5 - 1	4.86E+02		161000						105000					
CA pH 6.5 - 2	4.94E+02	548	165000	168500	0.00325				105000	105500	0.00519			
CA pH 6.5 - 2	6.02E+02		172000						106000					
CA pH 6.5 - 3	6.76E+02	738.5	181000	180000	0.00410				161000	161000	0.00459			
CA pH 6.5 - 3	8.01E+02		179000						161000					
CA pH 8 - 1	5.01E+02	447.5	144000	135000	0.00331	0.00350	0.00064	0.00037	98300	98500	0.00454	0.00511	0.00167	0.00096
CA pH 8 - 1	3.94E+02		126000						98700					
CA pH 8 - 2	7.13E+02	669	160000	159000	0.00421				96400	95700	0.00699			
CA pH 8 - 2	6.25E+02		158000						95000					
CA pH 8 - 3	4.05E+02	410	137000	138000	0.00297				108000	108000	0.00380			
CA pH 8 - 3	4.15E+02		139000						108000					

Appendix 6.5.8. qRT-PCR data of Figure 3.25B. Expression of *ltmE* in wild-type, Δ*pacC* and *pacC*^{CA} mutant in culture.

	easA		EF-2		x / EF-2				RPS22		x / RPS22			
Sample	Value	Avg	Value	Avg	Value	Avg	Stdev	S.E.	Value	Avg	Value	Avg	Stdev	S.E.
WT pH 5 - 1	2.50E+02	230.5	87600	90200	0.00256	0.00230	0.00112	0.00064	53500	53850	0.00428	0.00408	0.00202	0.00117
WT pH 5 - 1	2.11E+02		92800						54200					
WT pH 5 - 2	3.70E+02	355	112000	108500	0.00327				57600	59200	0.00600			
WT pH 5 - 2	3.40E+02		105000						60800					
WT pH 5 - 3	1.55E+02	143.5	134000	132500	0.00108				72800	72900	0.00197			
WT pH 5 - 3	1.32E+02		131000						73000					
WT pH 6.5 - 1	5.99E+01	49.15	156000	153000	0.00032	0.00029	0.00003	0.00002	104000	103500	0.00047	0.00044	0.00004	0.00002
WT pH 6.5 - 1	3.84E+01		150000						103000					
WT pH 6.5 - 2	3.84E+01	38.4	136000	137000	0.00028				95100	95650	0.00040			
WT pH 6.5 - 2	3.84E+01		138000						96200					
WT pH 6.5 - 3	3.84E+01	38.4	152000	150000	0.00026				85800	85450	0.00045			
WT pH 6.5 - 3	3.84E+01		148000						85100					
WT pH 8 - 1	3.84E+01	38.4	134000	133500	0.00029	0.00030	0.00002	0.00001	80700	80750	0.00048	0.00049	0.00006	0.00003
WT pH 8 - 1	3.84E+01		133000						80800					
WT pH 8 - 2	3.84E+01	38.4	121000	120000	0.00032				70200	69700	0.00055			
WT pH 8 - 2	3.84E+01		119000						69200					
WT pH 8 - 3	3.84E+01	38.4	132000	133000	0.00029				88000	87200	0.00044			
WT pH 8 - 3	3.84E+01		134000						86400					
	easA		EF-2		x / EF-2				RPS22		x / RPS22			
Sample	Value	Avg	Value	Avg	Value	Avg	Stdev	S.E.	Value	Avg	Value	Avg	Stdev	S.E.
ΔpacC pH 5 - 1	1.32E+02	120	110000	109500	0.00110	0.00128	0.00060	0.00034	81900	81450	0.00147	0.00179	0.00098	0.00056
ΔpacC pH 5 - 1	1.08E+02		109000						81000					
ΔpacC pH 5 - 2	9.35E+01	78.25	98300	98050	0.00080				76900	77700	0.00101			
ΔpacC pH 5 - 2	6.30E+01		97800						78500					
ΔpacC pH 5 - 3	2.21E+02	225	116000	115500	0.00195				78100	78050	0.00288			
ΔpacC pH 5 - 3	2.29E+02		115000						78000					
ΔpacC pH 6.5 - 1	1.53E+02	151	155000	154500	0.00098	0.00093	0.00012	0.00007	88800	88650	0.00170	0.00160	0.00017	0.00010
ΔpacC pH 6.5 - 1	1.49E+02		154000						88500					
ΔpacC pH 6.5 - 2	1.51E+02	130.5	124000	129000	0.00101				76400	76900	0.00170			
ΔpacC pH 6.5 - 2	1.10E+02		134000						77400					
ΔpacC pH 6.5 - 3	1.12E+02	114.5	145000	145000	0.00079				80100	81000	0.00141			
ΔpacC pH 6.5 - 3	1.17E+02		145000						81900					
ΔpacC pH 8 - 1	7.68E+01	80.5	100000	101500	0.00079	0.00124	0.00063	0.00045	62800	62350	0.00129	0.00210	0.00114	0.00080
ΔpacC pH 8 - 1	8.42E+01		103000						61900					
ΔpacC pH 8 - 2		#DIV/0!	111000	109500	#DIV/0!				76500	76250	#DIV/0!			
ΔpacC pH 8 - 2			108000						76000					
ΔpacC pH 8 - 3	1.64E+02	159.5	94300	94450	0.00169				54600	55000	0.00290			
ΔpacC pH 8 - 3	1.55E+02		94600						55400					
	easA		EF-2		x / EF-2				RPS22		x / RPS22			
Sample	Value	Avg	Value	Avg	Value	Avg	Stdev	S.E.	Value	Avg	Value	Avg	Stdev	S.E.
CA pH 5 - 1	2.09E+02	201	154000	155000	0.00130	0.00124	0.00013	0.00008	119000	118000	0.00170	0.00180	0.00033	0.00019
CA pH 5 - 1	1.93E+02		156000						117000					
CA pH 5 - 2	1.88E+02	190.5	174000	174500	0.00109				124000	125000	0.00152			
CA pH 5 - 2	1.93E+02		175000						126000					
CA pH 5 - 3	2.54E+02	240.5	182000	179500	0.00134				111000	111000	0.00217			
CA pH 5 - 3	2.27E+02		177000						111000					
CA pH 6.5 - 1	2.02E+02	167.5	157000	159000	0.00105	0.00088	0.00025	0.00018	107000	106000	0.00158	0.00135	0.00033	0.00023
CA pH 6.5 - 1	1.33E+02		161000						105000					
CA pH 6.5 - 2	1.38E+02	117.7	165000	168500	0.00070				105000	105500	0.00112			
CA pH 6.5 - 2	9.74E+01		172000						106000					
CA pH 6.5 - 3		#DIV/0!	181000	180000	#DIV/0!				161000	161000	#DIV/0!			
CA pH 6.5 - 3			179000						161000					
CA pH 8 - 1	1.50E+02	114.05	144000	135000	0.00084	0.00095	0.00019	0.00011	98300	98500	0.00116	0.00134	0.00017	0.00010
CA pH 8 - 1	7.81E+01		126000						98700					
CA pH 8 - 2	1.28E+02	132	160000	159000	0.00083				96400	95700	0.00138			
CA pH 8 - 2	1.36E+02		158000						95000					
CA pH 8 - 3	1.33E+02	160.5	137000	138000	0.00116				108000	108000	0.00149			
CA pH 8 - 3	1.88E+02		139000						108000					

Appendix 6.5.9. qRT-PCR data of Figure 3.25C. Expression of *easA* in wild-type, Δ*pacC* and *pacC*^{CA} mutant in culture.

	dmaW		EF-2		x / EF-2				RPS22		x / RPS22			
Sample	Value	Avg	Value	Avg	Value	Avg	Stdev	S.E.	Value	Avg	Value	Avg	Stdev	S.E.
WT pH 5 - 1	3.01E+01	30.1	87600	90200	0.00033	0.00028	0.00005	0.00003	53500	53850	0.00056	0.00049	0.00007	0.00004
WT pH 5 - 1	3.01E+01		92800						54200					
WT pH 5 - 2	3.01E+01	30.1	112000	108500	0.00028				57600	59200	0.00051			
WT pH 5 - 2	3.01E+01		105000						60800					
WT pH 5 - 3	3.01E+01	30.1	134000	132500	0.00023				72800	72900	0.00041			
WT pH 5 - 3	3.01E+01		131000						73000					
WT pH 6.5 - 1	3.01E+01	30.1	156000	153000	0.00020	0.00021	0.00001	0.00001	104000	103500	0.00029	0.00032	0.00003	0.00002
WT pH 6.5 - 1	3.01E+01		150000						103000					
WT pH 6.5 - 2	3.01E+01	30.1	136000	137000	0.00022				95100	95650	0.00031			
WT pH 6.5 - 2	3.01E+01		138000						96200					
WT pH 6.5 - 3	3.01E+01	30.1	152000	150000	0.00020				85800	85450	0.00035			
WT pH 6.5 - 3	3.01E+01		148000						85100					
WT pH 8 - 1	7.38E+01	51.95	134000	133500	0.00039	0.00085	#DIV/0!	#DIV/0!	80700	80750	0.00064	0.00079	0.00045	0.00026
WT pH 8 - 1	3.01E+01		133000						80800					
WT pH 8 - 2	3.01E+01	30.1	121000	120000	0.00025				70200	69700	0.00043			
WT pH 8 - 2	3.01E+01		119000						69200					
WT pH 8 - 3	8.91E+01	112.55	132000	133000	0.00085				88000	87200	0.00129			
WT pH 8 - 3	1.36E+02		134000						86400					
	dmaW		EF-2		x / EF-2				RPS22		x / RPS22			
Sample	Value	Avg	Value	Avg	Value	Avg	Stdev	S.E.	Value	Avg	Value	Avg	Stdev	S.E.
ΔpacC pH 5 - 1	5.78E+01	83.4	110000	109500	0.00076	0.00060	0.00023	0.00017	81900	81450	0.00102	0.00083	0.00027	0.00019
ΔpacC pH 5 - 1	1.09E+02		109000						81000					
ΔpacC pH 5 - 2		#DIV/0!	98300	98050	#DIV/0!				76900	77700	#DIV/0!			
ΔpacC pH 5 - 2			97800						78500					
ΔpacC pH 5 - 3	4.74E+01	49.75	116000	115500	0.00043				78100	78050	0.00064			
ΔpacC pH 5 - 3	5.21E+01		115000						78000					
ΔpacC pH 6.5 - 1	4.74E+01	59.8	155000	154500	0.00039	0.00040	0.00001	0.00001	88800	88650	0.00067	0.00069	0.00001	0.00001
ΔpacC pH 6.5 - 1	7.22E+01		154000						88500					
ΔpacC pH 6.5 - 2	4.38E+01	53.05	124000	129000	0.00041				76400	76900	0.00069			
ΔpacC pH 6.5 - 2	6.23E+01		134000						77400					
ΔpacC pH 6.5 - 3	2.99E+01	56.75	145000	145000	0.00039				80100	81000	0.00070			
ΔpacC pH 6.5 - 3	8.36E+01		145000						81900					
ΔpacC pH 8 - 1	1.44E+02	155	100000	101500	0.00153	0.00123	0.00049	0.00028	62800	62350	0.00249	0.00201	0.00091	0.00053
ΔpacC pH 8 - 1	1.66E+02		103000						61900					
ΔpacC pH 8 - 2	7.42E+01	72.85	111000	109500	0.00067				76500	76250	0.00096			
ΔpacC pH 8 - 2	7.15E+01		108000						76000					
ΔpacC pH 8 - 3	1.15E+02	142	94300	94450	0.00150				54600	55000	0.00258			
ΔpacC pH 8 - 3	1.69E+02		94600						55400					
	dmaW		EF-2		x / EF-2				RPS22		x / RPS22			
Sample	Value	Avg	Value	Avg	Value	Avg	Stdev	S.E.	Value	Avg	Value	Avg	Stdev	S.E.
CA pH 5 - 1	6.64E+01	114.7	154000	155000	0.00074	0.00062	0.00020	0.00012	119000	118000	0.00097	0.00088	0.00022	0.00013
CA pH 5 - 1	1.63E+02		156000						117000					
CA pH 5 - 2	1.64E+02	129.05	174000	174500	0.00074				124000	125000	0.00103			
CA pH 5 - 2	9.41E+01		175000						126000					
CA pH 5 - 3	6.00E+01	69.65	182000	179500	0.00039				111000	111000	0.00063			
CA pH 5 - 3	7.93E+01		177000						111000					
CA pH 6.5 - 1	4.08E+01	70.4	157000	159000	0.00044	0.00050	0.00008	0.00005	107000	106000	0.00066	0.00064	0.00003	0.00002
CA pH 6.5 - 1	1.00E+02		161000						105000					
CA pH 6.5 - 2		#DIV/0!	165000	168500	#DIV/0!				105000	105500	#DIV/0!			
CA pH 6.5 - 2			172000						106000					
CA pH 6.5 - 3	9.57E+01	99.35	181000	180000	0.00055				161000	161000	0.00062			
CA pH 6.5 - 3	1.03E+02		179000						161000					
CA pH 8 - 1	1.14E+02	116	144000	135000	0.00086	0.00060	0.00029	0.00017	98300	98500	0.00118	0.00083	0.00035	0.00020
CA pH 8 - 1	1.18E+02		126000						98700					
CA pH 8 - 2	4.92E+01	45.1	160000	159000	0.00028				96400	95700	0.00047			
CA pH 8 - 2	4.10E+01		158000						95000					
CA pH 8 - 3	1.19E+02	90.25	137000	138000	0.00065				108000	108000	0.00084			
CA pH 8 - 3	6.15E+01		139000						108000					

Appendix 6.5.10. qRT-PCR data of Figure 3.25D. Expression of *dmaW* in wild-type, Δ*pacC* and *pacC*^{CA} mutant in culture.

	lpsA		EF-2		x / EF-2				RPS22		x / RPS22			
Sample	Value	Avg	Value	Avg	Value	Avg	Stdev	S.E.	Value	Avg	Value	Avg	Stdev	S.E.
WT pH 5 - 1	4.44E+02	458	87600	90200	0.00508	0.00449	0.00052	0.00030	53500	53850	0.00851	0.00794	0.00051	0.00029
WT pH 5 - 1	4.72E+02		92800						54200					
WT pH 5 - 2	4.52E+02	446	112000	108500	0.00411				57600	59200	0.00753			
WT pH 5 - 2	4.40E+02		105000						60800					
WT pH 5 - 3	5.52E+02	566.5	134000	132500	0.00428				72800	72900	0.00777			
WT pH 5 - 3	5.81E+02		131000						73000					
WT pH 6.5 - 1	7.21E+02	686.5	156000	153000	0.00449	0.00440	0.00009	0.00005	104000	103500	0.00663	0.00685	0.00080	0.00046
WT pH 6.5 - 1	6.52E+02		150000						103000					
WT pH 6.5 - 2	5.93E+02	591	136000	137000	0.00431				95100	95650	0.00618			
WT pH 6.5 - 2	5.89E+02		138000						96200					
WT pH 6.5 - 3	6.69E+02	661	152000	150000	0.00441				85800	85450	0.00774			
WT pH 6.5 - 3	6.53E+02		148000						85100					
WT pH 8 - 1	8.07E+02	794	134000	133500	0.00595	0.00608	0.00011	0.00006	80700	80750	0.00983	0.00992	0.00059	0.00034
WT pH 8 - 1	7.81E+02		133000						80800					
WT pH 8 - 2	7.31E+02	735.5	121000	120000	0.00613				70200	69700	0.01055			
WT pH 8 - 2	7.40E+02		119000						69200					
WT pH 8 - 3	8.35E+02	818	132000	133000	0.00615				88000	87200	0.00938			
WT pH 8 - 3	8.01E+02		134000						86400					
	lpsA		EF-2		x / EF-2				RPS22		x / RPS22			
Sample	Value	Avg	Value	Avg	Value	Avg	Stdev	S.E.	Value	Avg	Value	Avg	Stdev	S.E.
ΔpacC pH 5 - 1	5.14E+02	500	110000	109500	0.00457	0.00445	0.00010	0.00006	81900	81450	0.00614	0.00606	0.00047	0.00027
ΔpacC pH 5 - 1	4.86E+02		109000						81000					
ΔpacC pH 5 - 2	4.17E+02	432	98300	98050	0.00441				76900	77700	0.00556			
ΔpacC pH 5 - 2	4.47E+02		97800						78500					
ΔpacC pH 5 - 3	4.98E+02	506	116000	115500	0.00438				78100	78050	0.00648			
ΔpacC pH 5 - 3	5.14E+02		115000						78000					
ΔpacC pH 6.5 - 1	6.95E+02	670.5	155000	154500	0.00434	0.00599	0.00203	0.00117	88800	88650	0.00756	0.01035	0.00320	0.00185
ΔpacC pH 6.5 - 1	6.46E+02		154000						88500					
ΔpacC pH 6.5 - 2	1.12E+03	1065	124000	129000	0.00826				76400	76900	0.01385			
ΔpacC pH 6.5 - 2	1.01E+03		134000						77400					
ΔpacC pH 6.5 - 3	7.41E+02	781	145000	145000	0.00539				80100	81000	0.00964			
ΔpacC pH 6.5 - 3	8.21E+02		145000						81900					
ΔpacC pH 8 - 1	1.00E+03	975	100000	101500	0.00961	0.00898	0.00213	0.00123	62800	62350	0.01564	0.01452	0.00457	0.00264
ΔpacC pH 8 - 1	9.50E+02		103000						61900					
ΔpacC pH 8 - 2	7.18E+02	724	111000	109500	0.00661				76500	76250	0.00950			
ΔpacC pH 8 - 2	7.30E+02		108000						76000					
ΔpacC pH 8 - 3	9.86E+02	1013	94300	94450	0.01073				54600	55000	0.01842			
ΔpacC pH 8 - 3	1.04E+03		94600						55400					
	lpsA		EF-2		x / EF-2				RPS22		x / RPS22			
Sample	Value	Avg	Value	Avg	Value	Avg	Stdev	S.E.	Value	Avg	Value	Avg	Stdev	S.E.
CA pH 5 - 1	1.14E+03	1125	154000	155000	0.00726	0.00706	0.00017	0.00010	119000	118000	0.00953	0.01017	0.00091	0.00053
CA pH 5 - 1	1.11E+03		156000						117000					
CA pH 5 - 2	1.30E+03	1220	174000	174500	0.00699				124000	125000	0.00976			
CA pH 5 - 2	1.14E+03		175000						126000					
CA pH 5 - 3	1.21E+03	1245	182000	179500	0.00694				111000	111000	0.01122			
CA pH 5 - 3	1.28E+03		177000						111000					
CA pH 6.5 - 1	1.21E+03	1205	157000	159000	0.00758	0.00771	0.00098	0.00057	107000	106000	0.01137	0.01067	0.00081	0.00047
CA pH 6.5 - 1	1.20E+03		161000						105000					
CA pH 6.5 - 2	1.13E+03	1145	165000	168500	0.00680				105000	105500	0.01085			
CA pH 6.5 - 2	1.16E+03		172000						106000					
CA pH 6.5 - 3	1.58E+03	1575	181000	180000	0.00875				161000	161000	0.00978			
CA pH 6.5 - 3	1.57E+03		179000						161000					
CA pH 8 - 1	1.21E+03	1275	144000	135000	0.00944	0.00996	0.00101	0.00058	98300	98500	0.01294	0.01421	0.00126	0.00073
CA pH 8 - 1	1.34E+03		126000						98700					
CA pH 8 - 2	1.50E+03	1480	160000	159000	0.00931				96400	95700	0.01546			
CA pH 8 - 2	1.46E+03		158000						95000					
CA pH 8 - 3	1.56E+03	1535	137000	138000	0.01112				108000	108000	0.01421			
CA pH 8 - 3	1.51E+03		139000						108000					

Appendix 6.5.11. qRT-PCR data of Figure 3.25E. Expression of *lpsA* in wild-type, Δ*pac*C and *pac*C^{CA} mutant in culture.

	perA		EF-2		x / EF-2				RPS22		x / RPS22			
Sample	Value	Avg	Value	Avg	Value	Avg	Stdev	S.E.	Value	Avg	Value	Avg	Stdev	S.E.
WT pH 5 - 1	1.30E+03	1295	87600	90200	0.01436	0.01496	0.00458	0.00264	53500	53850	0.02405	0.02661	0.00871	0.00503
WT pH 5 - 1	1.29E+03		92800						54200					
WT pH 5 - 2	2.18E+03	2150	112000	108500	0.01982				57600	59200	0.03632			
WT pH 5 - 2	2.12E+03		105000						60800					
WT pH 5 - 3	1.42E+03	1420	134000	132500	0.01072				72800	72900	0.01948			
WT pH 5 - 3	1.42E+03		131000						73000					
WT pH 6.5 - 1	3.09E+03	3080	156000	153000	0.02013	0.01572	0.00397	0.00229	104000	103500	0.02976	0.02416	0.00487	0.00281
WT pH 6.5 - 1	3.07E+03		150000						103000					
WT pH 6.5 - 2	1.98E+03	2000	136000	137000	0.01460				95100	95650	0.02091			
WT pH 6.5 - 2	2.02E+03		138000						96200					
WT pH 6.5 - 3	1.82E+03	1865	152000	150000	0.01243				85800	85450	0.02183			
WT pH 6.5 - 3	1.91E+03		148000						85100					
WT pH 8 - 1	1.95E+03	1945	134000	133500	0.01457	0.01392	0.00231	0.00133	80700	80750	0.02409	0.02289	0.00508	0.00293
WT pH 8 - 1	1.94E+03		133000						80800					
WT pH 8 - 2	1.95E+03	1900	121000	120000	0.01583				70200	69700	0.02726			
WT pH 8 - 2	1.85E+03		119000						69200					
WT pH 8 - 3	1.56E+03	1510	132000	133000	0.01135				88000	87200	0.01732			
WT pH 8 - 3	1.46E+03		134000						86400					
	perA		EF-2		x / EF-2				RPS22		x / RPS22			
Sample	Value	Avg	Value	Avg	Value	Avg	Stdev	S.E.	Value	Avg	Value	Avg	Stdev	S.E.
ΔpacC pH 5 - 1	1.07E+03	1034.5	110000	109500	0.00945	0.01030	0.00080	0.00046	81900	81450	0.01270	0.01405	0.00199	0.00115
ΔpacC pH 5 - 1	9.99E+02		109000						81000					
ΔpacC pH 5 - 2	1.03E+03	1020	98300	98050	0.01040				76900	77700	0.01313			
ΔpacC pH 5 - 2	1.01E+03		97800						78500					
ΔpacC pH 5 - 3	1.33E+03	1275	116000	115500	0.01104				78100	78050	0.01634			
ΔpacC pH 5 - 3	1.22E+03		115000						78000					
ΔpacC pH 6.5 - 1	1.38E+03	1370	155000	154500	0.00887	0.00841	0.00087	0.00050	88800	88650	0.01545	0.01458	0.00116	0.00067
ΔpacC pH 6.5 - 1	1.36E+03		154000						88500					
ΔpacC pH 6.5 - 2	9.91E+02	1155.5	124000	129000	0.00896				76400	76900	0.01503			
ΔpacC pH 6.5 - 2	1.32E+03		134000						77400					
ΔpacC pH 6.5 - 3	1.07E+03	1075	145000	145000	0.00741				80100	81000	0.01327			
ΔpacC pH 6.5 - 3	1.08E+03		145000						81900					
ΔpacC pH 8 - 1	1.45E+03	1485	100000	101500	0.01463	0.01460	0.00098	0.00056	62800	62350	0.02382	0.02336	0.00361	0.00209
ΔpacC pH 8 - 1	1.52E+03		103000						61900					
ΔpacC pH 8 - 2	1.46E+03	1490	111000	109500	0.01361				76500	76250	0.01954			
ΔpacC pH 8 - 2	1.52E+03		108000						76000					
ΔpacC pH 8 - 3	1.51E+03	1470	94300	94450	0.01556				54600	55000	0.02673			
ΔpacC pH 8 - 3	1.43E+03		94600						55400					
	perA		EF-2		x / EF-2				RPS22		x / RPS22			
Sample	Value	Avg	Value	Avg	Value	Avg	Stdev	S.E.	Value	Avg	Value	Avg	Stdev	S.E.
CA pH 5 - 1	2.24E+03	2240	154000	155000	0.01445	0.01453	0.00037	0.00021	119000	118000	0.01898	0.02099	0.00277	0.00160
CA pH 5 - 1	2.24E+03		156000						117000					
CA pH 5 - 2	2.47E+03	2480	174000	174500	0.01421				124000	125000	0.01984			
CA pH 5 - 2	2.49E+03		175000						126000					
CA pH 5 - 3	2.70E+03	2680	182000	179500	0.01493				111000	111000	0.02414			
CA pH 5 - 3	2.66E+03		177000						111000					
CA pH 6.5 - 1	3.05E+03	3020	157000	159000	0.01899	0.01592	0.00290	0.00168	107000	106000	0.02849	0.02270	0.00710	0.00410
CA pH 6.5 - 1	2.99E+03		161000						105000					
CA pH 6.5 - 2	2.65E+03	2620	165000	168500	0.01555				105000	105500	0.02483			
CA pH 6.5 - 2	2.59E+03		172000						106000					
CA pH 6.5 - 3	2.38E+03	2380	181000	180000	0.01322				161000	161000	0.01478			
CA pH 6.5 - 3	2.38E+03		179000						161000					
CA pH 8 - 1	3.00E+03	2980	144000	135000	0.02207	0.02236	0.00421	0.00243	98300	98500	0.03025	0.03159	0.00219	0.00126
CA pH 8 - 1	2.96E+03		126000						98700					
CA pH 8 - 2	2.86E+03	2910	160000	159000	0.01830				96400	95700	0.03041			
CA pH 8 - 2	2.96E+03		158000						95000					
CA pH 8 - 3	3.72E+03	3685	137000	138000	0.02670				108000	108000	0.03412			
CA pH 8 - 3	3.65E+03		139000						108000					

Appendix 6.5.12. qRT-PCR data of Figure 3.25F. Expression of *perA* in wild-type, Δ*pacC* and *pacC*^{CA} mutant in culture.

Fold RPS22							
A	In culture			In planta			Fold change
	Value	SD		Value	SD	S.E.	
ltmE	0.007189797	0.001128809	6.52E-04	1.996515685	0.350800504	2.03E-01	277.6873635
ltmP	N.D.	N.D.	N.D.	52.70239094	10.37983758	5.99E+00	N.A.
ltmM	N.D.	N.D.	N.D.	15.23944538	3.334762402	1.93E+00	N.A.
easA	0.00044191	3.72744E-05	2.15E-05	0.469112184	0.206527804	1.19E-01	1061.557137
dmaW	0.000319254	3.09692E-05	1.79E-05	0.345291492	0.120865866	6.98E-02	1081.556156
lpsA	0.006849048	0.000800573	4.62E-04	0.281994191	0.121226857	7.00E-02	41.17275549
perA	0.02416455	0.004866068	2.81E-03	1.430417381	0.376146217	2.17E-01	59.19486998

Fold EF-2							
B	In culture			In planta			Fold change
	Value	SD	S.E.	Value	SD	S.E.	
ltmE	0.004651363	0.000858412	4.96E-04	0.942049214	0.19098699	1.10E-01	202.5318834
ltmP				24.86989426	5.508238647	3.18E+00	
ltmM				7.186639856	1.686757913	9.74E-01	
easA	0.000285845	3.29734E-05	1.90E-05	0.222175159	0.102914436	5.94E-02	777.2585496
dmaW	0.000205702	1.22879E-05	7.09E-06	0.163182002	0.060121814	3.47E-02	793.2922942
lpsA	0.004402488	8.66054E-05	5.00E-05	0.132543914	0.055916483	3.23E-02	30.10659429
perA	0.015720864	0.003969527	2.29E-03	0.67595156	0.196542897	1.13E-01	42.99709951

Appendix 6.5.13. qRT-PCR data of Figure 3.26. Comparison of secondary metabolite gene expression in culture and *in planta*.

	pacC		EF-2		x / EF-2				RPS22		x / RPS22			
Name	Value	Avg	Value	Avg	Value	Avg	Stdev	S.E.	Value	Avg	Value	Avg	Stdev	S.E.
WT	64.8	178.9	1240	1255	0.14255	0.11843	0.02715	0.06837	1270	1165	0.15356	0.14350	0.02837	0.08285
WT	293		1270						1060					
WT	53.2	100.6	1140	1130	0.08903				675	902.5	0.11147			
WT	148		1120						1130					
WT	70.1	97.05	813	784.5	0.12371				537	586.5	0.16547			
WT	124		756						636					
ΔpacC	4.67	5.175	663	664	0.00779	0.00393	0.00390	0.00227	379	653.5	0.00792	0.00391	0.00396	0.00226
ΔpacC	5.68		665						928					
ΔpacC	1.23	2.85	735	715	0.00399				302	746	0.00382			
ΔpacC	4.47		695						1190					
ΔpacC	0	0	554	541.5	0.00000				601	474.5	0.00000			
ΔpacC	0		529						348					
ΔpacC/pacC	45.5	135.25	685	693	0.19517	0.17083	0.02468	0.09863	349	734.5	0.18414	0.15953	0.03419	0.09211
ΔpacC/pacC	225		701						1120					
ΔpacC/pacC	71.3	106.15	713	728	0.14581				382	881	0.12049			
ΔpacC/pacC	141		743						1380					
ΔpacC/pacC	98	97.25	579	567	0.17152				374	559	0.17397			
ΔpacC/pacC	96.5		555						744					
pacC-CA #14	30.04	28.96	583	569.5	0.05085	0.07701	0.03115	0.04446	232	530	0.05464	0.07763	0.03694	0.04482
pacC-CA #14	27.88		556						828					
pacC-CA #14	29.36	28.65	409	417	0.06871				236	494	0.05800			
pacC-CA #14	27.94		425						752					
pacC-CA #14	30.38	29.76	262	267	0.11146				151	247.5	0.12024			
pacC-CA #14	29.14		272						344					

Appendix 6.5.14. qRT-PCR data of Figure 3.27A. Expression of *pac*C in wild-type, Δ*pac*C, Δ*pac*C/*pac*C and *pac*C^{CA} mutant *in planta*.

	ltmE		EF-2		x / EF-2				RPS22		x / RPS22			
Name	Value	Avg	Value	Avg	Value	Avg	Stdev	S.E.	Value	Avg	Value	Avg	Stdev	S.E.
WT	1130	1095	1240	1255	0.87251	0.94205	0.19099	0.54389	1270	1165	0.93991	1.16169	0.33662	0.67070
WT	1060		1270						1060					
WT	928	899	1140	1130	0.79558				675	902.5	0.99612			
WT	870		1120						1130					
WT	916	908.5	813	784.5	1.15806				537	586.5	1.54902			
WT	901		756						636					
ΔpacC	749	737.5	663	664	1.11069	0.97773	0.11868	0.56449	379	653.5	1.12854	1.01570	0.14972	0.58641
ΔpacC	726		665						928					
ΔpacC	603	631	735	715	0.88252				302	746	0.84584			
ΔpacC	659		695						1190					
ΔpacC	522	509	554	541.5	0.93998				601	474.5	1.07271			
ΔpacC	496		529						348					
ΔpacC/pacC	587	620.5	685	693	0.89538	1.17931	0.31633	0.68087	349	734.5	0.84479	1.10473	0.38097	0.63782
ΔpacC/pacC	654		701						1120					
ΔpacC/pacC	819	817	713	728	1.12225				382	881	0.92736			
ΔpacC/pacC	815		743						1380					
ΔpacC/pacC	867	862	579	567	1.52028				374	559	1.54204			
ΔpacC/pacC	857		555						744					
pacC-CA #14	548	522.5	583	569.5	0.91747	1.31936	0.47785	0.76173	232	530	0.98585	1.27748	0.28705	0.73755
pacC-CA #14	497		556						828					
pacC-CA #14	709	770.5	409	417	1.84772				236	494	1.55972			
pacC-CA #14	832		425						752					
pacC-CA #14	303	318.5	262	267	1.19288				151	247.5	1.28687			
pacC-CA #14	334		272						344					

Appendix 6.5.15. qRT-PCR data of Figure 3.27B. Expression of *ltmE* in wild-type, Δ*pac*C, Δ*pac*C/*pac*C and *pac*C^{CA} mutant *in planta*.

	ltmP		EF-2		x / EF-2				RPS22		x / RPS22			
Name	Value	Avg	Value	Avg	Value	Avg	Stdev	S.E.	Value	Avg	Value	Avg	Stdev	S.E.
WT	30200	30450	1240	1255	24.26295	24.86989	5.50824	14.35864	1270	1165	26.13734	30.59902	9.04316	17.66635
WT	30700		1270						1060					
WT	22100	22250	1140	1130	19.69027				675	902.5	24.65374			
WT	22400		1120						1130					
WT	23200	24050	813	784.5	30.65647				537	586.5	41.00597			
WT	24900		756						636					
ΔpacC	24300	24250	663	664	36.52108	33.53508	4.73953	19.36149	379	653.5	37.10788	34.55301	2.53727	19.94919
ΔpacC	24200		665						928					
ΔpacC	25800	25750	735	715	36.01399				302	746	34.51743			
ΔpacC	25700		695						1190					
ΔpacC	14900	15200	554	541.5	28.07018				601	474.5	32.03372			
ΔpacC	15500		529						348					
ΔpacC/pacC	19000	18300	685	693	26.40693	33.46145	9.63912	19.31897	349	734.5	24.91491	31.46650	11.79284	18.16719
ΔpacC/pacC	17600		701						1120					
ΔpacC/pacC	21600	21500	713	728	29.53297				382	881	24.40409			
ΔpacC/pacC	21400		743						1380					
ΔpacC/pacC	25500	25200	579	567	44.44444				374	559	45.08050			
ΔpacC/pacC	24900		555						744					
pacC-CA #14	13200	13100	583	569.5	23.00263	31.52864	8.23965	18.20307	232	530	24.71698	30.89441	5.39330	17.83690
pacC-CA #14	13000		556						828					
pacC-CA #14	16500	16450	409	417	39.44844				236	494	33.29960			
pacC-CA #14	16400		425						752					
pacC-CA #14	8200	8580	262	267	32.13483				151	247.5	34.66667			
pacC-CA #14	8960		272						344					

Appendix 6.5.16. qRT-PCR data of Figure 3.27C. Expression of *ltmP* in wild-type, Δ*pac*C, Δ*pac*C/*pac*C and *pac*C^{CA} mutant *in planta*.

	ltmM		EF-2		x / EF-2				RPS22		x / RPS22			
Name	Value	Avg	Value	Avg	Value	Avg	Stdev	S.E.	Value	Avg	Value	Avg	Stdev	S.E.
WT	9710	9765	1240	1255	7.78088	7.18664	1.68676	4.14921	1270	1165	8.38197	8.78699	2.40030	5.07317
WT	9820		1270						1060					
WT	6030	5970	1140	1130	5.28319				675	902.5	6.61496			
WT	5910		1120						1130					
WT	6630	6665	813	784.5	8.49586				537	586.5	11.36402			
WT	6700		756						636					
ΔpacC	7090	7100	663	664	10.69277	9.37530	1.14548	5.41283	379	653.5	10.86458	9.71591	1.21056	5.60948
ΔpacC	7110		665						928					
ΔpacC	6240	6305	735	715	8.81818				302	746	8.45174			
ΔpacC	6370		695						1190					
ΔpacC	4600	4665	554	541.5	8.61496				601	474.5	9.83140			
ΔpacC	4730		529						348					
ΔpacC/pacC	6210	6510	685	693	9.39394	10.38321	1.89323	5.99475	349	734.5	8.86317	9.73426	2.68435	5.62008
ΔpacC/pacC	6810		701						1120					
ΔpacC/pacC	6700	6690	713	728	9.18956				382	881	7.59364			
ΔpacC/pacC	6680		743						1380					
ΔpacC/pacC	7370	7125	579	567	12.56614				374	559	12.74597			
ΔpacC/pacC	6880		555						744					
pacC-CA #14	4900	4815	583	569.5	8.45478	11.41583	2.71526	6.59093	232	530	9.08491	11.22469	1.96543	6.48058
pacC-CA #14	4730		556						828					
pacC-CA #14	5750	5750	409	417	13.78897				236	494	11.63968			
pacC-CA #14	5750		425						752					
pacC-CA #14	3110	3205	262	267	12.00375				151	247.5	12.94949			
pacC-CA #14	3300		272						344					

Appendix 6.5.17. qRT-PCR data of Figure 3.27D. Expression of *ltmM* in wild-type, Δ*pacC*, Δ*pacC*/*pacC* and *pacC*^{CA} mutant *in planta*.

	easA		EF-2		x / EF-2				RPS22		x / RPS22			
Name	Value	Avg	Value	Avg	Value	Avg	Stdev	S.E.	Value	Avg	Value	Avg	Stdev	S.E.
WT	290	274	1240	1255	0.21833	0.22218	0.10291	0.12827	1270	1165	0.23519	0.27478	0.14683	0.15864
WT	258		1270						1060					
WT	148	137	1140	1130	0.12124				675	902.5	0.15180			
WT	126		1120						1130					
WT	231	256.5	813	784.5	0.32696				537	586.5	0.43734			
WT	282		756						636					
ΔpacC	181	174.5	663	664	0.26280	0.21864	0.04332	0.12623	379	653.5	0.26702	0.22782	0.05195	0.13153
ΔpacC	168		665						928					
ΔpacC	134	126	735	715	0.17622				302	746	0.16890			
ΔpacC	118		695						1190					
ΔpacC	139	117.45	554	541.5	0.21690				601	474.5	0.24752			
ΔpacC	95.9		529						348					
ΔpacC/pacC	166	151	685	693	0.21789	0.27729	0.09082	0.16009	349	734.5	0.20558	0.26157	0.10910	0.15102
ΔpacC/pacC	136		701						1120					
ΔpacC/pacC	176	169	713	728	0.23214				382	881	0.19183			
ΔpacC/pacC	162		743						1380					
ΔpacC/pacC	230	216.5	579	567	0.38183				374	559	0.38730			
ΔpacC/pacC	203		555						744					
pacC-CA #14	110	119.5	583	569.5	0.20983	0.44229	0.20521	0.25536	232	530	0.22547	0.43004	0.17925	0.24829
pacC-CA #14	129		556						828					
pacC-CA #14	240	249.5	409	417	0.59832				236	494	0.50506			
pacC-CA #14	259		425						752					
pacC-CA #14	120	138.5	262	267	0.51873				151	247.5	0.55960			
pacC-CA #14	157		272						344					

Appendix 6.5.18. qRT-PCR data of Figure 3.27E. Expression of *easA* in wild-type, Δ*pacC*, Δ*pacC*/*pacC* and *pacC*^{CA} mutant *in planta*.

	dmaW		EF-2		x / EF-2				RPS22		x / RPS22			
Name	Value	Avg	Value	Avg	Value	Avg	Stdev	S.E.	Value	Avg	Value	Avg	Stdev	S.E.
WT	213	220.5	1240	1255	0.17570	0.16318	0.06012	0.09421	1270	1165	0.18927	0.20024	0.08382	0.11561
WT	228		1270						1060					
WT	105	110.5	1140	1130	0.09779				675	902.5	0.12244			
WT	116		1120						1130					
WT	156	169.5	813	784.5	0.21606				537	586.5	0.28900			
WT	183		756						636					
ΔpacC	201	217	663	664	0.32681	0.27139	0.08508	0.15669	379	653.5	0.33206	0.28552	0.10414	0.16484
ΔpacC	233		665						928					
ΔpacC	140	124	735	715	0.17343				302	746	0.16622			
ΔpacC	108		695						1190					
ΔpacC	167	170	554	541.5	0.31394				601	474.5	0.35827			
ΔpacC	173		529						348					
ΔpacC/pacC	235	225.5	685	693	0.32540	0.28543	0.13586	0.16479	349	734.5	0.30701	0.27343	0.14873	0.15787
ΔpacC/pacC	216		701						1120					
ΔpacC/pacC	79.2	97.6	713	728	0.13407				382	881	0.11078			
ΔpacC/pacC	116		743						1380					
ΔpacC/pacC	179	225	579	567	0.39683				374	559	0.40250			
ΔpacC/pacC	271		555						744					
pacC-CA #14	38.4	30.8	583	569.5	0.05408	0.18597	0.12621	0.10737	232	530	0.05811	0.18504	0.13666	0.10683
pacC-CA #14	23.2		556						828					
pacC-CA #14	68.1	82.65	409	417	0.19820				236	494	0.16731			
pacC-CA #14	97.2		425						752					
pacC-CA #14	97.9	81.6	262	267	0.30562				151	247.5	0.32970			
pacC-CA #14	65.3		272						344					

Appendix 6.5.19. qRT-PCR data of Figure 3.27F. Expression of *dmaW* in wild-type, Δ*pacC*, Δ*pacC*/*pacC* and *pacC*^{CA} mutant *in planta*.

	lpsA		EF-2		x / EF-2				RPS22		x / RPS22			
Name	Value	Avg	Value	Avg	Value	Avg	Stdev	S.E.	Value	Avg	Value	Avg	Stdev	S.E.
WT	215	241	1240	1255	0.19203	0.13254	0.05592	0.07652	1270	1165	0.20687	0.15831	0.05317	0.09140
WT	267		1270						1060					
WT	89.8	91.6	1140	1130	0.08106				675	902.5	0.10150			
WT	93.4		1120						1130					
WT	89.4	97.7	813	784.5	0.12454				537	586.5	0.16658			
WT	106		756						636					
ΔpacC	93.6	84.35	663	664	0.12703	0.09020	0.03468	0.05207	379	653.5	0.12907	0.09243	0.03266	0.05337
ΔpacC	75.1		665						928					
ΔpacC	59.5	61.05	735	715	0.08538				302	746	0.08184			
ΔpacC	62.6		695						1190					
ΔpacC	30.3	31.5	554	541.5	0.05817				601	474.5	0.06639			
ΔpacC	32.7		529						348					
ΔpacC/pacC	73.1	72	685	693	0.10390	0.10367	0.03419	0.05985	349	734.5	0.09803	0.09835	0.04120	0.05678
ΔpacC/pacC	70.9		701						1120					
ΔpacC/pacC	50	50.5	713	728	0.06937				382	881	0.05732			
ΔpacC/pacC	51		743						1380					
ΔpacC/pacC	64.9	78.1	579	567	0.13774				374	559	0.13971			
ΔpacC/pacC	91.3		555						744					
pacC-CA #14	23.3	28.35	583	569.5	0.04978	0.08469	0.04466	0.04890	232	530	0.05349	0.08074	0.03068	0.04661
pacC-CA #14	33.4		556						828					
pacC-CA #14	51.1	56.3	409	417	0.13501				236	494	0.11397			
pacC-CA #14	61.5		425						752					
pacC-CA #14	11.9	18.5	262	267	0.06929				151	247.5	0.07475			
pacC-CA #14	25.1		272						344					

Appendix 6.5.20. qRT-PCR data of Figure 3.27G. Expression of *lpsA* in wild-type, Δ*pacC*, Δ*pacC*/*pacC* and *pacC*^{CA} mutant *in planta*.

	perA		EF-2		x / EF-2				RPS22		x / RPS22			
Name	Value	Avg	Value	Avg	Value	Avg	Stdev	S.E.	Value	Avg	Value	Avg	Stdev	S.E.
WT	740	747.5	1240	1255	0.59562	0.67595	0.19654	0.39026	1270	1165	0.64163	0.83729	0.31761	0.48341
WT	755		1270						1060					
WT	584	601.5	1140	1130	0.53230				675	902.5	0.66648			
WT	619		1120						1130					
WT	698	706	813	784.5	0.89994				537	586.5	1.20375			
WT	714		756						636					
ΔpacC	652	684	663	664	1.03012	0.95761	0.08029	0.55288	379	653.5	1.04667	0.99678	0.14337	0.57549
ΔpacC	716		665						928					
ΔpacC	626	623	735	715	0.87133				302	746	0.83512			
ΔpacC	620		695						1190					
ΔpacC	517	526	554	541.5	0.97138				601	474.5	1.10854			
ΔpacC	535		529						348					
ΔpacC/pacC	691	700	685	693	1.01010	0.89740	0.10774	0.51811	349	734.5	0.95303	0.83084	0.11212	0.47969
ΔpacC/pacC	709		701						1120					
ΔpacC/pacC	644	645.5	713	728	0.88668				382	881	0.73269			
ΔpacC/pacC	647		743						1380					
ΔpacC/pacC	450	451	579	567	0.79541				374	559	0.80680			
ΔpacC/pacC	452		555						744					
pacC-CA #14	221	237.5	583	569.5	0.41703	0.51870	0.08857	0.29947	232	530	0.44811	0.51367	0.08087	0.29657
pacC-CA #14	254		556						828					
pacC-CA #14	223	241.5	409	417	0.57914				236	494	0.48887			
pacC-CA #14	260		425						752					
pacC-CA #14	148	149.5	262	267	0.55993				151	247.5	0.60404			
pacC-CA #14	151		272						344					

Appendix 6.5.21. qRT-PCR data of Figure 3.27H. Expression of *perA* in wild-type, Δ*pacC*, Δ*pacC*/*pacC* and *pacC*^{CA} mutant *in planta*.